



The University of
Nottingham

Department of Chemical and Environmental Engineering

Microwave Processing of Oil Contaminated Drill Cuttings

Igor S. M. Pereira M.Eng (Hons)

Thesis submitted to the University of Nottingham for the degree of Doctor of
Philosophy

September 2012

ABSTRACT

Easily accessible oil reserves are currently decreasing, leading to an increase in more complex offshore deep-sea drilling programs, which require increasingly greater depths to be drilled. Such wells are commonly drilled using oil based muds, which leads to the production of drilled rock fragments, drill cuttings, which are contaminated with the base oil present in the mud. It is a legal requirement to reduce oil content to below 1 wt% in order to dispose of these drill cuttings in the North Sea and microwave processing is suggested as a feasible method of achieving the desired oil removal. However, there are currently gaps in our understanding of the mechanisms behind, and variables affecting, the microwave treatment of oil contaminated drill cuttings. The work described in this thesis seeks to address some of these gaps in knowledge.

There were three main objectives for this thesis: (1) quantification, for the first time in the literature, of the main mechanisms driving oil and water removal during microwave processing of oil contaminated drill cuttings, (2) determination of key variables affecting performance during pilot scale continuous processing of oil contaminated drill cuttings and, for the first time, (3) treatment of drill cuttings with microwaves continuously at 896 MHz.

Bench scale experiments carried out in a single mode applicator were used to quantify the mechanisms involved in oil and water removal from drill cuttings. It was found that both vaporisation and entrainment mechanisms play a role in oil and water removal. Vaporisation was the main mechanism of water and oil removal, and typically accounted for >80-90% of the water and oil removed. For oil removal, vaporisation of the oil phase accounted for 70-100% of the overall removal. The absolute amount of water entrained and vaporised was found to increase with increasing energy input and power density. However, as a percentage of the overall

amount removed, entrainment was found to increase with increasing energy input. This was mainly due to higher heating rates at higher energy inputs, leading to pressurised, high velocity steam, which increased liquid carry-over (entrainment).

Both the drill cuttings sample composition and applicator type were found to have an effect on the extent of entrainment/vaporisation. Samples consisting of a higher overall liquid content, tended to have a greater amount of surface liquid content. This led to a greater potential of carry over when steam generated internally left the sample. Increasing the power again led an increase in entrainment in this case.

Different applicators were found to impact the electric field strength and power density within the water phase of the sample. Oil removal in multimode applicators progressed mainly through vaporisation (steam distillation) until the water content was sufficiently low to generate steam at a velocity high enough to entrain liquid droplets. When treatment was changed to single mode operation, entrainment occurred at an earlier stage, probably due to higher electric field strengths and power densities. It was also noted that the vaporisation mechanism of oil was more efficient at higher field strengths and powers, which could again be attributed to superheating and higher velocity steam, which enabled better mixing and heat transfer.

Experiments were also run to determine the main variables affecting the performance of continuous processing of cuttings. Overall continuous processing showed a substantial improvement in the energy required, 150 kWh/t vs. >250 kWh/t, to reduce the oil content of a drill cuttings sample to 1 wt%. It was found that the initial water and oil content of the sample, as well as the sample particle size distribution, had the greatest effect on the efficiency of continuous processing.

The effect of initial water and oil content on residual oil content was investigated methodically for the first time for continuous microwave processing of oil contaminated drill cuttings. An increase in initial oil content was found to have a

significant impact on the energy input required to treat the sample to 1 wt% oil content. As the oil content increased, the energy input required increased exponentially, mainly as a result of the change in the physical structure of the sample.

An increase in the water content led to an increase in energy input without any additional benefit to oil removal. However, as the water content was increased it was noticed that the theoretical energy input required to heat the entire sample approached the actual value measured for the energy input. This occurs as a result of the increasingly greater bulk dielectric properties of the sample as a result of higher levels of water content, which in turn leads to a higher efficiency in the conversion of microwave energy to heat in the sample.

The effect of particle size on oil content distribution and removal was investigated. Oil content was found to be substantially higher in particles of size <1.0 mm, with removal also being significantly higher in this particle size range. However, as the majority of the samples tested, $>80\%$, consisted of particles >1.0 mm, this improved removal is diluted by the performance of the coarser particles. The improved removal in finer particles is likely to be due to larger surface area, reduced path length within the particles and potentially higher electric field strength.

Finally, samples processed continuously using a continuous microwave setup at 896 MHz showed improvements over both continuous microwave treatment at 2.45 GHz and bench scale setups. Increasing the flowrate of the system at 896 MHz was also found to improve oil removal efficiency, which can be explained by the higher power requirements that would be required to maintain the energy inputs observed at the lower flowrate. Increasing the power leads to improved heating rates and thus increased removal rates through entrainment and vaporisation.

ACKNOWLEDGEMENTS

I would like to thank my supervisors, Professor Sam Kingman and Dr. John Robinson, for giving me the opportunity, advice and guidance needed to complete this PhD in the Department of Chemical and Environmental Engineering at the University of Nottingham.

I would like to thank the University of Nottingham, Brandt, which is part of the National Oilwell Varco and e2v for providing funding to my work.

I would like to thank Dr Aled Jones, Dr. Chris Dodds, Mr Andrew Batchelor, Dr. Christian Antonio, Dr. Jaouad El-Harfi, Dr. Georgios Dimitrakis and Dr. Richard Barranco for all the help and support, expertise and advice they gave me during my time at Nottingham. I would also like to thank all the workshop technicians, David Clift and the lab technicians for being flexible and helpful throughout my entire PhD. I would like to thank all my group colleagues and friends who not only helped me see issues, problems and opportunities from a different angle but were also there for me during hard times.

I would also like to thank the TD department at GSK Ulverston, Ian Morgan and David Grundy for supporting me during the difficult period of finishing my writing, whilst working.

I would like to thank my entire family for encouraging me to do my PhD and then for supporting me throughout the experimental work and now through writing.

Most of all I would like to thank my wife Catherine Rose Pereira for always supporting me in the hardest moments, and for helping me complete this work. Without her patience, help and love I would have not completed this.

CONTENTS

ABSTRACT	I
ACKNOWLEDGEMENTS	IV
CONTENTS	V
LIST OF FIGURES	VIII
LIST OF TABLES	XV
CHAPTER 1 – THESIS INTRODUCTION	1-1
1. Introduction	1-1
CHAPTER 2 – LITERATURE REVIEW	2-4
2. Introduction	2-4
2.1 Review of Oil Contaminated Drill Cuttings	2-4
2.2 Drilling muds	2-5
2.3 Drill cuttings mineralogy	2-7
2.4 Drill cuttings contamination	2-8
2.5 Review of current treatment and disposal practices	2-9
2.6 opportunity for microwave treatment of Cuttings	2-12
2.7 Microwave heating theory and application	2-13
2.8 The use of Microwaves as an alternative heating source	2-14
2.9 Microwave fundamental theory	2-15
2.9.1 Microwave interaction with dielectrics	2-15
2.9.2 Measurement of dielectric properties	2-17
2.9.3 Microwave heating mechanisms	2-18
2.9.4 Attenuation of microwaves during heating	2-20
2.9.5 Skin Depth	2-22
2.9.6 Dissipation of microwave power into the sample	2-23
2.9.7 selectivity in microwave heating	2-23
2.9.8 Microwave components and applicators	2-25
2.10 Review and analysis of gaps in previous works of microwave treatment of oil contaminated drill cuttings	2-30
2.11 Review of conventional and microwave heating	2-33
2.12 Review of conventional heating of wet porous materials	2-33
2.12.1 Heating mechanisms present during drying	2-33
2.12.2 conventional heating drying periods and rate	2-35
2.13 Review of microwave heating of wet porous materials	2-38
2.13.1 The effect of water type and content in microwave heating of Porous Materials	2-39
2.14 Conclusion	2-45
2.15 Thesis aims and objectives	2-46
CHAPTER 3 – ANALYTICAL TECHNIQUES	3-47
3. Introduction	3-47
3.1 Drill cuttings liquid Content and composition Analysis	3-47
3.2 Water content measurements	3-48

3.2.1	Introduction to DEAN & Stark Method	3-48
3.2.2	Method Description	3-48
3.2.3	Method Analysis	3-50
3.3	Oil content measurements	3-50
3.3.1	SOXHLET Method Description	3-51
3.3.2	Accelerated Solvent Extraction Method Description	3-53
3.3.3	Method Analysis	3-54
3.4	Oil Composition Measurements	3-55
3.4.1	gas chromatography (GC) and mass spectrometry (MS)	3-55
3.4.2	GC-MS method description	3-57
3.4.3	Method Analysis	3-58
3.5	Drill cuttings particle analysis	3-58
3.6	Sieving	3-59
3.6.1	Introduction to sieving	3-59
3.6.2	Sieving of agglomerated drill cuttings particles	3-59
3.6.3	Sieving of de-agglomerated drill cuttings particles	3-60
3.7 (MLA)	Scanning Electron Microscope (SEM) and Mineral Liberation Analysis	3-61
3.7.1	Introduction to Scanning Electron Microscope (SEM)	3-61
3.7.2	SEM method description	3-63
3.7.3	Introduction to Mineral Liberation Analysis (MLA)	3-64
3.7.4	MLA method description	3-65
3.8	X-ray Diffraction (XRD)	3-65
3.8.1	Introduction to XRD	3-65
3.8.2	XRD method description	3-67
3.9	Dielectric properties measurement	3-67
3.10	cylindrical cavity perturbation technique Introduction	3-67
3.11	Cylindrical Cavity perturbation method description	3-68
CHAPTER 4 – OIL AND WATER REMOVAL MECHANISMS		4-71
4. introduction		4-71
4.1	Drill Cuttings Sample Characterisation	4-73
4.2	Dielectric Properties	4-78
4.3	Nitrogen drying and microwave heating of drill cuttings	4-79
4.3.1	Experimental Setup	4-79
4.3.2	Results and Discussion	4-81
4.3.3	Nitrogen Drying	4-81
4.3.4	Microwave treatment of drill cuttings	4-87
4.3.5	Effect of Nitrogen Flow during microwave treatment	4-89
4.4	oil and water removal mechanisms during microwave treatment of drill cuttings	4-94
4.4.1	Experimental Setup	4-95
4.4.2	Experimental Configuration A	4-96
4.4.3	Experimental Configuration B	4-98
4.4.4	Experimental Configuration C	4-101
4.4.5	Results and Discussion	4-102
4.4.6	validation of Experimental configuration A	4-102

4.4.7	Quantification of Entrainment vs. Vaporisation	4-104
4.4.8	Investigation of oil vaporisation mechanisms	4-112
4.4.9	Effect of power density on extent of entrainment and vaporisation	4-116
4.4.10	Effect of sample type on extent of entrainment and vaporisation	4-124
4.4.11	Effect of nitrogen flow on extent of entrainment and vaporisation	4-137
4.4.12	Effect of applicator type on liquid removal mechanisms	4-141
4.5	Conclusion	4-147
CHAPTER 5 – CONTINUOUS MICROWAVE PROCESSING		5-149
5. introduction		5-149
5.1	Continuous pilot scale treatment of oily cuttings	5-152
5.2	General Experimental Setup	5-153
5.2.1	2.45 GHz pilot scale rig	5-153
5.3	Results and Discussion	5-155
5.3.1	Continuous Treatment of drill cuttings at pilot scale	5-155
5.3.2	Comparison of continuous and bench scale treatment	5-166
5.3.3	Effect of initial oil content on residual oil content and energy requirements.	5-172
5.3.4	Effect of initial water content on residual oil content and energy requirements.	5-178
5.3.5	Effect of particle size on oil removal	5-181
5.3.6	Variation in oil content distribution and removal with particle size	5-190
5.3.7	Variation in oil content distribution with particle size for different samples.	5-193
5.3.8	Variation in oil removal for different samples.	5-194
5.4	896MHz pilot scale rig	5-196
5.5	Results of 896 MHz Microwave RIG	5-197
5.5.1	Comparison of various rig setups.	5-199
5.6	Conclusion	5-201
CHAPTER 6 – THESIS CONCLUSION & FUTURE WORK		6-205
6.1	Oil and Water removal transfer mechanisms	6-205
6.2	Continuous microwave processing of drill cuttings at 2.45 GHz	6-207
6.3	Continuous microwave processing of drill cuttings at 896 MHz	6-208
6.4	Implications of Work on Industrial System Design	6-209
6.5	Future work	6-210
REFERENCES		6-212
APPENDIX 1 – ADDITIONAL CHARACTERISATION DATA		6-224
APPENDIX 2 – MICROWAVE SURFACE TEMPERATURE DATA		6-226
APPENDIX 3 – WEIGHT LOSS AND DRYING RATE DATA		6-229

LIST OF FIGURES

Figure 2.1 - Average depth of crude oil, natural gas and dry exploratory and developmental wells drilled (feet/well) over the past 60 years (Energy Information Administration, 2011).	2-6
Figure 2.2 - Electromagnetic Spectrum (Metaxas & Meredith, 1983).	2-14
Figure 2.3 - Interaction between microwaves and dielectrics using parallel capacitors as an example.	2-15
Figure 2.4 - Microwave heating mechanisms relative to the electromagnetic spectra.	2-20
Figure 2.5 - Microwave interaction with different types of material.	2-21
Figure 2.6 - Heterogeneous material containing two phases with different dielectric properties.	2-24
Figure 2.7 - Variation of moisture content with time and of the drying rate with time for a wet porous material.	2-36
Figure 2.8 - Illustration of different types of physically bound water.	2-40
Figure 2.9 - Variation of bulk dielectric loss of material with moisture content and temperature.	2-40
Figure 2.10 - Difference in liquid spread due to different wettability characteristics.	2-43
Figure 3.1 - Dean and Stark apparatus used for water content measurements (Dean & Stark, 1920).	3-49
Figure 3.2 - SOXHLET apparatus used for oil content measurements.	3-51
Figure 3.3 - Dionex ASE 200 apparatus used for oil content measurements (Dionex, 1999)	3-53
Figure 3.4 - Basic gas chromatography setup.	3-56
Figure 3.5 - Mass Spectrometer Setup.	3-57
Figure 3.6 - Scanning Electron Microscope (SEM) principle of operation and interaction with Sample.	3-61
Figure 3.7 - Diffraction of X-rays in a lattice with equally spaced ions/atoms.	3-66
Figure 3.8 - Setup used for measuring dielectric properties using the cavity perturbation method.	3-69

Figure 4.1 - Approach used for confirming oil removal mechanisms and quantification.	4-72
Figure 4.2 - SEM photograph of drill cuttings particles.	4-74
Figure 4.3 - De-agglomerated drill cuttings particle size distribution for Samples A, B and C.	4-75
Figure 4.4 - MLA analysis of samples A and B for particles of size range - 53+38 μm .	4-76
Figure 4.5 - XRD analysis of Sample A	4-77
Figure 4.6 - XRD analysis of Sample B	4-77
Figure 4.7 - Variation of dielectric properties of a drill cuttings sample B containing 3.7 ± 0.3 and 12.0 ± 0.8 wt% respectively.	4-78
Figure 4.8 - Setup for the nitrogen and microwave drying of oil contaminated drill cuttings using a multimode cavity of dimensions 425 (W) x 425 (L) x 545 mm (H).	4-80
Figure 4.9 - Variation of sample weight with time for Sample A.	4-82
Figure 4.10 - Sample weight loss vs. Time for Sample A.	4-83
Figure 4.11 - Variation of water content (wt%) with time (mins) for Sample A.	4-84
Figure 4.12 - Variation of oil content (wt%) with time (mins) for Sample A.	4-85
Figure 4.13 - Variation of counts with time (mins).	4-86
Figure 4.14 - Variation of sample weight with time for samples treated using microwaves at $720 \text{ W} \pm 18$ and a Nitrogen flow of 15 L/min and for samples treated using nitrogen only at 16°C at 20 L/min.	4-87
Figure 4.15 - Difference between vaporisation and evaporation mechanisms.	4-88
Figure 4.16 - Variation of residual oil content for drill cuttings samples treated at $720 \text{ W} \pm 18$ and a Nitrogen flow of 15 L/min and for samples treated using nitrogen only at 16°C at 20 L/min.	4-89
Figure 4.17 - Effect of nitrogen on oil removal during microwave treatment.	4-90
Figure 4.18a - Variation of oil content with nitrogen flowrate for Sample A treated at 720 W at 5, 15 and 25 L/min nitrogen @ 16°C .	4-92
Figure 4.18b - Hypothetical variation of oil content with increasing Nitrogen flowrate or Modified Reynolds Number vs. processing times.	4-93

Figure 4.19 - Detailed Investigation structure for Entrainment vs. Vaporisation experiments	4-94
Figure 4.20 - Configuration A Experimental Setup.	4-96
Figure 4.21 - Configuration B experimental setup.	4-99
Figure 4.22 - Configuration C experimental setup.	4-101
Figure 4.23 - Oil composition for Sample B feed sample, oil from the phase separator traps (Entrained – 1-2) and oil from the condenser section (Vaporised – traps 3-5) for Sample B treated at 490 W and 41 kJ.	4-103
Figure 4.24 - Variation of oil and water content vs. energy input for sample B treated using configuration A at 490 W and 16, 27 and 41 kJ.	4-105
Figure 4.25 - Measured and calculated total weight loss vs. Energy input for Sample B treated using configuration A at 490 W and 16, 27 and 41 kJ.	4-107
Figure 4.26 - Variation of weight loss due to vaporisation and entrainment with energy input for Sample B treated using configuration A at 490 W and 16, 27 and 41 kJ.	4-109
Figure 4.27 - Variation of oil and water percentages for %entrainment for Sample B treated using configuration A at 490 W and 16, 27 and 41 kJ.	4-111
Figure 4.28 - Variation of oil and water percentages for %vaporisation for Sample B treated using configuration A at 490 W and 16, 27 and 41 kJ.	4-112
Figure 4.29 - Sample C, 1.18 g/cm ³ , treated with a 2.2 kW VEIT steam generator.	4-114
Figure 4.30 - Sample C, 0.85 and 1.18 g/cm ³ , treated with a 2.2 kW VEIT steam generator.	4-115
Figure 4.31 - Total weight loss for Sample B treated using configuration A at 490 W and 3508 W at energy inputs of 16 to 58 kJ.	4-117
Figure 4.32 - Variation of power density for Sample B treated using configuration A at 490 W and 3508 W at energy inputs of 16 to 58 kJ.	4-118
Figure 4.33 - Variation of weight loss due to vaporisation and entrainment with energy input for Sample B treated using configuration A at 3508W and 17, 45 and 58 kJ.	4-119
Figure 4.34 - Variation of oil and water percentages for %entrainment for Sample B treated using configuration A at 3508W at 17, 45 and 58 kJ.	4-120
Figure 4.35 - Variation of water content with energy input for Sample B treated using configuration A at 490 W and 3508 W at energy inputs of 16	4-121

to 58 kJ.

Figure 4.36 - Variation of oil content with energy input for Sample B treated using configuration A at 490 W and 3508 W at energy inputs of 16 to 58 kJ	4-122
Figure 4.37 - Variation of oil and water percentages for %entrainment for Sample B treated using configuration A at 3508W at 17, 45 and 58 kJ.	4-123
Figure 4.38 - Variation of oil content with energy input for Sample C treated using configuration A at 419 W 15, 18 and 39 kJ and Sample B treated using configuration A at 490 W 16, 27 and 41 kJ.	4-124
Figure 4.39 - Comparison of calculated and measured weight loss for Sample C treated at 419 W and 0-39 kJ.	4-126
Figure 4.40 - Variation of measured weight loss due to vaporisation and entrainment with energy input for Sample B and C treated using configuration A at 490 and 419 W respectively, at energy inputs of 16-41 kJ.	4-127
Figure 4.41 - Drill cuttings samples B and C.	4-128
Figure 4.42 - Variation of oil and water percentages for %entrainment for Sample C treated using configuration A at 419 W respectively at 15, 18 and 39 kJ.	4-129
Figure 4.43 - Variation of oil and water percentages for %vaporisation for C treated using configuration A at 419 W respectively at 15, 18 and 39 kJ.	4-130
Figure 4.44 - Variation of measured weight loss due to vaporisation and entrainment with energy input for Sample C treated using configuration A at 419 and 3266 W respectively, at energy inputs of 15-52 kJ.	4-133
Figure 4.45 - Hypothetical diagram for the removal of oil and water vapours from a bed of drill cuttings of Sample C. The change in removal behaviour is shown for a sample treated at constant power but with increasingly longer durations/energy input.	4-135
Figure 4.46 - Variation of oil and water percentages for %entrainment for Sample C treated at 3266 W using configuration A at 19, 37 and 52 kJ.	4-135
Figure 4.47 - Variation of oil and water percentages for %vaporisation for Sample C treated at 3266 W using configuration A at 19, 37 and 52 kJ.	4-136
Figure 4.49 - Variation of percentage of entrainment vs. Vaporisation for nitrogen flowrates of 2 and 7 L/min at approx. 80 ± 5 °C.	4-138
Figure 4.49 - Variation of percentage of entrainment vs. Vaporisation for nitrogen flowrates of 2 and 7 L/min at approx. 80 ± 5 °C.	4-139

Figure 4.50 - Variation of oil and water percentages for %entrainment (a) and %vaporisation (b) for Sample B treated at 490 W and 41 kJ using a nitrogen flowrate of 2 and 7 L/min.	4-140
Figure 4.51 - Oil removal vs. Water removal for Sample B treated at 490 W and 16-41 kJ.	4-142
Figure 4.52 - Variation of % oil removed through entrainment with water removal (%) for Sample B.	4-143
Figure 4.53 - Variation of water and oil content with energy input for Sample B treated at 490 W and 508 W using Configuration A and B respectively.	4-144
Figure 4.54 - Oil removal vs. Water removal form Sample B treated using configuration A and B at 490 and 508 W respectively.	4-145
Figure 4.55 - Variation of water and oil content with energy input for Sample B treated at 490 W using Configuration A and 508 and 2550 W using Configuration B.	4-146
Figure 5.1 - Relationship between various variables affecting oil removal.	5-150
Figure 5.2 - Applicator configurations used in experiments.	5-154
Figure 5.3 - Complete diagram of pilot scale rig for the treatment of oil contaminated drill cuttings. Microwave system used to continuously treat oil contaminated drill cuttings. Microwaves propagate from both applicators at 2.45 GHz. a) Hopper, b) Screw feeder, c) Conveyor belt, d) Untreated drill cuttings (Oil rich) are fed into the microwave applicator, e) Chokes used to prevent microwave leakage, f) Chokes used to prevent cross-coupling, g) and i) Microwave applicators where the sample is subjected to a high power density, j) and k) Vapours and extracted fumes are removed to the extraction system, l) microwave treated (oil-lean) drill cuttings exit the cavity and are collected (m) at the end of the line for testing, n) and o) microwave inlet perpendicular to belt, p) nitrogen bottle.	5-155
Figure 5.4 - Variation of oil content with energy input for a sample containing approximately 3.7 wt% oil and 12 wt% water treated with microwaves.	5-156
Figure 5.5 - Separate heating of oil and water phases, compared to dry drill cuttings material using microwaves.	5-161
Figure 5.6 - Water content vs. energy input for a drill cuttings sample with an initial oil and water content of 3.7 ± 0.4 and 12 ± 0.8 wt% respectively.	5-163
Figure 5.7 - Variation of average, maximum and minimum bulk temperature with energy input (kWh/t) for drill cuttings samples containing 3.7 ± 0.4 and 12 ± 0.8 wt% oil and water content respectively.	5-164
Figure 5.8 - Variation energy input with temperature and equivalent dielectric properties at that temperature.	5-165

Figure 5.9 - Variation of oil content with energy input for drill cuttings with an oil and water content of 3.7 ± 0.3 and 12 wt% respectively, treated using the pilot scale and bench scale setup (See Chapter 4, Section 4.4.3).	5-167
Figure 5.10 - Power density (kW/kg of water/hr) vs. energy input (kWh/t) for drill cutting samples containing 3 and 12 wt% oil and water content respectively, treated using a bench scale and pilot scale setup.	5-170
Figure 5.11 - Variation of oil content with energy input for drill cuttings containing different initial oil content.	5-173
Figure 5.12 - Variation in oil removal requirement with energy input for drill cuttings Samples 1A to 1C.	5-174
Figure 5.13 - Variation of oil content with energy input for drill cuttings containing different initial water content.	5-178
Figure 5.14 - Hypothetical variation of oil removal with water content.	5-180
Figure 5.15 - Particle size distribution for Sample 2A.	5-182
Figure 5.16 - Variation of oil content with particle size for untreated Sample 2A.	5-183
Figure 5.17 - Calculated variation of particle surface area vs. particle radius for a fixed volume of 4.19 mm ³ .	5-184
Figure 5.18 - variation of oil content with energy input for Sample 2A as obtained through a bulk sample measurement, and as calculated by the sum of oil content contributed by each particle size.	5-186
Figure 5.19 - Variation of oil content with particle size for Sample 2A treated at 70 kWh/t.	5-187
Figure 5.20 - Variation of water and oil content with particle size for Sample 2A feed material.	5-189
Figure 5.21 - Variation of oil content with particle size for Sample 2A treated at 70-183 kWh/t.	5-190
Figure 5.22 - Variation of oil removal with particle size for Sample 2A treated at 70-183 kWh/t.	5-191
Figure 5.23 - Variation of oil content with energy input (kWh/t) for particles of size <1mm (Triangles) and agglomerates >1mm (Squares).	5-192
Figure 5.24 - Comparison of the variation in oil content with particle size for samples 2A-2C.	5-193
Figure 5.25 - Cumulative particle size distribution for Samples 2A, 2B and 2C.	5-194

Figure 5.26 - Oil removal vs. particle size for Samples 2A, 2B and 2C at 103 ± 7 kWh/t.	5-195
Figure 5.27 - Variation of oil content with energy input for sample treated using the 896 MHz system.	5-198
Figure 5.28 - Comparison of residual oil content with energy input for samples treated using the 2.45 GHz and 896 MHz continuous system.	5-200
Figure A.1 - XRD analysis of Samples A and B after glycolation.	6-224
Figure A.2 - XRD analysis of sample after heat treatment to 400 °C.	6-224
Figure A.3 - XRD analysis of sample after heat treatment to 600 °C.	6-225
Figure A.4 - Variation of surface T (°C) for water, oil and dried cuttings during MW treatment for 30 secs.	6-226
Figure A.5 - Sample B	6-227
Figure A.6 - Sample C.	6-228
Figure A.7 - Continuous processing cavity used for batch treatment of drill cuttings.	6-229
Figure A.8 - Variation of weight vs. time for Sample A treated at 490W in a multimode cavity setup as shown in Figure A.6	6-231
Figure A.9 - Online measurements vs. manual weighing measurements for samples treated at 180 seconds and an average power of 490 W.	6-231
Figure A.10 - Normalised weight vs. time for Sample 4 treated in a high power density multimode cavity at 490 W.	6-232
Figure A.11 - Variation of sample weight, water and oil content with time.	6-233
Figure A.12 - Drying rate for drill cutting samples treated at 490 W. Drying rate calculated based on Data presented on Figure A.10 and Figure A.6.	6-234
Figure A.13 - Drying rate for drill cutting samples treated at 490, 1000 and 1990 W. Drying rate calculated based on Data presented on Figure A.10 and Figure A.6.	6-235

LIST OF TABLES

Table 2.1 - Advantages and disadvantages of oil and water based fluids.	2-7
Table 2.2 - Oil content discharge limits imposed in different global regions.	2-8
Table 2.3 - Description of current commercial drilling waste treatment and disposal processes.	2-10
Table 2.4 - Advantages and disadvantages of each process available for the treatment and/or disposal of oil contaminated drill cuttings. Cost is provided in U\$ per metric tonne and based on three main sources (Bernier, et al., 2003; Puder & Veil, 2006; Piper, et al., 2005).	2-12
Table 2.5 - Microwaves as an alternative source for heating.	2-15
Table 2.6 - Dielectric constant, loss and Tan δ of some pure materials. (1) (Ellison, et al., 1996) (2) (Erle, et al., 2000), (3) (Westphal, 1997), (4) (Evans, 1997), (5) @ 400 °C and 4 GHz (Orzechowski, et al., 2006), (6) (Nelson, et al., 1989). With the exception of Kaolinite all measurements were at 20-25 °C and 2-2.5 GHz.	2-17
Table 2.7 - Different types of polarisation present during electromagnetic heating.	2-19
Table 2.8 - Attenuation factor for low and high loss materials.	2-21
Table 2.9 - Moisture removal mechanisms during drying.	2-37
Table 4.1 - Drill cuttings initial oil and water content.	4-74
Table 4.2 - Parameters used for the estimation of the modified Reynolds number for Nitrogen flowing through a packed bed.	4-91
Table 4.3 - Experimental conditions for samples B and C used in the determination of the extent of entrainment and vaporisation present during microwave processing of drill cuttings.	4-98
Table 4.4 - Experimental conditions for Samples B and C using configuration B.	4-100
Table 4.5 - Configuration C experimental conditions.	4-102
Table 4.6 - Sample weight, absolute water and oil content present in the sample and removed from the sample for different energy inputs (16, 27 and 41 kJ). The data applies for Sample B treated using configuration A at 490 W and 90 secs.	4-106
Table 4.7 - Values of variables used for the heat balance of Sample B and C treated at 490 and 419 W respectively (all data from (Perry &	4-132

Green, 1997) unless otherwise stated).

Table 5.1 – Replicated from Chapter 4 - Dielectric constant, loss and Tan δ of some pure materials. (1) (Ellison, et al., 1996) (2) Erle et al (Erle, et al., 2000), (3) Westphal (Westphal, 1997), (4) (Evans, 1997), (5) Orzechowski et al (@ 400 °C and 4 GHz) (Orzechowski, et al., 2006), (6) Nelson et al (Nelson, et al., 1989).	5-158
Table 5.2 - Power, flowrate, processing time, energy input and water content data for bench and continuous processing of cuttings.	5-169
Table 5.3 - Initial oil and water content of Samples 1A, 1B and 1C.	5-172
Table 5.4 - Initial oil and water content of Samples 1A, 1B and 1C.	5-178
Table 5.5 - Drill cuttings samples treated using microwaves at 2.45GHz and analysed at different particle size ranges.	5-181
Table 5.6 - Details of experiment conditions for samples shown in Figure 5.28.	5-199
Table A.1 - Power and treatment times used for the microwave treatment of oil contaminated drill cuttings with a high power multimode cavity.	6-230

CHAPTER 1 - Thesis Introduction

1. INTRODUCTION

The literature is divided between two main schools of thought regarding future oil demand (Dargay & Gately, 2010; Benes, et al., 2012). The first school of thought believes the world oil demand will continue to increase through to 2030, whereas the second school of thought believes oil demand has or will peak shortly, and will decrease over the next 2 to 3 decades (Zittel & Schindler, 2002; Miller, 2011; Kjärstad & Johnsson, 2009). The latter appears to have developed greater strength in the last few years, especially due to reduced investment and worsening financial conditions following the 2008 economic downturn. Nevertheless, both schools of thought rely on the continuing ability to supply oil when required, either through the development of adequate technology or through the discovery of new sources.

Previous research has hypothesised that future oil production levels are likely to remain similar to current levels and at best will decrease from 85 million barrels/day in 2007 to 50-70 million barrels/day in 2030 (Alekklett, et al., 2010). The decrease in production is primarily attributed to dwindling reserves in current onshore and shallow water wells. It is therefore proposed that the trend for enhanced oil recovery from offshore reservoirs will continue to increase (Sandrea & Sandrea, 2007). Additionally, there is expected to be an increase in the drilling of deeper offshore wells of higher complexity, resulting in significantly higher drilling costs. Deeper wells also produce a proportionally greater amount of drilling waste, which poses both significant cost and environmental issues.

The literature shows that for drilling operations in the North Sea approximately half the cost of drilling fluids is allocated to drilling waste management (Minton & McGlaughlin, 2003). In general, a significant portion of the cost of offshore drilling

waste management can be attributed to the disposal of oil contaminated drill cuttings. For example, for deep wells drilled in the Gulf of Mexico, drill cuttings disposal costs of >\$200,000/well were reported in the year of 1999 ((EPA), 1999). Therefore, with the potential increase in number of offshore wells and escalating costs of drilling offshore, cost reductions in waste management could become increasingly important in delivering oil cost effectively.

Part of the reason for escalating production costs in waste management can be attributed to tighter regulations, which limit significantly or eliminate completely the disposal of oily wastes into the sea. Strict offshore disposal guidelines (OSPAR, 2000) have been specified in the North Sea, which require the residual oil content present within the material to be limited to <1 wt% oil content. This requirement has forced companies to dispose of cuttings locally via re-injection (Veil, et al., 2003) or thermal desorption (Seaton, et al., 2006), or to ship the material to shore for further disposal (Canadian Association of Petroleum Producers, 2001). This can add additional cost to the >\$200,000/well figure previously quoted.

Re-injection is limited to platforms with the appropriate surrounding formations to allow retrofitting of the required equipment. In addition, leakage is possible both during and post injection and could have significant impact on the surrounding maritime environment. As a result, re-injection is cost effective in only a limited number of cases and does not provide a solution that fits all rigs. Thermal desorption systems, which can be used to treat and dispose of drill cuttings locally, do not currently provide an economically feasible solution. Other drawbacks include the heavy weight of the necessary equipment and large footprint requirements. Transportation to shore is often used as it can be the only feasible option, however, tighter onshore disposal regulations are coming into practice. In addition, transport of waste involves high numbers of crane lifts and long shipping distances, which pose a significant safety risk to both operators and the environment

In conclusion, there is a clear rationale for the disposal of drill cuttings offshore, eliminating transportation requirements. Treatment methods, such as thermal desorption, are highly preferable over re-injection based waste management systems for 2 reasons: (i) it provides an actual treatment to the waste therefore eliminating any associated hazards, (ii) can be retrofitted to a larger number of platforms as it is not formation dependent. However, current thermal desorption technologies have significant drawbacks, which limit their usefulness. Therefore, there is a clear rationale to develop a system, which is capable of operating more efficiently, safely and at a lower cost than the current solution. In order to compete with current conventional thermal desorption systems, the proposed new system would ideally be capable of treating at a feed flowrate of 1-5 tonnes per hour of oil contaminated drill cuttings with an energy consumption <200 kWh/t. This research builds upon previous work (Shang, et al., 2006) in order to explore this opportunity and further develop the understanding required to continue the development and implementation of commercial continuous microwave treatment of oil contaminated drill cuttings, as an alternative technology to the existing thermal desorption system.

CHAPTER 2 – Literature Review

2. INTRODUCTION

This chapter introduces the key concepts which underpin the subjects discussed in detail in this thesis. Also presented are more detailed reviews of published studies which are directly relevant to the work described in this thesis. The literature review is divided into the following sections:

1. *Drill cuttings* – provides an introduction into the processing of drill cuttings and a background review of current disposal methods; including advantages, disadvantages and approximate costs.
2. *Microwave heating* – details the basic theory behind both microwave heating and applicator design.
3. *Review of previous work* – provides a detailed overview of previous work on the microwave heating of drill cuttings.
4. *Review of other work* – provides a detailed overview of other work related to either an aspect of the experiments run in this project or useful in the analysis of the results obtained.

2.1 REVIEW OF OIL CONTAMINATED DRILL CUTTINGS

Drill cuttings are mixtures of rock fragments, which are generated during the drilling of oil wells. More specifically drill cuttings are heterogeneous agglomerates, which consist of a mixture of: (1) drilling mud and (2) rock formation (Al-Ansary & Al-Tabbaa, 2007; Khan & Islam, 2007).

2.2 DRILLING MUDS

Drilling muds are specific fluid formulations that perform a number of key functions during drilling including (Fink, 2003; Caenn & Chillingar, 1996; Gray & Darley, 1980): transporting cuttings from the bottom of the hole to the surface, keeping the drill bit cool and clean, reducing friction between the drill string and casing, maintaining the stability of the well, preventing fluid loss into the surrounding formation, preventing damage of the producing formation, well-logging for information acquisition and preventing any damage to the environment and personnel.

Drilling muds can be separated into three main continuous base fluid categories: gas based fluids, oil based fluids and water based fluids. A general composition of each of these muds is provided in the literature (Khan & Islam, 2007). Gas based drilling fluids use a continuous gas, air, mist or foam phase and can be used for drilling shallow wells in hard formations, low pressure reservoirs, in underbalanced operations or where drilling would result in high fluid losses. These fluids are only used where the volume of water and oil produced is expected to be small (Chilingarian & Vorabutr, 1981).

Water based fluids are the most frequently used type of drilling fluid (Caenn & Chillingar, 1996), and are generally used for drilling stable formations. Water based muds consist of a continuous fresh water or brine phase and a number of additives that are added to improve the performance of the mud by reducing fluid loss, increasing mud weight, improving temperature stability and increasing lubricity amongst others (Fink, 2003; Caenn & Chillingar, 1996). Over the past two decades a large amount of progress has been made in water based mud formulation, which is discussed in detail as a viable alternative solution to oil based fluids by a number of authors (Caenn & Chillingar, 1996; Cameron & Baroid, 2005; Dye, et al., 2006).

Despite this progress, synthetic and natural oil based fluids continue to be used in complex drilling operations due their high reliability and performance (Lee, 1998; Canadian Association of Petroleum Producers, 2001), and are likely to be used with greater frequency as a result of the current trend for the drilling of deeper wells (Figure 2.1). Oil based drilling fluids consist of a continuous oil phase and a dispersed fresh water or brine phase (Hudgins, 1994) and are typically used in drilling complex formations. Typical oil to water ratios for drilling in a completed well in shallower and deeper sections are: (1) 60/40 to 70/30 and (2) 75/25 to 85/15 (Devereux, 1998).

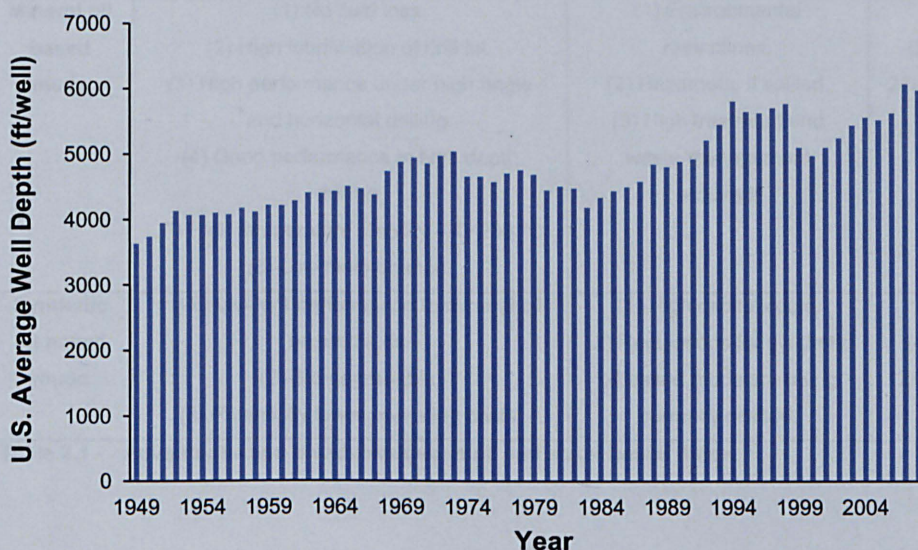


Figure 2.1 - Average depth of crude oil, natural gas and dry exploratory and developmental wells drilled (feet/well) over the past 60 years (Energy Information Administration, 2011).

The oil phase can be divided into two types: natural and synthetic oil. Natural oil initially referred to crude oil and later to components distilled from crude oil, for example diesel (Aromatic carbons<25% and PAH<2-4wt%). Later crude oil and diesel were replaced by mineral oils and linear paraffins, which provided higher performance and lower toxicity (Aromatic carbons<5-0.5% and PAH<2-0.001wt%) (Erickson, et al., 1988; Munro, et al., 1998). Synthetic oils (Aromatic carbons<0.5wt% and PAH<0.001wt%) are the latest type of oil base used and are compounds that result from chemical reactions of common hydrocarbon feedstocks and include olefins, esters and synthetic linear paraffins (Growcock & Harvey, 2005). Table 2.1

shows a comparison between the advantages and disadvantages of using oil and water based muds (Erickson, et al., 1988; Caenn & Chillingar, 1996).

Fluid Type	Advantages	Disadvantages	Cost
Water based muds	(1) Fast drilling in stable formations. (2) Drilling through salt formations. (3) Low damage to the environment. (4) Little treatment required. High temperature stability – T<205 °C	(1) Fluid loss to clay based formations. (2) Requires a large number of additives. (3) Increasingly tighter legislation on additives. (4) Worse performance at high angle and horizontal drilling.	Low-Moderate
Mineral oil based muds	(1) No fluid loss. (2) High lubrication of drill bit. (3) High performance under high angle and horizontal drilling. (4) Good performance in high depth drilling. (5) High temperature stability – T<230 °C (6) Low maintenance.	(1) Environmental restrictions. (2) Hazardous if spilled. (3) High treatment and waste management required.	High (250U\$-2500U\$/m ³)
Synthetic oil based muds	(1) Equivalent performance to mineral oil based muds. (2) Bio-degradable. (3) Potentially lower operating costs.	(1) High capital costs. (2) Regulations for synthetic oil based muds are being currently drafted.	High (750U\$-12500U\$/m ³)

Table 2.1 - Advantages and disadvantages of oil and water based fluids.

2.3 DRILL CUTTINGS MINERALOGY

The mineralogical composition of drill cuttings is entirely dependent on the location and formations present during drilling. Dhir *et al*, 2010 provided quantification, in weight%, of the different minerals and their corresponding compounds present in four different types of drill cuttings each obtained in different locations in the North Sea. The major components identified were Quartz, Barite, Calcite, Halite, Kaolinite, Muscovite, Albite and Siderite, although in three of the four samples, over 45% of the sample was composed of other non-identified amorphous phases. The bulk and individual particle densities varied between 0.79 and 1.05 g/cm³ and 2.52 and 2.78 g/cm³ respectively and were measured using BS EN 1097-3 and BS EN 1097-7. The potential for creating synthetic drill cuttings by adding materials that were either

identical to the composition previously stated or performed in the same manner has also been investigated previously (Al-Ansary & Al-Tabbaa, 2007).

2.4 DRILL CUTTINGS CONTAMINATION

Drill cuttings contaminated with water based muds, depending on the additives used, do not require any treatment before direct disposal into the sea (Neff, 2005). However, drill cuttings contaminated with oil based mud became a serious environmental issue, as the oil phase was found to be toxic to living organisms and the surrounding maritime environment when discharged directly into the sea (Jorissen, et al., 2009; Breuer, et al., 2004). These initial studies resulted in the re-formulation of muds with low toxicity mineral oil, plant derived oils and later on with synthetic oils. Although the toxicity of oil based muds has been significantly reduced in recent years, studies have still shown a considerable environmental impact if discharged into the sea without treatment. This has resulted in stringent legislation being employed whereby oil content discharge limits have been imposed throughout the world, as shown in Table 2.2 (Wait & Sharma, 2009; Bernier, et al., 2003). The discharge limits provided below are for mineral oil based muds only (synthetic oil based muds can be higher).

Discharge limit (wt%)	Country
>10 or Case- by-case	Argentina, Angola, Albania, Algeria, Bulgaria, China, Chile, Colombia, Congo,
	Malaysia, Indonesia, Ecuador, Cote D'Ivoire, Iran, Iraq, Kuwait, Oman,
	Panama, Peru, Qatar, Romania, Saudi Arabia, Senegal, Turkey, Ukraine
10	Egypt, France (Mediterranean Sea), Israel, Italy, Lebanon, Libya, Monaco,
	Morocco, Spain (Mediterranean Sea), Syria, Thailand, Turkey (Mediterranean Sea), United Arab Emirates.
1	Nigeria, UK (North Sea), Australia, Canada, Denmark, Finland, France,
0	Netherlands, Norway (Barents Sea), Portugal, Spain, Sweden.
	Azerbaijan, Kazakhstan (Caspian Sea), Belgium, Brazil, Ireland, Mexico, Russia, Trinidad, USA (Gulf of Mexico).

Table 2.2 - Oil content discharge limits imposed in different global regions.

These limits imposed on residual oil content have resulted in increased costs of drilling waste management and has encouraged research and development in this area in order to develop better performing, non-toxic drilling fluids as well as treatment and disposal processes that can be employed offshore to treat and/or safely dispose of these cuttings. Thus, the offshore treatment of drill cuttings is the main concern of this project, which aims to provide a treatment solution capable of treating oily cuttings to the required 1wt% oil content threshold imposed by OSPAR in the North Sea (OSPAR, 2000).

2.5 REVIEW OF CURRENT TREATMENT AND DISPOSAL PRACTICES

Current disposal practices can be divided into onshore and offshore solutions. Offshore solutions are limited to re-injection (Minton & Secoy, 1992) and thermal desorption treatment (Scomi Oiltools, 2010; MI SWACO, 2006; Halliburton, 2007; TWMA, 2010). Cuttings which cannot be disposed of offshore are shipped back to shore for appropriate treatment and disposal. Onshore solutions include: Landfill disposal, bioremediation (land treatment (Barker, et al., 1992) and composting (Ji, et al., 2004)), stabilisation and solidification (Al-Ansary & Al-Tabbaa, 2007; Leonard & Stegemann, 2010) and thermal treatment processes (Seaton, et al., 2006; Piper, et al., 2005). Less conventional methods and non-commercial solutions include: supercritical extraction (Elridge, 1996), liquefied gas extraction and salt caverns injection (Veil, et al., 1996; Veil, 1997). Table 2.3 provides a short description of each of these processes.

Process	Description
<i>Discharge</i>	The drill cuttings are released directly into the Sea. Discharge of oil contaminated drill cuttings is regulated by local authorities and legislation.
<i>Re-injection</i>	Drill cuttings ground into particles <100 µm are pumped into underground formations or wells which are no longer in use. Once in the formation or well, the cuttings are confined by a cemented casing. Waste leakages and migration can be a hazard.
<i>Landfill</i>	Drill cuttings are buried into sites that are designed and lined to contain hazardous waste. Hazardous liquids contained within the liquid may leach and migrate to the surrounding environment if the lining is not appropriately designed.
<i>Bioremediation</i>	Drill cuttings are biodegraded to CO ₂ and water using natural biologic process with specific bacteria. The constant supply of the correct bacteria, oxygen, nutrients, moisture content, salinity, pH and temperature are required for successful operation. Two main techniques are used: land treatment and composting.
<i>Stabilisation and solidification</i>	Drill cuttings are mixed with a cementing agent (fly ash, kiln dust, Portland cement or silica) forming stable blocks of material, which can then be either re-used as construction material or disposed of in a landfill.
<i>Thermal Treatment</i>	Thermal desorption vaporises the water and oil within the drill cuttings and recovers it by passing it through a condenser. Depending on the temperature ranges used thermal cracking of the oil may be present. Incineration uses high temperatures to completely oxidise the hydrocarbons present in the drill cuttings and carbonise the sample. Dust, oil and water vapours leaving the system may be hazardous.

Table 2.3 - Description of current commercial drilling waste treatment and disposal processes.

The reader is directed to the technical reports produced by the Canadian Association of Petroleum Producers, 2001 and by the International Association of Oil & gas Producers (Bernier, et al., 2003) for a more detailed discussion of each of the commercially available disposal methods. These reports provide a description of the types of drilling waste the method can be applied to, limitations and current developments, advantages and disadvantages, how performance is measured, factors which affect use and how it has been or is implemented globally. Argonne National Laboratory has also released a comprehensive report concerning the options, cost and availability of the various facilities for disposal and treatment of drilling waste (Puder & Veil, 2006). Table 2.4 summarises the key advantages, disadvantages and cost (excludes transportation) for each of these commercial methods.

Process	Advantages	Disadvantages	Cost (\$/t)
<i>Discharge</i>	(1) No specialist equipment needed. (2) Does not require shipment to shore - not affected by weather. (3) Low energy requirements. (4) Only requires few operators. (5) No storage requirements.	(1) Potential damage to the environment. (2) Potential costs incurred with site clean-up. (3) Continuous analysis of discharged material required.	N/A
<i>Re-injection</i>	(1) Does not require shipment to shore – not affected by weather. (2) Disposal of mixed wastes is possible. (3) Limited contamination of surface and ground water.	(1) Mistakes can lead to high cleaning-up costs. (2) Labour and energy intensive. (3) Equipment shutdown can halt drilling. (4) Limited by availability of suitable formations/wells. (5) Can impact stability of adjacent wells. (6) Harder to use with exploration wells. (7) Limited experience with drilling in floating platforms – technical limitations in deep sea. (8) Not a treatment.	130 (Onshore) 300 (Offshore)
<i>Landfill (Treated and Untreated)</i>	(1) Can accommodate any level of residual oil content.	(1) High transportation costs. (2) Limited space available. (3) Safety issues with transporting waste from offshore platform to disposal site. (4) Possibility of incurring high landfill clean-up costs in the future. (6) Not a treatment.	75 -210
<i>Bioremediation (Land farming and composting)</i>	(1) Treatment rather than just disposal. (2) Biodegradation of hydrocarbons. (3) Accepted as good practice in many areas. (4) Composting: little equipment, limited land, improved efficiency.	(1) Can have high transportation costs. (2) Potential damage to ground water and surrounding environment. (3) Limited to yearly seasons and ground temperature. (4) Long term – 60 days to 4 years. (5) Limited land space. (6) Stringent regulations (7) Safety and environmental issues with transport from offshore to onshore facility.	40
<i>Stabilisation/Solidification</i>	(1) Little equipment. (2) Reduced leaching of hazardous materials from waste to the environment.	(1) Labour intensive. (2) Large space requirements. (3) Volume of waste is increased.	100

<i>Thermal Treatment (Thermal desorption & Incineration)</i>	(3) High processing rates.	(4) Safety and environmental issues with transport from offshore to onshore facility. (5) Not a treatment.	110-250
	(1) Treatment rather than just disposal. (2) High processing rate. (3) Small footprint in comparison to other processes. (4) Recovers oil and water from cuttings for re-use. (5) Incineration provides a reduced, carbonized material with no residual waste.	(1) High air pollution. (2) Safety issues - vaporised oil and water are flammable and explosive. (3) Long cool down time required. (4) Reliability issues. (5) Cracking of hydrocarbons removed. (6) High labour cost. (7) Safety and environmental issues with transport from offshore to onshore facility. (8) Unfavourable public perception.	

Table 2.4 - Advantages and disadvantages of each process available for the treatment and/or disposal of oil contaminated drill cuttings. Cost is provided in U\$ per metric tonne and based on three main sources (Bernier, et al., 2003; Puder & Veil, 2006; Piper, et al., 2005).

2.6 OPPORTUNITY FOR MICROWAVE TREATMENT OF CUTTINGS

From the treatment solutions described on Table 2.4 it is clear that, apart from bioremediation and thermal processes, all methods essentially involve inerting the waste material and/or disposing of it in a contained manner. Disposal of contaminated cuttings without treatment always provides an increased risk of leaching to the environment and/or possible significant waste management costs in the future, as a result of cleaning up landfills or waste storage facilities. Thus, a process capable of treatment, whilst reducing waste and increasing the potential for drilling mud recycling is essential.

The large land and treatment time required when using bioremediation make it unsuitable as a primary waste disposal method, as it cannot be used effectively offshore due to space limitations. It can also have significant transportation costs and require long times to reach the site where the waste is processed, increasing the potential for hazards. Furthermore, even treatment of the material can be complicated

and add extra costs. These disadvantages are not present however, when using thermal incineration, and desorption in particular. Thermal desorption provides a unique treatment solution whereby oil and water can be removed from the cuttings, separated and potentially recycled back into the system, whilst providing an inert cuttings material, which could be theoretically used as a filler in construction work for example (Dhir, et al., 2010) or disposed off directly into the sea. However, the high operating cost, especially when used offshore, safety, reliability and operational (long cool down time, labour intensive) issues as well as high air pollution, prevent this method of treatment from becoming the main solution to treat drill cuttings. Also, current offshore systems are relatively bulky and can require a significant amount of retrofitting and floor space in offshore platforms leading to further increases in cost.

Microwaves have been investigated previously as an alternative process to conventional thermal desorption due to its selective and volumetric heating capabilities, faster heating and cooling rates, smaller footprint and capability of continuous reliable operation (Robinson, et al., 2009). A review of microwave heating theory and applications as well as previous work is presented in Section 2.7 of this thesis. The advantage of microwave heating arises from the way in which microwaves interact with and heat materials as well as the reduced size of the equipment used and required for processing.

2.7 MICROWAVE HEATING THEORY AND APPLICATION

Microwaves are electromagnetic waves in the frequency range of 0.3 to 300 GHz ($\lambda = 0.001 - 1\text{m}$), situated between infrared and radio waves in the electromagnetic spectrum (Figure 2.2), and are used in a variety of broad applications including, cellular phones, radar, telecommunications and heating (Thostenson & Chou, 1999).

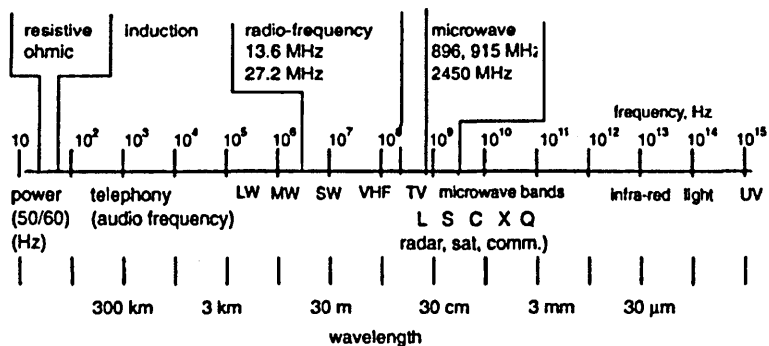


Figure 2.2 - Electromagnetic Spectrum (Metaxas & Meredith, 1983)

Microwave heating is normally operated at 0.915 and 2.45 GHz in the UK, under the Federal Communications Commission (FCC) for the Industrial, Scientific and Medical (ISM) processes (Metaxas & Meredith, 1983). Further guidance for other less used frequencies and standards in other countries is provided by the literature (Metaxas & Meredith, 1983).

2.8 THE USE OF MICROWAVES AS AN ALTERNATIVE HEATING SOURCE

The use of microwave heating as an alternative heating source has been employed successfully in a number of fields (Meredith, 1998), but has been largely restricted to small and pilot scale experiments (Kennedy, 1995), mainly as a result of high capital cost and the lack of understanding of how microwaves work (Reader, 2006; Schiffmann, 2006; Bäder & Schlunder, 1996). Detailed reviews encompassing the basics of microwave theory and processes are provided by Metaxas and Meredith, 1983, Bykov *et al*, 2001, and Thostenson and Chou, 1999. Table 2.5 shows some of the key applications and authors who have successfully demonstrated in lab scale experiments the potential of microwaves for heating.

Field	Authors
Chemical reactions	(Lidström, et al., 2001), (Kappe, 2002)
Ore processing/ Grinding/Leaching	(Al-Harabsheh & Kingman, 2004), (Scott, et al., 2008), (Pickles, 2009), (Yoshikawa, et al., 2007)
Waste treatment	(Remya & Lin, 2011), (Appleton, et al., 2005)
Sintering	(Oghbaei & Mirzaee, 2010)
Food drying/curing	(Tang, et al., 2002), (Orsat, et al., 2007),
Wood drying	(Vongpradubchai & Rattanadecho, 2009)

Table 2.5 - Microwaves as an alternative source for heating.

2.9 MICROWAVE FUNDAMENTAL THEORY

2.9.1 MICROWAVE INTERACTION WITH DIELECTRICS

Microwaves can be treated as a constantly alternating electromagnetic field, applying a series of alternating potentials as it passes through a dielectric material (typically an insulator). Assuming the alternating potentials can be represented locally by a single parallel plate capacitor, then charges present initially in a random state in the material realign or move towards their oppositely charged plates (Figure 2.3) leading to polarisation within the dielectric (Gabriel, et al., 1998).

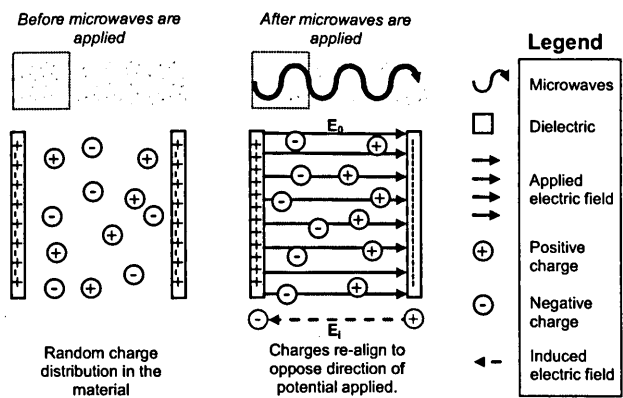


Figure 2.3 - Interaction between microwaves and dielectrics using parallel capacitors as an example.

This leads to charges within the material gaining potential energy, where the amount gained is dependent on how charges are initially distributed and present within the

structure of each material as well as the electric field strength applied. The potential energy gained by each charge through polarisation of the material can be quantified in relative terms by the dielectric constant (ϵ'). For an alternating field at a given frequency, the charges in either plate of the capacitor will alternate with time leading to a constant re-orientation of the charges within the material. Depending on the frequency of the applied field and the structure of the material between the capacitor plates, this can result in a lag between the applied field and the polarisation of the charges (Thostenson & Chou, 1999). This lag results from several collisions occurring during the realignment or movement of mobile charges, including dipolar molecules and ions, and/or vibration and distortion of lattice structures in materials where charges are fixed (Thostenson & Chou, 1999). These collisions and lattice vibrations result in the dissipation of the potential energy gained through polarisation into heat, and can be quantified by the dielectric loss of the material (ϵ''). The relationship between the dielectric constant and loss of a given pure material can be mathematically expressed by the complex permittivity (Equation 2.1).

$$\epsilon^* = \epsilon_0(\epsilon' - j\epsilon'') \quad \text{[Equation 2.1]}$$

Where ϵ^* is the complex permittivity ($\frac{F}{m}$), ϵ_0 is the permittivity of free space and is equal to $8.854 \times 10^{-12} \left(\frac{F}{m}\right)$ (Benenson, et al., 2001), ϵ' is the dielectric constant (dimensionless units) and ϵ'' is the dielectric loss (dimensionless units) (Metaxas & Meredith, 1983). For a given dielectric constant, the effectiveness of microwave heating can be compared between samples by calculating the $\tan \delta$, which is the ratio of dielectric loss to dielectric constant. Table 2.6 provides the dielectric loss, constant and $\tan \delta$ of some pure materials that are relevant to the work carried out in this thesis. For comparison purposes a material is considered a good microwave absorber for $\tan \delta \geq 0.1$ and a poor microwave absorber for $\tan \delta \leq 0.001$ (Bykov, et al., 2001). In addition, for more general applications, Kappe and Stadler, 2005 also provide a good summary table of the dielectric properties of key chemical solvents.

Material	ϵ'	ϵ''	$\tan \delta$
Water ⁽¹⁾	76.660	9.400	0.123
Mineral oil ⁽²⁾	2.400	0.180	0.075
Calcite ⁽³⁾	2.280	0.026	0.001
Sand (Dry) ⁽⁴⁾	2.910	0.005	0.002
Kaolinite (Dry) ⁽⁵⁾	1.91	0.12	0.063
Chlorite ⁽⁶⁾	7.200	0.126	0.018
Mica ⁽⁷⁾	8.690	0.091	0.011

Table 2.6 - Dielectric constant, loss and $\tan \delta$ of some pure materials. ⁽¹⁾ (Ellison, et al., 1996) ⁽²⁾ (Erle, et al., 2000), ⁽³⁾ (Westphal, 1997), ⁽⁴⁾ (Evans, 1997), ⁽⁵⁾ @ 400 °C and 4 GHz (Orzechowski, et al., 2006), ⁽⁶⁾ (Nelson, et al., 1989), ⁽⁷⁾ (Shang, et al., 2007). With the exception of Kaolinite all measurements were at 20-25 °C and 2-2.5 GHz.

2.9.2 MEASUREMENT OF DIELECTRIC PROPERTIES

As it is evident from Section 2.9.1 the measurement of dielectric properties of the materials present during heating is essential in predicting the efficiency of the process and how heating may be distributed through the different phases. The methods used for the measurement of dielectric properties are shown below. For a more detailed overview of the different methods the reader is referred to the literature (Venkatesh & Raghavan, 2005).

2.9.2.1 Cavity Perturbation

A small sample is inserted in a cylindrical resonant cavity of exact dimensions and the dielectric constant and loss are calculated from the shift in resonant frequency and absorption characteristics measured (based on standard TM and TE modes) (Venkatesh & Raghavan, 2005; Bengtsson & Risman, 1971). ASTM 2001 and D2520-90 are the used standards for solid and liquid sample measurements respectively. This method is suited for low bulk dielectric loss materials, homogeneous materials. The method has a high accuracy, requires little data and sample quantity, and can be used for temperature measurements.

2.9.2.2 Waveguide and Coaxial

The sample is placed either in a waveguide or measured through a coaxial probe placed in an annular sample. The dielectric constant and loss are calculated using the transmission line theory by measuring the phase and amplitude of the reflected microwave signal. In comparison to the cavity perturbation technique this method can be cheaper, and can be used with liquids and sludges. As this method typically uses a substantial amount of sample, a representative measurement of the rest of the sample can be more easily achievable in comparison to the cavity perturbation technique and open-ended probe. However, unlike the cavity perturbation technique, it is not possible to directly carry out measurements at temperature.

2.9.2.3 Open-ended Probe

Analogous in principle to the waveguide and coaxial transmission, but operates with an open-ended probe placed directly at the surface of the material. The operational advantages of this method are high accuracy for high loss materials and ease of carrying out the measurement. The main disadvantage arises from potential lack of reproducibility and limited capability if measurements with variations in temperature are required.

2.9.3 *MICROWAVE HEATING MECHANISMS*

As suggested in Section 2.9.1 microwave heating is likely to occur through two main mechanisms: (1) polarisation and (2) conduction. Heating through polarisation occurs mainly due to collisions and lattice vibrations or lateral movement resulting from the continuous reversal of the electric field during the propagation of microwaves through the material. However, in reality, several forms of polarisation mechanisms have been identified spanning the entire electromagnetic spectrum, which are summarised below in Table 2.7 (Kao, 2004).

Polarisation Mechanism	Description	Dominant Frequency (Hz)
<i>Electronic polarisation</i>	Electrons within the electron cloud of an atom initially present at a given arrangement with a given symmetry are displaced relative to their initial position due to an applied electromagnetic field.	10^{15}
<i>Atomic/ionic polarisation</i>	Atoms/ions are displaced relative to each other causing the lattice of the structure to vibrate.	10^{12}
<i>Dipole polarisation</i>	Molecules/ions with a permanent dipole re-orient their position according to the applied electromagnetic field. In an alternating field this causes constant movement and collision between adjacent molecules.	10^9
<i>Interfacial polarisation (Maxwell-Wagner)</i>	Charges present within a solid material, which are constrained locally or by the interface of difference phases in a multiphase material will also displace in accordance to the electric field leading to polarisation in the interfaces of the various material phases and/or voids.	10^4

Table 2.7 - Different types of polarisation present during electromagnetic heating.

Conduction is similar in principle to polarisation, where charges (electrons or ions for example) are free to move and are displaced within the material when an electric potential is applied. In a conducting material these charges are significantly more mobile within the material and are displaced for significant distances resulting in a number of collisions with immobile atoms or molecules within the material, leading to ohmic heating (Lidström, et al., 2001). The number and frequency of collisions is dependent on the nature of the material. Based on these polarisation mechanisms and conductivity losses, the dielectric loss for a pure material can be re-written to include all forms of polarisation and conduction (Equation2.2) (Kao, 2004; Metaxas & Meredith, 1983; Gupta & Wong Wai Leong, 2007).

$$\epsilon'' = \frac{\sigma_c}{\omega \epsilon_0} + \epsilon_e'' + \epsilon_a'' + \epsilon_d'' + \epsilon_{m-w}''$$

[Equation 2.2]

Where σ_c is the conductivity (S/m) of the material due to free electrons or ions, ω is the angular frequency (Hz) and ϵ_e'' , ϵ_a'' , ϵ_d'' , ϵ_{m-w}'' are the dielectric loss (Dimensionless units) due to electronic, atomic, dipole and interfacial polarisation respectively. Figure 2.4 shows the dominance of the various heating mechanisms with frequency in the heating of wet materials (Metaxas & Meredith, 1983; Kao, 2004; Roebuck & Goldblith, 1972). Attention is directed in particular to the frequency range of 10^9 Hz, as this is the frequency range in which conventional microwave heating operates, showing the dominating heating mechanism to be dipole polarisation of free and bound water (Mehdizadeh, 2010), although microwave heating will also occur to some extent through conduction and to a lesser extent interfacial polarisation.

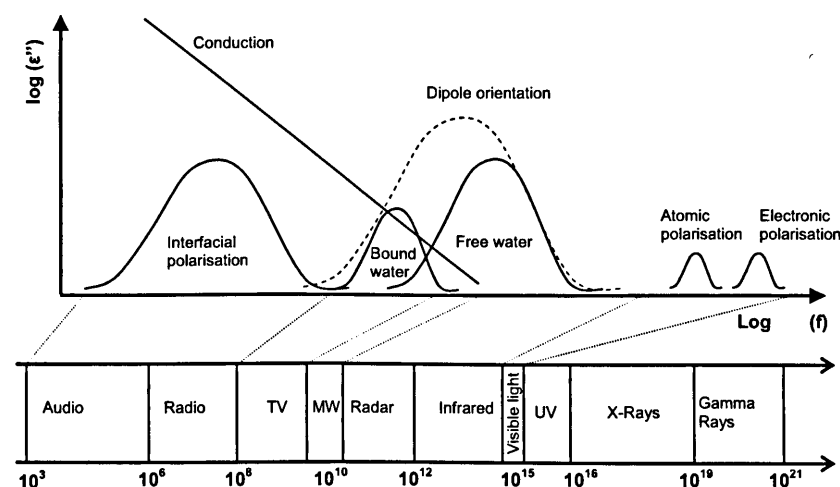


Figure 2.4 - Microwave heating mechanisms relative to the electromagnetic spectra.

2.9.4 ATTENUATION OF MICROWAVES DURING HEATING

The interaction between microwaves and a material is dependent entirely on its structure and composition (Bykov, et al., 2001), and will lie between two extremes, reflecting off the material's surface in a perfect conductor or propagate through the material without dissipation in a perfect insulator. For a material that is neither a perfect insulator or conductor, energy from the microwaves is lost to polarisation and

heating of the material, which causes the wave to attenuate as it propagates through the material (Figure 2.5).

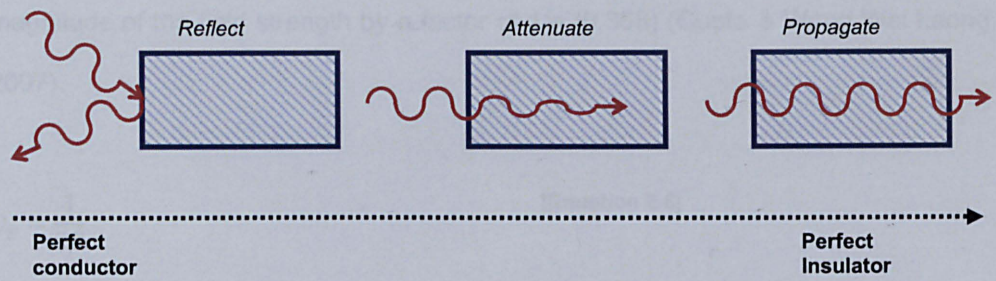


Figure 2.5 - Microwave interaction with different types of material.

The attenuation of microwaves within a phase can be quantified by the attenuation factor which is estimated from Lambert’s law and can be calculated for a pure material using Equation 2.3 (Ayappa, et al., 1991; Budd & Hill, 2011; Gupta & Wong Wai Leong, 2007).

$$\beta = 2\pi f \sqrt{\left(\frac{\epsilon' \epsilon_0 \mu' \mu_0}{2}\right) \frac{(\sqrt{1 + \tan^2 \delta} - 1)}{2}}$$

[Equation 2.3]

Where β is the attenuation factor (m^{-1}), f is the frequency (Hz), ϵ' is the dielectric constant, μ_0 is the permeability of free space ($\mu_0 = 4\pi \times 10^{-7} \text{ H/m}$), μ' is the permeability of the material, and $\tan \delta$ is the ratio of dielectric loss to constant. The permeability only needs to be accounted for materials which interact with the magnetic component of microwaves. For high and low loss materials β can be simplified as shown in Table 2.8.

Low loss ($\tan \delta \gg 1$)	$\beta = \sqrt{\pi^2 f^2 \mu_0 \mu' \epsilon_0 \epsilon''}$	[Equation 2.4]
High Loss ($\tan \delta \ll 1$)	$\beta = \pi \lambda_0 \left(\frac{\epsilon''}{\sqrt{\epsilon'}} \right)$	[Equation 2.5]

Table 2.8 - Attenuation factor for low and high loss materials.

Alternatively, the penetration depth (D_p in meters) (Equation 2.6) is often used as a comparative measurement of the attenuation of microwaves for materials and is defined as the distance from the surface of the sample required to attenuate the magnitude of the field strength by a factor of $1/e$ (0.368) (Gupta & Wong Wai Leong, 2007).

$$D_p = \frac{1}{2\beta} \quad \text{[Equation 2.6]}$$

2.9.5 SKIN DEPTH

The interaction between electromagnetic waves and conductors leads to the induction of high currents and a magnetic field at the surface of the material, flowing in an opposite direction to that of the electric field component. The induced current and magnetic field further induce subsequent layers, remaining parallel to the first induced layer but alternating in direction of flow at each layer. The skin depth measures the distance (m) by which the strength of the current induced at the surface are reduced to $1/e$ (0.368) of its initial value (Equation 2.7) (Meredith, 1998).

$$D_s = \sqrt{\frac{2}{\sigma_c \omega \mu_0}} \quad \text{[Equation 2.7]}$$

Where D_s is the skin depth (m). The applied currents lead to movement of free electrons within the material, and subsequently to ohmic losses due to collisions (Equation 2.8) (Meredith, 1998).

$$P_s = 0.5R|H_t|^2 \quad \text{[Equation 2.8]}$$

Where P_s is the power dissipated per surface area of conductor (W/m^2), R is the equivalent resistance (Ω), which is equal to $1/D_s \sigma_c$, and H_t is the magnetic field strength (A/m).

2.9.6 DISSIPATION OF MICROWAVE POWER INTO THE SAMPLE

The exponential attenuation of the electric field during the propagation of microwaves into dielectrics suggests that power is dissipated beyond the material's surface, leading to volumetric heating of the material. The dissipation of power per unit volume of material is quantified by the Poynting theorem, which equates the power dissipated into the material to the power stored in the electromagnetic waves and is presented in its simplest form by Equation 2.9 (Stratton, 2007).

$$P_d = \pi f \epsilon_0 \epsilon'' |E|^2 \quad \text{[Equation 2.9]}$$

Where P_d is the power dissipated into the sample (W/m^3), f is the field frequency (Hz), E is the field strength in V/m. P_d is alternatively known as the power density, and is a significant parameter during microwave processing as it directly dictates the rate at which the material is heated.

2.9.7 SELECTIVITY IN MICROWAVE HEATING

The microwave heating of heterogeneous materials containing multiple distinct phases is a complex matter, which arises due to the difference in dielectric properties of each phase (Bykov, et al., 2001). This was discussed in greater detail in other literature works (Asami, 2002), which investigated how this difference could be exploited to characterise heterogeneous systems. The work provided a number of models, which allow for the calculation of the combined bulk dielectric properties of various heterogeneous systems, based on their individual dielectric properties and the physical structure of the system in question. This effect was also described in detail during investigations of dielectric heating of foodstuffs (van der Veen, et al., 2004), where heating occurred at significantly higher rates in certain phases in comparison to other phases. Data obtained through modelling for power dissipation in materials containing multiple phases, showed significantly higher power density in

phases with higher dielectric constant and loss than surrounding phases with comparatively lower values of dielectric constant and loss (Ayappa, et al., 1991). The difference in heating rates due to differences in dielectric properties between phases being heated was confirmed by studies, which showed significant differences in the temperature distribution between phases with different dielectric properties, during the microwave heating of foods (Sakai & Wang, 2004). This effect has direct significance to the work being carried out here as the material in this case consists of a number of phases. Figure 2.5 illustrates this concept for a two phase material.

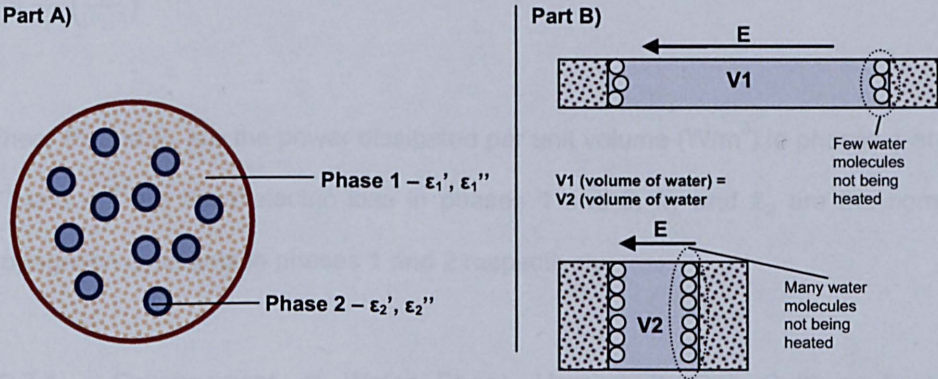


Figure 2.6 - Heterogeneous material containing two phases with different dielectric properties.

Figure 2.6 (Part A) shows a heterogeneous material which consists of two basic phases; a matrix which binds all phases together, and then another phase that is present throughout selected parts of the volume of the bulk material. Based on this concept the bulk dielectric constant and loss can be treated as a function of the loss and constant of each individual phase in the material (Equation 2.10) and can be estimated from the literature, or determined experimentally, for a given sample structure, size and composition (Asami, 2002).

$$\epsilon_{bulk}^* = f(\epsilon_1', \epsilon_1'', \epsilon_2', \epsilon_2'', \dots, \epsilon_n', \epsilon_n'') \quad [\text{Equation 2.10}]$$

Where ϵ_i' and ϵ_i'' are the dielectric constant and loss for a given phase 'i'. Similar to the dielectric constant and loss, the microwave power dissipated in each individual

phase is also dependent on the dielectric properties of each phase and the sample structure, as the distribution of phases within the material affect the field distribution, strength, reflection and absorption. The relationship for power dissipated in each phase is complex and will depend on the system being heated, although the relationship between the loss and the power dissipated in each phase still holds, with a higher loss leading to greater dissipation efficiency. For a two phase material, with phases less absorbing than water, the power dissipation in each phase can be estimated according to Equation 2.11 (van der Veen, et al., 2004).

$$\frac{P_1}{P_2} = \frac{\epsilon_1''}{\epsilon_2''} \left(\frac{|k_1|^2}{|k_2|^2} \right)^2 \quad [\text{Equation 2.11}]$$

Where P_1 and P_2 are the power dissipated per unit volume (W/m^3) in phases 1 and 2, ϵ_1'' and ϵ_2'' are the dielectric loss in phases 1 and 2, k_1 and k_2 are the complex propagation constants in phases 1 and 2 respectively.

2.9.7.1 Enhancement of Water Phase Heating in Drill Cuttings from an Electromagnetic Point of View

In a system consisting of a poorly absorbing material (e.g. a rock matrix) and water, optimum heating could be achieved by ensuring water was held within the microstructure of the material in long thin channels parallel to the direction of the electric field. This could lead to enhanced heating as a result of a reduction in the amount of water being depolarised at the interfaces between the rock and water phases. This is represented in Figure 2.6 (Part B).

2.9.8 MICROWAVE COMPONENTS AND APPLICATORS

The general microwave setup includes the following four components: (1) microwave generators, (2) power supply, (3) microwave transmission components and (4) microwave heating applicators.

2.9.8.1 Microwave generators

Microwaves are generated in vacuum tubes, of which three main types can be used; Klystrons, travelling-wave tubes (TWTs) and Magnetrons (Roach, 1995; Love, 1995). Klystrons are used where reliable operation at high powers and low frequency noise characteristics is required (Roach, 1995). These operating conditions come at a cost of low efficiency in terms of converting electricity to microwave power (<3% overall (Meredith, 1998)), high equipment cost and low operating life. Klystrons are composed of two main parts: (1) the beam system, which consists of a cathode (electron gun) generating a beam of electrons, which traverse through the RF circuit and are then received by a collector, (2) and the RF circuit itself, which consists of an input RF cavity, where a RF wave is introduced, followed by a series of resonant cavities and an output RF signal cavity which guides the modulated RF waves outwards. The reader is referred to further literature sources for a detailed description on the operation of Klystrons (Meredith, 1998; Chodorow & Susskind, 1964; Staprans, et al., 1973).

Travelling-wave tubes are of similar structure to the klystron, however, no resonant cavities are present and the interaction between the electron beam and the RF wave occurs along the beam path from the cathode to the collector, and, as a result, are not a resonant structure (Bagad, 2009). This allows for variable frequency RF waves to be generated increasing the operational bandwidth. TWTs are typically used where wide bandwidths and high frequency operation is required. A detailed introduction on TWTs is provided elsewhere in the literature (Tsimring, 2007).

Magnetrons are resonant generators, where typically a series of resonant cavities (anode) form a hollow cylindrical cavity with a cathode being positioned at the centre. Electrons emitted initially from the cathode are constantly redirected in a continuous circular motion between the cathode and anode by the appropriate use of a high strength magnetic field (Meredith, 1998). Magnetrons are used where reliability

(Kitagawa & Kanuma, 1986) and high conversion efficiency (>30-70%) (Sisodia & Gupta, 2005) from electrical power to microwaves is required, or where high power at a narrow, constant frequency range is needed. Generally, the manufacturing cost of magnetrons tends to be significantly lower than klystrons and TWTs (Meredith, 1998).

2.9.8.2 Transmission lines

Microwaves leaving the generator are typically transmitted from the magnetron to the load via cylindrical, or more commonly, rectangular waveguides, which are normally available in straight and 90° bend sections (Thostenson & Chou, 1999; Meredith, 1998). The propagation of microwaves in a waveguide is achieved through two modes: Transverse Electric (TE) or Transverse Magnetic (TM). In a TE and TM mode the electric and magnetic field propagate transversely to the direction of travel respectively. The transverse wave can have several maxima and minima depending on the mode of propagation, allowing for multiple possible mode patterns during transmission. The number of maxima and minima are typically denoted as a subscript, for example TE₁₀ or TM₁₀.

2.9.8.3 Circulators and Tuners

In addition to waveguides, circulators and tuners are also used for the protection of the system and maximisation of energy absorption respectively. Circulators are a specially designed waveguide containing three ports; one which is connected to the magnetron, one connected to the load and one connected to a water load. The circulator allows power leaving from the magnetron to be directed into the load, whilst, redirecting any reflected power to the water load avoiding damage to the magnetron. Tuners are added to further maximise absorption of microwave in the load by matching the impedance of the microwave generator to the load, where impedance is defined by the ratio of the electric and magnetic field components with respect to the direction of propagation (Das & Das, 2007). Of the various types of

tuners used, three stub and E-H plane tuners are the most common (Thostenson & Chou, 1999), and can be operated manually and automatically. Equation 2.12 provides the relationship between the power output by the generator, the power reflected and the power absorbed.

$$P_{abs} = P_{forward} - P_{reflected}$$

[Equation 2.12]

2.9.8.4 Applicators

Applicators are dimension specific cavities connected to the microwave generator via waveguides and allow for energy to be transferred from the microwaves to a load, resulting in heating, which causes a temporary or permanent change in the material's parameters and/or properties (Mehdizadeh, 2010). The shape and dimensions of the applicator directly affect the electromagnetic field distribution and intensity within the cavity and, thus, the sample. Although applicators can be custom made to meet the requirements of a given specific process, applicators can be divided into standard categories: resonant and a-periodic structures. In resonant structures microwaves form standing waves, which result from the superimposition of forward and reflected waves, whereas in a-periodic structures microwaves are absorbed by the load itself and subsequently by a dummy load. Different types of applicators, a general description and their advantages are provided below (Meredith, 1998; Metaxas & Meredith, 1983; Thostenson & Chou, 1999; Mehdizadeh, 2010; National materials advisory board, 1994):

Single Mode Applicators - Single mode applicators support the resonance of only one mode (Metaxas & Meredith, 1983; Thostenson & Chou, 1999). This type of applicator normally consists of a cylindrical cavity, with its radius restricted to approximately 1 wavelength, although different shapes and sizes are also possible (Mehdizadeh, 2010).

The field distribution in a single mode cavity is uneven and consists of a single “hot spot”, where the microwave field strength is high. High frequency purity required from the generated microwaves normally results in robustness issues during operation.

Multimode applicators - Multimode applicators support multiple resonating modes in rectangular cavities of various dimensions.

The performance of a multimode applicator is a function of: (1) the shape of the applicator, (2) the dimensions of the waveguide feeding microwaves into the cavity, (3) the dielectric properties of the sample and the location of the material in the cavity.

When the sample size is \gg penetration depth, operation is a-periodic, whilst the opposite leads to resonant operation. Cavity design is normally based on trial and error and experience. (Metaxas, 1993).

Axial Travelling Waveguide applicators – Microwaves propagate in the same direction or counterflow as the moving load usually conveyed by a belt. The actual cavity can be as simple as a given length of rectangular waveguide or can be more complex containing corrugations, or consisting of a different type of waveguide (helical for example) (Meredith, 1998).

Transverse Travelling Waveguide Applicators - Microwaves propagate perpendicular to the direction of motion of material. As a result microwave energy decays exponentially as it propagates away from the applicator inlet, heating non-uniformly. The occasional formation of standing waves due to reflections is also difficult to control (Meredith, 1998).

A more detailed overview of single and multimode microwave applicators is provided by Thostenson and Chou (Thostenson & Chou, 1999), whilst Meredith (Meredith, 1998) provides a comprehensive review of the different types of applicators available

and other additional components, including chokes, mode stirrers and movement of the load. Chokes are responsible for containing microwaves within the applicator, preventing leakage, whilst mode stirrers can be added to improve even heating of the sample by modulating the microwave signal into further modes.

2.10 REVIEW AND ANALYSIS OF GAPS IN PREVIOUS WORKS OF MICROWAVE TREATMENT OF OIL CONTAMINATED DRILL CUTTINGS

This section provides an overview of previous work carried out on the microwave treatment of drill cuttings, critically reviewing issues with the data and conclusions obtained thus far, highlighting any unanswered questions. Based on this, the main objectives of this thesis are presented in a concise manner followed by a further review of other literature works that have been used for support and developing a better understanding of the topics being investigated.

Previous work on the microwave treatment of oil contaminated drill cuttings has been carried out in two main areas: fundamental investigations (bench scale) (Shang, et al., 2006) and large scale processing of cuttings (Robinson, et al., 2009). Fundamental investigations determined some of the key variables affecting the treatment of the cuttings, including water content and flowrate of nitrogen, which has been consistently used as a sweep gas. Large scale processing concentrated on the performance and parameters affecting the treatment of drill cuttings at a larger scale, for example, power, treatment time and applicator configuration.

Bench scale investigations showed, to some extent, that initial water content had a significant impact on oil removal. Whilst the magnitude of nitrogen flowrate passing through the bed of cuttings did not appear to have an effect on oil removal, low temperature nitrogen was found to negatively affect oil removal. In larger scale tests, oil removal efficiency from drill cuttings was found to improve with increasing power and overall energy input. Finally, work carried out so far has suggested that oil is

removed through vaporisation and entrainment, however, specific experiments to determine the relative importance of each of these mechanisms is still lacking.

Although a good insight into the variables affecting the efficiency of microwave processing of oil contaminated drill cuttings was gained during work carried out to date, it is clear that a more rigorous, methodical approach could provide significant benefit when evaluating the fundamental effects of each variable in the oil removal process. For example, in the initial work, it is not entirely clear from the results shown how either sample mass or nitrogen impacted oil removal, as other parameters also changed simultaneously. As a result, the following questions still exist:

- How exactly does nitrogen affect the oil removal process and what is the effect of its flowrate during combined microwave and nitrogen processing? What is the effect of system configuration on this effect?
- Water directly affects oil removal. How are oil and water removal related and how can these be quantified? How are these related to the mechanisms of oil and water removal? Are the differences dependent on equipment setup or the feed conditions of samples processed?
- How exactly does the power and energy input affect oil and water removal. Is this relationship the same regardless of the applicator type?

More importantly, the main issue that is yet to be directly addressed is the actual confirmation and quantification of the mass transfer mechanisms that are present during oil and water removal mechanisms during processing. This is important for the following reasons:

1. It provides, from a mass transfer point of view, the ability to directly determine the factors that may directly affect the oil removal and energy input requirements during continuous, large scale microwave processing.

2. It allows for the collection equipment and extraction system to be designed appropriately in the future, maximising oil removal and minimising heat and mass transfer limitations from occurring after microwave processing.

Other key variables, which have not yet been investigated, are; sample temperature distribution, sample texture and particle size. Measurement of temperature allows for heat balances to be carried out, which can be useful in providing an alternative measurement of efficiency for the process. In addition, the measurement of surface temperature distribution, for example, can also help confirm which mechanisms of removal suggested are present.

Particle size is also important from a mass transfer and industrial point of view, as size could affect the mechanism of removal, or have a direct impact in the performance of a particular mechanism. This in turn could result in a higher oil removal efficiency for particles of certain size ranges.

Different sample textures tend to arise from differences in sample mineralogy and initial oil and water content. The difference in texture can have a significant impact in oil and water removal as it affects the structure of the material, with some cuttings samples consisting of a dry bed of porous solid particles and others a sludge.

From an industrial point of view, it is important to determine how large scale operation varies from bench scale operation and how the variables identified affect oil removal at larger scale processing. Results obtained at larger scale can then be compared to bench scale experiments in order to validate the initial observations regarding mass transfer mechanisms of oil and water removal. This should allow data obtained at bench scale to be used for calibration of larger scale processing. The robustness of larger scale operation also needs to be determined as most experiments carried out thus far have only used short treatment periods.

2.11 REVIEW OF CONVENTIONAL AND MICROWAVE HEATING

A further review of work using microwaves for heating or drying wet porous materials is presented, as these are directly relevant to this work. This section of the review is split into the following two main areas:

- (1) Review of conventional heat and mass transfer, paying particular attention to a review on basic drying principles, mechanisms and theoretical models.
- (2) Qualitative investigation of drying mechanisms during microwave heating of porous materials is reviewed, paying particular attention to heat and mass transfer for the microwave heating of porous materials. The effect of moisture content, material composition and structure, as well as particle size, on microwave heating and drying of porous materials is discussed in greater detail. Their influence on power and energy input requirements, according to the literature, are presented.

2.12 REVIEW OF CONVENTIONAL HEATING OF WET POROUS MATERIALS

2.12.1 HEATING MECHANISMS PRESENT DURING DRYING

Drying is defined as the removal of water and/or other solutes from a solid porous material (Ho & Udell, 1995) and can occur through two distinct mechanisms: evaporation and vaporisation (boiling). Note that, although these terms are interchangeably used by different authors in the literature, the differences between evaporation and vaporisation are made clear in this case and the terms are used strictly according to the definition provided herein.

In evaporation of a pure liquid the latent heat of vaporisation is overcome at a temperature below the boiling point (McAdams, 1926), whereby liquid molecules of high energy, present at the surface, collide with surrounding vapour molecules

generating enough energy to overcome latent heat barrier. Evaporation is dependent on the vapour pressure of the liquid, the pressure exerted on the liquid by the surrounding gas, vapour saturation of the surrounding atmosphere and the flowrate and temperature of the surrounding gas (if used).

Vaporisation, however, occurs at or above the boiling point temperature, where the liquid's vapour pressure becomes equal to the surrounding pressure leading to the rapid conversion of molecules from liquid to gaseous state, limited only by the energy provided locally in each portion of the liquid body to overcome latent heat. For liquids composed of multiple phases there is no single boiling point, but rather for a given mixture composition and pressure, a temperature where the combined vapour pressure of the various vapours present in the mixture at that temperature becomes equal to atmospheric pressure. For homogeneous mixtures, the composition of each component affects the final vapour pressure as shown by Equation 2.13 (Richardson, et al., 2002).

For an ideal mixture: $P_{total} = \sum x_i P_i^0$ [Equation 2.13]

Where P_{total} is the total pressure (bar) exerted in the system by the vapour and x_i and P_i^0 are the liquid mole fraction and partial pressure (bar) of component "i" respectively. However, in emulsions the vapour pressure of each pure component is used instead, regardless of the initial mixture composition (Equation 2.14). This results in lower boiling points than the boiling point of either pure component. Steam distillation takes advantage of this phenomenon to allow for water immiscible organic compounds to be boiled at significantly lower boiling points (Coker, 2010).

For an emulsion: $P_{total} = \sum P_i^0$ [Equation 2.14]

Vaporisation occurs throughout the volume of the liquid and is dependent on the temperature of the surface exerting the heating. The boiling of liquid can be achieved

through convection, nucleation and/or film heating (Richardson, et al., 2002). Nucleate boiling occurs when the temperature of the surface heating the liquid is close to that of the temperature of the liquid, and vapour bubbles form at distinct points of the surface rising through the volume of the liquid. Film boiling occurs when the temperature at the surface heating the liquid is significantly greater than that of the liquid, forming a film of vapour between the surface and the bulk of the liquid. A transition boiling mechanism occurs at surface temperatures intermediate to those in nucleate and film boiling.

For the purpose of this thesis drying through vaporisation is defined as the heating and removal of solutes through boiling. Evaporation is the removal of solutes at temperatures below the boiling point.

2.12.2 CONVENTIONAL HEATING DRYING PERIODS AND RATE

The drying of water from porous materials is characterized by three main periods (Sherwood, 1929; Sherwood, 1929; Mujumdar & Devahastin, 2004): warming-up, constant rate and falling rate (Shepherd, et al., 1938). These are categorized by the variation of water content (mass of moisture/mass of dry material) with time and drying rate (mass of weight loss/time) with water content as shown in Figure 2.7.

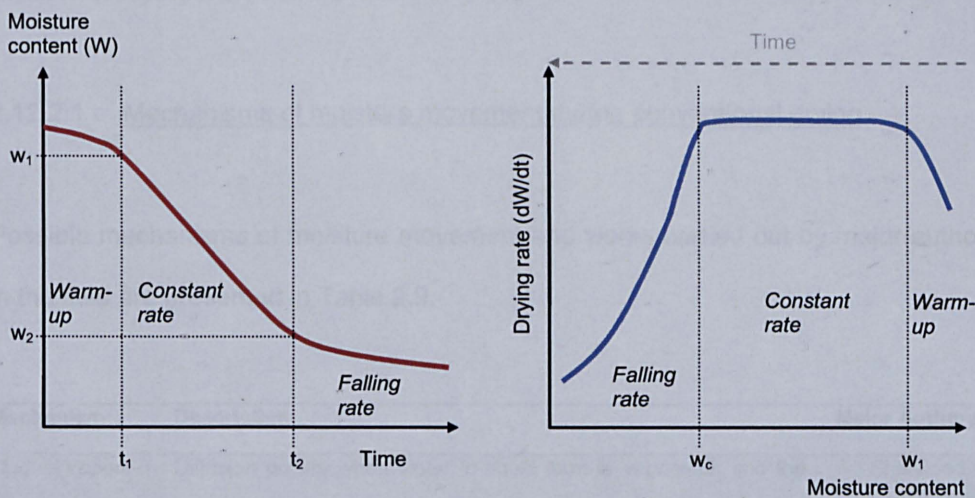


Figure 2.7 - Variation of moisture content with time and of the drying rate with time for a wet porous material.

In the warming up period the moisture content decreases slowly with time as the sample increases in temperature, resulting in an equivalent increase in drying rate with increasing time and decreasing moisture content. In the constant rate period the moisture content remains constant with time and moisture content, and is present whenever the moisture content of the material is greater than the critical moisture content.

The critical moisture content indicates the point above, which the moisture content at the surface of the particle/material ceases to be fully saturated. Below the critical moisture content the drying rate decreases with time and moisture content.

The falling rate is typically categorised by two regions (Moyers & Baldwin, 1997); the first region is characterized by removal of moisture mainly through areas of the surface that still remain partly saturated. As the water content decreases the removal becomes entirely dependent on mass transfer limiting the internal movement of moisture to the surface of the material. The second zone is characterised by moisture removal being fully dependent on internal mass transfer. Richardson *et al*, 2002 and Moyers and Baldwin, 1997, provide an in-depth review of quantitative and qualitative aspects of drying wet porous materials.

2.12.2.1 Mechanisms of moisture movement during conventional drying

Possible mechanisms of moisture movement and works carried out by major authors in the field are presented in Table 2.9.

Mechanism	Description	Major Authors
Liquid/Vapour	Diffusion occurs when water in liquid form is vaporised, and the	Sherwood
Diffusion	vapour moves in a random motion from areas of high to low	(Sherwood,

	concentration of moisture content. This can occur externally at the surface where water evaporates and leaves the material, or internally within the voids and pores present in the material, where water is vaporised and travels from within the material outwards. Thus, diffusion is a function of the thickness and moisture concentration distribution within the material.	1929; Sherwood, 1929; Sherwood, 1930) Newman (Newman, 1931) Tyrrell (Tyrrell, 1964)
<i>Capillary flow</i>	Internal moisture movement is governed primarily by capillary forces and gravity, where attractive intermolecular forces between the liquid surface and the internal pore surface of the material lead to liquid flow and movement. Capillary moisture movement is a function of capillary forces, pore/void size and gravity only.	Ceaglske and Hougen (Ceaglske & Hougen, 1937)
<i>Evaporation- condensation (Temperature gradient driven flow)</i>	Vapour diffusion can occur at a faster rate in the presence of condensable vapours and liquids in porous material due to capillary and thermal gradient effects occurring locally. These can be further improved if a gradient in vapour concentration and temperature is present in a macro scale. Vapours formed within the pore due to evaporation diffuse from local high temperatures to low temperatures. As the vapour contacts liquid within the pores, it condenses resulting in a momentum transfer through the liquid body, and subsequent evaporation at the other end.	Gurr <i>et al</i> (Gurr, et al., 1952),

Table 2.9 - Moisture removal mechanisms during drying.

2.12.2.2 Mathematical models used for predicting drying in wet porous materials

A significant amount of work is present in the literature regarding the prediction of moisture content distribution, drying rates and temperature distribution through numerical combined heat and mass transfer models. The majority of models have been designed to estimate the drying characteristics of moisture from rigid porous materials, and are based on one or more of the mechanisms of moisture movement previously described in Table 2.9 (Stangle & Aksay, 1990; Berger & Pei, 1973) as well as general vapour/liquid continuity equations (Whitaker & Chou, 1983). Complex models capable of accurately predicting momentum, heat and mass transfer and chemical reactions in a disordered porous medium are also presented in previous work (Stangle & Aksay, 1990).

2.13 REVIEW OF MICROWAVE HEATING OF WET POROUS MATERIALS

Meredith, 1998, Jones and Rowley, 1996, provide a general overview of microwave and radio frequency (RF) drying of porous materials and their applications. These works investigate some of the key variables affecting the microwave heating and drying of wet porous materials, including:

1. *Moisture content* – the type, purity, quantity and distribution of water content within a porous material significantly affects the bulk and local efficiency of microwave heating of the material, in particular in cases where the dielectric constant and loss of water is significantly higher than other phases present.
2. *Material structure* – the structure of the material being heated can limit internal moisture movement from within the material to its surface. Porous structures, which are relatively open, containing little tortuosity (textiles for example), impose little to no mass transfer limitations during drying. Materials where the pore structure is significantly more complex, such as clays and wood, can cause significant mass transfer limitations, leading to changes in internal pressures, temperature and physical properties of the material.
3. *Power* – the power applied and absorbed by the material determines the amount of energy being dissipated per second. For a given volume this provides the power density which is an important parameter in determining the heating rate during processing.
4. *Energy* – the energy input is the overall amount of energy supplied to the material over the course of treatment, and can be estimated by integrating the power applied and/or absorbed over time. The absolute energy used by the system can be estimated based on the power applied, whereas the effective energy absorbed by the material can be calculated from the power absorbed.

2.13.1 THE EFFECT OF WATER TYPE AND CONTENT IN MICROWAVE HEATING OF POROUS MATERIALS

Water can exist in two forms in porous materials: free and bound. Different definitions of bound and free water are used by different authors (Meredith, 1998; Richardson, et al., 2002). In this case the following definitions are used:

1. *Free water* is liquid water that is directly influenced by gravity, free to diffuse, or move within larger pores of materials, or water that is present at the surface of the particles comprising the material. **(Richardson, et al., 2002).**
2. *Bound water* can be divided into two further types. Physically bound water (interstitial water) is water that is adsorbed in the internal surface of the pores, retained in small capillaries or between layers of atoms making up the solid (Figure 2.8) **(Saarenketo, 1998)**. Chemically bound water (constitutional water) is water that is part of the chemical structure of the solid material. **(Harris, 1972).**

In water wet porous materials, where the dielectric properties of water are significantly greater than in the surrounding phases, the absorption of microwaves becomes a function of the moisture content and how the water is held within the material. As bound water is physically more restricted than free water (Cosenza & Tabbagh, 2004), the bulk dielectric loss of the material decreases with a decreasing moisture content, reducing the efficiency in which microwave energy is absorbed and dissipated as heat in the water phase (Meredith, 1998). Figure 2.9 shows the relationship between the bulk dielectric loss of the material with moisture content and temperature (Perkin, 1983).

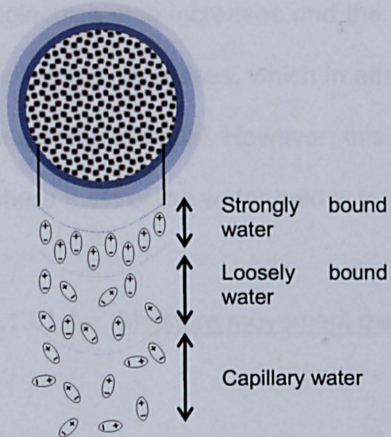


Figure 2.8 - Illustration of different types of physically bound water.

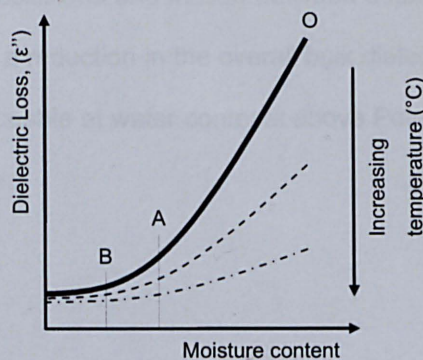


Figure 2.9 - Variation of bulk dielectric loss of material with moisture content and temperature.

In segment OA the majority of the water content present is held as free water and the dielectric loss of the material decreases linearly with decreasing moisture content and increasing temperature. At point A the critical moisture content is reached and dry patches begin to appear at the surface of the material, where the majority of the remaining water shifts from being free to bound. As drying progresses and the moisture content further decreases to point B, the surface of the material becomes dry and all internal moisture left is tightly bound either physically or chemically.

This reduction in dielectric loss due to bound water is a result of the limited mobility present in bound water molecules, and results in a decrease in microwave energy dissipation in the form of heat. During physically bound water removal, the energy input increases significantly as a result of an increase in unbinding energy requirements for removal to occur and more effective heat losses from the water phase to surrounding phases through conduction. In the case of chemically bound water, even higher temperatures and levels of energy input are required; for swelling clays, such as Kaolinite, dehydroxilation temperatures often in excess of 400-500 °C need to be reached before any further water removal occurs (Yeskis, et al., 1985; Frost & Vassallo, 1996).

The effect of temperature on the bulk dielectric loss of a water wet porous material is also shown in Figure 2.8. As the temperature increases the space between water

molecules also increases and the number of collisions and friction between adjacent molecules decreases, which in effect leads to a reduction in the overall bulk dielectric loss of the material. However, this is only noticeable at water contents above Point B, where most of the water held is in its free state.

2.13.1.1 Moisture movement mechanisms

Moisture removal mechanisms during microwave heating of porous samples have been investigated in detail in the literature (Perkin, 1983). Most heat and mass transfer models of microwave heating of porous materials have been developed to estimate moisture content, temperature and local pressures of food materials, wood and rigid porous structures such as bricks. Two common mechanisms have been identified throughout all microwave heating and drying works investigated:

1. *Pressure driven mechanism* – unlike conventional heating methods, microwaves heat the material volumetrically and are capable of generating vapour at fast rate internally. This increases the pressure locally, and results in several pressure gradients from within the material outwards, which increase the rate of liquid removal and drying.
2. *Liquid expulsion* – At higher liquid saturations, internal pressure causes a further removal mechanism whereby liquid is physically driven to the surface due to pressure exerted by the internally generated vapour. This liquid may be moisture situated nearer the surface, or moisture which has been vaporised internally, but condensed as it approached the surface of the material, which is significantly cooler than the core. This can cause build up of liquid at the surface of the material, limiting the overall mass transfer significantly.

These mechanisms directly impact the drying rate curves and periods, resulting in multiple drying rate maxima with moisture content, rather than the smooth

relationship observed during conventional heating. These less predictable drying curves result from power being applied constantly and the non-homogeneous drying characteristics during microwave heating of wet porous material. Constant shifts in removal mechanisms observed throughout the entire drying operation, normally cause the drying rate to increase and decrease throughout the entire drying period, although the overall trend of decreasing drying rate with moisture content is still followed in most cases.

It is important to note that the work discussed above mostly investigated the drying behaviour of water alone, and may differ significantly from cases where more than one solute is being heated and removed. Examples of such applications may include: (1) the removal of hazardous substances from soils/waste during microwave treatment, (2) heating and drying of food materials containing multiple mobile phases (oily foods for example), (3) drying of porous pharmaceutical powders, which may contain water as well as other solvents. As a result, there is a clear gap in the literature regarding the removal mechanisms of more than one solute during heating and drying, which needs to be addressed if systems are to be designed appropriately. Studying these systems can also allow for the adjustment of existing heat and mass transfer models to predict results more accurately.

2.13.1.2 Effect of material composition and structure on microwave heating

The material composition of porous materials can directly influence the efficiency of bulk and selective heating. The effect of multiphase materials on the bulk and local dielectric properties have been previously discussed in Section 2.9.7, in this Section the following additional key points are addressed:

1. Influence of material composition on water content retention
2. Influence of material structure on mass transfer

Effect of material composition on water content retention - The material composition directly determines the wettability of the material and how the material holds moisture content within its structure. Wettability is a measure of how much a liquid spreads in a given surface, which is directly related to forces of attraction between the surface and the fluid (Ahmed, 2001). Strong attractions between the surface and the fluid lead to a high spread area and strong adherence, whilst strong repulsion results in the fluid taking a shape tending towards a sphere, which gives the minimum amount of contact with the surface (Figure 2.10)

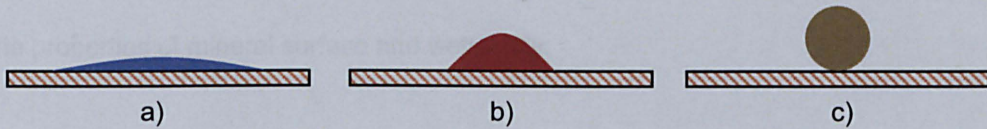


Figure 2.10 - Difference in liquid spread due to different wettability characteristics.

The surface material in Figure 2.9 is hydrophilic, which results in a high angle of spread and good surface adherence when water is in contact with the surface. A liquid, which is to some extent polar, or has some polar contents in it, is represented by b) and still spreads over the surface but to a lower extent in comparison to a). c) represents a liquid that is entirely non-polar and beads when in contact with the surface. In a rock composed of several mineral phases, containing water and oil there are four different states of wettability (Donaldson & Alam, 2008):

1. *Water-wet systems* – is the case where water occupies >50% of the materials surface. All small pores and voids are occupied by water. The surface of the larger pores and of the particle is also covered by a film of water, as long as the sample is saturated enough. If oil is present, then at high saturations it is present as globules in larger pores within the water phase or above the film of water. At lower saturations it can occupy regions where minerals are hydrophobic or surfaces in larger pores.
2. *Fractionally-wet systems* – there is no clear particular trend in the wetting of surface in these systems. Minerals which are both water and oil wet are

present randomly and at sufficiently high quantities, such that wettability is dependent on the exact location within the material.

3. *Mixed-wet systems* – in these systems the small pores are wetted by water, whereas the larger pores are wetted by oil.
4. *Oil-wet systems* – is the exact opposite of water-wet systems, where the roles of oil and water are reversed.

No particular mineral is more or less prone to being water or oil wet, and local conditions and components present within the water and oil can significantly change the properties of mineral surface and wettability.

Effect of material structure on mass transfer – The internal pore and void structure can have a significant effect on mass transfer during drying (Zhang, et al., 2010). The tortuosity and permeability are two parameters that are indicative of the ease in which fluids can flow through the material (Wilmanski, 2010; Ahmed, 2001). The tortuosity is defined by Equation 2.15 below.

$$\tau = \frac{L_{actual}}{L} \quad \text{[Equation 2.15]}$$

Where $L_{effective}$ is the actual effective distance between two points within the porous material and L is the linear distance between the two points. Thus, the higher the tortuosity value, the greater the actual path length the vapour and liquid need to travel before leaving the sample and the greater the resistance to mass transfer.

The inherent initial structure of the material provides a good estimation of how much resistance to mass transfer is present during drying, but does not account for changes in structure during drying and its effect on the drying mechanisms and rate. Although much of the modelling work is carried out in rigid bodies, many drying and heating processes occur in materials that can change significantly with drying time. For non-rigid body porous materials this can impact the tortuosity and structure

significantly, directly affecting the pore network and consequently the drying rate. The change in porous structures due to various drying techniques, for example conventional air drying, microwave drying, vacuum drying, osmotic dehydration and freeze drying, has been investigated in detail in the literature (Krokida & Maroulis, 2000).

2.14 CONCLUSION

The decreasing number of easily accessible oil reserves has led to more complex offshore deep-sea drilling programs, which require increasingly greater depths and higher angles to be drilled. These drilling conditions often require the use of oil based muds, which provide the operators with enhanced control, overall reduced down time and higher drilling efficiency. However, this leads to the contamination of drilled rock fragments, drill cuttings, with the base oil present in the mud, which is required by law to be removed below 1 wt% in the North Sea before any offshore disposal can take place. Current offshore and onshore waste management solutions are becoming increasingly un-economical to run, resulting in a significant commercial opportunity for the development of a system that can treat cuttings offshore cost effectively.

Microwaves provide fast heating rates selectively and volumetrically overcoming heat transfer limitations present in processes heated conventionally. Microwaves have, so far, been shown to be a potential alternative process to conventional thermal desorption systems at bench and pilot scale tests. However, the understanding of the mass transfer mechanisms present during the oil and water removal is currently lacking and is necessary if the process is to be operated, designed and optimized to deliver optimal performance at larger scale.

Currently the literature hypothesises that oil and water are removed through evaporation, vaporisation and entrainment, with experiments so far supporting this hypothesis. The primary objective of this thesis is to confirm the existence of these

mechanisms and determine and quantify the extent of each mechanism during microwave heating of drill cuttings. It is also clear that understanding how these mechanisms change with different operating parameters and sample properties is necessary for future optimisation and design of the system.

Other work in the area of conventional and microwave drying and heating of saturated materials was investigated and provides a starting point for the qualitative comparison of removal mechanisms. However, work presented in the literature has often concentrated in drying of single solutes, and descriptions of the drying of multiple solutes from heterogeneous material is lacking in the literature. As a result of this, direct comparison between mechanisms observed in literature cannot be applied in this case, without some degree of bias. Ultimately, this work aims to provide a significant advancement in the understanding of heat and mass transfer of oil and water from drill cuttings during microwave treatment, as well as aiding in the overall progress of understanding microwave heating and drying of multiple mobile phases in complex multiphase porous materials.

2.15 THESIS AIMS AND OBJECTIVES

The main aim of this thesis is to determine the mass transfer mechanisms governing oil and water removal during microwave processing. This should allow for improved interpretation of results obtained at pilot scale, leading, potentially, to the redesign of future system iterations. The key objectives are as follows:

- Determine and quantify the main oil and water removal mechanisms during microwave processing of drill cuttings.
- Continue previous work to determine key variables affecting operating efficiency at pilot scale.
- Investigate microwave processing of drill cuttings at 896 MHz

CHAPTER 3 – Analytical Techniques

3. INTRODUCTION

This chapter provides a detailed description and review, where appropriate, of the methods used repeatedly throughout this work; typically in the characterisation of a sample before and/or after treatment. The following methods are covered:

(1) Drill Cuttings liquid content and composition analysis:

- a. Water content measurements – Dean and Stark Method.
- b. Oil content measurements – Accelerated Solvent Extraction Method.
- c. Oil composition – Gas chromatography and Mass Spectrometry.

(2) Drill cuttings particle analysis:

- a. Scanning electron microscope (SEM).
- b. X-ray Diffraction (XRD)
- c. Mineral Liberation Analysis (MLA)
- d. Deagglomeration of oil contaminated drill cuttings.
- e. Sieving :
 - i. Deagglomerated particles
 - ii. Agglomerated particles.

(3) Dielectric property measurements

3.1 DRILL CUTTINGS LIQUID CONTENT AND COMPOSITION ANALYSIS

This section describes the method used for determining the water and oil content of treated samples. It also describes the method used for the measurement of the composition of the oil extracted from the drill cuttings. In addition, a review of issues identified with the measurement method and actions taken to minimise these issues is presented where necessary.

3.2 WATER CONTENT MEASUREMENTS

3.2.1 INTRODUCTION TO DEAN & STARK METHOD

The method used to measure the water content of oil contaminated drill cuttings is that proposed by Dean and Stark (ASTM D-95) (Dean & Stark, 1920). The method was primarily developed to determine the water content in petroleum and organic emulsions, and works through two main principles: (1) distillation and (2) gravity settling. A water immiscible solvent, toluene for example, is brought to its boiling point and penetrates through the water-organic emulsion, distilling the water. The water and toluene vapours are then re-condensed back into a vertical trap and separate over time, leading to water and solvent layers, which can be measured from the volumetric markings in the trap.

3.2.2 METHOD DESCRIPTION

Following the principle described above, drill cuttings samples were first weighed (around 30-60g) and placed in a round flask (sample holder). Toluene (CAS #108-88-3) was then added until the entire sample was submersed, and then brought to its boiling point, passing through the sample vaporising the water. The water/toluene vapour was then condensed and held in a graduated trap placed at the bottom of the condenser. Due to immiscibility and difference in density (approx. 1000 kg/m^3 vs. 870 kg/m^3) water sunk to the bottom of the trap, whilst toluene formed a layer at the top (Figure 3.1). The volume of water collected was then monitored with time (approximately every hour), and once the volume remained constant over a period of 2 consecutive hours, the final reading was taken. Typical running times required for measurement were between 5-8 hours.

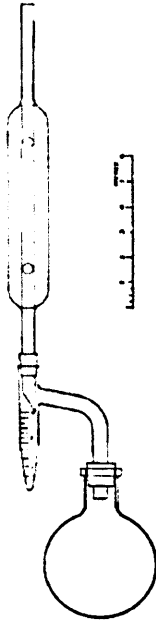


Figure 3.1 - Dean and Stark apparatus used for water content measurements (Dean & Stark, 1920).

The volume of water collected can be directly converted to a mass, as the density of water between 10 – 15 °C can be approximated to 1 kg/dm³. The overall water content, on a weight basis, is then given by the mass of water calculated from the trap divided by the initial sample weight as shown by Equation 3.1 below.

$$x_{H_2O}(wt\ frac.) = \frac{V_{H_2O}(ml) \times \rho_{H_2O}(g/ml)}{M_{sample}\ (g)} \quad \text{[Equation 3.1]}$$

Where $V_{H_2O}(ml)$ is the volume of water collected in the Dean and Stark trap, $\rho_{H_2O}(g/ml)$ is the density of the water, approximated to 1 g/ml in this case, and $M_{sample}\ (g)$ is the mass of the drill cuttings sample initially placed in the sample holder flask. The accuracy of this method has been reported in the literature to be in the range of ± 0.1 wt% (Dean & Stark, 1920).

3.2.3 METHOD ANALYSIS

Two issues were identified in preliminary experimental runs with the Dean & Stark method, and were also reported in the literature. The issues and the actions taken to minimise them are described in detail below.

Residual water droplets present within the rest of the test equipment – as water is vaporised and re-condensed some droplets inevitably remain in the condenser walls or in the return section of the trap. This volume of water not initially collected in the trap was minimised by allowing the apparatus to cool for a period of 1 hour and then by gently tapping the condenser, which led to droplets falling down into the trap. However, the water in the return section could not be recovered. The significance of this volume of uncollected water in the measuring trap can be reduced by increasing the sample size. This increases the overall absolute amount of water that can be removed from the sample and thus reduces the overall magnitude of the error.

Accuracy of measurement dependent on equipment used – the accuracy of the measurement of water collected in the trap is directly linked to the gradation of the collection trap. Traps with 0.1 ml were used for all tests, giving a minimum measurement error of ± 0.1 wt%. Finer gradation levels required smaller traps. When smaller traps were used it was found that water formed clusters in the collection pipe and did not fall, as expected, into the bottom of the trap (as observed with larger traps.).

3.3 OIL CONTENT MEASUREMENTS

In solvent extraction the organic material is contacted to a solvent, which is chosen based on its own chemical properties and those of the organic material to be extracted. The solvent is selected so that the organic material has a higher degree of

solubility in the solvent than its current medium. Two oil extraction methods were utilised in this case:

- (1) SOXHLET
- (2) Accelerated Solvent Extraction

3.3.1 SOXHLET METHOD DESCRIPTION

The SOXHLET apparatus consists of three main sections: the distillation flask, the extractor and the condenser. The drill cuttings sample is first weighed (typically 5-10g) and placed in a thimble, which is then held vertically within the extractor section. The distillation flask is then filled with solvent, Dichloromethane in this case (CAS #75-09-2), and connected to the extractor, which is finally connected to a condenser at the top (Figure 3.2).

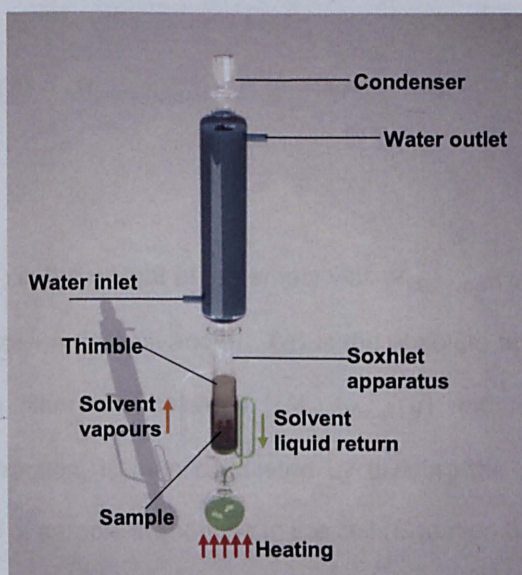


Figure 3.2 - SOXHLET apparatus used for oil content measurements.

The solvent is then heated and brought to a low boiling state. The solvent vapour propagates through the extractor and condensing in the condenser, falling down in the sample holder section of the extractor, where it permeates through the thimble contacting the sample and extracting the organic compounds present within it. Once

the solvent reaches a certain level in the sample holder section within the extractor it siphons back down to the distillation flask with extracted oil/organic content. This cycle is repeated for the entirety of the extraction procedure until it is stopped. Extractions were carried out for the duration of 24 hours in this case, in order to ensure full extraction of the oil phase from the drill cuttings into the solvent.

Once the extraction is completed the oil in the solvent-oil mixture present was concentrated by removing the Dichloromethane under vacuum at approximately 40-50 °C. Once the volume is concentrated to around 10 ml, it was transferred to 12ml cylindrical vials of known weight and placed under a fume hood, where the remainder of the dichloromethane was allowed to evaporate. The weight of the 12 ml vial with the solvent-oil mixture is then measured every 24 hours, normally requiring 2 days (3 days since the initial transfer) for the weight to stabilise to a final value. Once the weight has stabilised the oil content of the sample can be calculated using Equation 3.2:

$$M_{oil}(g) = M_{vial\ final}(g) - M_{vial\ initial}(g) \quad \text{[Equation 3.2]}$$

Where $M_{vial\ initial}(g)$ is the weight of the empty vial, $M_{vial\ final}(g)$ is the final weight of the vial containing solvent-free oil and $M_{oil}(g)$ is the absolute amount of oil extracted, calculated from the difference between $M_{vial\ final}(g)$ and $M_{vial\ initial}(g)$. The oil content, in weight fraction, is then calculated by dividing the mass of oil extracted over the initial mass of sample introduced in the cell (Equation 3.3).

$$x_{oil}(wt\ frac.) = \frac{M_{oil}(g)}{M_{sample}(g)} \quad \text{[Equation 3.3]}$$

Where $M_{sample} (g)$ is the initial mass of drill cuttings sample placed in the Thimble and $x_{oil}(wt\ frac.)$ is the calculated weight fraction based on the amount of oil collected divided by the mass of the drill cuttings sample.

3.3.2 ACCELERATED SOLVENT EXTRACTION METHOD DESCRIPTION

A DIONEX ASE (Accelerated Solvent Extraction) 200 was also used with Dichloromethane (CAS #75-09-2) to carry out the extraction of oil content from drill cuttings samples (Figure 3.3).

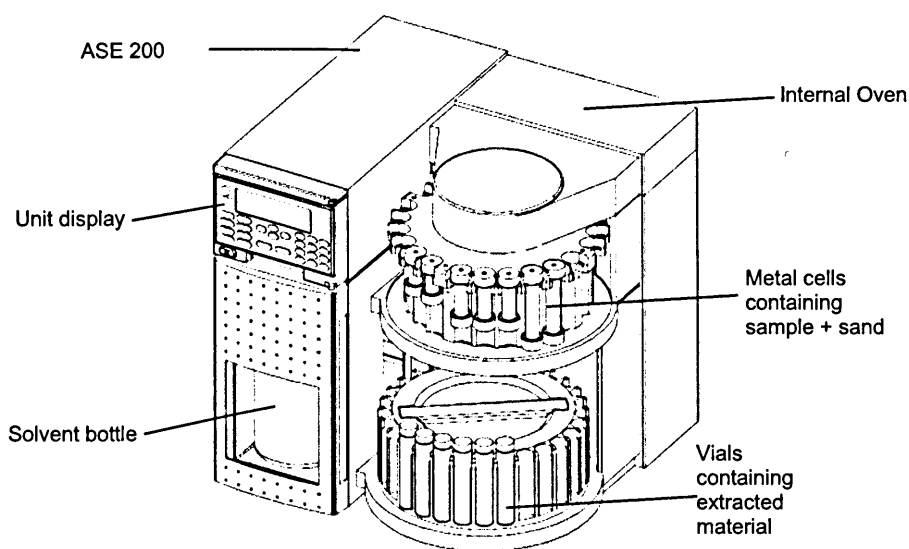


Figure 3.3 - Dionex ASE 200 apparatus used for oil content measurements (Dionex, 1999)

Samples weighing between ≤ 2 grams were placed in a 60 ml stainless steel cell, which was then filled with Ottawa sand (CAS #14808-60-7). The sand prevents voids from forming within the cell, and provides added porosity to the sample, which allows for solvent to pass through the sample without blocking the cell. The solvent is then injected into the cell, and the extractive process is started.

The method used for extraction follows the same concept as that of normal SOXHLET and goes through the following procedure:

1. The internal oven pre-heats the cell containing the solvent and the sample for 5 minutes, followed by heating up to 100 °C for another 5 minutes.
2. The chamber is then held static at approximately 100 bar for a total of 15 minutes before flushing and purging the solvent from the cell into the 60 ml glass collection vial.

The collection vials with the oil-solvent mixture are then placed under a fume hood without their lids so that the bulk of the solvent is evaporated for a period of approximately 48 hours. The remaining solvent and organic content are then transferred to 12 ml vials and the same procedure as that shown for the SOXHLET method is followed, allowing for the sample's oil content to be determined.

3.3.3 *METHOD ANALYSIS*

Castro and Priego-Capote (Luque de Castro & Priego-Capote, 2010) have reviewed the different methods used for the extraction of organic material from samples, including the simplest form of SOXHLET (as described above) and its variations (e.g. accelerated solvent extraction methods). One of the main conclusions of the report was that SOXHLET based methods offered greater flexibility and results accuracy in comparison to alternative technologies. In previous work SOXHLET generally provided a measurement accuracy of 0.05 wt% (Shang, et al., 2006). However, the variability between measurements of the same sample has been found to vary depending on the homogeneity of the sample, and in this work has typically ranged from 0.1 to 0.4 wt%.

Oil content measurements for 2 homogeneous drill cuttings feed samples were measured using conventional SOXHLET apparatus and the accelerated solvent extraction method. For the same drill cuttings feed material, the oil content was measured as 2.91 wt% for conventional and 2.93 wt% for accelerated solvent extraction methods respectively. Given the heterogeneity of samples tested, with a

measured variation in either method of approximately 0.3 wt% is present, these results confirm the accuracy of the ASE against the traditional SOXHLET method. Two other variables were also checked in order to determine their impact on oil content measurement accuracy:

1. Number of extraction cycles – oil content measured for samples with a single cycle was 6.15 wt%, for a double cycle was 6.16 wt%. The difference in measurement was significantly lower than the error generated by the inherent variation in the sample's initial oil content ($\pm 0.3\text{wt}\%$).

2. Using a mixture of solvents 7%Hexane (CAS# 110-54-3) and 93% Dichloromethane (CAS# 75-09-2), to allow for the extraction of aromatic components – oil content measured for a samples with an initial oil content of approximately 3 wt% and treated at 25 kW was: (1) for pure Dichloromethane: 0.3 wt%, (2) for mixed DCM (93%) and Hexane (7%): 0.1 wt%. The difference between either measurement is again within error due to variation of initial oil content in the sample ($\pm 0.3\text{wt}\%$).

This suggests that measurements can be carried out using the accelerated solvent extraction method for a single cycle and with pure DCM and still yield an accurate oil content.

3.4 OIL COMPOSITION MEASUREMENTS

3.4.1 GAS CHROMATOGRAPHY (GC) AND MASS SPECTROMETRY (MS)

Gas chromatography (GC) allows for the separation of components with different boiling points present in a liquid mixture, and is typically used for the identification of unknown components in a mixture. The method works by vaporising the required sample at a given rate (mobile phase) and passing it through a column (stationary phase) using a sweep gas (Figure 3.4) (McNair & Miller, 2009).

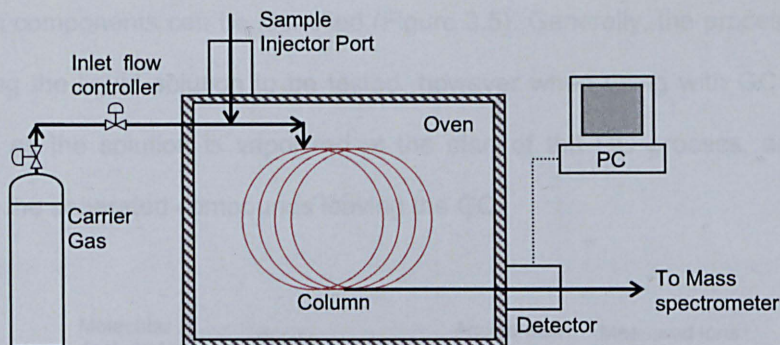


Figure 3.4 - Basic gas chromatography setup.

Capillary columns are generally used and can be made of different materials, which interact with the components passing through it differently depending in the chemical structure of the compounds. Separation then occurs through two main mechanisms (Stuart, 2003):

1. *Differing vapour pressures* – Components enter and leave the column at different times due to differences in vapour pressure.
2. *Interaction of column material* – Components physically interact (strongly or weakly) with the column material leading to further separation.

Thus, depending on the vapour pressure of the component and amount of interaction between the mobile and stationary phase, each component will enter and leave the column at different times. The time taken for the mobile phase to pass through the column is termed the retention time and can be compared for a given setup against existing values in the literature. Thus, using GC by itself is useful for a mixture where there is a good idea of the components present in the mixture and there are well established procedures. However, for unknown mixtures it is possible to connect a GC to a mass spectrometer (MS), which allows for the direct identification of the components leaving the column (Sparkman, et al., 2011).

Mass spectrometry essentially involves the measurement of the weight and frequency of ions arising from the ionisation organic and/or inorganic compounds, such that

unknown components can be identified (Figure 3.5). Generally, the process starts by vaporising the liquid solution to be tested, however when using with GC this is not required as the solution is vaporised at the start of the GC process, and the MS receives the separated compounds leaving the GC.

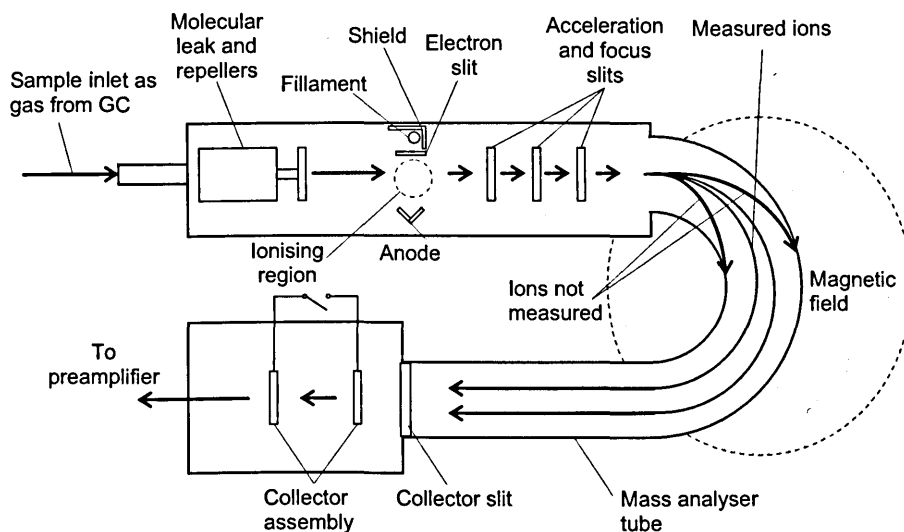


Figure 3.5 - Mass Spectrometer Setup.

After the sample is fed into the mass spectrometer the gas is ionised typically by an electron beam. The different ions are then accelerated through a number of charged slits before entering a curved tube under an applied magnetic field. The magnetic field then directs the ions around the tube into the mass analyser and finally the detector. The actual path taken by each ion is dependent on its mass, with heavier particles tending towards the outside and lighter particles towards the inside. If the ions are too light or too heavy they collide with the wall of the tube and are not detected. The detector effectively detects the presence and frequency of a given ion mass based on what is received from the mass analyser.

3.4.2 GC-MS METHOD DESCRIPTION

Oil extracted from the samples using the accelerated solvent extraction method described above in Section 3.3.2, was analysed using gas chromatography and mass

spectrometry. A Varian CP-3800 gas chromatographer in full scan mode was connected to a Varian 1200 mass spectrometer (EI mode, 70 eV). The chromatographer used an injection in split mode (injection temperature 280 °C; split ratio 50:1). Separation was achieved on a VF-1MS fused silica capillary column (50 m x 0.25 mm ID, 0.25 µm thickness), with helium as the carrier gas, and an oven programme of 50°C (hold for 2 min) to 300°C (hold for 33 min) at 5°C min⁻¹.

3.4.3 METHOD ANALYSIS

The measurement of oil composition was carried out for two purposes:

1. Determining hydrocarbon components present in the mixture in order to allow for physical properties such as specific heat capacity and boiling points to be estimated.
2. Supporting data to show that method used to quantify extent of entrainment and vaporisation worked in practice.

The direct comparison to previously obtained data (Shang, et al., 2006) shows that the composition of oil obtained is similar to that previously measured. Thus, the results obtained here-in using this method of analysis can be used with confidence.

3.5 DRILL CUTTINGS PARTICLE ANALYSIS

This section describes the following methods in detail:

- Sieving:
 - De-agglomerated drill cuttings
 - Agglomerated drill cuttings
- Particle imaging and mineral composition identification:
 - SEM
 - XRD
 - MLA

3.6 SIEVING

3.6.1 INTRODUCTION TO SIEVING

Sieving allows materials originally containing a range of discrete particulate sizes to be split into groups of particles of a specific particle size range. The sieving of drill cuttings samples was carried out in two distinct ways:

- (1) Sieving of agglomerated drill cuttings particles
- (2) Sieving of de-agglomerated drill cuttings particles

The former was carried out in order to determine the agglomerate particle size distribution for the various samples tested, whereas the latter was carried out in order to carry XRD and MLA analysis of the sample.

3.6.2 SIEVING OF AGGLOMERATED DRILL CUTTINGS PARTICLES

Approximately 1kg of feed and treated drill cuttings samples were sieved using the following 200 mm diameter frame sieve sizes: 0.3, 0.425, 0.6, 0.85, 1.18, 2.36, 3.35, 4.75 and 6.35 mm. All sieves were stacked in ascending order, with the sieve with the largest aperture on top and that with the smallest aperture in the bottom.

Sieving was carried out by hand, rather than using an automatic sieve shaker, as a trial run showed some types of drill cuttings samples deagglomerated and reagglomerated when using the automated sieve shaker system. From the 1kg sample, 50g were loaded at a time into the top sieve size. The sieves were then tapped 10 times allowing for particles to descend through the various sieve sizes. The material at the top sieve was then re-spread and the cycle started again. This cycle was carried out between 5-10 times for each 50g of sample loaded in the top sieve, and continued until the entire sample was sieved. This process was carried out exactly in the same manner for all feed and treated samples. Each size fraction was

then weighed and collected in individual plastic sample containers, before being measured for oil and water content as described in Sections 3.1 and 3.2 above.

3.6.3 SIEVING OF DE-AGGLOMERATED DRILL CUTTINGS PARTICLES

Deagglomeration of the individual mineral particles in untreated drill cuttings samples was carried out using the following methodology:

- (1) Sample riffled down from $\geq 200\text{g}$ to approximately 15g.
- (2) Dissolved 15g of sample in 210-240 ml of highly purified water (conductivity $\leq 0.2 \mu\text{S/cm}$).
- (3) Dispersed sample in water by stirring.
- (4) Placed equal amounts of water-sample solution into 50 ml centrifuge tubes
- (5) Centrifuged for a duration of 10 minutes at 3000 rpm.
- (6) Drained water layer from centrifuge samples, re-dissolved samples in fresh water and mixed to ensure good contact between sample and newly added water.
- (7) Repeated steps 5-6 x 5 times.
- (8) Rinsed sample from centrifuge tubes and left sample to settle for 24 hours in a 200 ml of water (250 ml beaker).

After settling for 24 hours, particles $\leq 2\mu\text{m}$ remained suspended in the water phase, whilst particles $>2\mu\text{m}$ settled in the bottom of the beaker (Moore & Reynolds Jr., 1997). The water-particles suspension was then drained into a separate glass container. The settled phase was wet sieved through a $38\mu\text{m}$ sieve and the upper and lower size fractions were collected in individual containers. All three containers with fractions, $\leq 2 \mu\text{m}$, $2\text{--}38 \mu\text{m}$ and $>38 \mu\text{m}$, were then left to dry for a duration of 24 hours in an oven with a setpoint of 105°C . The $\leq 2 \mu\text{m}$ and $2\text{--}38 \mu\text{m}$ size fractions were milled using a pestle and mortar and stored in appropriate containers. After drying sieving was carried out for the fraction $>38\mu\text{m}$ using standard 200mm diameter

$\sqrt{2}$ sieve series: 0.3, 0.212, 0.15, 0.106, 0.075, 0.053 and 0.038 mm. Sieves were stacked from the smallest size to the largest size and placed in an automated sieve shaker for 10 minutes. Each size fraction was then weighed and collected in an individual container for MLA analysis.

3.7 SCANNING ELECTRON MICROSCOPE (SEM) AND MINERAL LIBERATION ANALYSIS (MLA)

3.7.1 INTRODUCTION TO SCANNING ELECTRON MICROSCOPE (SEM)

Scanning electron microscopes (SEM) can be used for obtaining information on the topography, morphology, composition and, to a lesser extent, crystallographic structure. However, SEM is generally limited to surface or near surface measurements and works as shown in Figure 3.6 (Reimer, 1998).

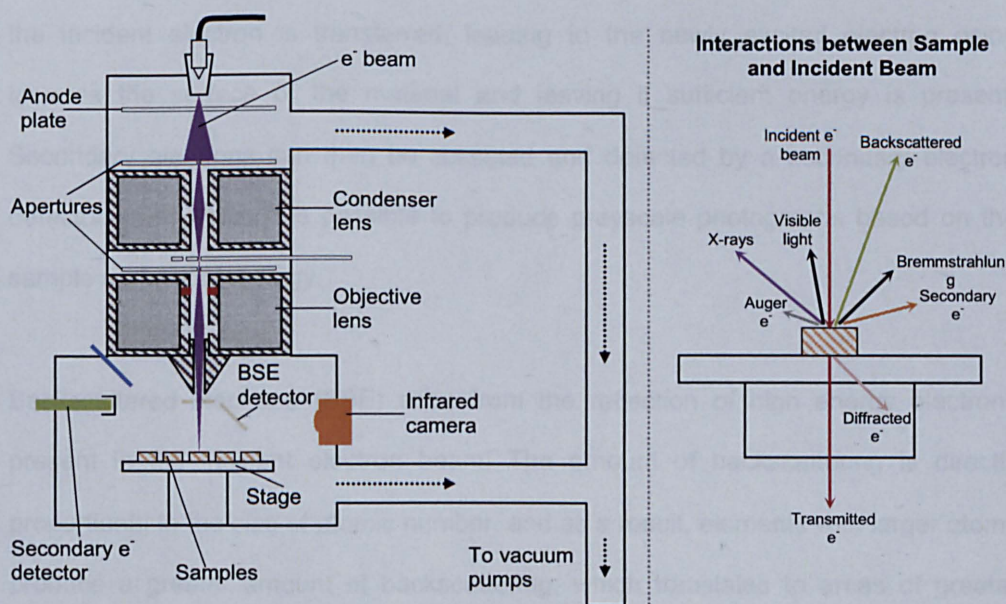


Figure 3.6 - Scanning Electron Microscope (SEM) principle of operation and interaction with Sample.

A focused, monochromatic electron beam, generated using an electron gun at high vacuum, is accelerated towards the anode, passing subsequently through a magnetic

lens, before making contact with the sample. A number of interactions can occur when the electron beam hits the sample. These interactions are also shown in Figure 3.6 and can be divided into inelastic and elastic (Carlton, 2011; Yacobi, et al., 1994):

- *Elastic*: (i) transmission of electrons straight through the sample, (ii) diffraction of electrons.
- *Inelastic*: (iii) backscattering of electrons, (iv) emission of secondary reflections, (v) auger electrons, (vi) X-rays, (vii) Bremsstrahlung, (viii) visible light and (ix) heat.

The emission of secondary electrons, backscattered electrons and X-rays can be used for gathering information when using an SEM setup.

Secondary electrons arise from the transfer in energy from an electron in the incident electron beam to electrons present within the material. A great part of the energy of the incident electron is transferred, leading to the newly excited electron rising towards the surface of the material and leaving if sufficient energy is present. Secondary electrons can then be collected and detected by a secondary electron detector, from which it is possible to produce greyscale photographs based on the sample surface's topology.

Backscattered electrons (BSE) arise from the reflection of high energy electrons present in the incident electron beam. The amount of backscattering is directly proportional to the size of atomic number, and as a result, elements with larger atoms produce a greater amount of backscattering, which translates to areas of greater intensity (brightness) in the resulting photographs. Thus, backscattered electrons provide, in effect, a density map of the elements present in the surface, and can be used for helping determine the composition and morphology of the sample.

X-ray emissions arise, when electrons move from higher to lower shell vacancies, which occurs as the near surface atoms need to return to an unexcited state. The overall energy and quantity of emitted X-rays is detected via an energy dispersive X-ray spectrum (EDS or EDXS) detector, and, for the spot measured, can be correlated back to specific elements and abundance. This provides information, which can help determine the composition of the sample.

3.7.2 SEM METHOD DESCRIPTION

Scanning electron microscope (SEM) photographs were taken for cross-sections of dry drill cuttings agglomerate in view of better understanding the structure of the agglomerates.

A computer controlled FEI Quanta 600 Scanning Electron Microscope equipped a backscattered electron (BSE) detector, an EDAX X-ray detector and an automated sample holder capable of accommodating 14 x 30mm mounts was used. Spot sizes between 4.5 and 6.0 were used between 10-25 kV at working distances of approximately 10 mm \pm 0.5.

Approximately 100g of a drill cuttings sample containing various agglomerate sizes were oven dried at 105 °C. 1-2g samples were riffled down from the bulk sample (100g) and introduced into 30mm ID polythene mounts. A mixture (15:2 wt/wt ratio) of Struers' EpoFix epoxy resin and EpoFix hardner (CAS# 223-24-3) was added to each mount so that the height of liquid in the mounts was approximately 20-25 mm (method modified from (Nielsen & Maiboe, 2000) to suit). Once added the sample was stirred lightly in order to ensure good contact with the resin and eliminate air pockets.

The mount containing the resin and the sample was then deaerated by placing the mount under vacuum in a Struers' EpoVac for a duration of approximately 15-20

mins. Once this was completed the blocks were allowed to cure for a period of 24 hours, before being removed from the mount. The epoxy resin blocks were then ground and polished using a Struers' Terrain horizontal rotary wheel system.

Grinding was initially necessary in order to expose a cross section of the block which contained a significant number of particles. Grinding was carried out using consecutively finer grinding discs: MD-Piano 120, 220 and 1200 discs. Polishing was carried out after grinding and is necessary for obtaining clear images using the SEM and accurate measurement of backscattered electrons using the BSE detector. Polishing was carried out using three consecutively finer polishing discs with Struers' DiaDuo-2 diamond suspension, which is required during polishing to ensure even surface finish, cooling and lubrication. The discs used for polishing were as follows: MD-Plan (9 µm), MD-Dac (3 µm) and MD-Dur (1 µm).

3.7.3 *INTRODUCTION TO MINERAL LIBERATION ANALYSIS (MLA)*

Mineral liberation analysis combines data automatically gathered from BSE detectors and EDS detectors to determine the mineralogy of the various particles present in the sample (Gu, 2003; Fandrich, et al., 2007). The data from the BSE detectors allows the identification of individual particles to be carried out based on differences in density, the data from EDS detectors is then used to perform an elemental analysis of each of the particles identified from the BSE detectors. From this data it is possible to determine the minerals present in the sample and quantity. The data and image output can also be used in a number of other analyses. The quality of results is ultimately determined by the resolution of BSE images, which in turn is dependent on the time required for the scan to be completed, thus a balance between resolution accuracy is typically considered.

3.7.4 *MLA METHOD DESCRIPTION*

Approximately 1-2g untreated, deagglomerated drill cuttings of size fraction - 0.053+0.038 mm (as per Section 3.6.3.), were mounted and prepared using the same procedure as that shown in Section 3.7.2 above. Samples are then exposed to X-rays using the same setup as that described in Section 3.7.2 above. A number of backscattered electron (BSE) images of the sample are generated producing a gray scale image, with each shade of gray being also representative of specific X-ray spectra. By combining BSE and X-ray spectra data and using specialist MLA software (Deyssel, 2007) it is possible to correlate, an individual mineral phase with a unique average atomic number (AAN) to a specific shade of gray. It is then possible to show each of the individual phases in a colour coded image, where visual identification of individual minerals is facilitated.

Previous works have used mineral liberation analysis for quantification purposes; however, in this case the technique was used solely for qualitative purposes. The purpose of using the technique was solely to confirm the potential presence of certain minerals in the sample. This analysis is useful, as the confirmation of the presence of Pyrite, for example, would suggest localised heating could occur (as pyrite is a high microwave energy absorber (Jones, et al., 2007))

3.8 X-RAY DIFFRACTION (XRD)

3.8.1 *INTRODUCTION TO XRD*

An X-ray beam directed onto a crystalline material with a repeating atomic structure and equidistant planes, will lead to scattering in various directions when coming in contact with ions/atoms present in the lattice structure, as shown in Figure 3.7.

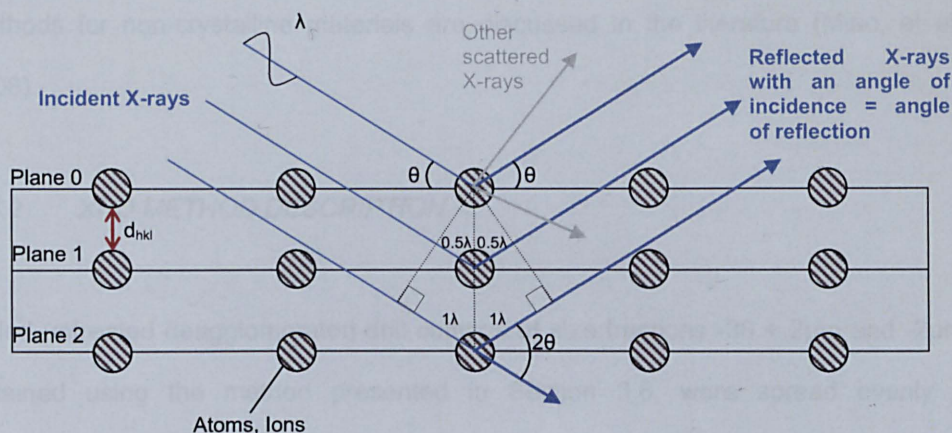


Figure 3.7 - Diffraction of X-rays in a lattice with equally spaced ions/atoms.

Reflected X-rays can lead to constructive diffraction:

- (1) The angle of incidence is equal to the angle of reflection
- (2) The path difference between X-rays reflected at different (hkl) planes is 1 wavelength.

This can be mathematically represented by Bragg's Law (Norton & Suryanarayana, 1998) (Equation 3.4), which correlates the angle of incidence of the X-ray beam and the interplanar spacing to the wavelength of the X-rays.

$$n\lambda = 2d_{hkl}\sin\theta$$

[Equation 3.4]

Where 'n' is an integer representing the equivalent number of X-ray wavelengths for a given diffracted X-ray (i.e. $n=1$ is the X-ray resulting from diffraction at the surface of the material), λ is the wavelength of the incident X-ray, typically between 0.01 nm to 10 nm (Joshi, 2010), d_{hkl} is the interplanar spacing, and θ is the angle of incidence.

The diffraction pattern obtained for a given crystalline material is unique to its mineral structure and composition, and as a result X-ray diffraction can be used for identification of unknown crystalline materials present at a given sample. This technique was used to identify crystalline materials only in this case, however

methods for non-crystalline materials are discussed in the literature (Miao, et al., 2008).

3.8.2 XRD METHOD DESCRIPTION

Milled untreated deagglomerated drill cuttings of size fractions $-38 + 2\mu\text{m}$ and $-2\mu\text{m}$, obtained using the method presented in Section 3.6, were spread evenly in aluminium platelets. The samples were then analysed using an automated 3kW Hiltonbrooks Generator attached to a Phillips PW 1050 diffractometer operating at 40kV and 20mA. The X-rays were generated from a copper anode and were passed through an automatic divergence slit producing X-rays of wavelength $\lambda = 1.54056 \text{ \AA}$. 2θ angles were measured automatically at a rate of $2^\circ/\text{min}$ and intervals of 0.05° between 5 and 95° . A dedicated computer running Diffraction Technology Traces V.3 matched the spectra obtained for the sample tested against standards from the JCPDS-ICDD database, allowing specific minerals to be identified. After initial analysis samples were also treated with acetic acid and glycolated in order to remove carbonates and identify interlayer clays respectively. Once the treatments were carried out samples were analysed again.

3.9 DIELECTRIC PROPERTIES MEASUREMENT

3.10 CYLINDRICAL CAVITY PERTURBATION TECHNIQUE INTRODUCTION

The measurement of dielectric properties using a cylindrical resonant cavity is typically used for materials with a low dielectric loss, and where accuracy and measurements at temperature are required. The cylindrical cavities used for measurement are designed to have the dimensions required for resonance to occur at specific frequencies (normally at ISM or near ISM frequencies of 915 and 2450 MHz).

For a given sample volume and weight, the technique allows for the indirect measurement of the dielectric loss and constant by measuring shifts in the resonating frequency and quality factor (Q-factor) of the cavity, typically with the aid of a Vector Network Analyser (VNA). The Q-factor is given by the ratio of energy stored against the energy dissipated by the cavity. In this case, the following Maxwell's equations (Equation 3.5 and 3.6) were used for processing the data obtained (Meng, et al., 1995).

$$\epsilon' = 1 + 2J_1^2(X_{l,m}) \left(\frac{\bar{V}_1}{\bar{V}_2} \right) \left(\frac{f_2 - f_1}{f_1} \right) \quad [\text{Equation 3.5}]$$

$$\epsilon'' = J_1^2(X_{l,m}) \left(\frac{\bar{V}_1}{\bar{V}_2} \right) \left(\frac{1}{Q_2} - \frac{1}{Q_1} \right) \quad [\text{Equation 3.6}]$$

Where J_1 is the first order Bessel function, $X_{l,m}$ is the m^{th} root of the first kind Bessel function (Baricz, 1994), \bar{V}_1 and \bar{V}_2 are the volumes of the empty cavity (15190473 mm³ in this case) and the sample respectively, f_1 and f_2 are the empty cavity's resonant frequency (2470 and 911 MHz in this case) and the cavity's resonant frequency with the sample respectively, Q_1 and Q_2 are the empty cavity's Q-factor and the Q-factor of the cavity with the sample respectively. The reader is referred to the literature for further information on cavity perturbation and other dielectric property measurement techniques (Terselius & Ranby, 1978; Metaxas & Meredith, 1983; Venkatesh & Raghavan, 2005).

3.11 CYLINDRICAL CAVITY PERTURBATION METHOD DESCRIPTION

Figure 3.8 below shows the setup used for the measurement of dielectric properties of drill cuttings samples.

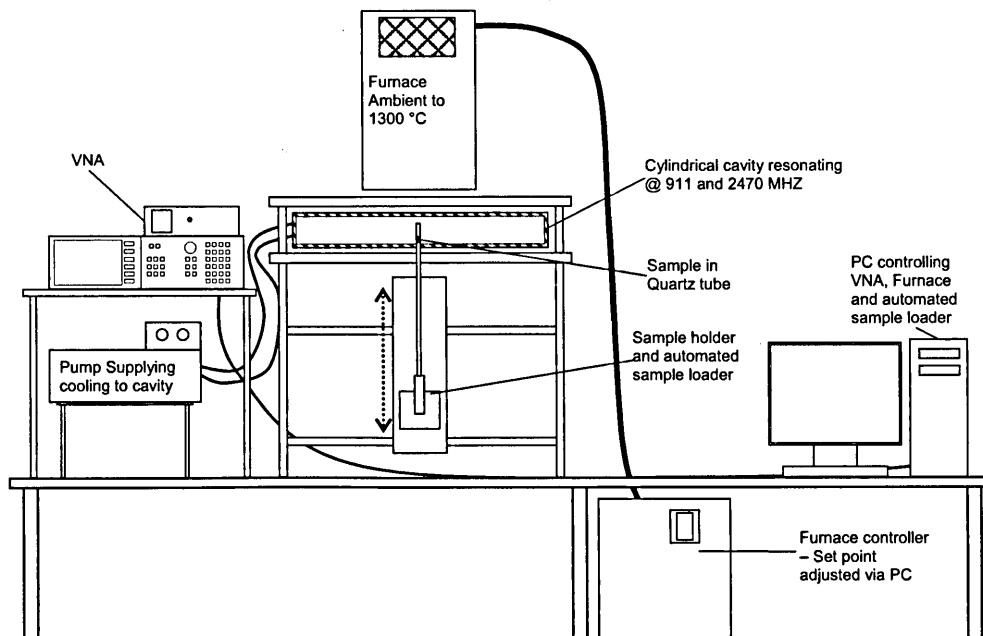


Figure 3.8 - Setup used for measuring dielectric properties using the cavity perturbation method.

The system consisted of: (1) a water cooled cylindrical copper resonant cavity connected to a (2) HP 8753C VNA, allowing measurements to be taken at resonant modes TM_{0n0} at 2470 (n=5,) and 911 MHz (n=2), (3) a 3kW Carbolite® furnace is mounted directly above the cavity and allows samples to be heated up to 1300 °C and (4) an automated mechanical arm mechanism is used for loading the sample holder into the cavity and furnace automatically. The computer, which is attached to each of the above parts of the system, is used for automatically controlling the entire measurement process and recording the frequency shift ($\Delta f/f_2$) and the quality factor (Q_2), which is measured through the VNA.

Empty sample holders (2.98 mm cylindrical Quartz tubes) are loaded into the automated mechanical arm, and an “empty tube” measurement is taken at room temperature, establishing a baseline ‘ Q_1 ’ and ‘ f_1 ’. Drill cuttings samples, typically weighing between 0.01 to 0.05g, were then placed in the same sample holders measured empty. The tubes are tapped 10 times to ensure sample density is uniform across all measurements. The samples are then generally measured at temperatures ranging from 20 °C to 800 °C at intervals of 10 or 20 ° depending on the resolution required. The furnace power rating used during heating of the sample was as follows:

0.06 to 0.12 kW for the first 200 °C, 0.3 to 0.4 kW for the next 200 °C and approx. 0.9 kW for the remainder of the time. The sample was held at 10 mins at the temperatures where measurements were taken before actually carrying the measurement out. The data was then automatically recorded and the dielectric constant and loss (ϵ'') automatically calculated as per Equations 3.5 and 3.6 above.

The variation in measurement for the same sample was measured by taking measurements at room temperature of three different samples taken from the same bulk sample. The variation due to sample heterogeneity for the dielectric constant and loss were calculated to be ± 0.11 and ± 0.02 respectively.

CHAPTER 4 – Oil and Water Removal Mechanisms

4. INTRODUCTION

The objective of this chapter is to determine the mechanisms involved in the removal of oil from oil contaminated drill cuttings using microwaves. Previous work (Shang, et al., 2006; Robinson, et al., 2009) has suggested the following potential mechanisms for the removal of oil from oil contaminated drill cuttings during microwave processing:

- Evaporation – removal of oil and water content through evaporation using a sweep gas such as air or nitrogen.
- Vaporisation (boiling)
 - Direct vaporisation of the oil phase or through heat transfer from other phases.
 - Steam distillation as a result of internal generation of steam during microwave heating of the water phase.
- Entrainment – physical removal of oil droplets through the rapid vaporisation of water content present in the cuttings during microwave heating.

Based upon previous work, the main mechanism responsible for removal is expected to be vaporisation, for two reasons:

1. The measured energy input used was found to be greater than the minimum amount of energy input required for vaporising the oil and water content and heating the rock during microwave treatment (**Robinson, et al., 2009**). If entrainment was the main mechanism the energy input used would be expected to be less than that required to vaporise the water and the oil and heat the rock.

2. Evaporation is a form of vaporisation that can be achieved at a temperature below the boiling point of the liquid. The rate of removal is highly dependent on sweep gas flowrate, surface area available, vapour pressure, external pressure and temperature. The low vapour pressure of the oil phase (predominantly alkanes as shown in the previous works (Shang, et al., 2006)), even at higher temperatures, and the limited available surface area for evaporation are likely to significantly limit mass transfer and the rate of oil removal. This makes the rate and extent of removal achievable through this mechanism negligible in comparison to both of the other mechanisms.

Thus, in order to confirm the above hypothesis it was necessary to first confirm the presence of these mechanisms and secondly to, quantify the extent of removal due to each individual mechanism. In order to carry this out the approach shown in Figure 4.1 was used.

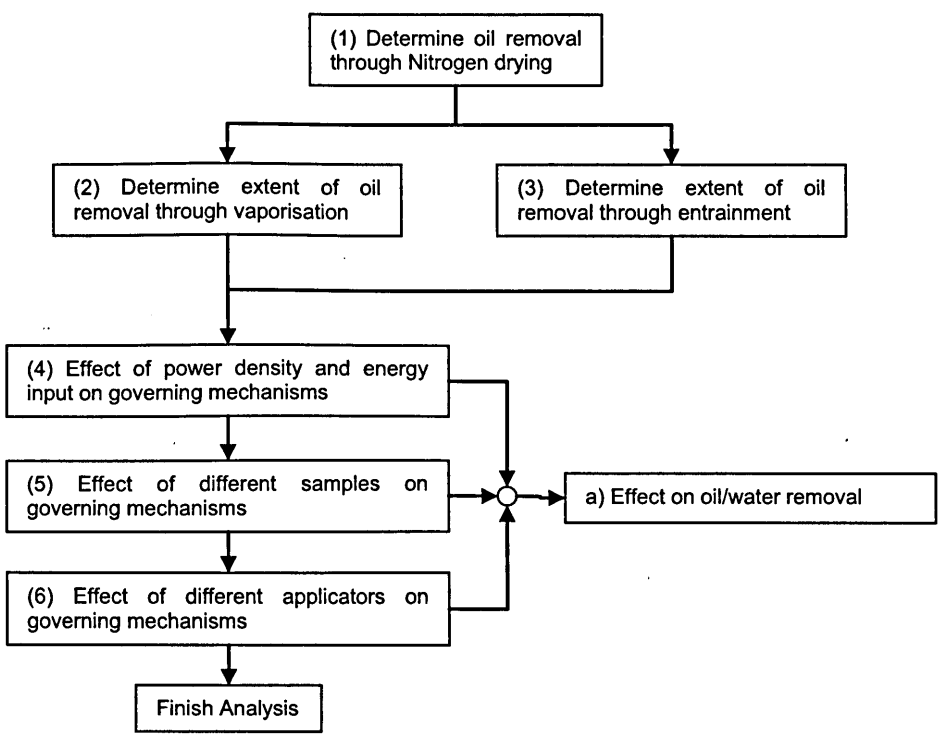


Figure 4.1 - Approach used for confirming oil removal mechanisms and quantification.

Based on Figure 4.1, the first step was to determine whether oil could be removed through nitrogen drying alone, as nitrogen is used throughout all experiments for a safety purposes. This would also allow for adjustments to be made to the results obtained during microwave treatment if nitrogen drying was found to be a significant factor in oil and water removal.

The extent of oil removal through vaporisation and entrainment was quantified using a specific rig setup which allowed for physical measurement of the weight of oil and water removed through entrainment and vaporisation. This was done in order to obtain a baseline on the ratio of entrainment to vaporisation for a range of operating conditions. The effect of power density and energy input, different rock samples and applicators, on the mechanisms present was then determined by measuring the differences in oil and water content before and after treatment. The results of the above experiments allowed the main oil removal mechanism present during microwave treatment of oil contaminated drill cuttings to be determined.

4.1 DRILL CUTTINGS SAMPLE CHARACTERISATION

Drill cuttings consist of agglomerates containing a blend of minerals, typically kaolinite, quartz, illite, montmorillonite, barite and traces of pyrite (Dhir, et al., 2010), which is held together by a binding agent; generally one or more of the clays present and/or calcite. Figure 4.2 shows electron scanning microscope photographs of agglomerated drill cuttings particles at 70x and at 2000x magnification, the method and parameters used for taking SEM photographs are described in detail in Section 3.7 of Chapter 3.

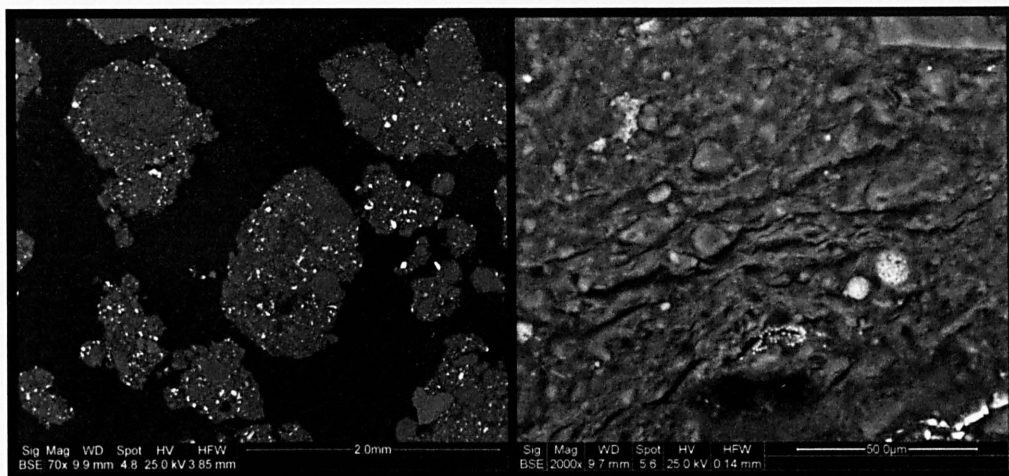


Figure 4.2 - SEM photograph of drill cuttings particles.

Drill cuttings with an initial oil and water content and density as shown in Table 4.1 were used for these experiments.

Sample	Oil Content (wt%)	Water content (wt%)
Sample A	5.4 ± 0.8	7.9 ± 0.9
Sample B	3.7 ± 0.4	12 ± 0.8
Sample C	7.8 ± 0.4	5.5 ± 0.8

Table 4.1 - Drill cuttings initial oil and water content.

Samples A, B and C were de-agglomerated through the methods described in Section 3.6.3 of Chapter 3. Figure 4.3 shows the de-agglomerated particle size distribution for Samples A, B and C.

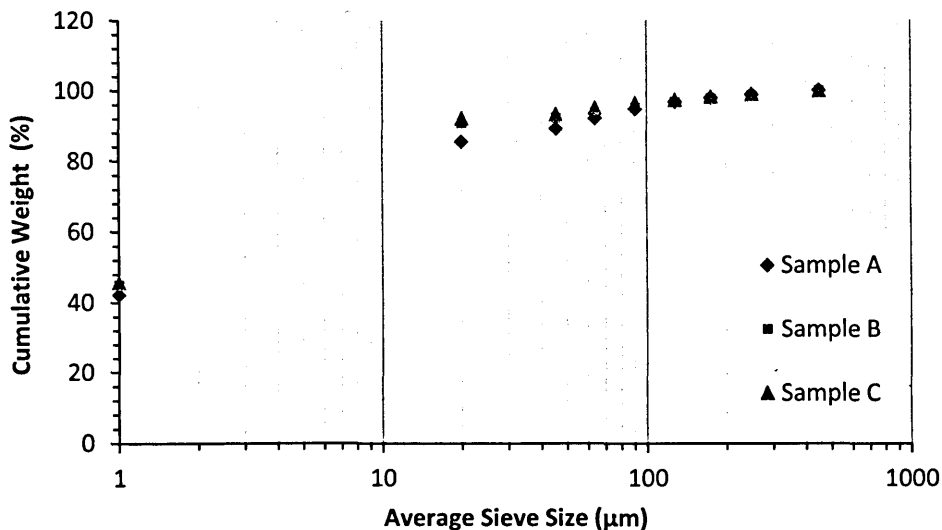


Figure 4.3 - De-agglomerated drill cuttings particle size distribution for Samples A, B and C.

According to the data presented in Figure 4.3 >85-90% of all three samples consist of particles <20μm, and at >40% of the sample consists of particles <2μm, suggesting high clay contents. The distribution of the particle size across all three samples did not change significantly, which was expected as all drill cuttings samples received for treatment are drill cuttings that came from formations that were drilled with oil based muds, which are typically used in deep wells with complex sections of high clay content, where water loss to formation can be high. Figure 4.4 below shows the SEM photograph and corresponding MLA analysis image of particles of size -53+38 μm for samples A and B.

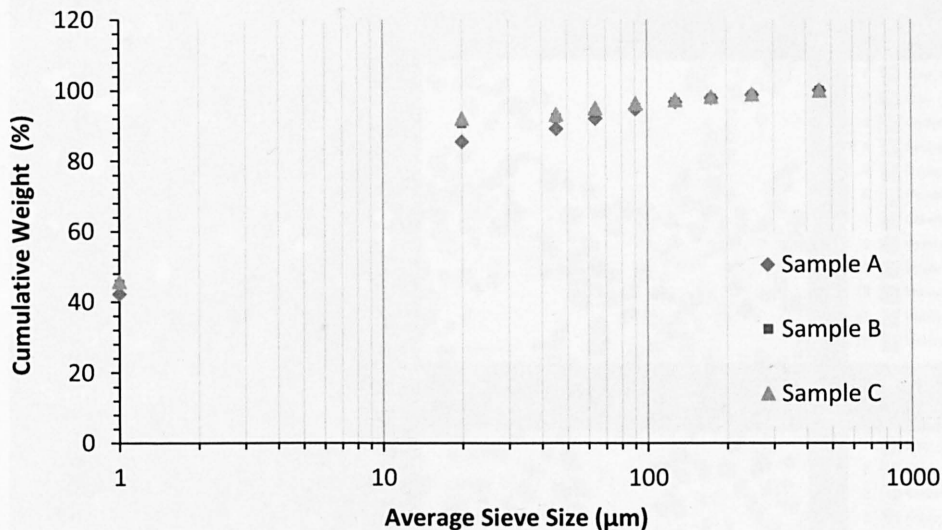


Figure 4.3 - De-agglomerated drill cuttings particle size distribution for Samples A, B and C.

According to the data presented in Figure 4.3 >85-90% of all three samples consist of particles <20μm, and at >40% of the sample consists of particles <2μm, suggesting high clay contents. The distribution of the particle size across all three samples did not change significantly, which was expected as all drill cuttings samples received for treatment are drill cuttings that came from formations that were drilled with oil based muds, which are typically used in deep wells with complex sections of high clay content, where water loss to formation can be high. Figure 4.4 below shows the SEM photograph and corresponding MLA analysis image of particles of size -53+38 μm for samples A and B.

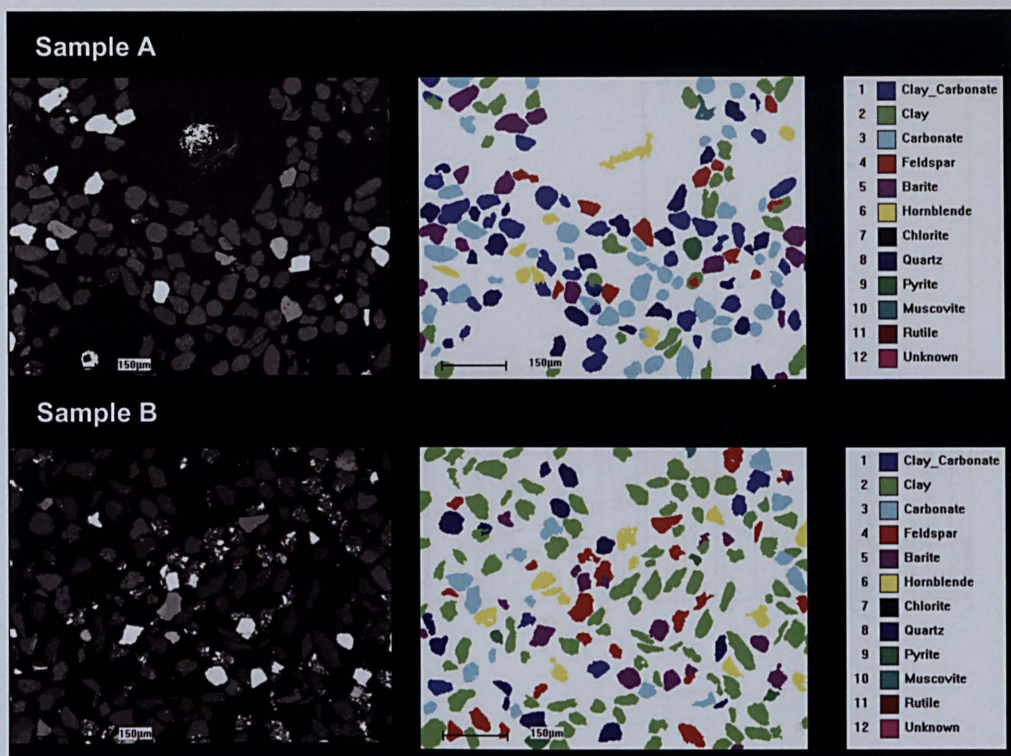


Figure 4.4 - MLA analysis of samples A and B for particles of size range -53+38 µm.

Figure 4.4 provides an identification of minerals that are present in drill cuttings tested and is in agreement with data reported in the literature. Note the experiment was carried out for qualitative purposes only and the above images alone cannot be used for quantification purposes. Nevertheless, by analysing this data in Figure 4.4 with the data in Figure 4.3 it appears that a great portion of the sample consists of clay, clay-carbonate and carbonate minerals. Figure 4.5 and 4.6 below show the XRD analysis of Samples A and B for particles <2 µm after acetic acid treatment.

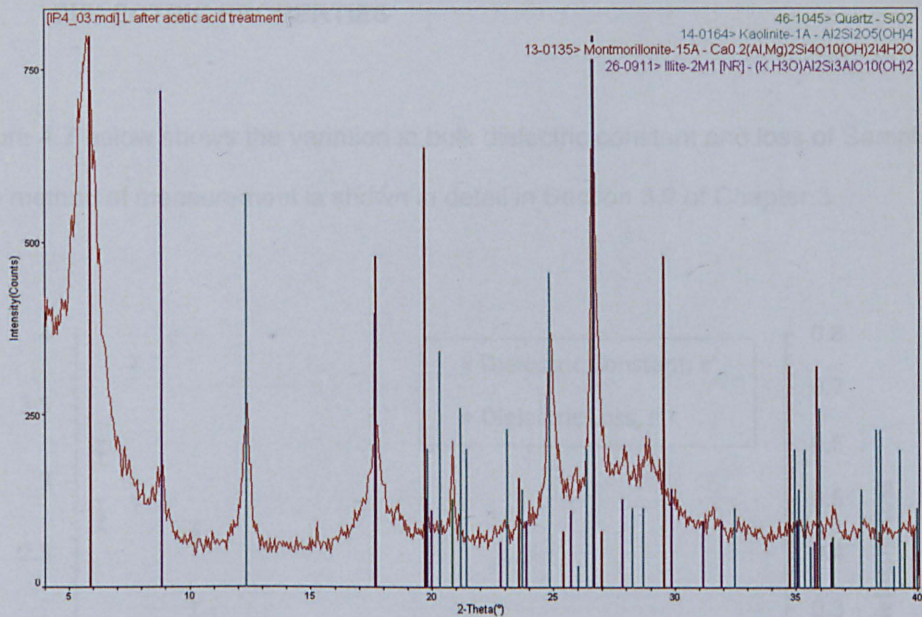


Figure 4.5 - XRD analysis of Sample A

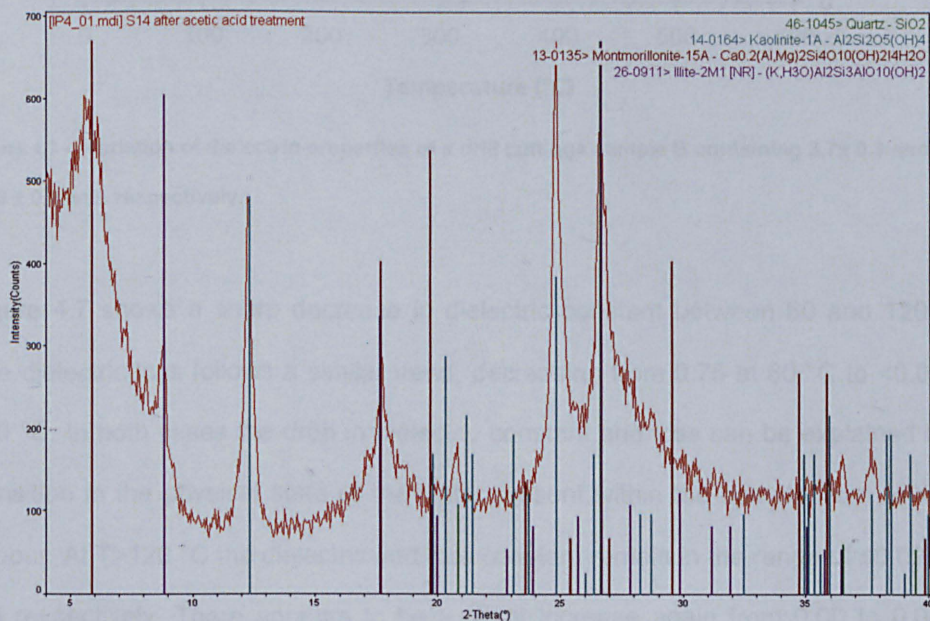


Figure 4.6 - XRD analysis of Sample B

From Figure 4.5 and 4.6 both samples it appears that the clays present in the sample are a blend of Kaolinite, illite, montmorillonite. Quartz was also identified within the sample. The results of glycolation are shown in Appendix 1.

4.2 DIELECTRIC PROPERTIES

Figure 4.7 below shows the variation in bulk dielectric constant and loss of Sample B. The method of measurement is shown in detail in Section 3.9 of Chapter 3.

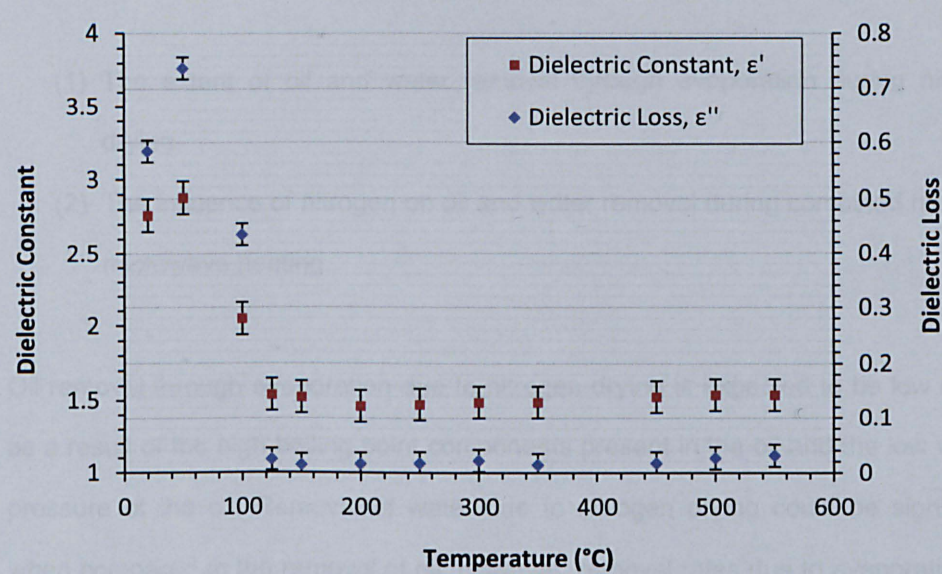


Figure 4.7 - Variation of dielectric properties of a drill cuttings sample B containing 3.7 ± 0.3 and 12.0 ± 0.8 wt% respectively.

Figure 4.7 shows a sharp decrease in dielectric constant between 60 and 120 °C. The dielectric loss follows a similar trend, decreasing from 0.75 at 60 °C to <0.02 at 120 °C. In both cases the drop in dielectric constant and loss can be explained by a transition in the physical state of the water present within the sample from liquid to vapour. At $T > 120$ °C the dielectric and loss constant remain in the range of ≤ 0.02 and 1.5 respectively. There appears to be a slight increase again from 0.00 to 0.04 at $T = 400 - 600$ °C. This is in agreement with the typical de-hydroxylation temperature range for clays containing interlayer water and is confirmed through the XRD analysis of samples heat treated at 400 and 600 °C (Frost & Vassallo, 1996). However, this observation should be applied with care, as the variation in the sample is relatively high (represented by error bars in Figure 4.7 above.)

4.3 NITROGEN DRYING AND MICROWAVE HEATING OF DRILL CUTTINGS

In previous work on the microwave treatment of drill cuttings nitrogen has been typically used as a sweep and inerting gas (Shang, et al., 2006). However, no experiments have been carried out to determine:

- (1) The extent of oil and water removal through evaporation during nitrogen drying.
- (2) The influence of nitrogen on oil and water removal during combined nitrogen-microwave heating.

Oil removal through evaporation due to nitrogen drying is expected to be low mainly as a result of the high boiling point components present in the oil and the low vapour pressure of the oil. Removal of water due to nitrogen drying could be significant, when compared to the removal of oil. However, removal rates due to evaporation are expected to be orders of magnitude lower than removal through vaporisation and entrainment, which are likely to be the main mechanisms of oil and water removal during microwave treatment. Consequently, during combined nitrogen drying and microwave heating of the cuttings, nitrogen flowrate is not expected to have any significant impact in the removal efficiency of the oil or water, and is only necessary from a safety point of view.

4.3.1 EXPERIMENTAL SETUP

Drill cuttings of Sample A weighing 150g were loaded in a cylindrical reactor, with an inside diameter of 0.071m, to a sample height of 40 mm \pm 2.5. The reactor was placed at the centre of a multimode cavity of dimensions 425 (W) x 425 (L) x 545 mm (H). The same sample placement was used throughout all experiments in order to maintain reproducibility between samples.

Nitrogen was fed from below the reactor passing through the cuttings before leaving the cavity through a designated extraction point. The cavity was connected to a magnetron, capable of outputting a maximum power of 3 kW, through an e-plane bend connected perpendicularly to the cavity attached to a straight waveguide section and a 3-stub tuner. A junction circulator was used to protect the magnetron by deflecting reflected microwaves to a continuous flow of cooling water, which absorbed any remaining unabsorbed power. This setup is shown in Figure 4.8.

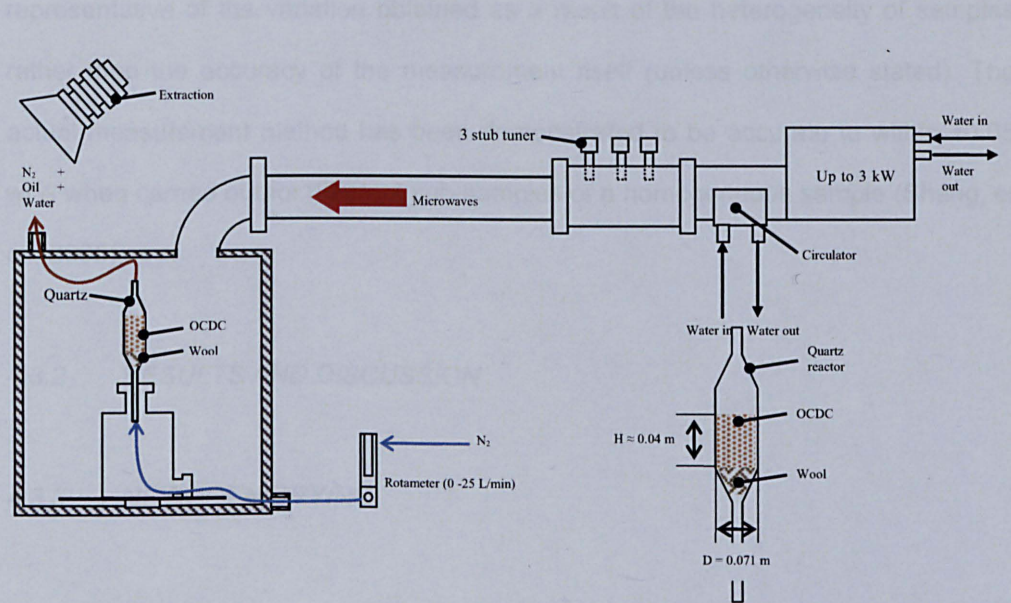


Figure 4.8 - Setup for the nitrogen and microwave drying of oil contaminated drill cuttings using a multimode cavity of dimensions 425 (W) x 425 (L) x 545 mm (H).

Nitrogen drying: Nitrogen at 16 °C was fed at a volumetric flowrate of 20 L/min. Initial and final weights were measured up to 120 minutes in 10 minute intervals, with a new sample being used for each measurement. For example, one sample was set up and measured after 10 minutes, removed and stored; a new sample was prepared and dried for 20 minutes, until the final measurement was carried out at 120 minutes. Weight loss and water and oil content were measured for each sample. No microwaves were used.

Microwave drying: Analogous to the experiment above, nitrogen at 16 °C was passed through the bed during microwave treatment. Nitrogen flowrates of 5-25 L/min were

tested. Samples were then treated with microwaves at intervals of 30 seconds up to 180 seconds at an average forward power of $720\text{ W} \pm 15\text{ W}$ and reflected power of $8.5 \pm 15\text{ W}$. In each experiment the oil, water content and mass loss were measured. The results of these experiments are presented and discussed below in Section 4.3.2.

All error bars related to oil content measurements shown within this work are representative of the variation obtained as a result of the heterogeneity of samples rather than the accuracy of the measurement itself (unless otherwise stated). The actual measurement method has been demonstrated to be accurate to within $\pm 0.05\text{ wt\%}$ when carried out for different sub-samples of a homogeneous sample (Shang, et al., 2006).

4.3.2 *RESULTS AND DISCUSSION*

4.3.3 *NITROGEN DRYING*

Figure 4.9 shows the variation in Sample A's weight with time for drill cuttings dried using nitrogen at 20 L/min . The sample weight dropped with time decreasing by approximately 10g from the start of the experiment. The trend in Figure 4.9 can be divided into two sections; (1) rapid weight decrease with time from 150g to 146g between 0 and 30 minutes, (2) quasi-constant decrease in weight with time, reaching a weight of approximately 140g at 120 minutes.

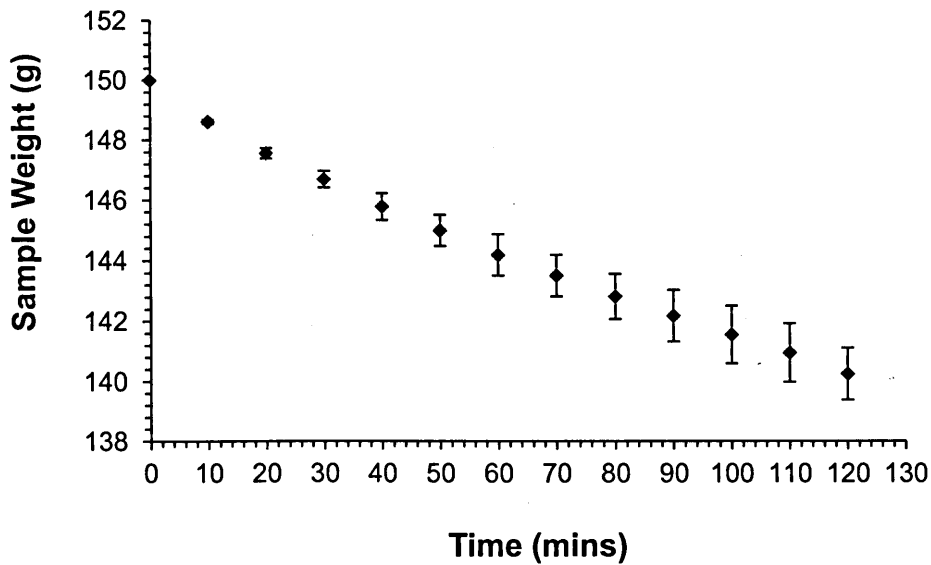


Figure 4.9 - Variation of sample weight with time for Sample A.

Based on the data from Figure 4.9 it is possible to calculate the variation of sample weight loss with time. This is done according to Equation 4.1:

$$\frac{dW_n}{dt_n} = \frac{w_n - w_{n+1}}{(t_n - t_{n+1})}$$

[Equation 4.1]

Where dW_n is the difference in weight (g) between a given time difference dt_n , which is the difference between a time (min) t_n and a time (min) t_{n+1} . w_n is the weight (g) of the sample at t_n and w_{n+1} is the weight of the sample at t_{n+1} . Figure 4.10 shows the variation of weight loss with time.

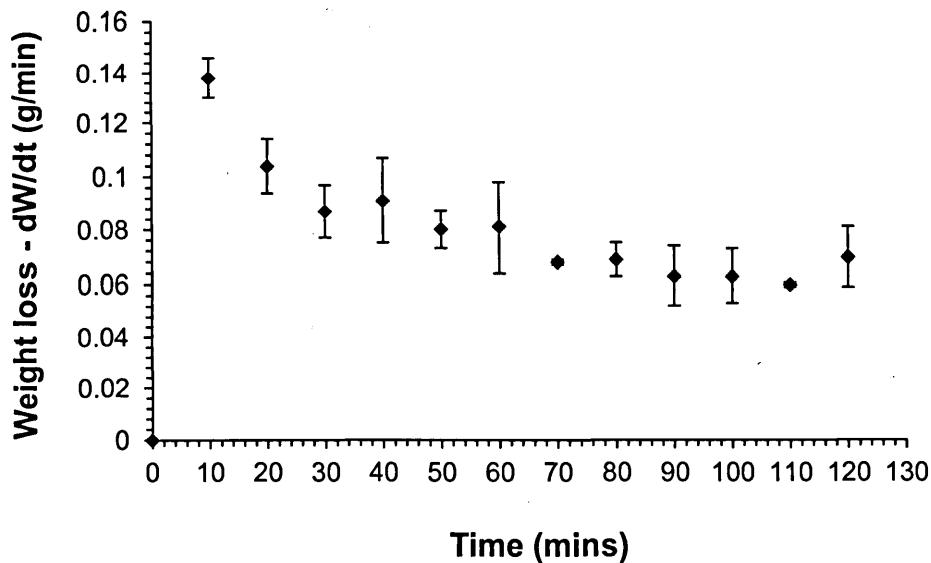


Figure 4.10 - Sample weight loss vs. Time for Sample A

Figure 4.10 shows as expected an overall decrease in weight loss with time and appears to have 3 main regions: (1) high weight loss between 0-30 mins, (2) transition period between high and low weight loss between 30-70 mins and finally (3) a low weight loss region >70 mins. The weight loss between 10 and 30 mins decreased from 0.14 g/min to 0.09 g/min, decreasing until 0.07 at 70 mins, before remaining fairly constant thereafter, oscillating around 0.07 ± 0.01 g/min. This trend agrees with data shown in the literature for evaporative drying (Hall, et al., 1984) and can be explained by the different stages of drying for a wet porous material. Surface and free water is dried initially at faster rates as a result of lower mass resistance and energy requirements for vaporisation (region 1), which leads to higher initial weight losses. However, as water content decreases below a given content (regions 2 and 3) water mass transfer limitations as well as energy requirements for vaporisation increase, resulting in the lower weight losses observed in Figure 4.9 above.

Thus, there is a clear reduction in sample weight with time as a result of nitrogen drying. However, in order to understand whether the observed weight loss is caused by removal of water, oil or a combination of both it was necessary to measure the oil and water content for each sample tested. Figure 4.11 shows the variation of water content with time for the same sample.

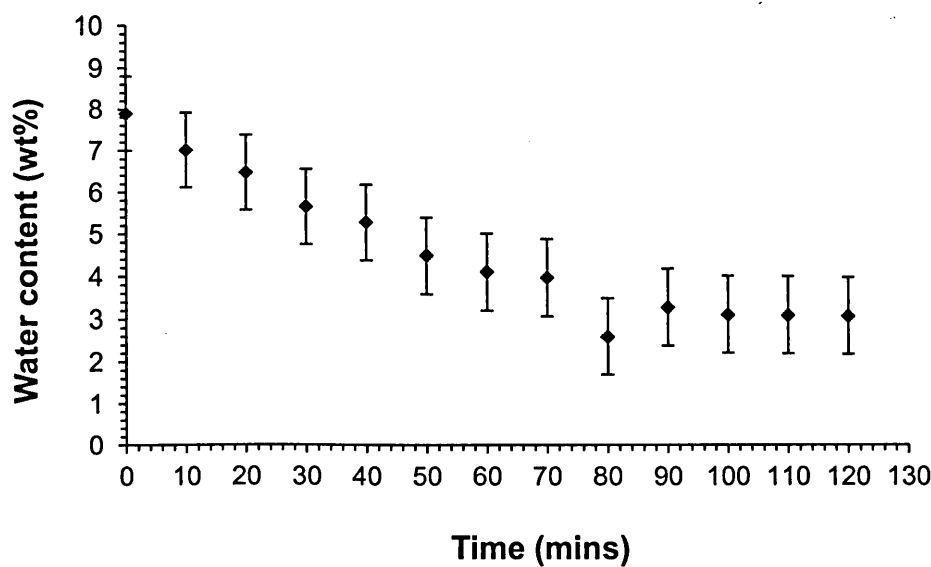


Figure 4.11 - Variation of water content (wt%) with time (mins) for Sample A

As seen from Figure 4.11, the water content decreased with time from 8 wt% initially present in the material, to approximately 3.5 wt% after 120 minutes of drying. It followed a similar pattern to that of Figure 4.10, with water content decreasing from just below 8wt% to 5.5 wt% between 0 and 30-40 mins, and then from 5.5 to 4 wt% in the transitional period (30-70 mins), before entering the region of low weight loss at >70 mins, where the water content only dropped from 4 to just over 3 wt% with time. Interestingly, the water content remains constant, whilst the actual sample weight continues to decrease. This effect could be a result of moisture being re-absorbed by the sample during the storage time between the end of the experiment and carrying out the water content measurement. The average rate of decrease in water content per treatment time during 0-50 mins of treatment was 0.07wt%/min. Figure 4.12 shows the equivalent of the above but for oil content.

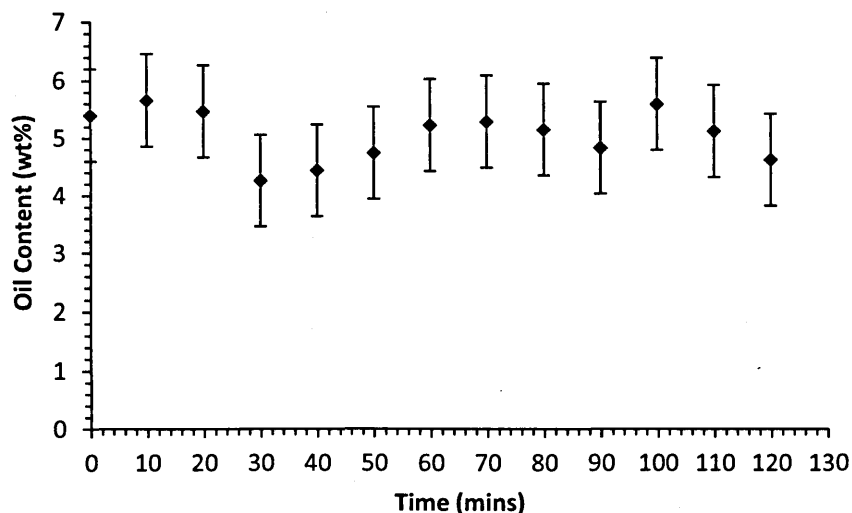


Figure 4.12 - Variation of oil content (wt%) with time (mins) for Sample A

Figure 4.12 shows an oscillation in the variation of oil content with time, but does not show any distinct increasing or decreasing trends with time. The variation observed in oil content with time is caused by the high natural variation of oil content present initially within the drill cuttings sample. However, if any oil removal was occurring an overall decrease in oil content with drying time would have been expected. The oscillation around a value of 5-6 wt% from 0 to 120 mins suggests little or no oil removal is observed during nitrogen drying. This could be explained by the nature of the oil composition present in the cuttings, which typically consists of alkanes chains between C10-C20, and will therefore have high boiling points and low vapour pressure at room temperature. In order to confirm this, the composition of oil extracted from one of the feed samples was measured using a Varian CP-3800 gas chromatograph connected to a Varian 1200 mass spectrometer, the details of which are provided in Section 3.4 in Chapter 3. Figure 4.13 shows the variation of counts (dimensionless) with time (mins) for oil extracted during the measurement of oil content for the samples tested above.

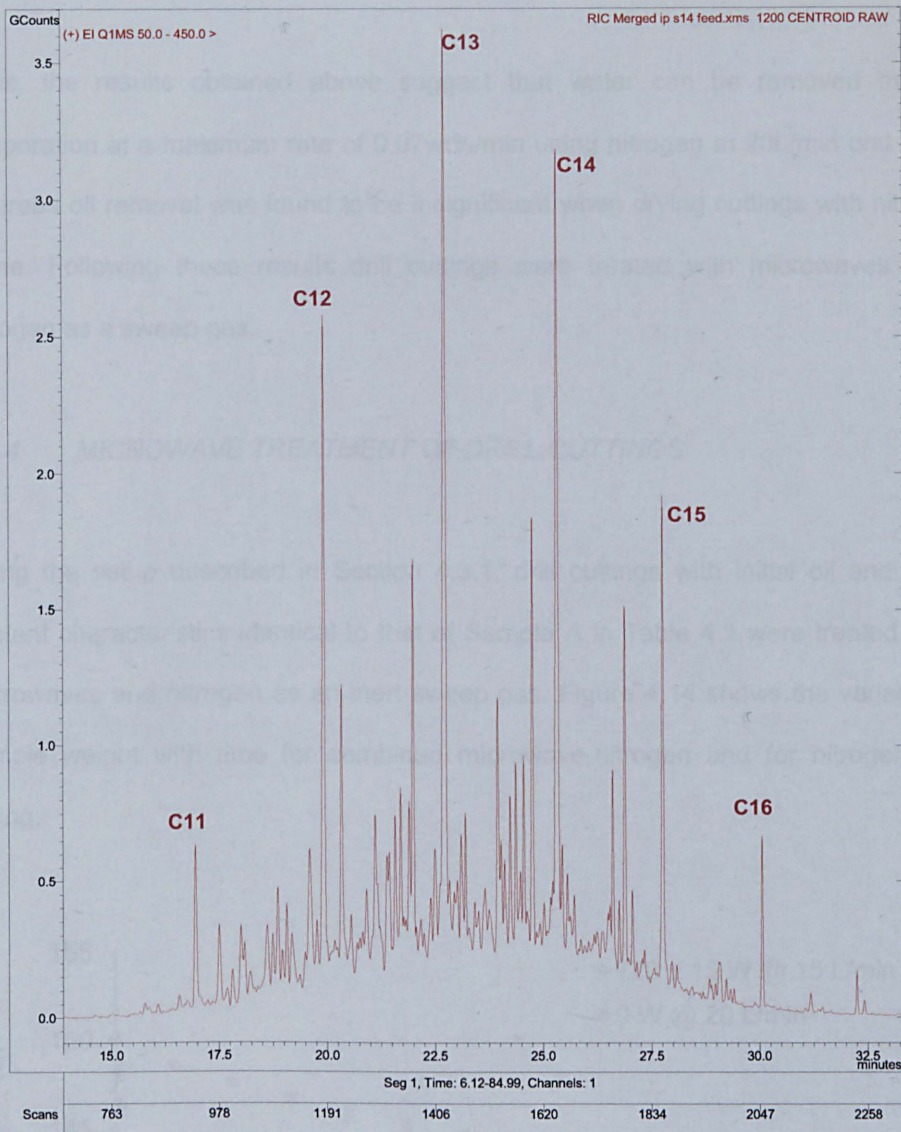


Figure 4.13 - Variation of counts with time (mins).

Figure 4.13 shows the components making up the oil that is present within the feed sample. Components ranging from C11 to C17 were identified with the bulk of the sample consisting of C12-C14 chains. As the lowest boiling component identified was C11, at 196 °C, removal of oil through evaporation due to Nitrogen at 15-20 °C is likely to be insignificant. Furthermore, by comparing the vapour pressure of C11, 0.0007 bar at standard temperature and pressure (STP), to water, 0.023 bar at STP, it is clear that evaporation will be significantly greater for water than for C11 at 16 °C and 1 atm (measurements of vapour pressure were carried out using ABB's PEL PhysPack).

Thus, the results obtained above suggest that water can be removed through evaporation at a maximum rate of 0.07wt%/min using nitrogen at 20L/min and 16°C, whereas oil removal was found to be insignificant when drying cuttings with nitrogen alone. Following these results drill cuttings were treated with microwaves using nitrogen as a sweep gas.

4.3.4 MICROWAVE TREATMENT OF DRILL CUTTINGS

Using the setup described in Section 4.3.1, drill cuttings with initial oil and water content characteristics identical to that of Sample A in Table 4.1 were treated using microwaves and nitrogen as an inert sweep gas. Figure 4.14 shows the variation of sample weight with time for combined microwave-nitrogen and for nitrogen only drying.

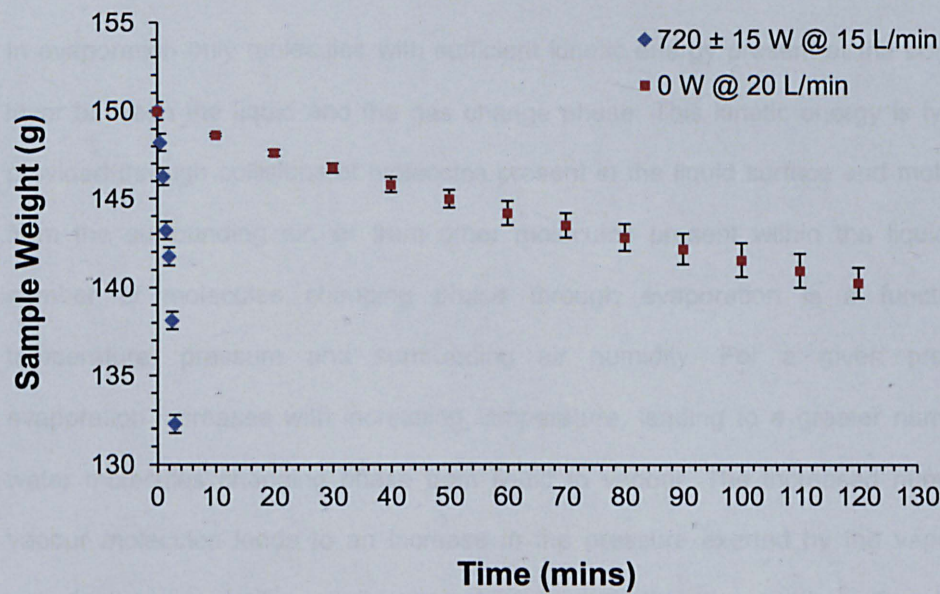


Figure 4.14 - Variation of sample weight with time for samples treated using microwaves at 720 W ± 18 and a Nitrogen flow of 15 L/min and for samples treated using nitrogen only at 16 °C at 20 L/min.

Figure 4.14 shows, as expected, a greater decrease in sample weight over a shorter period of time for samples treated using microwaves, 9 g/min, in comparison to

samples dried with nitrogen at 0.07g/min, which represents less than 1% of the microwave removal for every minute of treatment. This difference in removal occurs as a result of the shift in the removal mechanism, from evaporation only during nitrogen drying, to vaporisation and possibly entrainment during microwave treatment. Figure 4.15 shows the difference between vaporisation and evaporation mechanisms.

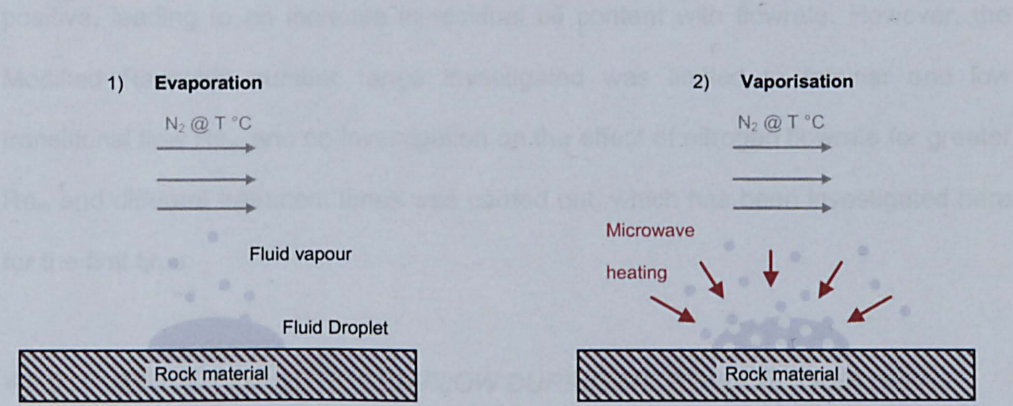


Figure 4.15 - Difference between vaporisation and evaporation mechanisms.

In evaporation only molecules with sufficient kinetic energy present at the boundary layer between the liquid and the gas change phase. This kinetic energy is typically provided through collisions of molecules present in the liquid surface and molecules from the surrounding air, or from other molecules present within the liquid. The number of molecules changing phase through evaporation is a function of temperature, pressure and surrounding air humidity. For a given pressure, evaporation increases with increasing temperature, leading to a greater number of water molecules changing phase from liquid to vapour. The increased number of vapour molecules leads to an increase in the pressure exerted by the vapour. In vaporisation (i.e. boiling) the temperature is such that the number of molecules having sufficient energy to change from liquid to vapour results in the pressure exerted by the vapour being equal to that of the surrounding. At this point, if sufficient energy is provided to the liquid phase such that it can overcome its latent heat of vaporisation, an immediate change of state from liquid to vapour phase is possible. These conditions lead to a significantly larger driving force for mass transfer.

The effect of nitrogen flowrate of sweep gas on oil removal has been investigated previously, and showed that nitrogen flow can potentially impact oil removal positively, by increasing even heating, and negatively, by condensing oil and water vapours back into the cuttings (Shang, et al., 2006). For the modified Reynolds number (Re_m) <15 nitrogen flow was seen to have a greater negative impact than positive, leading to an increase in residual oil content with flowrate. However, the Modified Reynolds number range investigated was limited to laminar and low transitional flow Re_m and no investigation on the effect of nitrogen flowrate for greater Re_m and different treatment times was carried out, which has been investigated here for the first time.

4.3.5 EFFECT OF NITROGEN FLOW DURING MICROWAVE TREATMENT

Figure 4.16 below shows the measured residual oil content with processing time for the same Sample A, previously shown in Figure 4.12, using microwaves at 720 W and 15 L/min of Nitrogen and Nitrogen only at 20 L/min.

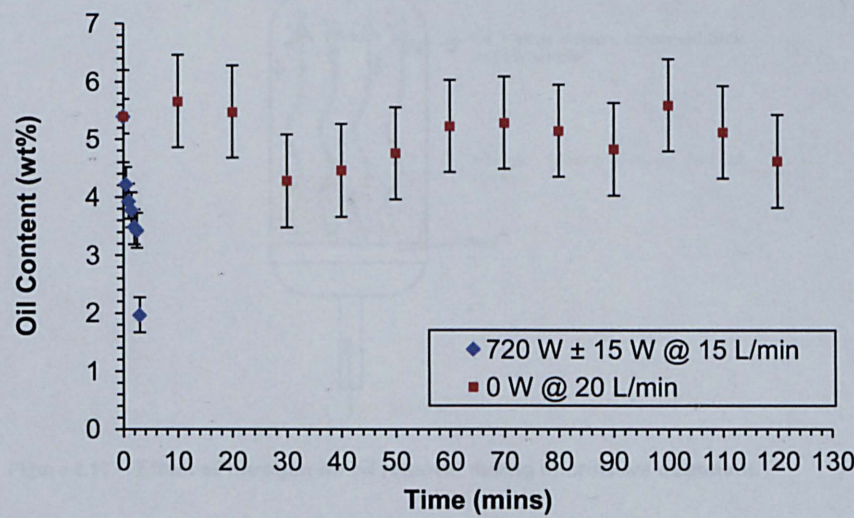


Figure 4.16 - Variation of residual oil content for drill cuttings samples treated at 720 W ± 18 and a Nitrogen flow of 15 L/min and for samples treated using nitrogen only at 16 °C at 20 L/min.

As seen from Figure 4.16, the oil content decreased from an initial value of 5 wt% to 2 wt% after 3 minutes of microwave heating at 720 W with a Nitrogen flow of 15 L/min. For a nitrogen flow of 20 L/min, the sample oil content oscillated around 5 wt% and, given the heterogeneity of the feed, did not see any significant decrease in oil content over time. The differences in residual oil content between treatment methods can be explained purely by the overall difference in energy input supplied to the sample in each method.

This data clearly shows that oil removal through evaporation using Nitrogen at 16°C as an oil removal mechanism is, as expected, insignificant during microwave treatment of oil contaminated cuttings. However, an increase in nitrogen flow is expected to enhance vapour transport from the cuttings surface into the extraction duct, and reduce the overall concentration gradient around the cuttings, further increasing the driving force for evaporation and vaporisation Figure 4.17.

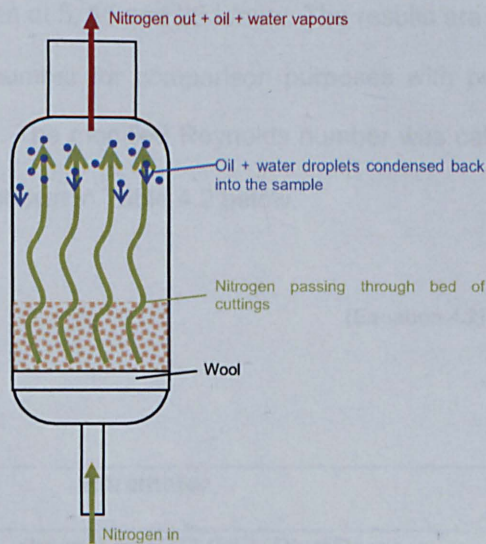


Figure 4.17 - Effect of nitrogen on oil removal during microwave treatment.

The impact of nitrogen flowrate on oil removal is expected to be greater in samples treated for shorter periods of time than longer periods. This is thought to be the case as a result of the shift in vapour removal mechanism occurring due to decreasing liquid content. Liquid content present as free/surface fluid can be removed easily from

the cuttings as the energy required for removal is approximately equal to that theoretically required to heat and vaporise the fluid. However, as the liquid content decreases liquid content is held in a bound state rather than in a free state. There are various degrees of bound fluid (Saarenketo, 1998), and as the liquid content decreases the energy requirements for unbinding the liquid increases.

As a result of this shift in drying behaviour, the main mass transfer rate limiting factor for oil and water removal during the initial microwave drying process is the removal of oil and water vapours and droplets from the material's surface or near-surface to the extraction points. At later drying stages the main rate limiting factor is driving vapours present within the pores and structure of the cuttings to the surface. As a result, increasing nitrogen flowrate is expected to have a greater impact initially, where the nitrogen can enhance vapour removal from the cuttings surface by increasing the concentration gradient and vapour pressure of the water and oil. Figure 4.18 shows the variation of oil content with nitrogen flowrate for samples treated with microwaves at 720 W and Nitrogen at 5, 15 and 25 L/min. The results are also shown against the modified Reynolds number for comparison purposes with previous published work (Shang, et al., 2006). The modified Reynolds number was calculated using Equation and the parameters shown in Table 4.2 below.

$$Re_m = \frac{\rho_{N_2} v_{N_2} D_b}{\mu_{N_2} (1 - \epsilon_b)}$$

[Equation 4.2]

Parameter	Value
Nitrogen density, ρ_{N_2} (kg/m ³) @ STP (PEL PhysPack)	1.25
Nitrogen viscosity, μ_{N_2} (Pas) @ STP (PEL PhysPack)	1.766 x 10 ⁻⁵
Superficial velocity of Nitrogen, v_{N_2} (m/sec)	0.021 , 0.063 and 0.110
Diameter of bed, D_b (m)	0.071
Bed void fraction, ϵ_b (Perry & Green, 1997)	0.38

Table 4.2 - Parameters used for the estimation of the modified Reynolds number for Nitrogen flowing through a packed bed.

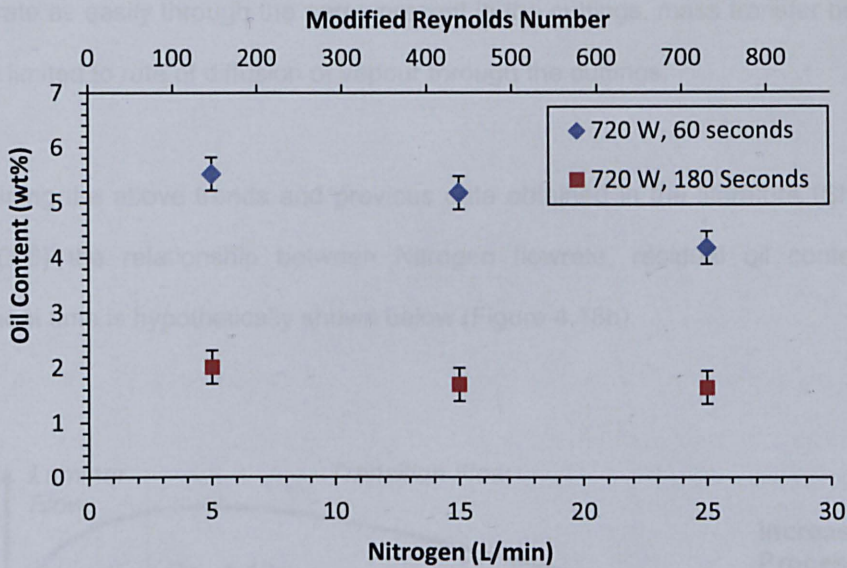


Figure 4.18a - Variation of oil content with nitrogen flowrate for Sample A treated at 720 W at 5, 15 and 25 L/min nitrogen @ 16 °C.

As seen in Figure 4.18 for samples processed for a duration of 60 seconds the oil content decreased with increasing nitrogen flowrate, with a significant decrease being observed between 15 and 25 L/min from 5.2 to 4.5 wt%. This equated to an overall increase in the modified Reynolds number from 150 at 5 L/min to over 700 at 25 L/min. For the modified Reynolds number laminar flow is present between 0-10, followed by transition flow between laminar and turbulent flow between $Re_m = 10$ and $Re_m = 2000$, and turbulent flow at $Re_m > 2000$. The data shows that when processing for shorter durations, increasing the flow increases oil removal as a result of increasing turbulence. Turbulence can improve mass transfer of vapours generated at the surface or near the surface of the cuttings through the bed and into the bulk sweep gas.

For samples treated for a longer duration of 180 seconds with the same nitrogen flowrate (5-25 L/min) and over the same modified Reynolds number (150 to 700) range, little difference was noticed in the residual oil content with varying nitrogen flowrate. During longer treatment times, the limitation in mass transfer shifts from transferring vapours generated at the surface of the particles to the mass transfer of vapour within the particles' pores (vapour diffusion). As nitrogen is unlikely to

penetrate as easily through the pores present in the cuttings, mass transfer becomes purely limited to rate of diffusion of vapour through the cuttings.

Combining the above trends and previous data obtained in the literature (Shang, et al., 2006) the relationship between Nitrogen flowrate, residual oil content and treatment time is hypothetically shown below (Figure 4.18b).

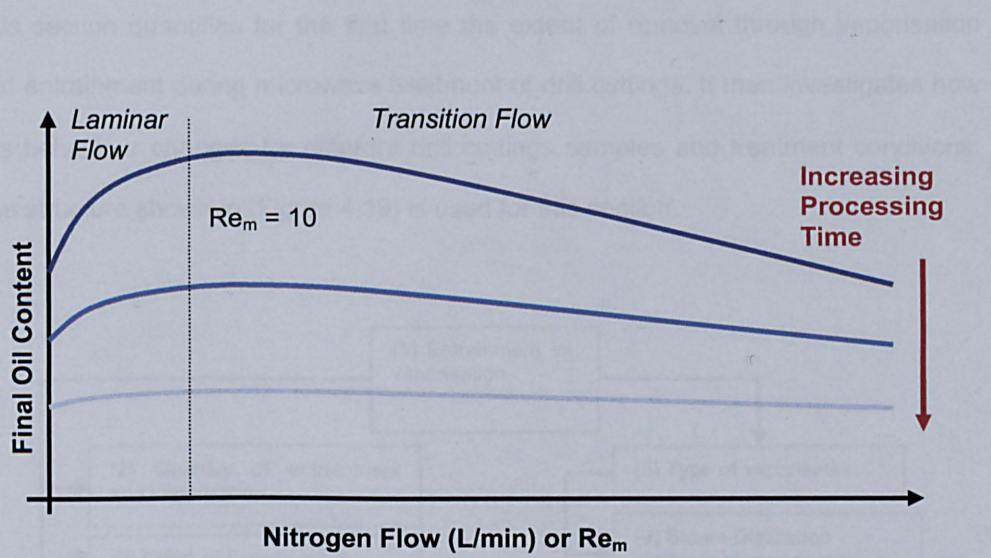


Figure 4.18b - Hypothetical variation of oil content with increasing Nitrogen flowrate or Modified Reynolds Number vs. processing times.

As seen in Figure 4.18b an increase in nitrogen flow and Re_m has a negative impact in oil content at low Re_m values, as the benefit of increased mass transfer is outweighed by re-condensation of oil and water vapours. As Re_m increases towards turbulent flow the benefits of improved mass transfer begin to outweigh re-condensation, improving the overall oil and water removal. Increased processing time (or reduced liquid content) leads to less significant changes in oil content with increasing Re_m .

Following these results Nitrogen flowrates were selected to give a flowrate with a $Re_m \geq 100$. In order to minimise re-condensation, it was therefore decided to re-heat Nitrogen to 80 °C.

4.4 OIL AND WATER REMOVAL MECHANISMS DURING MICROWAVE TREATMENT OF DRILL CUTTINGS

The data presented in Section 4.3 strongly suggests that the majority of the water and oil removal (>99%) must be through either vaporisation and/or entrainment.

This section quantifies for the first time the extent of removal through vaporisation and entrainment during microwave treatment of drill cuttings. It then investigates how this behaviour changes for different drill cuttings samples and treatment conditions. The structure shown in (Figure 4.19) is used for this section.

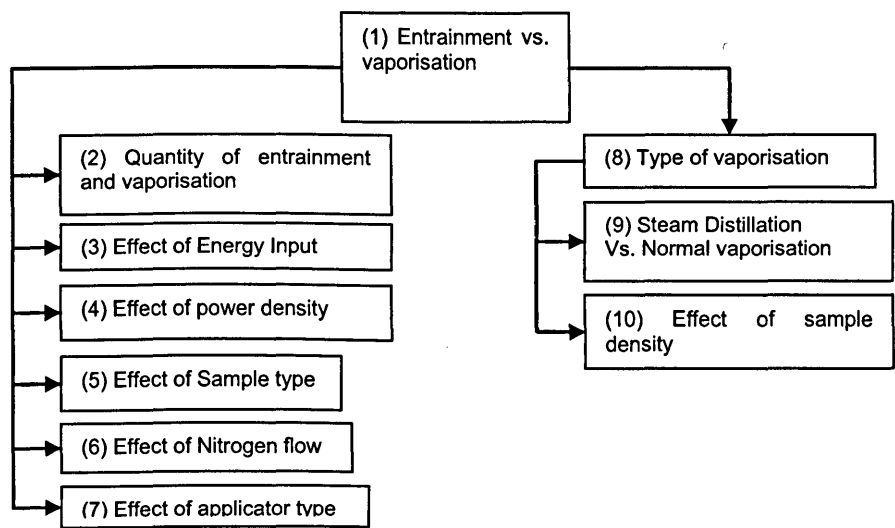


Figure 4.19 - Detailed Investigation structure for Entrainment vs. Vaporisation experiments

The extent of entrainment is expected to be greatest during the initial sections of the experiment where the highest level of liquid content is available, which is likely to facilitate the carryover of droplets in steam/gas passing through the cuttings.

Power density is expected to enhance entrainment, as steam will be formed at a faster rate leading to higher gas speeds exiting the cutting and therefore greater potential for carrying liquid out of the cuttings in liquid form.

Where nitrogen flows through the bed of cuttings, a decrease in hot nitrogen flow is expected to have a negative impact in oil and water removal for 2 reasons: (1) lower mass transfer as discussed previously, (2) greater potential for condensation (as nitrogen is heated in this case).

The applicator type is expected to have an impact on the overall power density, and thus the ratio of entrainment to vaporisation. The single mode applicator is expected to have the highest percentages for oil removed through entrainment, whereas samples treated using the multimode applicator are expected to have the lowest levels of entrainment due to low velocity steam generated during microwave heating.

Removal through vaporisation is expected to occur mainly through steam distillation, based on data previously shown in the literature (Robinson, et al., 2009). Oil removal was observed for all components present in the oil, although a shift towards the heavier components was present in treated samples, which would suggest lighter components were preferentially removed, which is expected from a steam distillation based mechanism. Also, had the mechanism been driven by individual vaporisation of each of the components, temperatures in excess of 400 °C would have been required for removal to take place, which is unlikely to be achievable in this case as the bulk of the heating is carried out in the water phase (free and weakly bound), which is likely to be removed at ≈100-120 °C. An increase in steam generation, and thus flowrate, is expected to yield an increase in vaporisation efficiency.

4.4.1 *EXPERIMENTAL SETUP*

4 Different experimental setups were used in this case:

- (1) Configuration A – Setup used to primarily measure the extent of entrainment and vaporisation of drill cuttings samples treated with microwaves. The effect of power density, processing time, sample type and nitrogen flow are also investigated.

(2) Configuration B – Setup used to determine the effect of using a different applicator on the extent of each mechanism by measuring oil removal against power density. The results of configuration A (Single Mode) and B (Continuous processing applicator) were then also compared to C (Multimode).

(3) Configuration C – Setup used to investigate steam distillation as a potential vaporisation mechanism.

4.4.2 EXPERIMENTAL CONFIGURATION A

The first setup (Configuration A) was used in order to physically measure the extent of entrainment and vaporisation present during microwave processing (Figure 4.20).

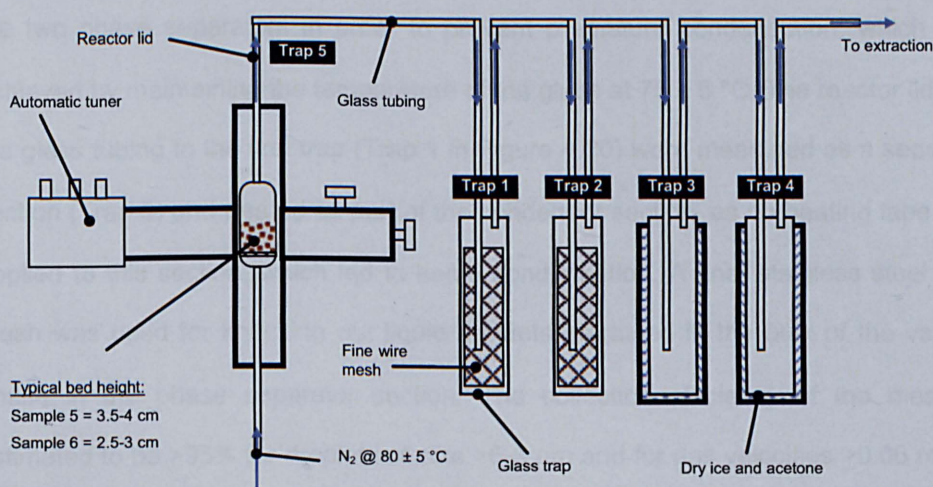


Figure 4.20 - Configuration A Experimental Setup.

Drill cuttings of Samples B and C in Table 4.3 were placed in cylindrical quartz reactor of internal diameter 0.071m. The reactor contained a perforated (5-7 mm diameter holes) support shelf, which allowed for even distribution of nitrogen throughout the bed. Approximately 121g of sample were used for each experiment. The sample height was 0.04-0.035m and 0.02-0.025m Samples B and C respectively.

Nitrogen heated to 80 °C was connected to the bottom of the reactor in order to provide an inert atmosphere. This also minimised condensation of vapours within the reactor and improved heat and mass transfer through the drill cuttings bed. Nitrogen flowrates of 7 ($Re_m = 203$) and 2 ($Re_m = 58$) L/min were tested in order to determine the effect of hot nitrogen flowrate on the overall performance of the system. Drill cuttings were also treated with hot Nitrogen only in order to confirm that no significant oil and water removal is observed for the durations used during microwave processing.

Vapours removed during microwave heating of the sample were captured in a phase separator section (Entrainment – Traps 1 & 2) followed by a condenser section (Vaporisation – Traps 3 & 4) before being sent into the main building extraction service. A heating tape was used between the end of the reactor lid and the end of the two phase separators in order to prevent premature condensation, which was achieved by maintaining the temperature of the glass at 75 ± 5 °C. The reactor lid and the glass tubing to the first trap (Trap 1 in Figure 4.20) were measured as a separate section (Trap 5) and treated as part of the condenser section, as no heating tape was applied to this section, which led to some condensation. A fine, stainless steel wire mesh was used for knocking out liquid droplets entrained in the bulk of the vapour phase in the phase separator section. The collection efficiency of the mesh is estimated to be >95% for droplets of size >6-8 μm and for gas velocities >0.06 m/sec (Perry & Green, 1997) – the system in this case has an approximate gas velocity >0.17m/sec (Ludwig, 1997). The condensers were cooled by using a mixture of dry ice (CAS#: 124-38-9) and acetone (CAS#: 67-64-1).

A single mode cavity was used for these experiments and was connected to the magnetron via a 0.5m straight waveguide section to an automatic tuner, followed by another 0.3m straight waveguide attached to a circulator, which was used to protect the magnetron by absorbing reflected microwaves. A magnetron capable of outputting up to 6kW was used (Figure 4.20).

The initial and final weight of the sample, initial and final bed height, mass of liquid (oil and water) collected in each trap (1-5) and water and oil content of the treated and untreated sample were measured ($\pm 0.01\text{g}$) and recorded. It was not possible to physically collect and separate the oil and water collected in Trap 5. As a result of this the comparison between entrained and vaporised oil and water only takes into account traps 1-4. Each sample was then treated for 3 different energy inputs and 2 different powers as detailed below in Table 4.3.

Sample	P_f (W)	P_r (W)	P_{eff} (W)	E_{eff} (kJ)
B	492	2.1	490	16, 26.6, 41.2
B	3512	3.4	3508	17.1, 44.9, 58.6
C	429	10.3	419	15.0, 18.2, 38.4
C	3444	177.4	3266	18.5, 37.1, 51.2

Table 4.3 - Experimental conditions for samples B and C used in the determination of the extent of entrainment and vaporisation present during microwave processing of drill cuttings.

Where P_{eff} is the average effective power (W), P_f is the average power forward (W) and P_r is the average power reflected (W) and E_{eff} is the effective energy (kJ). The average effective power (P_{eff}) is calculated as shown by Equation 4.3.

$$P_{eff} = P_f - P_r \quad \text{[Equation 4.3]}$$

The effective energy (E_{eff}) was calculated according to Equation 4.4 below. Where t is the processing time in seconds.

$$E_{eff} = \frac{P_{eff}}{1000} \times t \quad \text{[Equation 4.4]}$$

4.4.3 EXPERIMENTAL CONFIGURATION B

This setup was used in order to investigate the effect of using a different applicator type on the oil and water removal mechanisms, as well as allowing, the sample

surface temperature to be measured with time and energy input, for the first time. This was then used as supporting data for the results obtained using the entrainment/vaporisation rig (Configuration A) above.

Drill cuttings of Samples B and C were placed in a cylindrical Pyrex® container with an internal diameter of 0.071 m and filled to a height of 3 cm, giving an average sample mass of 120 and 240g for Sample B and C respectively. Samples were then positioned at the centre of a round PTFE (Polytetrafluoroethylene) plate used as a support, in the centre of a multimode cavity with dimensions 425 (W) x 425 (L) x 545 mm (H), as shown in Figure 4.21. The position of the sample in the tray was the same during all experiments. Microwaves were fed through a 90° E-Bend attached to the top of the multimode cavity, facing the surface of the sample perpendicularly. The bend was connected to two further 90° E-Bends, an automatic tuner, a short straight waveguide section of 30cm, followed by a circulator and the magnetron, which was capable of outputting a maximum power of 6 kW.

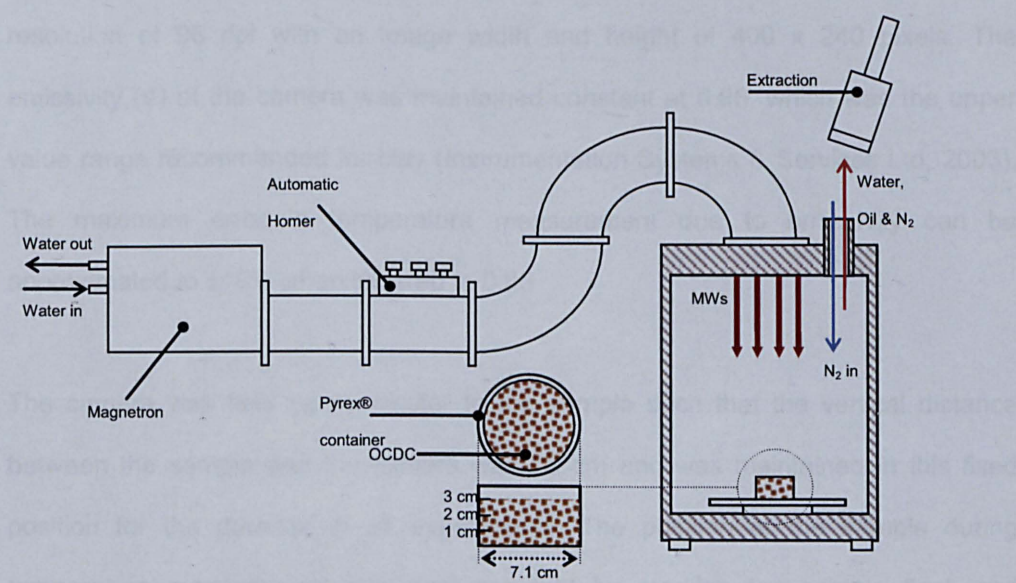


Figure 4.21 - Configuration B experimental setup.

The sample was treated at the powers and times shown below in Table 4.4. The cavity was flushed with nitrogen prior to the experiment and fed continuously into the cavity during the experiment at a flowrate of 5 L/min in order to maintain an inert atmosphere during heating. An extraction point was placed directly above the

extraction aperture in the cavity in order to collect the water and oil vapour given off during microwave treatment.

Sample #	Effective Power (W)	Times (secs)
B	523	30, 60, 90, 120, 150, 180, 210, 240, 270
B	2554	7.5, 15, 22.5, 30, 37.5, 45, 52.5, 60
C	508	30, 60, 90, 120, 150, 180, 210, 240, 270
C	2550	7.5, 15, 22.5, 30, 37.5, 45, 52.5, 60

Table 4.4 - Experimental conditions for Samples B and C using configuration B.

Temperature measurements were carried out using an optical thermal imaging camera, Raytek ThermoView Ti30, with a spectral and temperature measurement range of 7-14 μm and 0 to 250 $^{\circ}\text{C}$ ($\pm 2\%$) respectively. The camera used a single laser dot, which meets the IEC class 2 and FDA Class II requirements, and had a field of view (FOV) of 17 $^{\circ}$ (Horizontal) X 18 $^{\circ}$ (Vertical). The final image had a resolution of 96 dpi with an image width and height of 400 x 240 pixels. The emissivity (ϵ) of the camera was maintained constant at 0.95, which was the upper value range recommended for clay (Instrumentation Systems & Services Ltd, 2003). The maximum error in temperature measurement due to emissivity can be approximated to $\pm 10\%$ when lowered to 0.85.

The camera was held perpendicular to the sample such that the vertical distance between the sample and the camera was 75 cm and was maintained in this fixed position for the duration of all experiments. The position of the sample during temperature measurement was kept constant by marking the sample flask and aligning it to a mark made on the tray as well as a mark made in the thermal insulating brick mats, which were used to support the sample as the temperature measurements were taken. The measurement procedure involved removing the sample from the cavity immediately after microwaves were turned off and taking the thermal image of the sample's surface. The images were analysed and extracted

using the camera's own proprietary software: InsideIR version 1.2.1. During this experiment, the initial sample weight, final sample weight, oil and water content and temperature distribution of the sample were recorded.

4.4.4 *EXPERIMENTAL CONFIGURATION C*

Drill cuttings from Sample C were used for these experiments. Samples weighing $50.4\text{g} \pm 4.4$ were placed in a fine wire mesh tray, which was fitted into a 4 cm diameter cylindrical glass reactor. The inlet of the reactor was connected to a 2.2kW VEIT steam generator (Model# 2365), which generated $3.75\text{ bar} \pm 0.25$ steam at a rate of $3\text{ kg/hour} \pm 0.3$. The operation of the steam generator is described in detail in its operation manual. The outlet of the reactor was connected to a straight section of Quickfit® glass tubing followed by a 120° bend into a condenser. The condensed oil and water removed during steam distillation were collected in a reflux trap, with water being drained continuously off the bottom of the trap. The oil was lighter than the water and was extracted at the end of the experiment. Figure 4.22 shows the experimental setup used in this case.

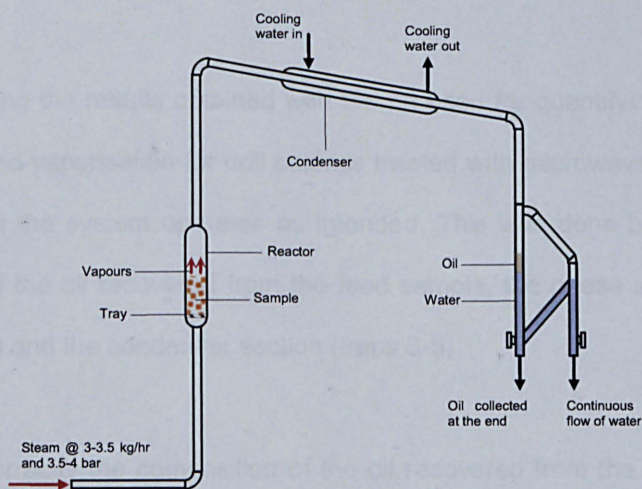


Figure 4.22 - Configuration C experimental setup.

Two different sample heights were used in order to test the effect of density on oil removal efficiency. Table 4.5 summarises the sample conditions for this experiment.

Sample C	
Av. Height 1 (cm)	Av. Height 2 (cm)
3.38 ± 0.53	4.80 ± 0.42
Av. Density 1 (g/cm ³)	Av. Density 2 (g/cm ³)
1.18 ± 0.01	0.85 ± 0.05

Table 4.5 - Configuration C experimental conditions.

Samples were treated for a total of 120 minutes. The volume of oil collected was monitored over time, and recorded in 15 minute intervals. The final oil content of the treated sample was also measured. The overall energy consumed for the duration of the experiment was recorded using an Elcomponent SPC mini data logger, acquiring data automatically every 20 seconds.

4.4.5 RESULTS AND DISCUSSION

Sections 4.4.6 to 4.4.12 provide the results and discussions to the various experiments carried out as per Figure 4.20.

4.4.6 VALIDATION OF EXPERIMENTAL CONFIGURATION A

Before analysing the results obtained with the rig used for quantifying the amount of entrainment and vaporisation for drill cuttings treated with microwaves, it is important to confirm that the system operates as intended. This was done by measuring the composition of the oil recovered from the feed sample, the phase separator section (traps 1 and 2) and the condenser section (traps 3-5).

If operating correctly the composition of the oil recovered from the phase separator section is expected to have an almost identical composition to the oil composition of the oil extracted from the feed material, whereas the oil recovered in the condenser section is expected to be slightly shifted towards the left, with a greater percentage of lighter hydrocarbon chains as a result of steam distillation/vaporisation effect (i.e.

lighter components will be removed first before heavier components). This assumes that there would still be some residual oil content in the feed sample (i.e. the heavier components). Figure 4.23 below shows the variation of oil composition for oil extracted from the feed sample, for oil obtained from the phase separator section for Sample B treated at 490 W and 41 kJ, and for oil obtained from the condenser section for the same sample.

Chromatogram Plots

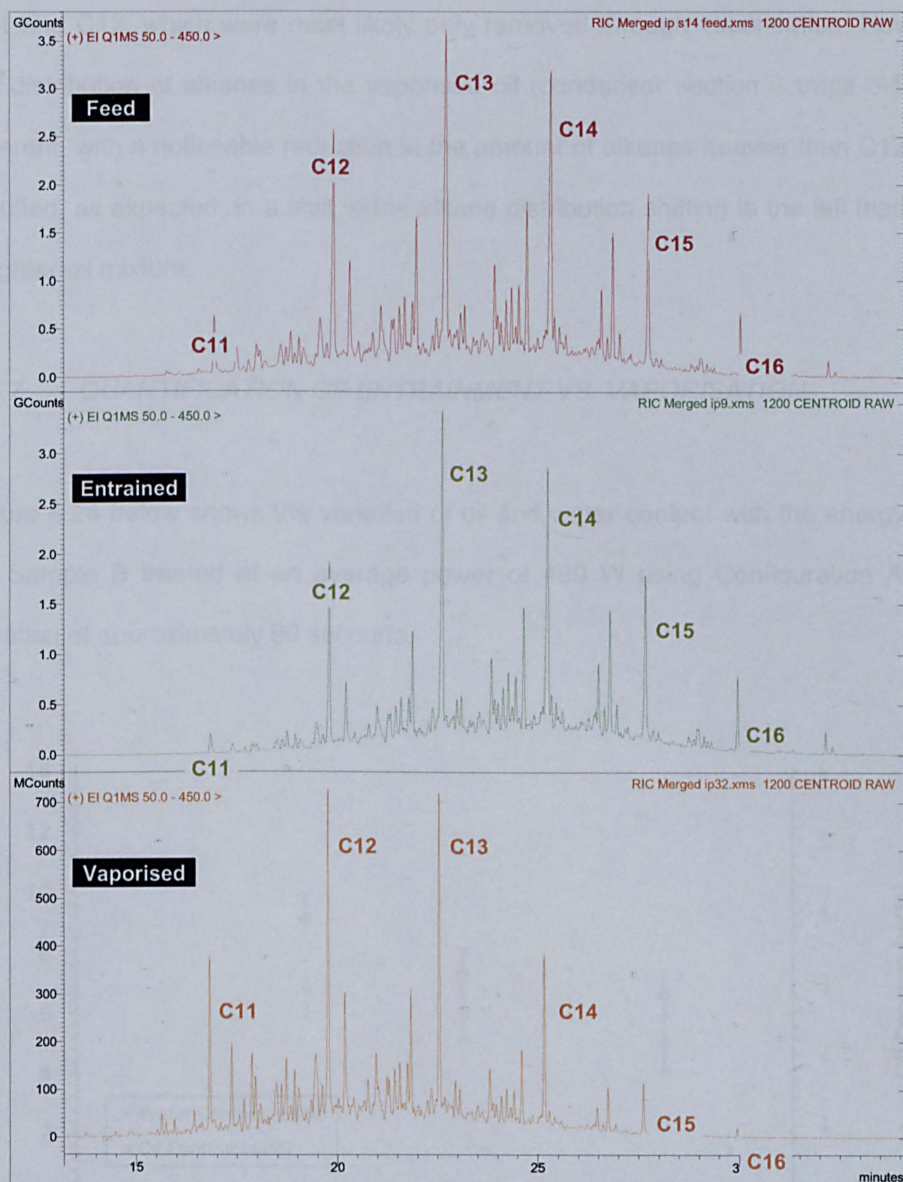


Figure 4.23 - Oil composition for Sample B feed sample, oil from the phase separator traps (Entrained – 1-2) and oil from the condenser section (Vaporised – traps 3-5) for Sample B treated at 490 W and 41 kJ.

The composition of the oil in the feed was similar to that reported in the literature (Robinson, et al., 2009) which is important as oil composition and removal comparisons between samples can be made without significant adjustments. Figure 4.23 shows that the range of alkanes in the feed and entrainment and vaporisation sections are similar, suggesting there is no significant decomposition of the oil. In terms of chain size distribution, the composition of the oil collected in the phase separator (traps 1-2) was very similar to that of the feed, except for lower quantities of C11 and C12, which were most likely only removed through vaporisation. However, the distribution of alkanes in the vaporised oil (condenser section – traps 3-5) was different, with a noticeable reduction in the amount of alkanes heavier than C12. This resulted, as expected, in a shift in the alkane distribution shifting to the left leading to a lighter oil mixture.

4.4.7 QUANTIFICATION OF ENTRAINMENT VS. VAPORISATION

Figure 4.24 below shows the variation of oil and water content with the energy input for Sample B treated at an average power of 490 W using Configuration A for a duration of approximately 90 seconds.

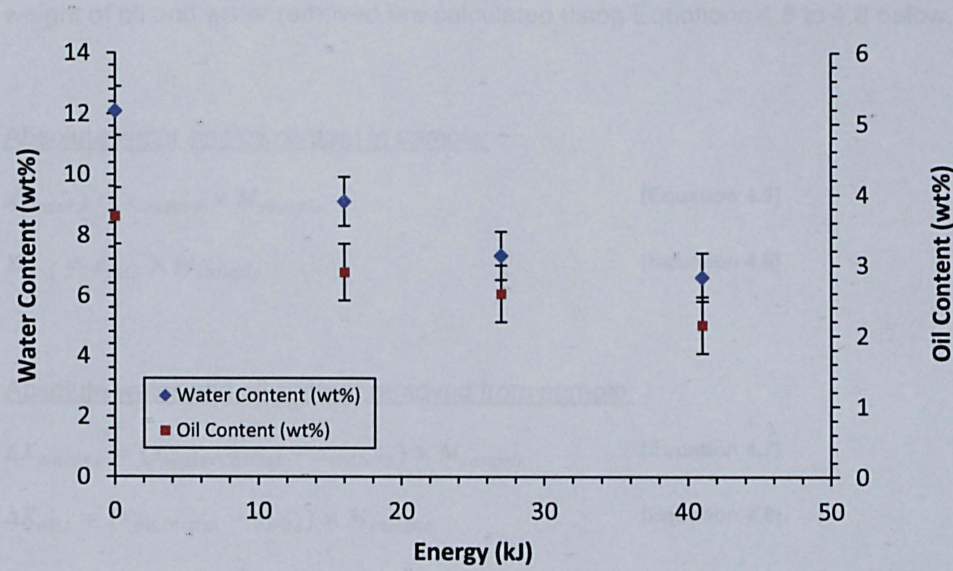


Figure 4.24 - Variation of oil and water content vs. energy input for sample B treated using configuration A at 490 W and 16, 27 and 41 kJ.

As seen from Figure 4.24 the oil and water content decreased with increasing processing time as expected. The water content decreased from around 12.1 wt% to just over 6.5 wt%, whereas the oil content decreased from 3.7 wt% to 2.2 wt%. As was the case with results obtained above (Figure 4.16), the greatest drop in oil and water content was observed within the first 30 seconds of processing. This is in line with the previous hypothesis that initially removal is easier as liquid is present in free form and mass transfer is limited mainly by the drill cuttings bed itself.

The data in Figure 4.24 can then be used to estimate the absolute total amount of oil and water in grams that would be removed at each of the given energy inputs tested (16, 27 and 41 kJ). This can then be compared to the overall amount of oil and water collected in Traps 1-4 (Figure 4.20) allowing for a full mass balance to be carried out.

Table 4.6 below shows the initial weight of each sample tested at 16, 27 and 41 kJ, the absolute weight of oil and water still present in the sample and the weight of oil and water removed from the sample (based on average water and oil content of Figure 4.24). The absolute weight of water and oil present in the sample and the weight of oil and water removed are calculated using Equations 4.5 to 4.8 below.

Absolute water and oil content in sample:

$$X_{water,i} = x_{water,i} \times M_{sample} \quad \text{[Equation 4.5]}$$

$$X_{oil,i} = x_{oil,i} \times M_{sample} \quad \text{[Equation 4.6]}$$

Absolute water and oil content removed from sample:

$$\Delta X_{water,i} = (x_{water,initial} - x_{water,i}) \times M_{sample} \quad \text{[Equation 4.7]}$$

$$\Delta X_{oil,i} = (x_{oil,initial} - x_{oil,i}) \times M_{sample} \quad \text{[Equation 4.8]}$$

Where X_{water} and X_{oil} are the amount of water and oil in the sample for a given time/energy input "i". $x_{water,i}$ and $x_{oil,i}$ are the water and oil weight fractions at the same given time/energy input "i". M_{sample} is the overall initial mass of the sample (Rock, oil and water). $x_{water,initial}$ and $x_{oil,initial}$ are the initial water and oil weight fractions respectively. $\Delta X_{water,i}$ and $\Delta X_{oil,i}$ are the amount of water and oil removed from the sample for a given time/energy input "i".

Energy (kJ)	M_{sample} (g)	$X_{water,i}$ (g)	$X_{oil,i}$ (g)	$\Delta X_{water,i}$ (g)	$\Delta X_{oil,i}$ (g)	$\Delta X_{water,i} + \Delta X_{oil,i}$ (g)
0	121.26	14.67	4.49	0	0	0
16	121.67	10.66	3.4	4.01	1.09	5.1
27	121.28	8.25	2.93	6.42	1.56	7.98
41	120.82	7.26	2.37	7.41	2.12	9.53

Table 4.6 - Sample weight, absolute water and oil content present in the sample and removed from the sample for different energy inputs (16, 27 and 41 kJ). The data applies for Sample B treated using configuration A at 490 W and 90 secs.

The data in Table 4.6 shows as expected an increase in the mass of oil and water removed from the sample with increasing energy input. It is also interesting to notice how the ratio of mass of oil removed per mass of water removed remains fairly constant at $0.27 \pm 0.3g$, suggesting a similar amount of water is used each time to remove an equivalent amount of oil. The data in Table 4.6 was then used for a mass balance comparison against data collected for Traps 1-5. Figure 4.25 shows the total weight loss, measured as the sum of the total amount of liquid physically collected in each Trap (Figure 4.20), and as calculated from the measured oil and water content data in Figure 4.24 and the data presented above, in Table 4.6.

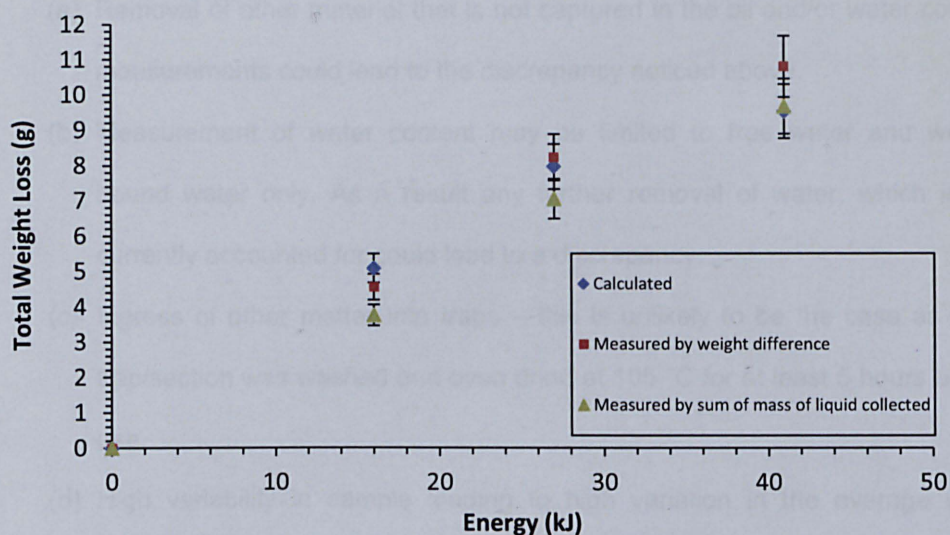


Figure 4.25 - Measured and calculated total weight loss vs. Energy input for Sample B treated using configuration A at 490 W and 16, 27 and 41 kJ.

As seen in Figure 4.25, the weight loss as measured by sample weight difference and the calculated weight loss at 16 and 27 kJ were close, with a $\leq 0.5\text{g}$ difference between the values.

The weight loss, as measured by the sum of liquid collected in the various traps (1-5), was constantly lower than the weight loss as measured by sample weight difference. The difference between measured values remained constant at approximately 1g. The discrepancy between the weight losses as measured by the two different methods used can be explained by vapours which were removed but were not captured in the condenser section.

At 41 kJ there was a noticeable discrepancy between the weight loss measured by difference in sample weight and that calculated from the water and oil content measurements. Figure 4.25 shows the calculated value underestimates the actual total weight loss measured by $>1.2\text{g}$. This discrepancy could be explained by the following:

- (a) Removal of other material that is not captured in the oil and/or water content measurements could lead to the discrepancy noticed above.
- (b) Measurement of water content may be limited to free water and weakly bound water only. As a result any further removal of water, which is not currently accounted for could lead to a discrepancy.
- (c) Ingress of other matter into traps – this is unlikely to be the case as each trap/section was washed and oven dried at 105 °C for at least 5 hours before use.
- (d) High variability in sample leading to high variation in the average water content (± 0.8 wt%). If the initial mass of water present is calculated with the maximum possible water content (12.9 wt%), then the calculated mass loss = 10.5, which is within error to the amount measured of 10.8g.

The measured total weight loss data presented in Figure 4.25 can be broken down further into weight loss due to vaporisation (Traps 3,4 and 5) and entrainment (Traps 1 and 2) for the energy inputs used. It is then possible to calculate the amount of entrainment and vaporisation as a percentage of the total weight loss using Equations 4.9 to 4.10 below.

$$\Delta X_{vap,i} = \sum_{vap} X_{water,i} + \sum_{vap} X_{oil,i} \quad \text{[Equation 4.9]}$$

$$\Delta X_{ent,i} = \sum_{ent} X_{water,i} + \sum_{ent} X_{oil,i} \quad \text{[Equation 4.10]}$$

Where $\Delta X_{ent,i}$ and $\Delta X_{vap,i}$ are the weight measured for liquid collected (water and oil) in the phase separator (Entrainment – Traps 1 and 2) and condenser sections (Vaporisation – Traps 3, 4 and 5) respectively. $\sum_{vap} X_{water,i}$ and $\sum_{vap} X_{oil,i}$ are the sum of the weight of water and oil respectively collected at a given time/energy input “i” in the condenser sections (Traps 3-5). $\sum_{ent} X_{water,i}$ and $\sum_{ent} X_{oil,i}$ are the sum of the weight of water and oil respectively collected at a given time/energy input “i” in the condenser sections (Traps 1-2). Note that all entrained liquid is assumed to be

collected in traps 1 and 2. Figure 4.26 shows the weight loss, as measured by the sum of liquid collected in traps, due to vaporisation and entrainment for energy inputs of 16, 27 and 41 kJ.

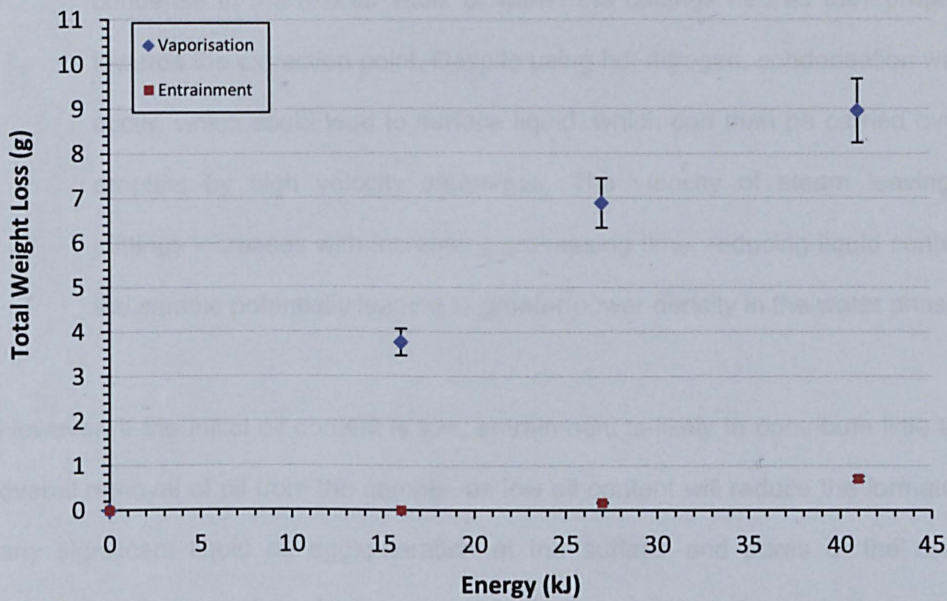


Figure 4.26 - Variation of weight loss due to vaporisation and entrainment with energy input for Sample B treated using configuration A at 490 W and 16, 27 and 41 kJ.

Figure 4.26 shows an increase in weight loss with increasing energy input as expected. It is also clear from Figure 4.26 that the majority of the liquid content (>93%) is removed through vaporisation under the conditions used in this case. No measurable entrainment was noticed until 27 kJ, which is unexpected as entrainment was initially expected to have a greater impact on removal in the beginning due a greater amount of free water available than at the end of treatment. However, this behaviour could be explained as follows:

- (a) As liquid content is removed from the sample the amount of energy dissipated per unit time and sample volume increases (power density), and as a result steam is generated at faster rates. If the rate of generation is fast enough, it may be possible to partially pressurise the sample (**Constant, et**

al., 1996), increasing the velocity of the steam leaving the cuttings structure. As entrainment is a function of gas/vapour velocity (Perry & Green, 1997), an increase in entrainment would be expected.

- (b) Oil and water removed as vapours during initial removal stages, can condense in the reactor walls or within the cuttings bed as they propagate towards the extraction point. Despite using hot nitrogen, condensation will still occur, which could lead to surface liquid, which can then be carried over as droplets by high velocity steam/gas. The velocity of steam leaving the cuttings increases with increasing processing time, reducing liquid content in the sample potentially leading to greater power density in the water phase..

However, if the initial oil content is low, entrainment is likely to contribute little to the overall removal of oil from the sample, as low oil content will reduce the formation of any significant liquid oil agglomeration at the surface and pores of the sample, increasing the overall surface area available for heat transfer and, thus removal through vaporisation. The amount of liquid removed through entrainment and vaporisation can then be broken down into its oil and water components. This allows for the identification of any preferential oil or water removal occurring as a result of entrainment or vaporisation. Figures 4.27 and 4.28 below show the variation of oil and water entrained and vaporised for samples A and B treated at 16, 27 and 41 kJ.

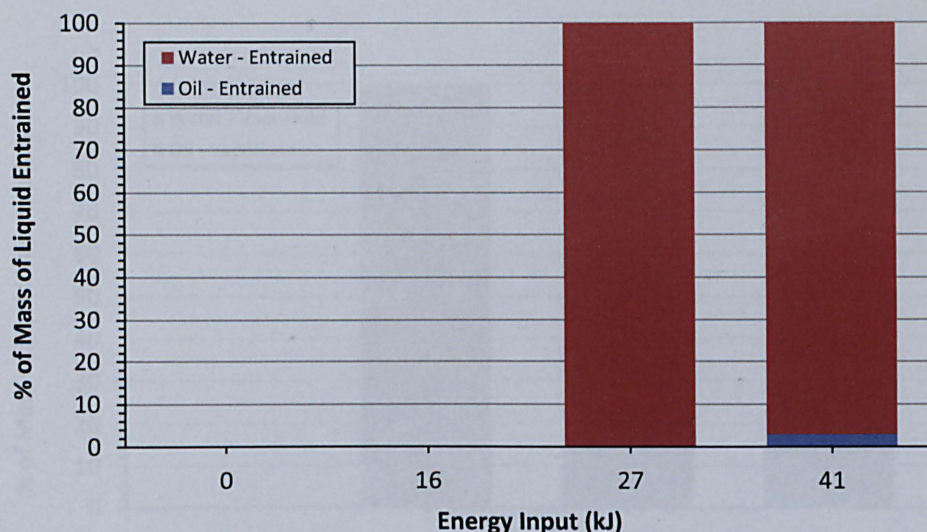


Figure 4.27 - Variation of oil and water percentages for %entrainment for Sample B treated using configuration A at 490 W and 16, 27 and 41 kJ.

As seen from Figure 4.27 the majority of the liquid entrained (>97%) is water, suggesting that for the above experimental conditions, even at the highest energy input, only a very small percentage (<1% at 41 kJ) of the overall oil removal is through entrainment. The low percentage of entrainment can be explained by the structure of this particular sample. From a qualitative point of view this particular sample did not contain any significant surface liquid, in comparison to, for example, Sample C, where there was a substantial layer of surface liquid. The lack of any significant surface liquid is likely to minimise the chance of entrainment leading to the results obtained in Figure 4.28.

In addition, the fairly open structure between drill cuttings particles allows for vapour to propagate more easily through the bed of cuttings, reducing the potential for pressure build-up within the bed itself and generation of high pressure and temperature steam. As discussed previously, increasing the internal pressure within the sample increases the driving force for steam generated within the cuttings to leave, which increases the potential for high velocity steam and consequently entrainment. Figure 4.28 shows the percentage of water and oil of the total amount removed through vaporisation for samples treated at 16, 27 and 41 kJ.

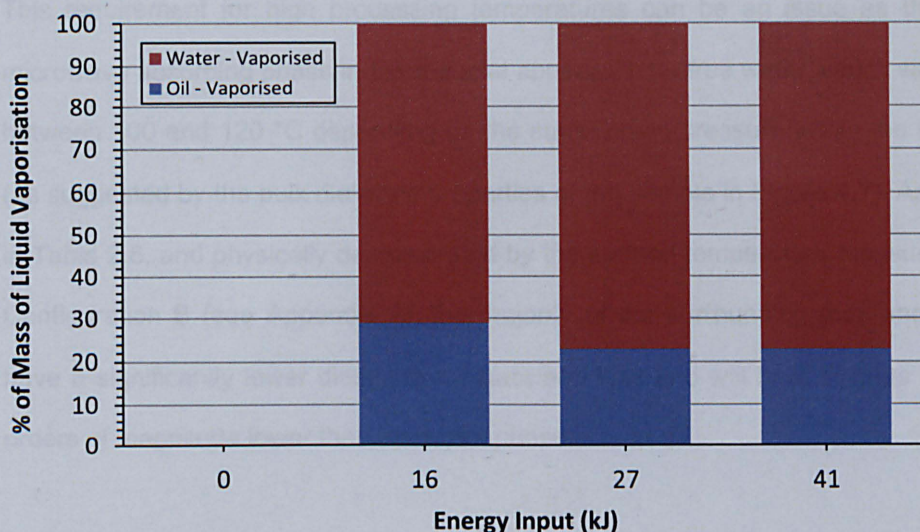


Figure 4.28 - Variation of oil and water percentages for %vaporisation for Sample B treated using configuration A at 490 W and 16, 27 and 41 kJ.

As seen from Figure 4.28 approximately 25-30% of the mass of liquid vaporised is oil. It is important to note that the ratio of percentage of water to oil with increasing energy input decreases from 2:1 to 3:1, suggesting that the volume of water required for oil removal increases with decreasing liquid content. This can be explained by the lower probability of contact between the remaining oil and water phases.

4.4.8 INVESTIGATION OF OIL VAPORISATION MECHANISMS

Oil can be vaporised in one of two ways, either through direct vaporisation of the liquid or through steam distillation of the oil phase. In direct vaporisation the oil phase is heated directly by microwaves (negligible due to very low dielectric properties), or through heat transfer, by the rock and water phase. The extent of vaporisation will depend on the sum of the vapour pressure multiplied by the vapour fraction of each component of the oil at a given temperature, being equal to that of the surrounding air/void pressure. However, as the vapour pressure of each component is dependent on its boiling point, lighter hydrocarbons will be vaporised preferentially at the beginning of heating. As a result, increasingly higher temperatures, and consequently energy input, are required in order vaporise the remaining oil.

This requirement for high processing temperatures can be an issue as the main microwave absorbing phase in the material appears to be free water, which vaporises between 100 and 120 °C depending on the surrounding pressure within the material (as suggested by the bulk dielectric properties of the sample in Figure 4.7). As shown in Table 2.6, and physically demonstrated by the surface temperature measurements Configuration B (see Appendix 2), the majority of the surrounding rock and the oil have a significantly lower dielectric constant and loss and will heat at rates that are orders of magnitude lower than the water phase.

These lower heating rates eventually lead to thermal equilibrium between the sample and the surrounding air, where the heat gained by the sample is equal to that lost. As a result, this would suggest that vaporising heavier hydrocarbon chains may require a significant amount of energy before vaporisation can be achieved, or may not be achievable at all if the temperature required is higher than that which can be reached during equilibrium. Nevertheless, the heating of ferromagnetic minerals, such as pyrite, and of bound water could result in high temperature hot spots leading to further removal of heavier hydrocarbons in the oil through direct vaporisation.

Steam distillation is, potentially, the other mechanism from which oil can be removed through during vaporisation. In steam distillation, vaporisation occurs at significantly lower temperatures, due to immiscibility between phases. In an emulsion the vapour pressure of the liquid is the sum of the actual vapour pressure of each component at a given temperature, rather than adjusted by the vapour fraction of each component. This leads to oil removal at temperatures lower than those that would be required to remove the same components through direct vaporisation.

In order to demonstrate that steam distillation is a viable mechanism for oil removal through vaporisation in this case, an experimental setup using Configuration C was used to treat oil contaminated drill cuttings (Sample C – bulk density $1.18 \pm 1 \text{ g/cm}^3$)

with steam over a treatment time of 120 mins. Figure 4.29 shows the variation of oil removal with time.

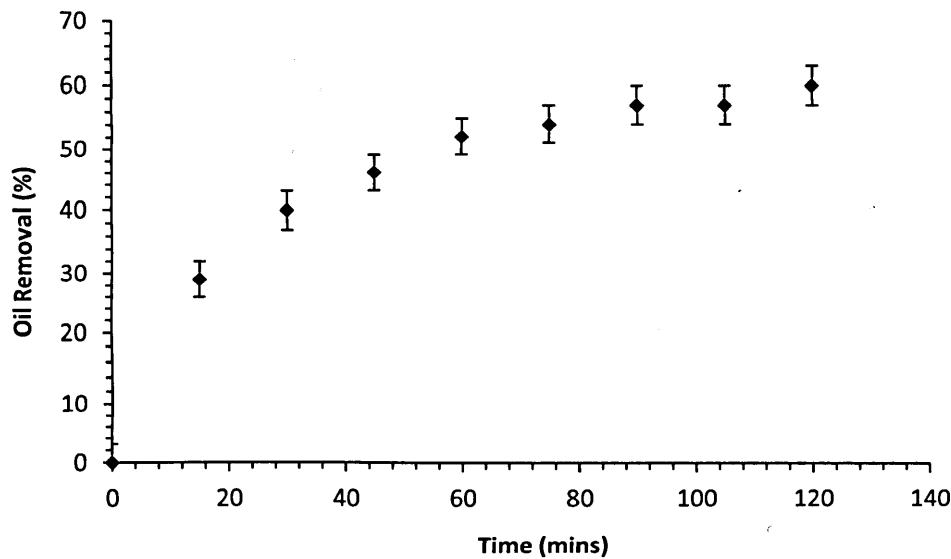


Figure 4.29 - Sample C, 1.18 g/cm³, treated with a 2.2 kW VEIT steam generator.

As seen from Figure 4.29 above, oil removal increases with processing time, however, >50% of the oil is removed within the first 40-50 minutes. Oil collection then plateaus at 55-60% as it reaches the end of the experiment. This is expected as the probability and extent of contact between the steam and the oil phases decreases with decreasing volume of oil present within the sample. This leads to an overall decrease in the amount of oil collected with time, and thus oil removal efficiency. In this case, 60% of the oil present in the cuttings was collected at $t \geq 90$ mins, which equates to a reduction in oil content from 7.8 wt% to 3.1 wt%

Figure 4.30 shows the variation in the amount of oil removed with time for samples with different bulk densities.

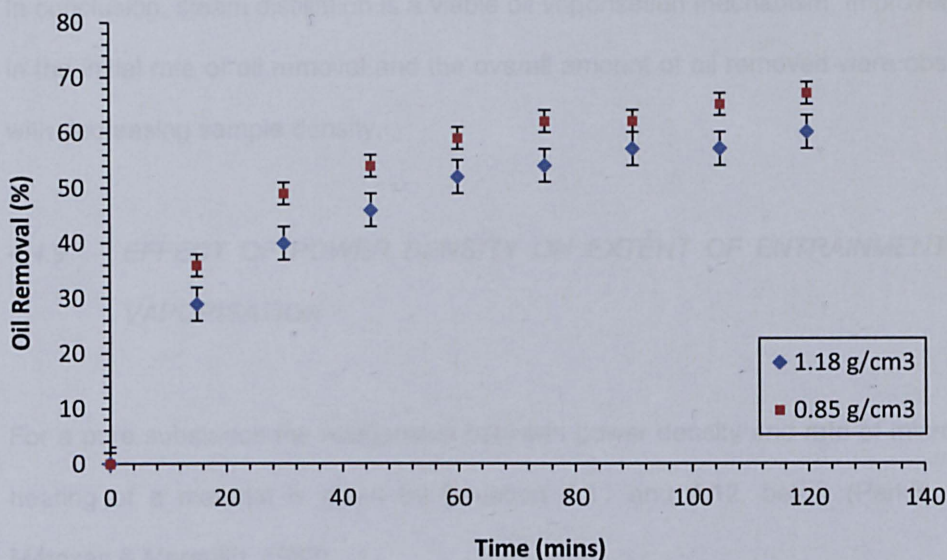


Figure 4.30 - Sample C, 0.85 and 1.18 g/cm³, treated with a 2.2 kW VEIT steam generator.

As seen from Figure 4.30 the volume of oil collected for samples with a density of 0.85 g/cm³ was around 5-10% greater at any point in time, leading to an overall improvement in oil removal from 60% (1.18 g/cm³) to 67% (0.85 g/cm³) at 120 mins. Interestingly the improvement is observed both at the initial stage of oil collection (0<t<50 mins), and also in final total amount of oil collected (t≥ 90 mins). This can be attributed to two factors:

- (1) Greater porosity in the less dense sample allows for a larger number of paths to be formed within the bed, increasing the overall mass transfer.
- (2) Improved contact likelihood as a result of higher overall surface area available for contact between the steam and the oil present in the sample. If the sample is compact, it is possible that some of the oil is locked away within the bed, which due to high compaction, becomes inaccessible to the steam passing through the bed.

The effect of density on removal is likely to be less significant during microwave treatment, as steam is generated within the material. If the water is well distributed throughout the material it is possible that oil removal is improved in comparison to conventional steam distillation.

In conclusion, steam distillation is a viable oil vaporisation mechanism. Improvements in the initial rate of oil removal and the overall amount of oil removed were observed with decreasing sample density.

4.4.9 EFFECT OF POWER DENSITY ON EXTENT OF ENTRAINMENT AND VAPORISATION

For a pure substance the relationship between power density and rate of microwave heating of a material is given by Equation 4.11 and 4.12. below (Perkin, 1983; Metaxas & Meredith, 1983).

$$P_d = 2\pi f \epsilon_0 \epsilon''_{eff} |E|^2 = \frac{Q}{Vt} \quad \text{[Equation 4.11]}$$

$$\frac{Q}{Vt} = \frac{m}{Vt} c_p \Delta T + \frac{m}{Vt} L = \frac{\rho}{t} c_p \Delta T + \frac{\rho}{t} L = P_d \quad \text{[Equation 4.12]}$$

Where P_d is the power density (W/m^3), f is the microwave frequency (Hz), ϵ_0 is the permittivity of free space ($8.85 \times 10^{-12} \text{ F/m}$), ϵ''_{eff} is the relative dielectric loss factor and E is the magnitude of the electric field (V/m). Q is the energy put into the sample (kJ) m is the mass of material (kg), t is the time (secs), V is the volume of material (m^3), c_p is the specific heat capacity (kJ/kg K), ΔT is the temperature difference ($^{\circ}\text{C}$), ρ is the density (kg/m^3) and L is the latent heat of vaporisation (kJ/kg). From equation 4.12 above it is clear that for a fixed sample mass, specific heat capacity and volume, increasing the power density leads to a proportional increase in the temperature driving force and a decrease in heating time (t), which in effect dictate the rate of heating and vaporisation.

As discussed above in Section 4.4.8, the rate of steam generation can have an impact in the amount of entrainment. Figure 4.31 shows the variation in total weight loss as measured by the difference in sample weight for Sample B treated at 16 to 58 kJ at 490 W and 3508 W. It is important to note that as the sample size and

experimental setup remains constant, an increase in power is directly proportional to an increase in the power density.

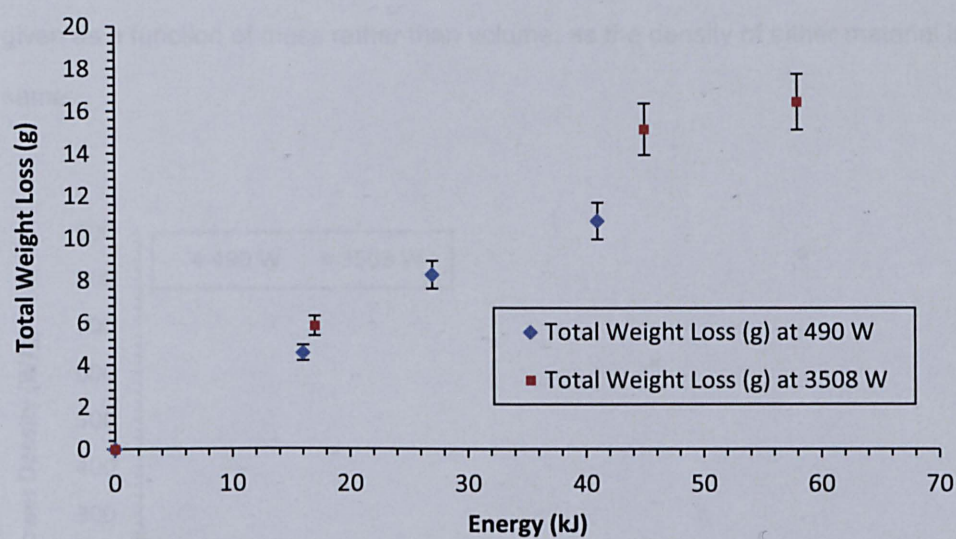


Figure 4.31 - Total weight loss for Sample B treated using configuration A at 490 W and 3508 W at energy inputs of 16 to 58 kJ.

Figure 4.31 shows an increasing weight loss with increasing energy input for the sample treated at 3512 W, as was the case with the sample treated at 490 W. The data shows a slightly higher overall weight loss for the same energy input at 3508 W, which can be explained by the higher overall power, and thus power density in the water phase. Figure 4.32 shows the difference in power density in the water phase between the samples treated at 490 W and the samples treated at 3508 W. The power density is calculated in accordance to Equation 4.13 below, which assumes microwaves are only dissipated in the water phase. This assumption will be accurate in most cases, but needs to be considered with decreasing water content, as this may lead to the portion of power dissipated in the other phases (oil and rock) increasing.

$$\frac{P_{d,i}}{\rho} = \frac{P}{X_{water,i}}$$

[Equation 4.13]

Where $\frac{P_{d,i}}{\rho}$ is the power density (W/g) for a given processing time/energy input “i”, P is the average effective power (W) and $X_{water,i}$ is the amount of water (g) present within the sample a given processing time/energy input “i”. Note the power density here is given as a function of mass rather than volume, as the density of either material is the same.

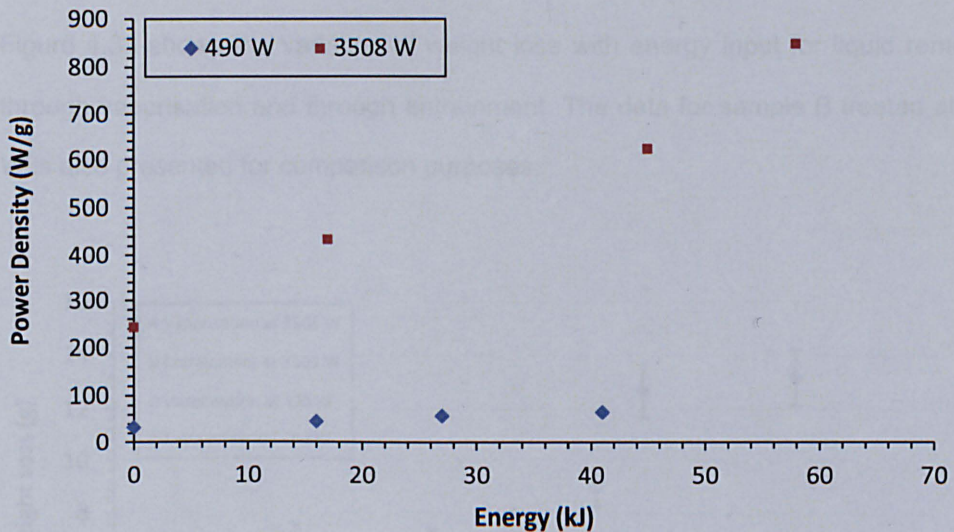


Figure 4.32 - Variation of power density for Sample B treated using configuration A at 490 W and 3508 W at energy inputs of 16 to 58 kJ.

Figure 4.32 shows an increase in power density with increasing energy input, for both samples treated at 490 and 3508 W, however, the power density at 3508 W is significantly higher and appears to increase exponentially with energy input. This supports the data presented in Figure 4.31 and can explain the greater weight loss observed at 3508 W. At higher power densities the following apply:

- (a) Heat transfer is improved – for a given energy input, higher power densities equate to lower processing times and therefore heat losses to the surrounding.
- (b) Increased internal pressure, steam temperature and velocity – increasing the power density leads to pressure driven vapour flow from within the cuttings at

higher velocity and turbulence. This can enhance both mass transfer from an entrainment point of view, as well as mass transfer from a vaporisation point of view, as better mixing can be achieved between the steam and the oil phase. However, it is expected that at higher steam velocities, benefits gained by improved entrainment will overcome benefits gained in vaporisation through better mixing.

Figure 4.33 shows the variation of weight loss with energy input for liquid removed through vaporisation and through entrainment. The data for sample B treated at 490 W is also presented for comparison purposes.

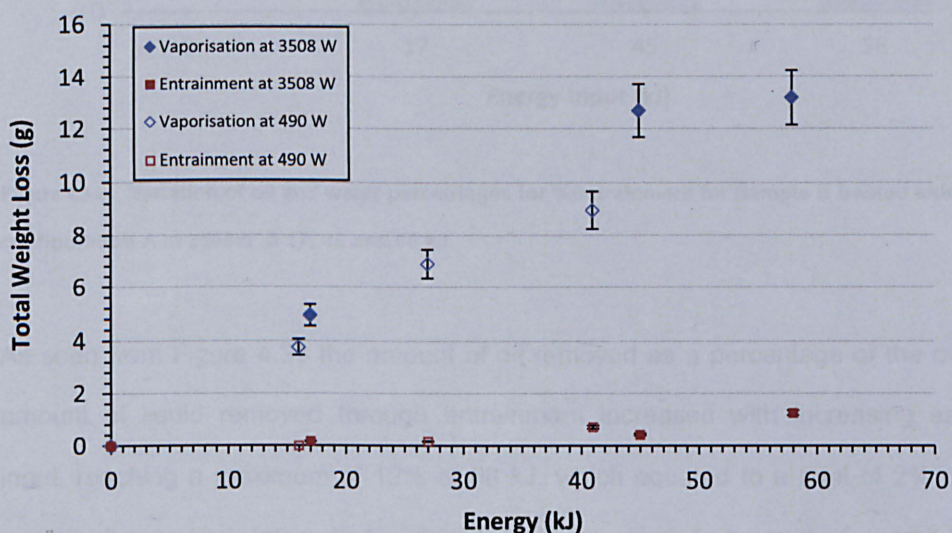


Figure 4.33 - Variation of weight loss due to vaporisation and entrainment with energy input for Sample B treated using configuration A at 3508W and 17, 45 and 58 kJ.

As expected, liquid removal through vaporisation is still significantly greater than liquid removed through entrainment. However, a small amount of entrainment (3%) was observed at an earlier energy input (17 kJ), which is expected as the average velocity of the steam leaving the sample is expected to be greater for the sample treated at 3508 W. Despite this initial improvement in entrainment over the sample treated at 490 W, entrainment appeared to be comparatively lower at higher energy inputs. Figure 4.34 below shows the variation of oil and water percentages for

entrainment for samples treated at 3508W and 17, 45 and 58 kJ. This is compared to the data shown in Figure 4.27.

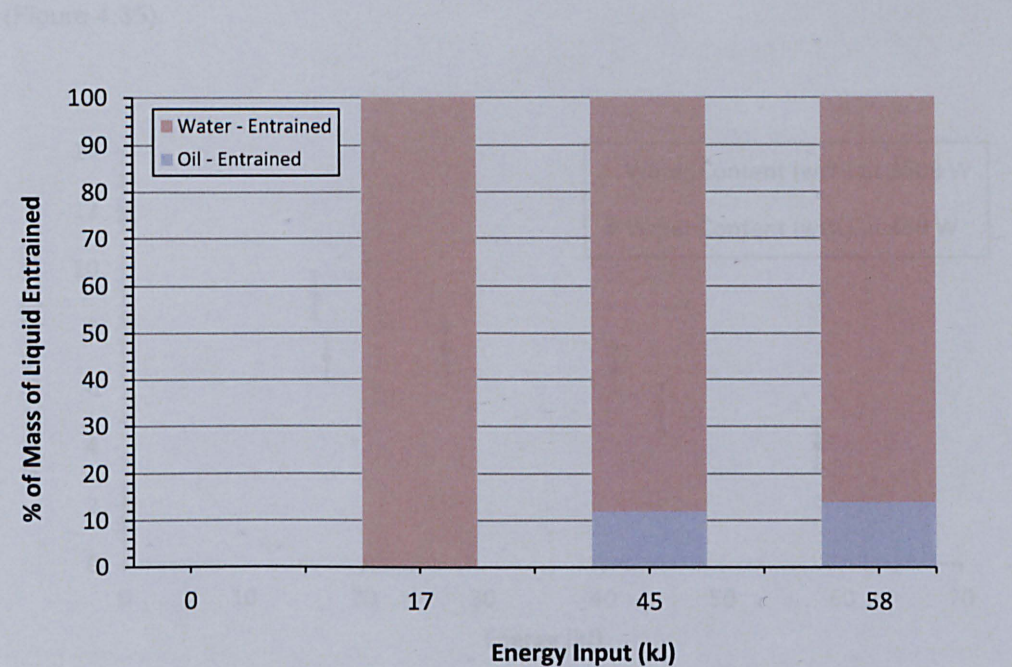


Figure 4.34 - Variation of oil and water percentages for %entrainment for Sample B treated using configuration A at 3508W at 17, 45 and 58 kJ.

As seen from Figure 4.34 the amount of oil removed as a percentage of the overall amount of liquid removed through entrainment increased with increasing energy input, reaching a maximum of 12% at 58 kJ, which equated to a total of 2% of the overall oil removed. Interestingly, despite a lower absolute amount of overall liquid removed through entrainment for the sample treated at 3508 W (0.43g at 3508 W vs. 0.71g at 490 W), the percentage and absolute amount of oil removed through entrainment was slightly greater for the sample treated at 3508 W.

This is a significant finding as it suggests that oil entrainment is preferential at higher power densities. This finding can be explained by the faster generation of steam at 3508 W (See Equation 4.13), which could lead to lower heat loss to other phases. Additionally, a greater degree of superheating could also occur, which could reduce both the amount of re-condensation and the overall water content available for entrainment. This would lead to an increase in the total amount of water removed

through vaporisation and is supported by the increase in overall weight loss observed in Figure 4.33 as well as the lower water content for the sample treated at 3508 W (Figure 4.35).

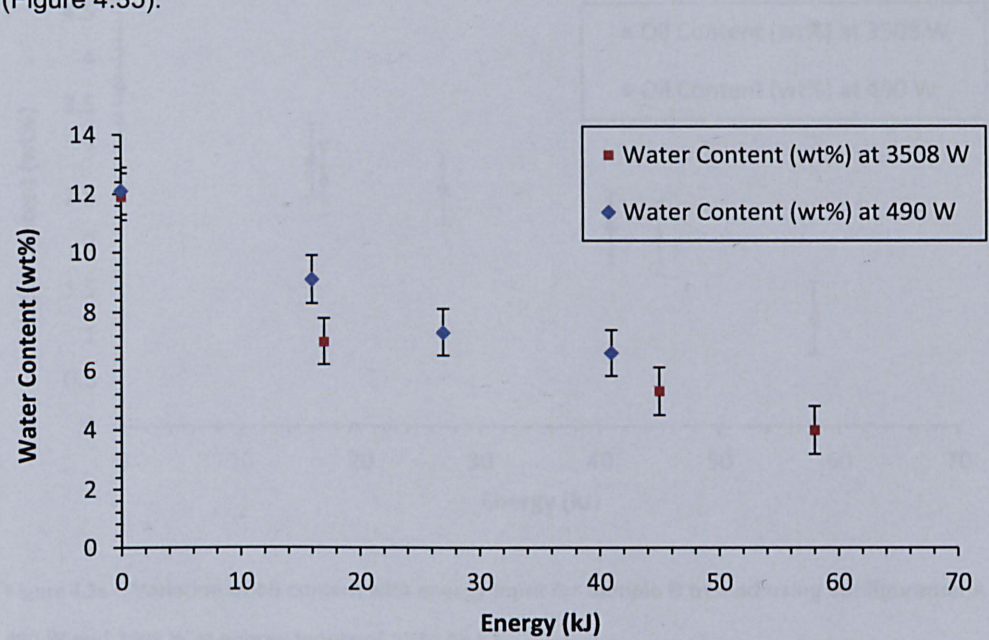


Figure 4.35 - Variation of water content with energy input for Sample B treated using configuration A at 490 W and 3508 W at energy inputs of 16 to 58 kJ.

Figure 4.35 shows a decrease in water content for samples treated both at 490 and 3508 W as expected. The data shows that at 41 kJ, the sample treated at 3508 W has, at most, approximately 1 wt% less water content in comparison to the sample treated at 490 W. Given the data in Figure 4.35 above, it is uncertain whether this increase in water removal leads to an equivalent increase in oil removal. Figure 4.36 below shows the equivalent variation in oil content samples treated at 490 and 3508W at 16- 58 kJ.

As seen from Figure 4.36 the oil content decreases with increasing energy input for both powers tested. However, unlike the water content, no significant difference exists between either trend, showing very similar oil contents at 40 kJ. The results obtained suggest instead that the increase in power density results in a shift in the mechanism of how the oil is removed from the structure, but does not affect the

overall oil removal, despite the improvement in the overall water removal at higher power densities.

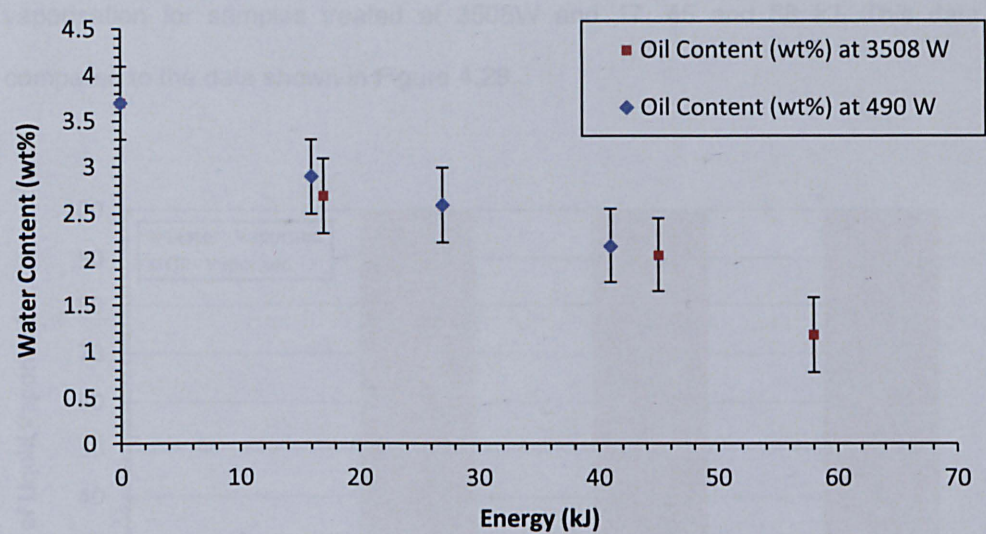


Figure 4.36 - Variation of oil content with energy input for Sample B treated using configuration A at 490 W and 3508 W at energy inputs of 16 to 58 kJ

The lack of improvement in oil removal with increasing power density in this case could be explained by the use of a single mode microwave applicator. According to the literature (Robinson, et al., 2009), the single mode applicator provided a significantly better performance in oil removal in comparison to a multi-mode applicator for equivalent energy inputs. This can be explained by the way in which the microwave field is distributed in a single mode. In a single mode applicator a standing wave is formed, providing greater field strength than multi-mode applicators, where there is no consistent wave superimposition, leading to significantly lower field strengths. This difference in behaviour is significant in this case, as 490 W and 3508 W of power being dissipated in a single mode applicator for a given energy input may not result in as a high an improvement as would be expected in a multi-mode applicator. This may be especially relevant if the removal of oil and water from the cuttings is time dependent, in which case for a fixed energy input, increasing the power will lead to lower processing times, which if short enough, could even lead to worse oil removal. The advantage of higher power densities may only be observed once the water content is sufficiently low, such that if the power density is too low, the

rate of heating equates to the rate of heat dissipation from the sample to the environment. Finally, Figure 4.37 shows the variation of oil and water percentages for vaporisation for samples treated at 3508W and 17, 45 and 58 kJ. This data is compared to the data shown in Figure 4.28.

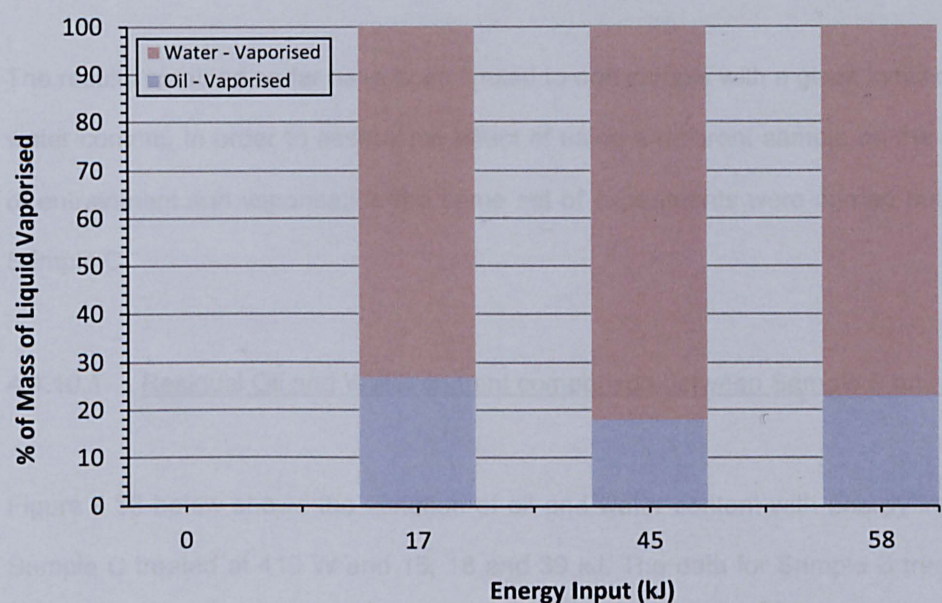


Figure 4.37 - Variation of oil and water percentages for %entrainment for Sample B treated using configuration A at 3508W at 17, 45 and 58 kJ.

Figure 4.37 initially shows a decrease (28% to 18%) in the percentage of oil in the mass of liquid removed through vaporisation between 17 and 45 kJ. This is followed by an increase back to 24% at 58 kJ. The decrease from 17 to 45 kJ was expected, however the magnitude of the drop is greater than that seen at 490W, and is probably a direct result of: (a) more water being removed at 45kJ for the sample treated at 3508 W in comparison to the sample treated at 490 W and (b) more oil being removed through entrainment. At 45 kJ an absolute amount of liquid of 2.28g was removed through vaporisation in comparison to 2.06g at 41 kJ at 490 W. Overall, at 3508 W and 45 kJ, 2.33g of oil were removed against 2.08g of oil at 490 W and 41 kJ, if normalised for “g of oil/kJ”, this equates to 0.052 g of oil/kJ at 3508 W and 0.051 g of oil/kJ at 490 W. As previously discussed this strongly suggests no improvement

in oil removal was seen at higher power densities in this case, even though a change in oil removal mechanism was observed.

4.4.10 EFFECT OF SAMPLE TYPE ON EXTENT OF ENTRAINMENT AND VAPORISATION

The results obtained so far have been limited to one sample with a given initial oil and water content. In order to assess the effect of using a different sample on the extent of entrainment and vaporisation the same set of experiments were carried out using Sample C.

4.4.10.1 Residual Oil and Water content comparison between Sample B and C

Figure 4.38 below shows the variation of oil and water content with energy input for Sample C treated at 419 W and 15, 18 and 39 kJ. The data for Sample B treated at 490 W and 16, 27 and 41 kJ is shown for comparison purposes.

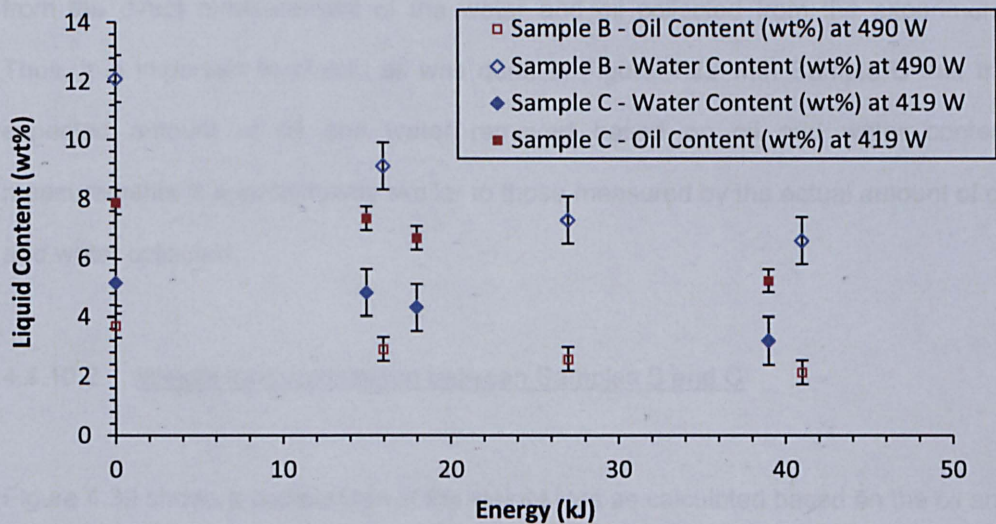


Figure 4.38 - Variation of oil content with energy input for Sample C treated using configuration A at 419 W 15, 18 and 39 kJ and Sample B treated using configuration A at 490 W 16, 27 and 41 kJ.

Figure 4.38 shows a decrease in oil and water content with energy input as expected for Sample C. For an energy input of approximately 40 kJ, Sample C treated at 419 W showed an approximate drop in oil content of 2.7 wt%, which equates to an oil removal of approximately 35%, whereas Sample B had a drop of 1.6 wt%, which equated to an oil removal of 42%. However, for the same energy input of approx. 40 kJ, 3.9g of oil were removed from Sample C in absolute terms, whereas only 2.1g of oil were removed from Sample B. Whereas the water content dropped over 6 wt% when treating Sample B at 490W and 41 kJ, the water content only dropped 2 wt% for Sample C treated at 419 W and 39 kJ. This equates, in absolute terms, to 7.5g for Sample B and 2.8g for Sample C. Thus, for Sample B treated at 490 W, 41 kJ of energy were required to remove a total liquid content of 7.6 wt%, which equated to 9.6g mass of liquid, whereas for Sample C treated at 419 W, 39 kJ of energy were required to remove a total liquid content of 4.7 wt%, which equated to a mass of 6.7g of liquid.

However, these values of oil and water mass removed are based on the water and oil content measurements, rather than the actual weight loss measurements obtained from the direct measurement of the water and oil collected from the experiment. Thus, it is important to check, as was done in Figure 4.25 with Sample B that the expected amount of oil and water removed based on oil and water content measurements is approximately similar to those measured by the actual amount of oil and water collected.

4.4.10.2 Weight loss comparison between Samples B and C

Figure 4.39 shows a comparison of the weight loss as calculated based on the oil and water content measurements, and as measured by the actual difference in the weight of the sample before and after the experiment, as well as measured by the sum of water and oil collected in each trap (1-5).

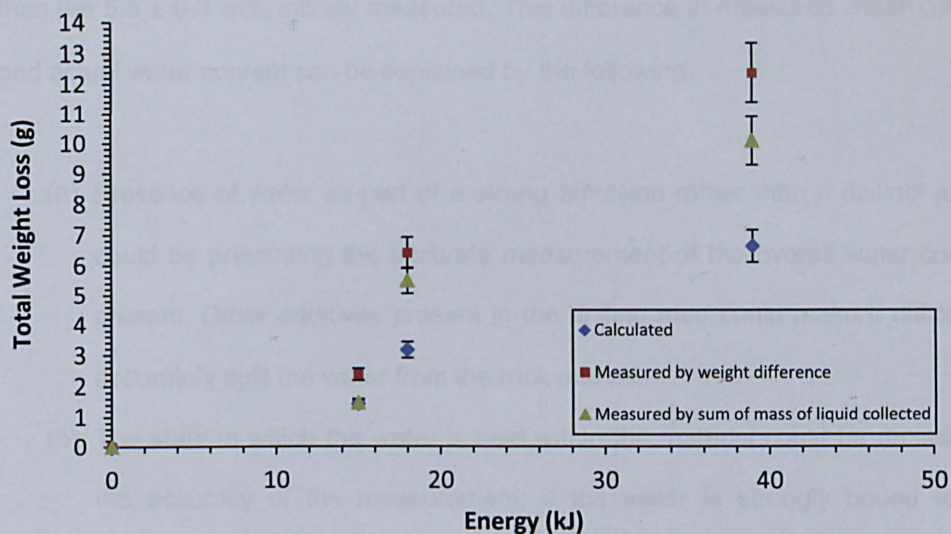


Figure 4.39 - Comparison of calculated and measured weight loss for Sample C treated at 419 W and 0-39 kJ.

Figure 4.39 shows an overall increase in total weight loss with energy input, as expected, regardless of the method used. However, there was a large discrepancy in the weight loss estimated based on the water and oil content in comparison to the weight loss measured through sample weight difference and by the sum of liquid collected in the traps. The difference between the latter two methods of measuring weight loss was lower, approximately 1g, which is of similar magnitude to the previous experiment (Figure 4.25). The difference could be explained, as before, by uncondensed vapours removed from the material.

However, the large difference observed between the calculated and measured weight loss values suggest that the method used for measuring the water and oil content for this particular sample may be inaccurate. The amount of oil collected in the vaporisation and entrainment sections for Sample C treated at 39 kJ was 3.8g, which is close to the suggested 3.9g estimated based on the water and oil content. The amount of water removed based on the water content for Sample C treated at 39 kJ was 2.8g, which is far less than the amount actually collected in the traps; 6.27g. This additional water increases the water content of the sample to just over 8 wt%, rather

than the 5.5 ± 0.8 wt% initially measured. This difference in measured water content and actual water content can be explained by the following:

- (a) Presence of water as part of a strong emulsion rather than a distinct phase could be preventing the accurate measurement of the overall water content present. Other additives present in the drilling mud could make it difficult to accurately split the water from the rock and oil.
- (b) The state in which the water is held within the material could be an issue in the accuracy of the measurement, if the water is strongly bound to the surface and/or present as part of the chemical structure of the clay.

For accuracy purposes the water and oil mass collected in traps (1-5) will be used for comparison and analysis from this point forward.

Figure 4.40 below shows the variation of weight loss as measured by the sum of oil and water collected in the traps (1-5) with energy input for Samples B and C treated at 490 and 419 W respectively.

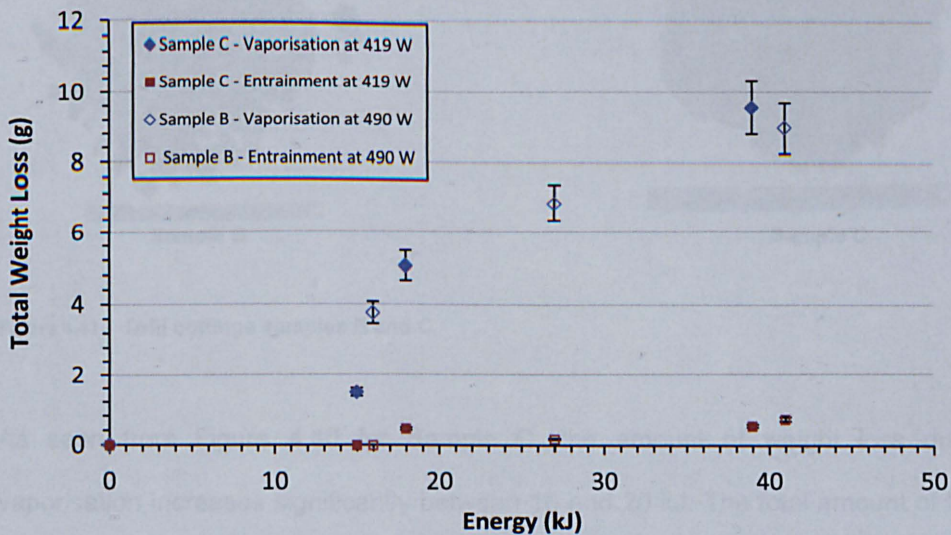


Figure 4.40 - Variation of measured weight loss due to vaporisation and entrainment with energy input for Sample B and C treated using configuration A at 490 and 419 W respectively, at energy inputs of 16-41 kJ.

As seen from Figure 4.40, the total weight loss due to vaporisation is similar for both Samples B and C; however, a greater amount of weight loss due to entrainment was noticed for Sample C at lower energy inputs. This can be explained by the difference in physical structure between one sample and the other. A significant amount of the liquid content of Sample C appears to be present at the surface of the sample, whereas in Sample B, a greater portion of liquid content is expected to be present within the cuttings (Figure 4.41). As previously discussed, this has a direct impact in the volume and overall surface area of liquid available for entrainment to occur as steam leaves the sample. Another key observation that can be made from Figure 4.40 is that the difference in total weight loss between 15 and 17 kJ is significant, 1.8g vs. 5g respectively, suggesting a minimum energy input is required before any liquid mass is removed from the sample. This is expected as energy needs to be supplied to the sample for heating, and then sufficient energy needs to be supplied for vaporisation to take place. Section 4.4.10.3 below, provides a heat balance for the system, which allows for the determination of minimum energy requirements for removing a given mass of liquid.

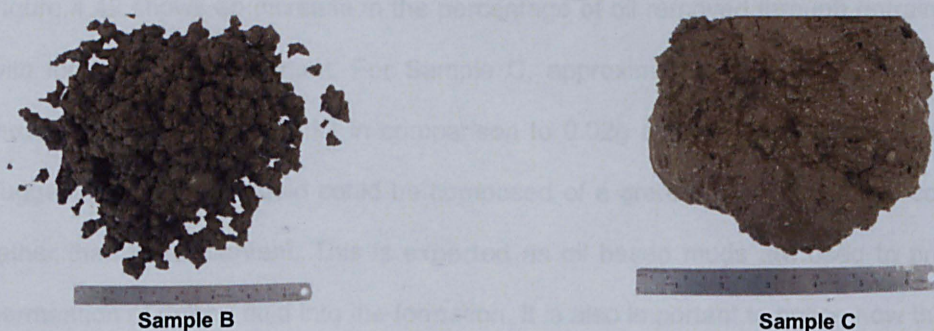


Figure 4.41 - Drill cuttings samples B and C.

As seen from Figure 4.40 for Sample C, the amount of weight loss due to vaporisation increases significantly between 15 and 20 kJ. The total amount of liquid removed through entrainment was approximately 0.55g at 17 kJ, accounting for 9% of the overall removal oil and water removal. The split between oil and water removed

through entrainment for Sample C is given below in Figure 4.42. This data is compared to Figure 4.27.

Figure 4.42 - Variation of oil and water percentages for %entrainment for Sample C treated using configuration A at 419 W respectively at 15, 18 and 39 kJ.

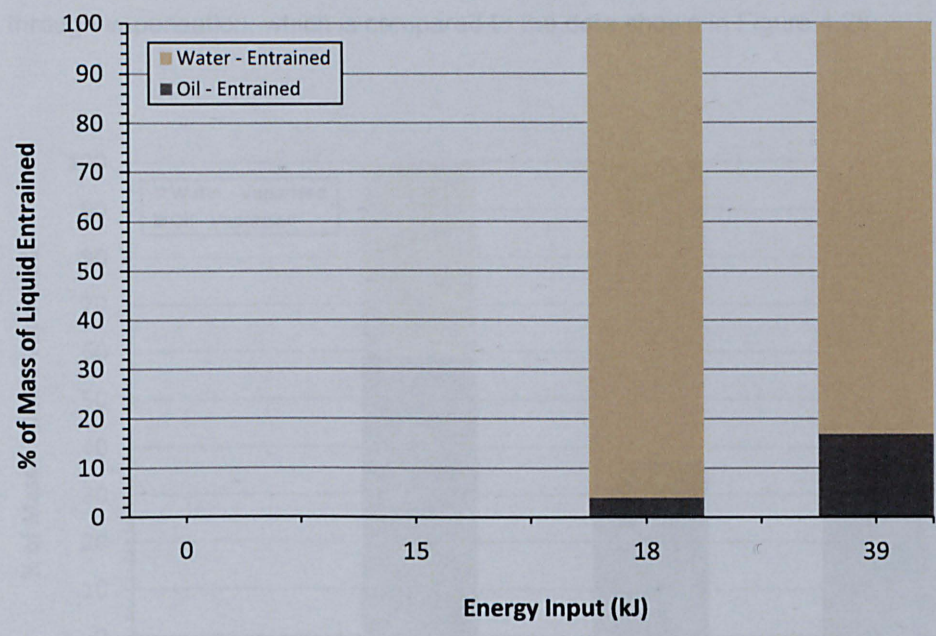


Figure 4.42 - Variation of oil and water percentages for %entrainment for Sample C treated using configuration A at 419 W respectively at 15, 18 and 39 kJ.

Figure 4.42 shows an increase in the percentage of oil removed through entrainment with increasing energy input. For Sample C, approximately 0.1g of oil is removed through entrainment at 39 kJ in comparison to 0.02g at 41 kJ for Sample B, which suggests the surface liquid could be composed of a greater proportion of oil content rather than water content. This is expected as oil based muds are used to prevent permeation of drilling fluid into the formation. It is also important to notice how the drill cuttings particles in Sample C pack close together resembling a thick sludge rather than individual particles, which appears to be the case in Sample B.

This packing could enhance entrainment as vapours generated within the mass of Sample C, will not be able to easily propagate through the structure potentially leading to greater internal pressures and superheating. As a result, oil removal could be slightly lower initially, as steam is generated with the centre and needs time to propagate through the sample mass, however, as treatment times increase, a better

oil removal could be observed for Sample C with an increase in entrainment being observed with increasing energy input (as observed in the data presented in Figure 4.42). Figure 4.43 shows the variation in percentage of oil and water removed through vaporisation, which is compared to the data shown in Figure 4.28.

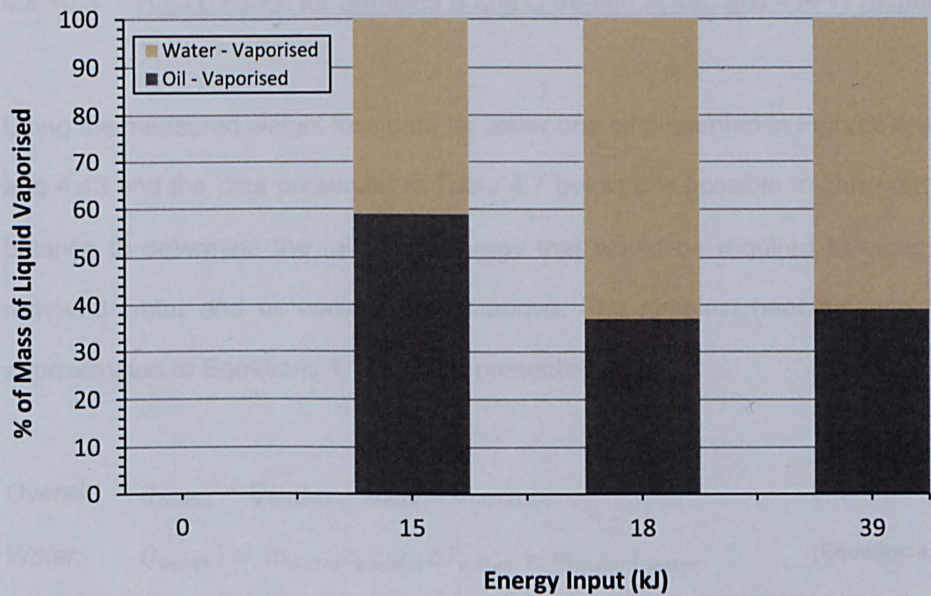


Figure 4.43 - Variation of oil and water percentages for %vaporisation for C treated using configuration A at 419 W respectively at 15, 18 and 39 kJ.

Figure 4.43 shows a greater proportion of oil in the liquid being removed through vaporisation for Sample C in comparison to Sample B. Interestingly, once entrainment starts at 18 kJ this percentage falls, suggesting a shift in mechanism occurs at this point. At 39 kJ the percentage of oil was seen to increase again despite an increase in entrainment. This result could be attributed to an overall increase in the performance of oil removal due to higher temperature and pressure steam being generated as a result of decreasing sample water content and increasing power density. For sample C oil accounted for 38 to 55% of the liquid removed through vaporisation in comparison to Sample B, with oil accounting for only 24 to 28%. From an oil removal efficiency point of view, which can be measured by mass of oil removed per kJ of energy input, Sample B had an efficiency of 0.05g of oil/kJ, whereas Sample C had an efficiency of 0.1 g of oil/kJ.

However, efficiency can also be compared in terms of energy input used vs. the minimum energy input theoretically required to remove a certain amount of oil and water through vaporisation. In order to achieve this a heat balance was carried out for Samples B and C treated at 490 and 419 W respectively.

4.4.10.3 Heat balance for Samples B and C treated at 490 and 419 W respectively

Using the measured weight loss data for water and oil presented in Figures 4.39, 4.42 and 4.43 and the data presented in Table 4.7 below it is possible to carry out a heat balance to determine the minimum energy that would be required to vaporise the removed water and oil content stated above. The simplest heat balance can be approximated to Equations 4.14 to 4.16 presented below.

$$\text{Overall: } Q_{total,i} = Q_{water,i} + Q_{oil,i} - Q_{losses,i} \quad [\text{Equation 4.14}]$$

$$\text{Water: } Q_{water,i} = m_{water}c_{p,water}\Delta T_{water} + m_{water}L_{water} \quad [\text{Equation 4.15}]$$

$$\text{Oil: } Q_{oil,i} = m_{oil}c_{p,oil}\Delta T_{oil} + m_{oil}L_{oil} \quad [\text{Equation 4.16}]$$

Where Q_{total} is the total energy (kJ) that needs to be supplied to the sample in order to vaporise a given water and oil content, "i", $Q_{water,i}$ is the total energy (kJ) required for heating and vaporising the water phase, $Q_{oil,i}$ is the total energy (kJ) required for heating and vaporising the oil phase, $Q_{losses,i}$ is the total energy (kJ) lost in superheating the steam, heating the rock, the surrounding environment and in reheating re-condensed water and oil vapours. m_{water} is the mass of water that needs to be vaporised (kg), $c_{p,water}$ is the average specific heat capacity of the water (kJ/kg K), ΔT_{water} is the temperature difference between the initial water temperature and the final temperature at vaporisation (°C). L_{water} is the latent heat of vaporisation for the water at a given temperature and pressure (kJ/kg). The same nomenclature applies for the oil phase.

Variable	Value	Assumptions
$c_{p,water}$ (kJ/kg K)	4.18	Average specific heat capacity value between 20 and 100 °C.
$c_{p,oil}$ (kJ/kg K)	2	Average specific heat capacity value based on an equivalent Alkane based oil.
ΔT_{water} (°C)	80	Assuming a boiling point of 100 and a sample temperature of 20 °C.
ΔT_{oil} (°C)	80	Assuming heating and vaporisation can occur through steam distillation (i.e. boiling point is lowered to boiling point of water – over estimation).
L_{water} (kJ/kg)	2250	Approximate latent heat of vaporisation for water at standard temperature and pressure (STP).
L_{oil} (kJ/kg)	800	Approximate average latent heat of vaporisation for oil at standard temperature and pressure (STP) based on an equivalent Alkane based oil.

Table 4.7 - Values of variables used for the heat balance of Sample B and C treated at 490 and 419 W respectively (all data from (Perry & Green, 1997) unless otherwise stated).

Using Equations 4.14 to 4.16 and the data presented above in Table 4.7 it is possible to estimate the minimum energy per gram of water and oil that would be required to heat all oil and water content and then vaporise a given amount of water and oil content. Thus, the energy requirement for heating per gram of oil and water is: 0.16kJ/g and 0.33 kJ/g respectively, and the energy required for vaporisation is 0.8 kJ/g and 2.25 kJ/g respectively. For Sample C treated at 490 W and 15 kJ, the overall amount of water and oil initially present in the sample is 9.65g and 9.52g respectively and the amount of water vaporised is 0.61g and 0.87g respectively. This gives a minimum energy requirement of approximately 7 kJ, which is just less than 50% the amount of energy actually used at 15 kJ.

For a heat balance comparison between Sample B and C, a liquid mass of 2.1g of oil and 7.5g of water of Sample B treated at 490 W and 41 kJ and 3.9g of oil and 6.3g of water of Sample C treated at 419 W and 39 kJ was used. The minimum calculated energy required to remove the above water and oil content from Samples B and C to the nearest kJ is 21 and 20 kJ respectively. This gives an energy efficiency of actual energy used per minimum energy required, based on the amount of liquid removed only, of approximately 50% for Sample B and C. This efficiency could be lower in reality, as some of the oil is removed through entrainment and therefore does not need to be vaporised in order for it to be removed. However, as the oil content only accounts for a smaller portion of the overall energy requirement (10-30%), and as entrainment for Sample B and C is small this will be less significant.

4.4.10.4 Effect of power density on extent of entrainment and vaporisation for Sample C

Figure 4.44 shows the difference in measured weight loss for Sample C treated at 419 and 3266 W respectively.

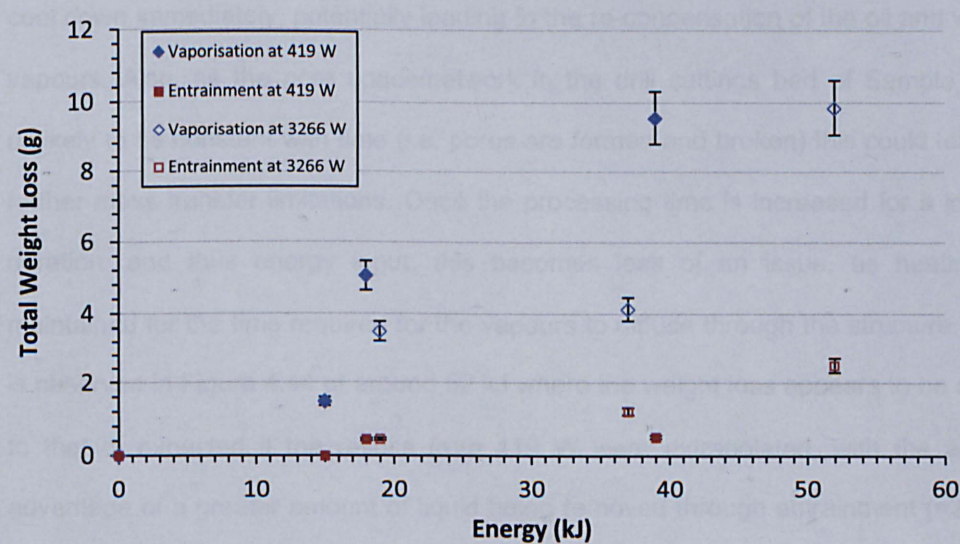


Figure 4.44 - Variation of measured weight loss due to vaporisation and entrainment with energy input for Sample C treated using configuration A at 419 and 3266 W respectively, at energy inputs of 15-52 kJ.

As seen in Figure 4.44, Sample C showed a different trend to Sample B when treated at a higher power. The weight loss was significantly lower at 37-39 kJ for the sample treated at 3266 W in comparison to the sample treated at 419 W.

Initially little difference is noticed between Sample C at 419 W and Sample C at 3266 W as the liquid content being removed is most likely present at the surface and mass transfer limitations are minimal. However, as the liquid content decreases, and removal becomes limited by diffusion within the cutting particles and within the cuttings bed, minimum diffusion time limitations become increasingly significant in the removal of oil and water from the material. As the mass of the sample is kept constant, an increase in power leads to a decrease in processing time for a given energy input. This decrease in processing time appears to be significant at around 40 kJ, where mass transfer appears to be limited by a minimum processing time, which is required for the water and oil vapours to diffuse through the structure.

In theory vapours will continue to diffuse once microwaves are stopped, however, unlike conventional heating, once microwaves are stopped the sample will begin to cool down immediately, potentially leading to the re-condensation of the oil and water vapours. Also, as the pore space/network in the drill cuttings bed of Sample C is unlikely to be constant with time (i.e. pores are formed and broken) this could lead to further mass transfer limitations. Once the processing time is increased for a longer duration, and thus energy input, this becomes less of an issue, as heating is maintained for the time required for the vapours to diffuse through the structure. This is observed in Figure 4.44 at around 52 kJ where the weight loss appears to be close to that of expected if the results from 419 W were extrapolated, with the added advantage of a greater amount of liquid being removed through entrainment ($\approx 20\%$). This concept is hypothetically shown in Figure 4.45 below.

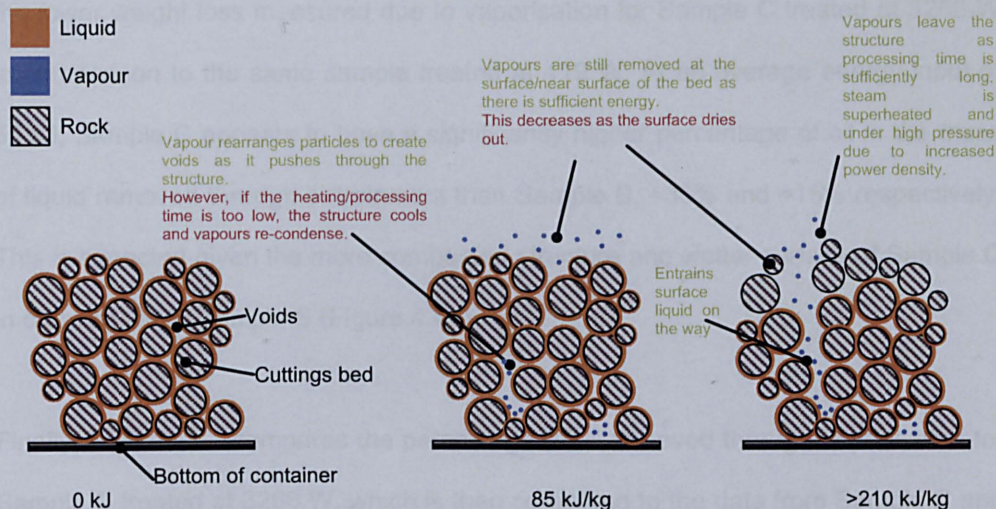


Figure 4.45 - Hypothetical diagram for the removal of oil and water vapours from a bed of drill cuttings of Sample C. The change in removal behaviour is shown for a sample treated at constant power but with increasingly longer durations/energy input.

Figure 4.46 below shows the percentage of oil removed through entrainment for Sample C treated at 3266 W, which is then compared to the data from Sample C and B treated at 419W (Figure 4.42) and 3508 W respectively (Figure 4.34).

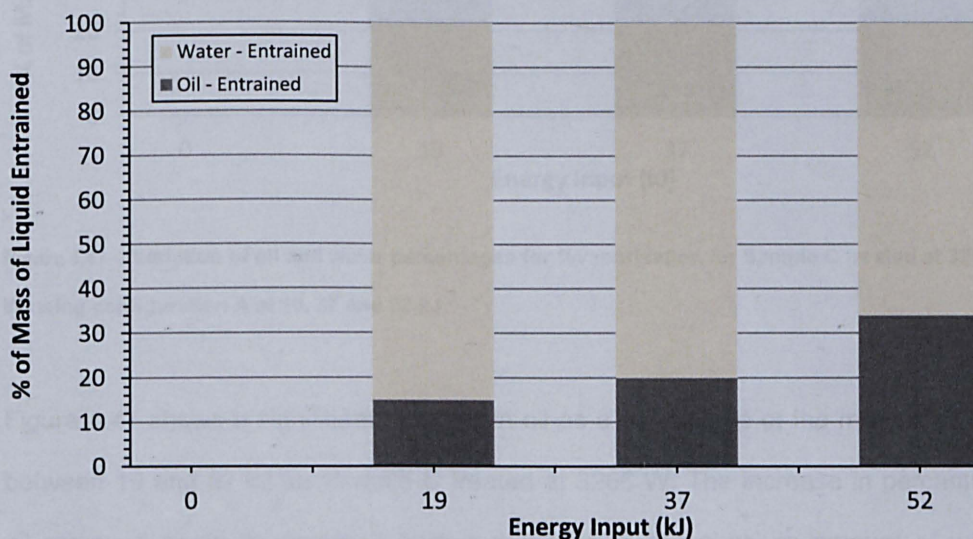


Figure 4.46 - Variation of oil and water percentages for %entrainment for Sample C treated at 3266 W using configuration A at 19, 37 and 52 kJ.

Figure 4.46 shows a clear increase in percentage of oil removal through entrainment between Sample C treated at 419 W and Sample C treated at 3266 W. This explains

the lower weight loss measured due to vaporisation for Sample C treated at 3266 W in comparison to the same sample treated at 419 W. At an average energy input of 55 kJ, Sample C appears to have a significantly higher percentage of oil in the mass of liquid removed through entrainment than Sample B, $\approx 35\%$ and $\approx 15\%$ respectively. This is expected given the more compacted structure and wetter surface of Sample C in comparison to Sample B (Figure 4.41).

Finally, Figure 4.47 compares the percentage of oil removed through vaporisation for Sample C treated at 3266 W, which is then compared to the data from Sample C and B treated at 419W (Figure 4.43) and 3508 W respectively (Figure 4.37).

remains the most significant of removal occurring for 30% liquid removed

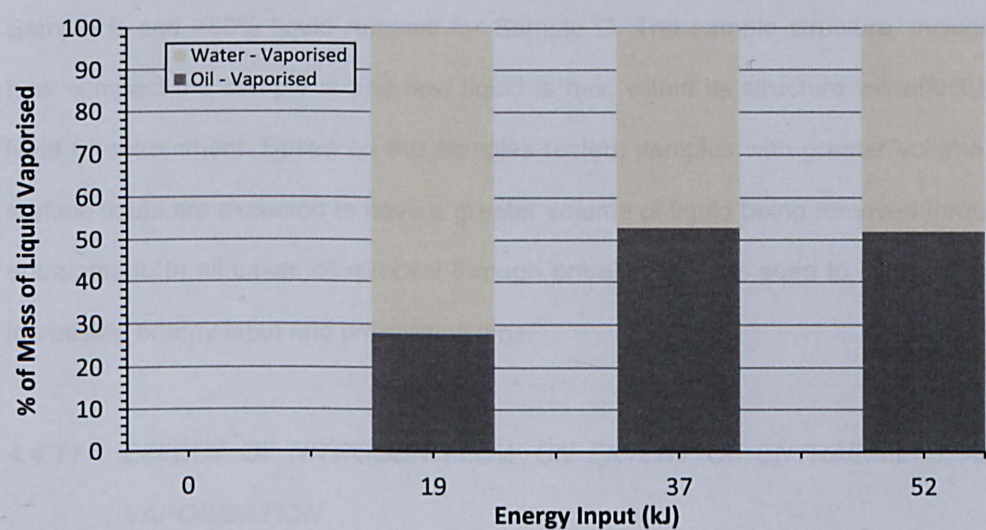


Figure 4.47 - Variation of oil and water percentages for %vaporisation for Sample C treated at 3266 W using configuration A at 19, 37 and 52 kJ.

Figure 4.47 shows a significant increase in oil as a percentage of the mass removed

between 19 and 37 kJ for Sample C treated at 3266 W. The increase in percentage oil removed could be resulting from a decrease in the absolute amount of water removed at 37 kJ for samples treated at 3266 W, rather than an absolute increase in oil removed. At 419 W and 39 kJ, over 6.27g of water were removed, whereas at 3266 W only 2.93g of water were removed. This is equivalent to a reduction of 53% in water removal for approximately the same energy input, whereas the oil removal only

decreased by 23%, from 3.81g at 419 W to 2.94g at 3266 W. This phenomenon could be explained by the hypothetical mechanism of water and oil vapour removal shown in Figure 4.45, strongly supported by the results shown above. Assuming the majority of the oil is present at the particles and bed surface, and the majority of the water is present within the bed and the particles, then the removal of water is expected to be hindered to a greater extent than the oil. This assumes, however, that sufficient steam can be generated at the surface to remove the required amount of oil.

In conclusion, the type of drill cuttings treated affects the oil and water removal mechanisms by a difference as high as 10%. For both samples tested vaporisation remained the main mechanism of removal accounting for >90% liquid removal for Sample B and >80% liquid removal for Sample C. The sample structure, including how compact the sample is and how liquid is held within its structure will affect the level of entrainment. Based on the samples tested, samples with greater volume of surface liquid are expected to have a greater volume of liquid being removed through entrainment. In all cases oil removal through entrainment was seen to increase with increasing energy input and processing time.

4.4.11 EFFECT OF NITROGEN FLOW ON EXTENT OF ENTRAINMENT AND VAPORISATION

Figure 4.48 shows the variation in weight loss against nitrogen flowrate for Sample B treated at 490 W and 41 kJ at 2 L/min ($Re_m = 58$) and 7 L/min ($Re_m = 203$).

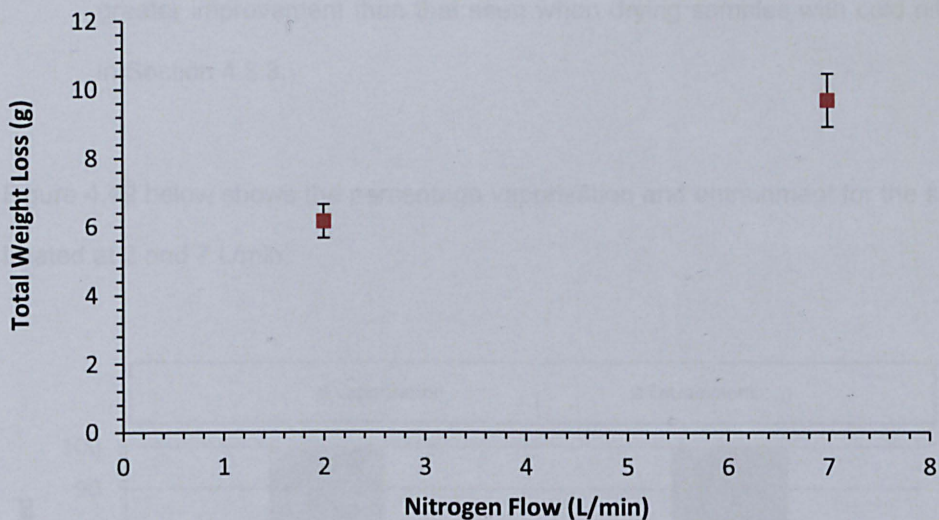


Figure 4.48 - Variation of total weight loss against nitrogen flowrate for Sample B treated at 490 W and 41 kJ at 2 L/min ($Re_m = 58$) and 7 L/min ($Re_m = 203$).

As seen from Figure 4.48 increasing the nitrogen flowrate from 2 to 7 L/min has a significant effect in the overall amount of liquid that is removed from the sample. Increasing the flowrate from 2 to 7 L/min resulted in an increase in mass loss from 6 to 10g, a 70% improvement in liquid removal efficiency. This is in agreement with previous data obtained for the variation of residual oil content with increasing nitrogen flowrate presented in Figure 4.18 in Section 4.3.5. As the overall weight loss is dependent on the water and oil content, increasing the nitrogen flowrate has, as expected, a similar effect in the overall weight loss. The improvement can be explained in simple terms by the following:

- (a) *Increased concentration gradient* – passing a sweep gas through the bed of cuttings, reduces stagnation and increases the concentration gradient between the sample surface and bulk gas. This concentration gradient then improves evaporation/vaporisation by providing an overall greater driving force, which prevents saturation.
- (b) *Reduced re-condensation* – passing hot nitrogen (approx. 80 ± 5 °C) through the bed, rather than cold can reduce re-condensation and give an even

greater improvement than that seen when drying samples with cold nitrogen in Section 4.3.3.

Figure 4.49 below shows the percentage vaporisation and entrainment for the sample treated at 2 and 7 L/min.

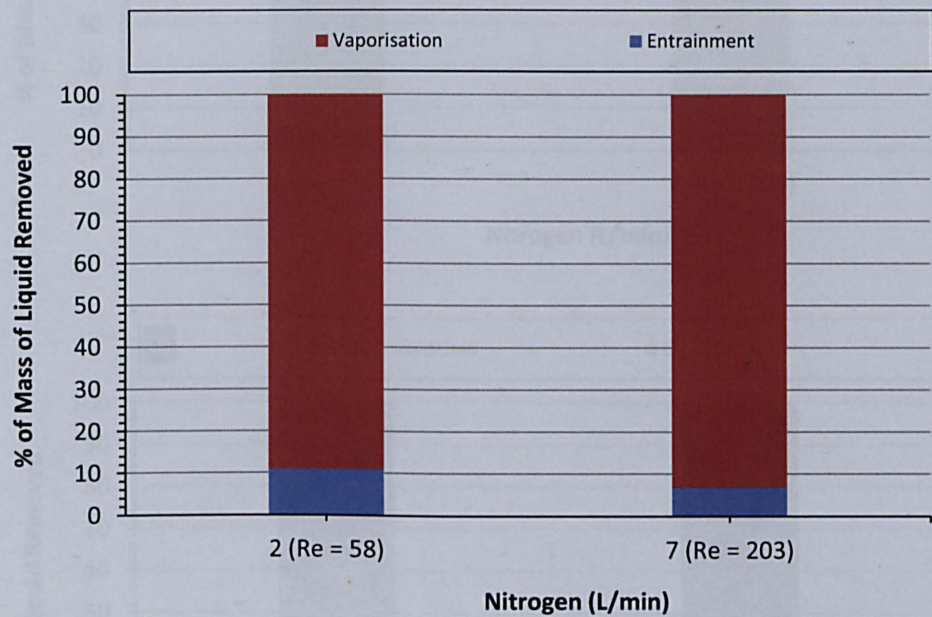


Figure 4.49 - Variation of percentage of entrainment vs. Vaporisation for nitrogen flowrates of 2 and 7 L/min at approx. 80 ± 5 °C.

As seen from Figure 4.49, increasing the nitrogen flowrate decreases the overall percentage of mass removed through entrainment. However, in absolute terms, no difference in entrainment is observed by increasing the nitrogen flowrate in either case. Figure 4.50 shows the split of oil and water as percentages of the mass removed through entrainment and vaporisation for both Nitrogen flowrates tested.

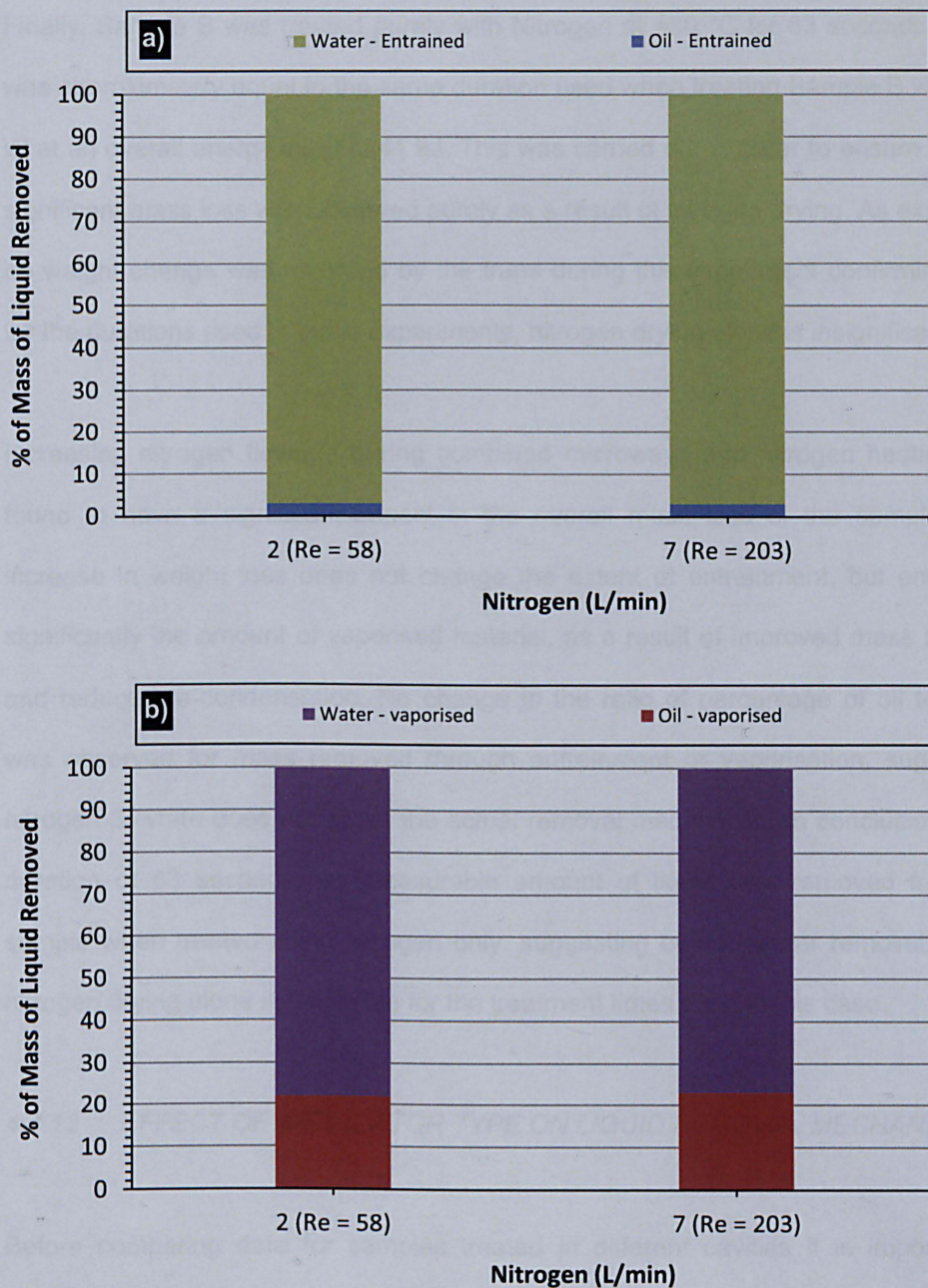


Figure 4.50 - Variation of oil and water percentages for %entrainment (a) and %vaporisation (b) for Sample B treated at 490 W and 41 kJ using a nitrogen flowrate of 2 and 7 L/min.

Figure 4.50 shows an identical split in terms of ratio of %oil:%water for samples treated using 2 and 7 L/min for both entrainment and vaporisation mechanisms (a) and (b). This suggests that increasing nitrogen flow through the bed does not actually change the behaviour of the oil and water removal mechanisms, but it rather just increases the overall volume of material vaporised and prevents re-condensation of material back into the sample.

Finally, Sample B was treated purely with Nitrogen at $\approx 80^\circ\text{C}$ for 83 seconds, which was approximately equal to the same duration used when treating Sample B with 490 W at an overall energy input of 41 kJ. This was carried out in order to ensure that no significant mass loss was observed purely as a result of nitrogen drying. As expected, no weight change was recorded by the traps during this experiment confirming that, for the durations used in these experiments, nitrogen drying alone is insignificant.

Increasing nitrogen flowrate during combined microwave and nitrogen heating was found to have a significant impact in the overall mass loss of the sample. This increase in weight loss does not change the extent of entrainment, but enhances significantly the amount of vaporised material, as a result of improved mass transfer and reduced re-condensation. No change in the ratio of percentage of oil to water was observed for mass removed through entrainment or vaporisation, suggesting nitrogen flowrate does not affect the actual removal mechanism. In conclusion, for a duration of 83 seconds, no measurable amount of liquid was removed from the sample when treated using nitrogen only, suggesting oil and water removal due to nitrogen drying alone is negligible for the treatment times used in this case.

4.4.12 EFFECT OF APPLICATOR TYPE ON LIQUID REMOVAL MECHANISMS

Before comparing data for samples treated in different cavities it is important to establish a way of determining a change in the mechanism of a sample. Figure 4.51 below shows the relationship between the percentage of oil and water removal for Sample B treated at 490 W and energy inputs of 16-41 kJ. Oil and water removal are calculated according to Equation 4.17 and 4.18 below, and use the data presented in Figure 4.38 in Section 4.4.10.1 above.

$$\% \text{Water Removal} = \frac{x_{\text{water,initial}} - x_{\text{water},i}}{x_{\text{water,initial}}} \times 100 \quad [\text{Equation 4.17}]$$

$$\% \text{oil Removal} = \frac{x_{\text{oil,initial}} - x_{\text{oil},i}}{x_{\text{oil,initial}}} \times 100 \quad [\text{Equation 4.18}]$$

Where $x_{water,initial}$ and $x_{oil,initial}$ are the initial water and oil content (wt%) respectively and $x_{water,i}$ and $x_{oil,i}$ are the water and oil content at a given energy input/processing time “i”.

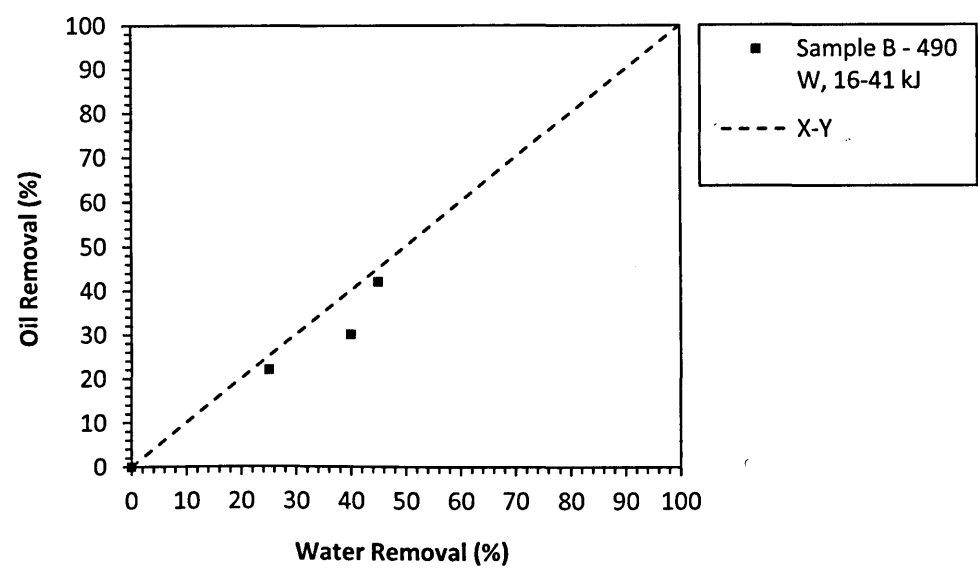


Figure 4.51 - Oil removal vs. Water removal for Sample B treated at 490 W and 16-41 kJ.

Figure 4.51 shows an increase in oil removal with water removal as expected. The data also shows that for the energy inputs tested, the amount of water removal required to remove an equivalent amount of oil was always higher than a 1:1 ratio. For example, if 30% oil removal is desired, than a 40% water removal is required. This relationship is dependent on the inherent physical structure of the sample, the initial oil and water content, power density and the overall energy input. However, it is interesting to note the increase in oil removal between 40 and 46% water removal, suggesting a greater percentage of oil being removed per percentage of water (towards a 1:1 ratio). This data can be compared to the actual percentage of oil removed through entrainment for the same water removal range (Figure 4.52).

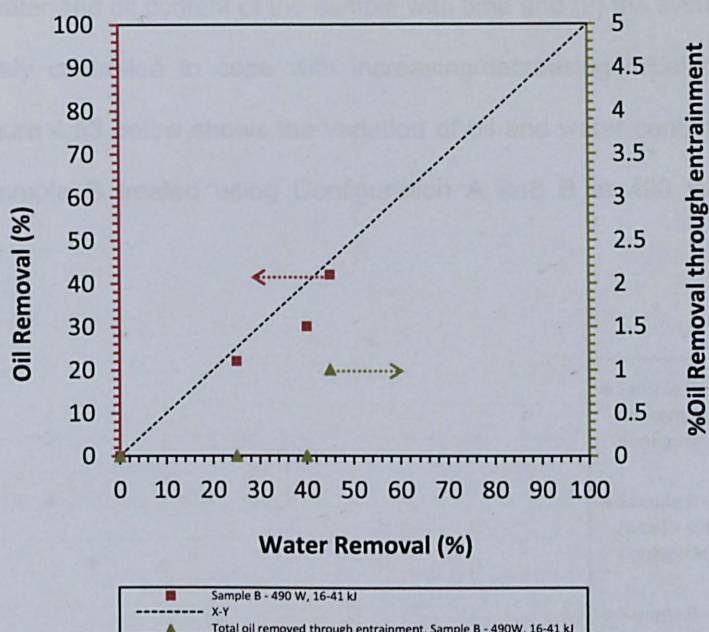


Figure 4.52 - Variation of % oil removed through entrainment with water removal (%) for Sample B.

Figure 4.52 shows an increase in the percentage of oil being removed through an entrainment mechanism (green triangles), from 0 to 1% for the same water removal range where there was an increase in the %oil removal per %water removal (red squares). Although the increase in %oil removal per %water removal between 40 and 50 kJ cannot be solely attributed to an increase in oil removal through entrainment, the data does suggest there is a shift in the overall removal mechanism from vaporisation only to a combination of vaporisation and entrainment. The presence of entrainment suggests steam was being generated at a high enough rate, which led to an increase the internal pressure within the particles, leading to superheated high velocity steam capable of physically carrying water and oil droplets. This increase in steam velocity and temperature not only enables the entrainment mechanism to occur, but it significantly enhances the rate of vaporisation of the oil within the sample, leading to an overall increase in % oil removal per % of water removed.

The ability to determine the shift in mechanism by plotting water and oil removal is significant, as it would allow for: (1) changes in the removal mechanism of different samples treated in various applicators to be assessed simply by measuring the

change of water and oil content of the sample with time and (2) the system could also be proactively controlled to cope with increasing/decreasing initial oil and water content. Figure 4.53 below shows the variation of oil and water content with energy input for Sample B treated using Configuration A and B at 490 W and 508 W respectively.

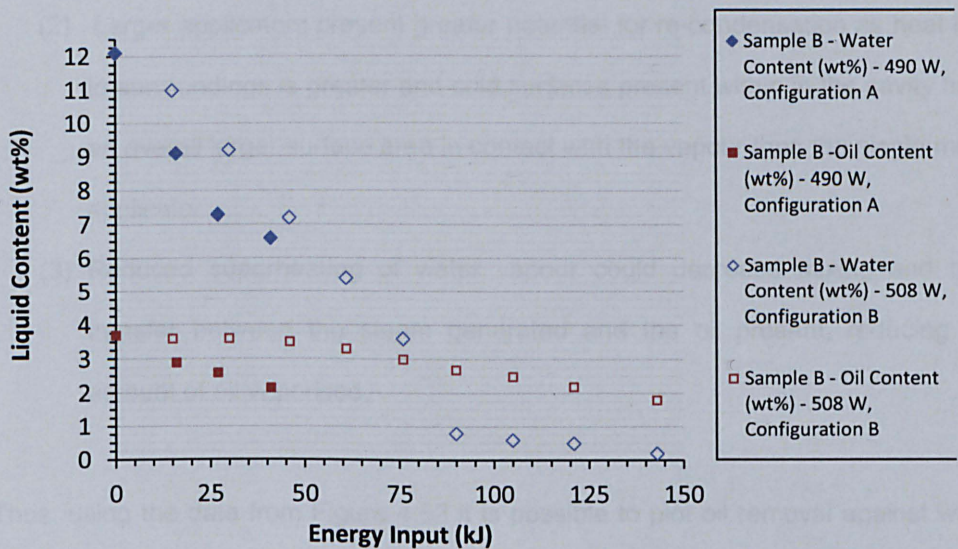


Figure 4.53 - Variation of water and oil content with energy input for Sample B treated at 490 W and 508 W using Configuration A and B respectively.

Figure 4.53 shows a decrease in the oil and water content with energy input for Sample B treated in both configurations A and B. The water content for Sample B treated using configuration A is slightly lower than that of configuration B for any given energy input, which is expected as the electrical field strength is greater in a single mode cavity than in a multimode cavity. However, a much greater difference was observed in the removal of oil content from the sample using configuration B, with no considerable oil removal observed up to 75 kJ. As an example, for the difference in oil removal performance; Sample B treated using configuration A for an energy input of 41 kJ led to a decrease in oil content from 3.7 to 2.2 wt%, giving an oil removal of 41%. For the same removal using configuration B an energy input of approximately 110-125 kJ was required, almost triple the amount using a single mode applicator. This could be explained by the following:

- (1) Nitrogen in single mode setup passes through the bed, potentially enhancing oil removal. As seen in Section 4.4.11, decreasing the nitrogen flowrate through the bed from 7 to 2 L/min led to a reduction in weight loss >30%. The nitrogen in configuration B serves purely the purpose of inerting the atmosphere.
- (2) Larger applicators present greater potential for re-condensation as heat loss to surroundings is greater and cold surfaces present within in the cavity have an overall larger surface area in contact with the vapour than the single mode applicator.
- (3) Reduced superheating of water vapour could decrease mixing and heat transfer between the steam generated and the oil present, reducing the amount of oil vaporised.

Thus, using the data from Figure 4.53 it is possible to plot oil removal against water removal in order to compare the removal mechanism between either configurations. This is shown in Figure 4.54 below.

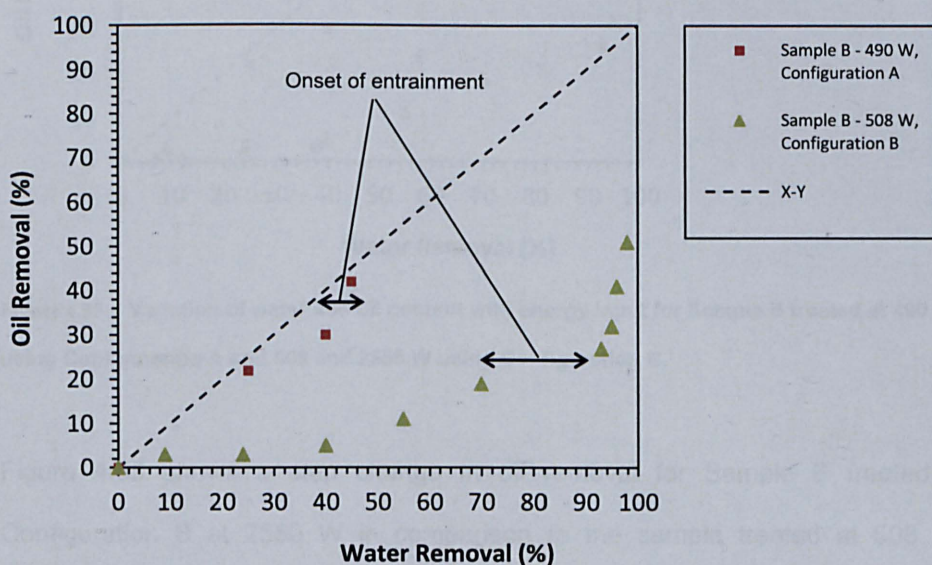


Figure 4.54 - Oil removal vs. Water removal form Sample B treated using configuration A and B at 490 and 508 W respectively.

As seen from Figure 4.54 there is a significant difference between Sample B treated using configuration A and using configuration B. In configuration B No significant oil removal is observed until 40% of the water has been removed from the sample. Oil removal then increases linearly with increasing water removal until 80-90% of the water has been removed. At a water removal >80% oil removal increases significantly, similar to the increase observed between 40-50% water removal for Sample B treated using configuration A. This suggests that high temperature and pressure steam generation will only occur in configuration B once >80% of the water has been removed. Up to that point oil and water removal will occur through low rate vaporisation only, with a significantly greater proportion of the liquid vaporised being water rather than oil. Figure 4.55 shows the effect of increasing power for configuration B.

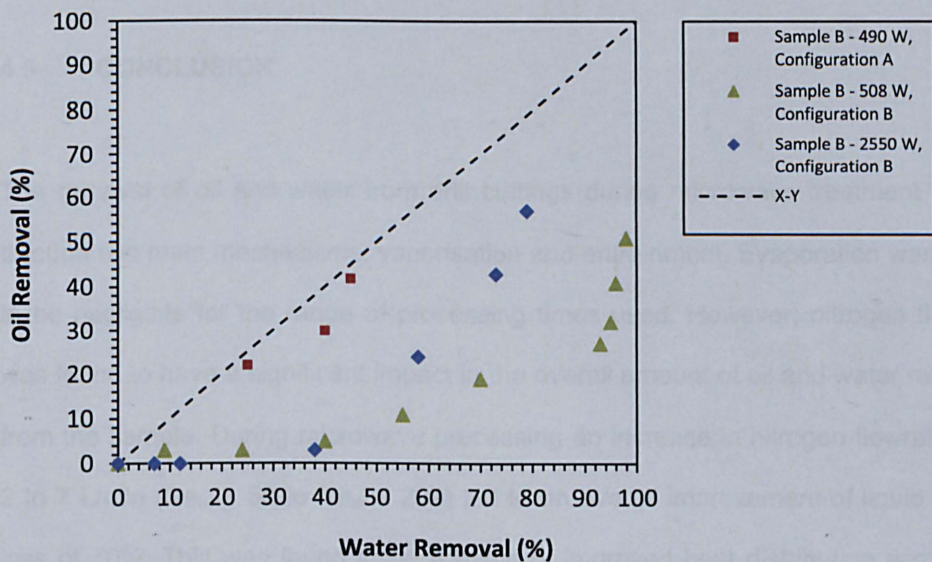


Figure 4.55 - Variation of water and oil content with energy input for Sample B treated at 490 W using Configuration A and 508 and 2550 W using Configuration B.

Figure 4.55 shows a step change in oil removal for Sample B treated using Configuration B at 2550 W in comparison to the sample treated at 508 W. As previously discussed, increasing the power in a multimode cavity has a significant impact on oil removal, as the rate of energy dissipated per volume of sample is still below the point above which mass transfer limitations become the rate limiting step. It

is also important to note how, in comparison to Sample B treated using configuration A, both samples treated at 508 and 2550 W using configuration B showed an initial plateau up to 30-40% water removal. This could be explained by vaporised oil re-condensing at the surface as a result of the hot nitrogen not passing through the bed as is the case in configuration A.

In conclusion, the applicator and setup configuration could have a significant impact on the oil and water removal mechanisms. In single mode applicators, where the electric field strength is higher, superheated and high velocity steam can be achieved at significantly higher levels of water content, allowing for a higher overall ratios of %oil removal to % water removal to be achieved, reaching approximately 1:1. However, in multimode cavities, where the electric field strength is significantly lower, the %oil removal to water ratio decreases to <1:3.

4.5 CONCLUSION

The removal of oil and water from drill cuttings during microwave treatment occurs through two main mechanisms: vaporisation and entrainment. Evaporation was found to be negligible for the range of processing times used. However, nitrogen flowrate was found to have a significant impact in the overall amount of oil and water removed from the sample. During microwave processing an increase in nitrogen flowrate from 2 to 7 L/min ($Re_m = 58$ to $Re_m = 203$) led to an overall improvement of liquid weight loss of 70%. This was found to be a result of improved heat distribution across the sample and improved mass transfer from the drill cuttings particle surface to the extraction points as well as a potential for reduced recondensation. Nevertheless, the increase in nitrogen flowrate did not result in any shifts in the oil:water ratio and so the removal mechanism, with the % removed through entrainment and vaporisation remaining constant at both flowrates.

Vaporisation was found to be the main removal mechanism for the experimental conditions tested, 500-3000 W for 120-240g samples, with oil being most likely removed through steam distillation. Generally, vaporisation accounted for >80-90% of the overall liquid removal. Vaporisation of the oil phase accounted for 70-100% of the overall removal. The absolute amount of material vaporised increased with increasing energy input and power, however, the percentage of the liquid removed through vaporisation was found to decrease with increasing energy input and power density. As a result, entrainment was found to increase with energy input and power density mainly as a result of steam being generated at higher velocities and pressures at the latter stages of treatment.

Both the drill cuttings sample and applicator type were also found to have a significant effect on the extent of oil and water removal through vaporisation and entrainment. Samples consisting of higher oil content and more surface liquid, resulted in a greater percentage of oil and water being removed through entrainment.

For given residual water and oil content curves, it was found that the onset of entrainment could be estimated by plotting oil removal against water removal. A positive change in the gradient of the line indicates entrainment onset. When using this relationship for a multimode and a single mode applicator setup (Configuration A and B) It was found that, in comparison to a single mode applicator, samples treated using a multimode applicator had a significantly greater amount of oil and water removed through vaporisation. However, data for samples treated using the multimode applicator at a higher power suggests that entrainment increases with increasing power density, as expected. This method of determining the removal mechanisms present can be useful as it provides an alternative way of determining shifts in mechanisms for different equipment setup and samples, without actually needing to quantify each mechanism.

CHAPTER 5 – Continuous Microwave Processing

5. INTRODUCTION

The main objectives of the work presented in this chapter are to determine the performance of a continuous microwave processing system and to develop the capability to treat oil contaminated drill cuttings on large samples so that a final oil content of 1 wt% is achieved. The work described in Chapter 4 provided an understanding of how oil is removed from drill cuttings during microwave treatment. This knowledge will be used to explain the experimental observations reported in this chapter, which focuses upon identifying the key variables affecting oil removal performance during continuous processing at pilot scale.

Previous work has suggested that oil removal can be affected by (1) properties inherent to the sample, (2) applicator design and (3) operating parameters. In practice little control is available over the initial conditions of the sample, however, understanding how the properties of the sample affect oil removal is crucial, as this directly affects the applicator design and operating parameters, which then need to be adjusted accordingly. Work on applicator design, specifically the shape and dimensions, has been carried out elsewhere and is not the focus of this work (Robinson, et al., 2009). The applicator used was optimised and designed for the belt conveyor system used in this work with only the applicator orientation and bed depth varied to determine their effects on oil removal.

This chapter aims to develop a detailed understanding of how sample properties and operating parameters affect oil removal efficiency in order to allow for future operation optimisation of the system. Oil removal efficiency in this case is defined as the difference between the initial and residual oil content, divided by the initial oil content

(Equation 4.18, Chapter 4). Figure 5.1 shows, which variables were investigated in order to understand how they affected oil removal from drill cuttings.

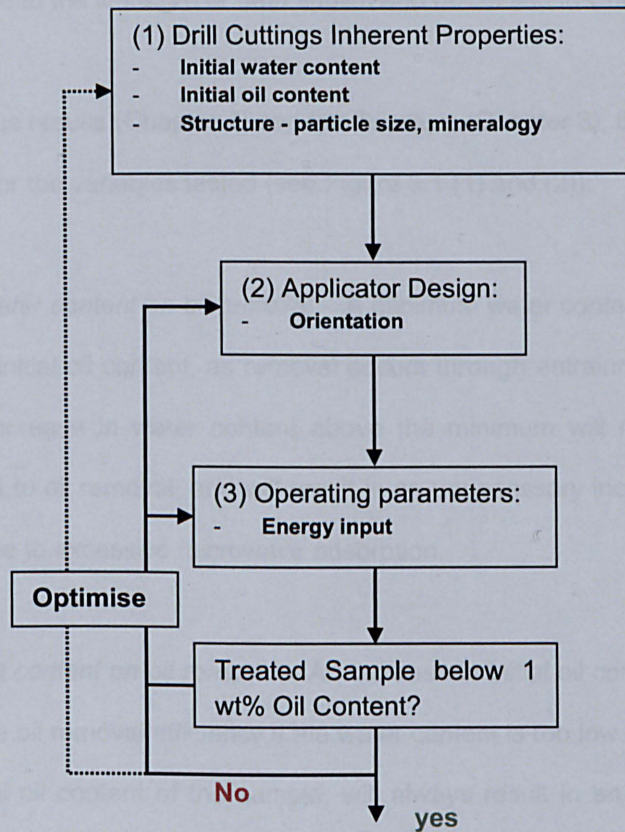


Figure 5.1 - Relationship between various variables affecting oil removal.

The results shown in this chapter follow the progression shown in Figure 5.1, where a single change is made to one of the variables shown in (1) or (2) for a given range energy inputs (3). The treated samples are then analysed for oil content and the results are compared to the literature or data obtained in bench scale experiments (Chapter 4).

The main objectives of this chapter can be summarised as follows:

- (1) To compare the performance of continuous pilot scale processing of drill cuttings with bench scale experiments.

- (2) To determine the effects of variables (1) and (2) on oil removal by determining the residual oil content as a function of energy input.
- (3) To explain the experimental observation obtained in each case through reference to the literature or data shown and discussed in Chapter 4.

Based on previous results (Chapter 4) and the literature (Chapter 3), the following are the hypotheses for the variables tested (see Figure 5.1 (1) and (2)):

Effect of initial water content on oil removal – A minimum water content is required to remove a given initial oil content, as removal occurs through entrainment and steam distillation. An increase in water content above the minimum will not provide any additional benefit to oil removal, and will result in an unnecessary increase in energy input required due to excessive microwave adsorption.

Effect of initial oil content on oil removal – An increase in initial oil content will lead to a decrease in the oil removal efficiency if the water content is too low. Additionally, an increase in initial oil content of the sample, will always result in an increase in the energy input required to process the sample.

Effect of particle size on oil content distribution and removal – Drill cuttings consist of particles which cover a range of particle sizes. Assuming the mineral constituents are equal across all particle sizes, the oil content is expected to be distributed equally across all particle sizes. For a given particle size range it is expected that oil removal will be greater in finer particles due to (1) increased individual particle surface area and (2) shorter path lengths water and oil vapours need to travel within the particles.

An additional aim of this chapter is to successfully demonstrate the treatment of drill cuttings at 896 MHz, in an industrial scale plant in comparison to bench scale and pilot scale treatment at 2.45 GHz. It is expected that at 896 MHz oil removal efficiency, measured as the percentage of oil removed based on the initial oil content,

will increase due to a larger sample bed surface area, which allows for better mass transfer from vapours formed within the cuttings. In addition, the decrease in frequency from 2.45 GHz to 896 MHz could result in an increase in microwave absorption efficiency due to increased contributions of Ionic Polarisation, Maxwell-Wagner Interface Polarisation and Conduction heating mechanisms. However, the latter could also lead to increased arcing, due to an increase in electric field strength required to maintain a similar magnitude power density in the water phase as observed at 2.45 GHz.

Results obtained for the continuous microwave treatment of drill cuttings at 896 MHz and 2.45 GHz will then be shown in an overall comparison chart of oil removal vs. energy input for all setups trialled thus far.

5.1 CONTINUOUS PILOT SCALE TREATMENT OF OILY CUTTINGS

This section begins by investigating the effect of initial water and oil content on the variation of residual oil content with energy input, it then moves on to determine the effects of bed depth and applicator orientation, before investigating the effect of particle size on oil content distribution and oil removal.

Section 5.2 provides a general experimental arrangement of the different applicator configurations used. Specific details of each of the experiments carried out are mentioned as required in each individual section. Standard techniques used for analysis are presented in the experimental Chapter 3.

5.2 GENERAL EXPERIMENTAL SETUP

5.2.1 2.45 GHZ PILOT SCALE RIG

Well mixed representative samples of oil contaminated drill cuttings were loaded into a rectangular hopper and fed through a continuous rectangular conveyor belt system using a screw feeder. The material was then passed at a given flowrate through the microwave cavity, where it was treated. The cavity was maintained inert at all times with a constant flow of Nitrogen (125 L/min), which was supplied at the inlet and outlet of the microwave cavity as well as in the applicator regions where material was treated. Nitrogen, steam and oil vapour leaving the material during treatment were collected by a dedicated extraction system (TAV 50), which was connected to the cavity at the exact points where material was treated. Steam and condensable vapours were then condensed in the shell side of a shell and tube heat exchanger, allowing for any oil collected to be recovered from the system. Extraction points were also present at the feed inlet between the screw feeder and the area of discharge into the belt, as well as at the discharge end of the cavity, where the treated drill cuttings were collected. The flow through the extraction points was controlled manually by opening and closing the extraction valves of each section as required. Treated material leaving the cavity was collected in metallic containers and placed in well ventilated areas under appropriate extraction.

The microwave cavity consisted of choke sections, which prevented microwave leakage, and the applicator region where treatment took place. Three different cavity configurations were used for tests, as shown in Figure 5.2.

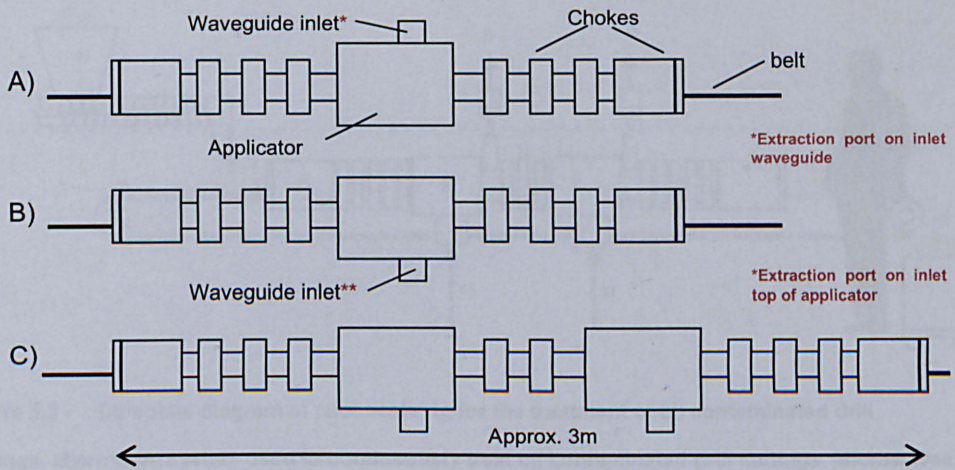


Figure 5.2 - Applicator configurations used in experiments.

Each arrangement is from here onwards referred to by its appropriate letter code. In arrangement A, the applicator was connected to the magnetron via three 90° bends and a series of straight sections followed by a water circulator unit. In arrangements B and C the applicator(s) were connected through a single 90° bend and a series of straight sections followed by a water circulator unit. In all cases the circulator was used to absorb any reflected power that was not absorbed by the load, and was important for protecting the magnetron during operation. Any heated water leaving the circulator unit is cooled by an air cooled heat exchanger and recycled back in a closed loop. Arc detectors were placed in the bend immediately after the applicator and just before the circulator in order to prevent any damage caused through arcing. Figure 5.3 shows a complete diagram of the system, the applicator configuration can be altered between A and C as required.

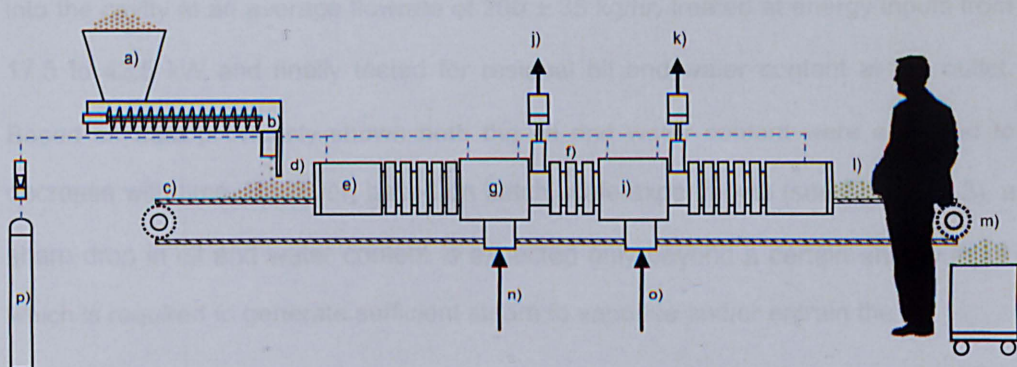


Figure 5.3 - Complete diagram of pilot scale rig for the treatment of oil contaminated drill cuttings. Microwave system used to continuously treat oil contaminated drill cuttings. Microwaves propagate from both applicators at 2.45 GHz. a) Hopper, b) Screw feeder, c) Conveyor belt, d) Untreated drill cuttings (Oil rich) are fed into the microwave applicator, e) Chokes used to prevent microwave leakage, f) Chokes used to prevent cross-coupling, g) and i) Microwave applicators where the sample is subjected to a high power density, j) and k) Vapours and extracted fumes are removed to the extraction system, l) microwave treated (oil-lean) drill cuttings exit the cavity and are collected (m) at the end of the line for testing, n) and o) microwave inlet perpendicular to belt, p) nitrogen bottle.

Flowrates ranging from 150 to 400 kg/hr and bed heights of 1.5 to 3 cm were used. In each case the oil and water content of the feed and product were measured at least 3 times using the standard procedures (ASTM D95 and DCM solvent extraction as per detailed in Chapter 3). Forward powers between 5 and 45 kW were used. The maximum power used with one single generator was 27.5 kW, the remainder was supplied using an additional 15 kW generator, which was installed in the second applicator in configuration C, as shown in Figure 5.2.

5.3 RESULTS AND DISCUSSION

5.3.1 CONTINUOUS TREATMENT OF DRILL CUTTINGS AT PILOT SCALE

Drill cuttings obtained from the North Sea containing an initial oil and water content of approximately 3 ± 0.3 and 12 ± 0.5 wt% respectively were treated using microwaves and an applicator arrangement equal to that of A) in Figure 5.2. The material was fed

into the cavity at an average flowrate of 200 ± 35 kg/hr, treated at energy inputs from 17.5 to 42.5 kW and finally tested for residual oil and water content at the outlet. Based on data previously shown both the oil and water content were expected to decrease with time. However, based on batch scale experiments (see Appendix 3), a sharp drop in oil and water content is expected only beyond a certain energy input, which is required to generate sufficient steam to vaporise and/or entrain the oil.

Figure 5.4 shows the variation of oil and water content with energy input, which was calculated as the product of the effective power input and the sample flowrate. The effective power input is the measured forward power minus the power reflected (as shown in Equation 4.3 in Chapter 4).

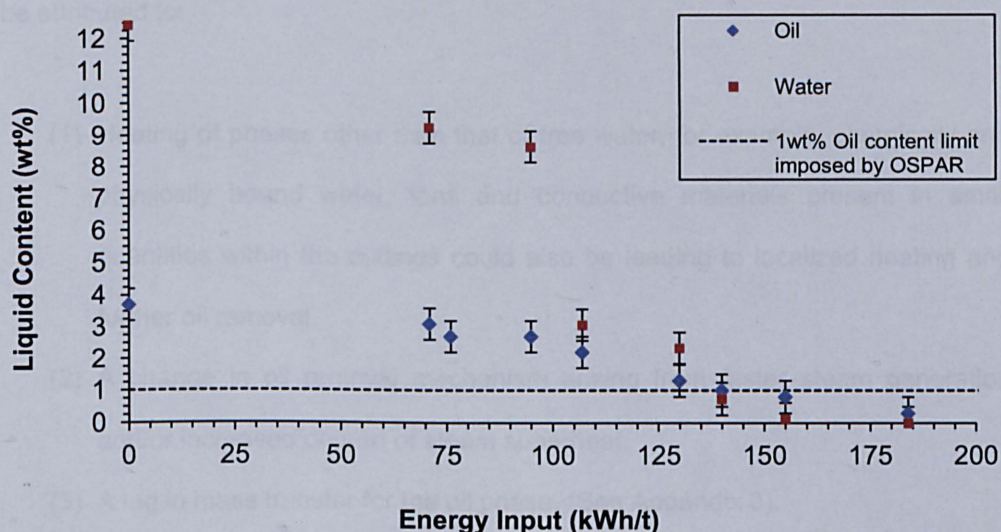


Figure 5.4 - Variation of oil content with energy input for a sample containing approximately 3.7 wt% oil and 12 wt% water treated with microwaves.

As expected the oil content decreased with increasing energy input from 3.7 to 0.4 wt% at 185 kWh/t, resulting in an overall oil removal of 92%. The gradient observed between 0 and 95 kWh/tonne, 0.01 wt%/kWh/t, was lower than that between 95 and 140 kWh/tonne at 0.03 wt%/KWh/t, suggesting a minimum energy input needs to be supplied to the sample before any significant oil removal is observed. This difference in the rate of oil removal per energy input supplied to the sample was also observed

during bench scale experiments (Chapter 4, Section 4.4.9) and can be attributed to the mechanisms responsible for removing the oil from the sample. In Chapter 4 two main mechanisms were identified; (1) steam distillation or vaporisation of the oil through steam generated in situ and/or (2) entrainment of the oil due to the rapid generation of steam within drill cutting particles, leading to an increase in pressure (Constant, et al., 1996) and velocity sufficient to entrain oil droplets present at the surface of particles. As a result oil removal is largely dependent on the vaporisation of the water content, which is the source of the minimum energy input requirements.

The water content was seen to decrease from just over 12 to 0.12wt%, resulting in an overall water removal of 99%. Interestingly, between 155 and 185 kWh/t, where <0.2 wt% water was present, oil content still decreased from 0.63 to 0.23 wt%. This could be attributed to:

- (1) Heating of phases other than that of free water, for example, chemically and physically bound water. Ions and conductive materials present in small quantities within the cuttings could also be leading to localized heating and further oil removal.
- (2) A change in oil removal mechanism arising from faster steam generation and/or increased degree of steam superheat.
- (3) A lag in mass transfer for the oil phase. (See Appendix 3).

5.3.1.1 Effect of dielectric properties on microwave heating of oily cuttings.

Oil contaminated drill cuttings consist of a series of minerals, water in various degrees of binding, oil and traces of additives present in the formulation of drilling muds. Dielectric properties data for the various phases is provided in Table 5.1 below (Replicated from Chapter 2 – Section 2.9.1.). With the exception of Kaolinite all measurements were at 20-25 °C and 2-2.5 GHz.

Material	ϵ'	ϵ''	Tan δ
Free water ⁽¹⁾	76.660	9.400	0.123
Mineral oil ⁽²⁾	2.400	0.180	0.075
Calcite ⁽³⁾	2.280	0.026	0.001
Sand (Dry) ⁽⁴⁾	2.910	0.005	0.002
Kaolinite (Dry) ⁽⁵⁾	1.91	0.12	0.063
Chlorite ⁽⁶⁾	7.200	0.126	0.018
Mica ⁽⁶⁾	8.690	0.091	0.011

Table 5.1 - Replicated from Chapter 4 - Dielectric constant, loss and Tan δ of some pure materials.

⁽¹⁾ (Ellison, et al., 1996) ⁽²⁾ Erle et al (Erle, et al., 2000), ⁽³⁾ Westphal (Westphal, 1997), ⁽⁴⁾ (Evans, 1997), ⁽⁵⁾ Orzechowski et al (@ 400 °C and 4 GHz) (Orzechowski, et al., 2006), ⁽⁶⁾ Nelson et al (Nelson, et al., 1989), ⁽⁷⁾ (Shang, et al., 2007).

When comparing dielectric properties between materials the following are key parameters:

- *Magnitude of dielectric constant* – provides an absolute measurement of the overall capacity of the material to absorb microwave energy.
- *Magnitude of dielectric loss* – directly affects the magnitude of the power dissipated per unit volume of the sample.
- *Loss tangent* – provides a conversion factor for how much of the absorbed energy is dissipated as heat.

Based on the above, the first consideration when comparing the dielectric properties of different materials is the actual magnitude of the dielectric constant and loss. Then, for materials of similar magnitude dielectric constant, the tangent loss can be used to differentiate between materials, where higher tangent losses lead to a more efficient energy to heat conversion.

As seen from Table 5.1, the dielectric constant and loss of free water is at least an order of magnitude higher than the other phases, which suggests the water phase is heated preferentially. Once the water phase is removed from the sample, the

dielectric constant and loss of the sample falls. This suggests that further heating of the remaining phases, is likely to be significantly lowered, as the magnitude of energy absorbed is significantly lower. In addition to the difference in magnitude between water and the other phases, the lower bulk tangent loss (<0.001 (Metaxas & Meredith, 1983)), results in poor energy to heat conversion.

For a given $\tan \delta$ and electric field strength, it is possible that the heat generated becomes much less the heat loss to the environment, which effectively leads to a stable or decreasing temperature trend with time. This is only possible if the sample properties change within a short space of time (i.e. within the time scales used within these experiments). The point at which the heat loss is \geq heat dissipation appears to be solely a function of the absolute amount of forward power, as increasing the power input by an order of magnitude will lead to a proportional increase in power dissipated in the material. As a result all materials, regardless of how low the dielectric constant and loss are, will heat if sufficient power is supplied. The latter assumes the energy losses to waveguides/applicators is minimal by comparison to the energy dissipated into the sample.

Figure 4.7 in Chapter 4 shows the actual variation in dielectric properties of a sample with an oil and water content of 3.7 ± 0.4 and 12.0 ± 0.8 wt% respectively. Measurements were carried out at 2.47 GHz in a cylindrical resonant cavity capable of temperature measurements as described in Chapter 3, Section 3.9.

From Figure 4.7 it can be seen that the dielectric constant and loss increase initially between 25 and 75 °C from 2.7 to 2.9 and from 0.58 to 0.72 respectively. This increase results from higher molecule mobility and an increased rate of collisions between molecules as they attempt to realign themselves to the charges in the electric field imposed by the electric field component of the microwaves. At $T > 100$ °C, the dielectric loss decreases significantly to ≤ 0.02 as free water is vaporised resulting in an increase in the physical space between molecules. This increase in

separation leads to a decrease in the number of overall collisions and consequently the dissipation of microwave energy as heat. The dielectric constant also decreases at $T > 100\text{ }^{\circ}\text{C}$, suggesting the degree of polarisation and energy absorption is significantly lower when free water is turned into steam. The calculated loss tangent at 50 and 120 $^{\circ}\text{C}$ are 0.2 and 0.005 respectively, which confirms the higher energy absorption and dissipation as heat prior to vaporisation.

Despite the low dielectric loss and, consequently low tangent loss, the bulk material will, as previously discussed, still heat if sufficient microwave power is applied, with the only difference being the greater inefficiency in the conversion of microwave energy to heat. Figure 5.5 shows the surface temperature of a borosilicate vial containing the oil base used in oil based drilling muds before and after microwave treatment at 750 W and 30 seconds. The vial containing oil was filled to the same height (3 cm) as that of the surrounding dry drill cuttings material, which contained negligible water and oil content $<0.2\text{ wt\%}$. The setup used is provided in Chapter 4, Section 4.4.3.

As seen from Figure 5.5, both the dry cuttings material and the oil phase heat when treated with microwaves. Further proof that this is the case, lies in the fact that the borosilicate vial, which has similar dielectric properties to that of sand as shown in Table 5.1, did not heat as much as the dry cuttings and oil phases with the temperature remaining close to that before treatment. The fact that the vial walls remained cold also suggest heat transfer between the rock and oil phase in the vial is minimal. The oil phase within the vial increased in temperature by 10 to 15 $^{\circ}\text{C}$ suggesting heating of the oil phase only using microwaves is possible albeit at a relatively low level.

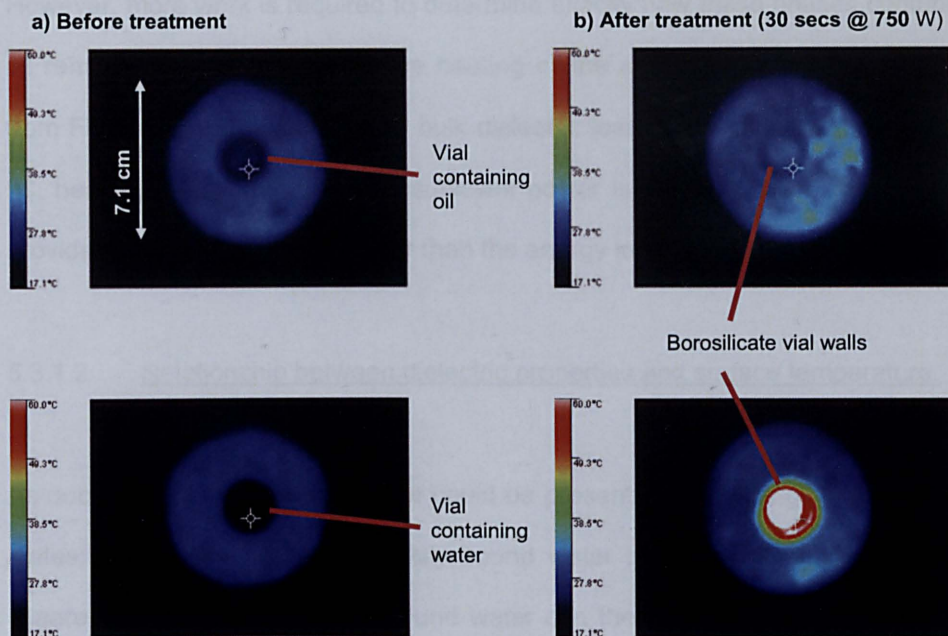


Figure 5.5 - Separate heating of oil and water phases, compared to dry drill cuttings material using microwaves.

The same experiment using the same parameters was carried out using water in the vial rather than oil, which resulted in a temperature rise of $>45^{\circ}\text{C}$ in the water phase. This can be converted to a heating efficiency by dividing the energy input into the sample by the temperature raised during that period. The volume of fluid present in the vial was calculated to be approximately $9.42 \times 10^{-6} \text{ m}^3$, based on a 3cm liquid height and an internal vial diameter of 2cm, this gives a heating efficiency of approximately 15 kWh/tonne/ $^{\circ}\text{C}$ for water and 50 kWh/tonne/ $^{\circ}\text{C}$ for oil. If the final reduction in oil is carried out through direct heating of the oil phase, then this could explain the significant increase in energy input per wt% oil reduction, in comparison to when oil is removed through steam distillation or entrainment as a direct result of stem generation.

Further heating of some of the mineral phases locally could also be occurring through conduction and/or Maxwell-Wagner interfacial polarisation. Strongly bound or chemically bound water could also be contributing to heating once the majority of the free and weakly bound water has been removed (Marcos & Rodriguez, 2011).

However, more work is required to determine exactly how these phases contribute to oil removal and overall microwave heating of the sample. Nevertheless, it is clear from Figure 4.7 that, although the bulk dielectric loss of the material is low at $T > 100$ °C, heating will still take place if sufficient power is provided, such that the energy provided into the sample is greater than the energy loss to the surrounding.

5.3.1.2 Relationship between dielectric properties and surface temperature.

As documented in Chapter 2 water could be present in drill cuttings in three different states: (1) free water, (2) physically bound water and (3) chemically bound water (Saarenketo, 1998). Physically bound water can then be further divided into weakly and strongly bound. Drill cuttings samples weighing 105 ± 7 g with an initial oil and water content of approximately 3.7 ± 0.4 and 12 ± 0.8 wt% respectively were treated at approximately 2500 W for 0-67.5 seconds. This was carried out at bench scale using the setup described in detail in Section 4.4.3 of Chapter 4. Figure 5.6 shows the variation of the recorded water content with energy input.

As expected, the water content decreased with energy input. It is clear that the drop in water content is greater between 100 and 200 kWh/t, in comparison to energy inputs < 100 and > 200 kWh/t respectively. The reduction in water content up to 100 kWh/t can be attributed to the minimum energy input required to carry out sensible heating of the sample to the boiling point of water.

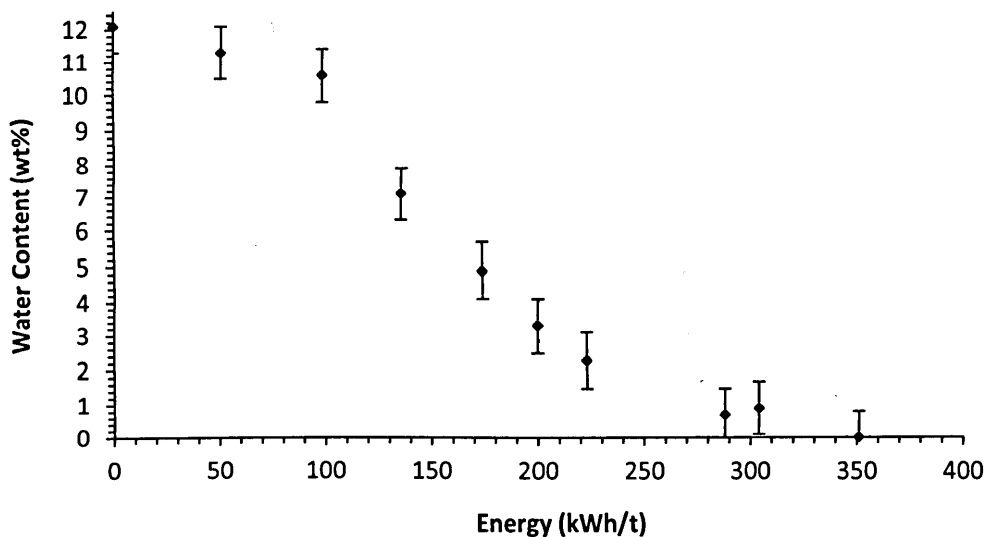


Figure 5.6 - Water content vs. energy input for a drill cuttings sample with an initial oil and water content of 3.7 ± 0.4 and 12 ± 0.8 wt% respectively.

Above 100 kWh/t steam is generated and removal improves as a result of enhanced mass transfer mechanisms, including pressure and temperature gradient driven removal, as discussed in Chapter 4. Above 300 kWh/t, the residual water content present is likely to be bound, requiring a substantially higher amount of energy input in order for removal to occur, which arises from a substantial decrease in the bulk dielectric properties of the sample (see properties at $T > 100$ °C in Figure 4.7), the state in which the water is present, and greater heat losses to the environment.

The average, maximum and minimum surface temperatures were then measured for the samples treated at the energy input shown above (Figure 5.7). Note the accuracy of surface temperature measurements is low and will vary significantly from internal temperatures. However, the data can be used as an indication of the magnitude and trends in sample temperature with energy input. Temperatures were measured using a Raytek ThermoView Ti30 with the setup described in Section 4.4.3 of Chapter 4.

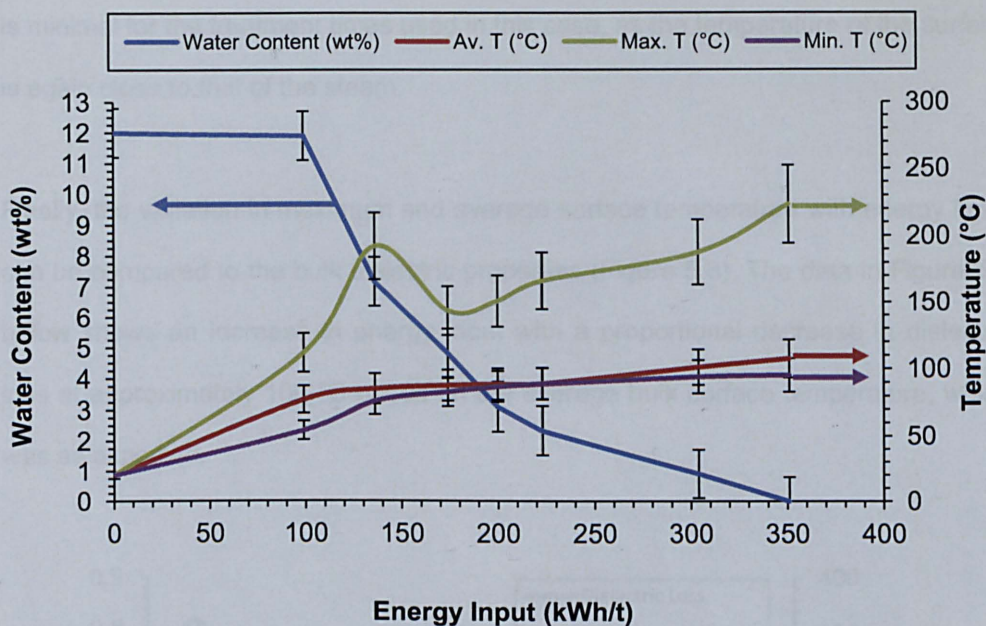


Figure 5.7 - Variation of average, maximum and minimum bulk temperature with energy input (kWh/t) for drill cuttings samples containing 3.7 ± 0.4 and 12 ± 0.8 wt% oil and water content respectively.

As expected, between 0 and 100 kWh/t the average surface temperature increases steadily as a result of sensible heating, once the sample reaches $90 \pm 10^\circ\text{C}$ the temperature remains constant between 100 and 200 kWh/t suggesting the vaporisation of free water is occurring. Above 200 kWh/t the average surface temperature increases towards 110°C suggesting superheating of the steam is occurring. Superheating could be occurring as the remainder of the water content present in the sample could be physically or chemically bound. This would correspond to a water content of <4 wt% according to the data shown in Figure 5.6.

Also, the maximum measured temperatures suggest localized heating may be occurring, which could be leading to substantial superheating of water. The fact the minimum and average sample temperature are within approx. $\pm 10^\circ\text{C}$ at energy inputs >140 kWh/t suggests the steam generated within the sample is distributed evenly within the volume of the sample as the entire surface is heated to at least 90°C . It also suggests that resistance to heat transfer between steam and other phases

is minimal for the treatment times used in this case, as the temperature of the surface is again close to that of the steam.

Finally, the variation in maximum and average surface temperature with energy input can be compared to the bulk dielectric properties (Figure 5.8). The data in Figure 5.8 below shows an increase in energy input with a proportional decrease in dielectric loss at approximately 100 °C based on the average bulk surface temperature, which was as expected.

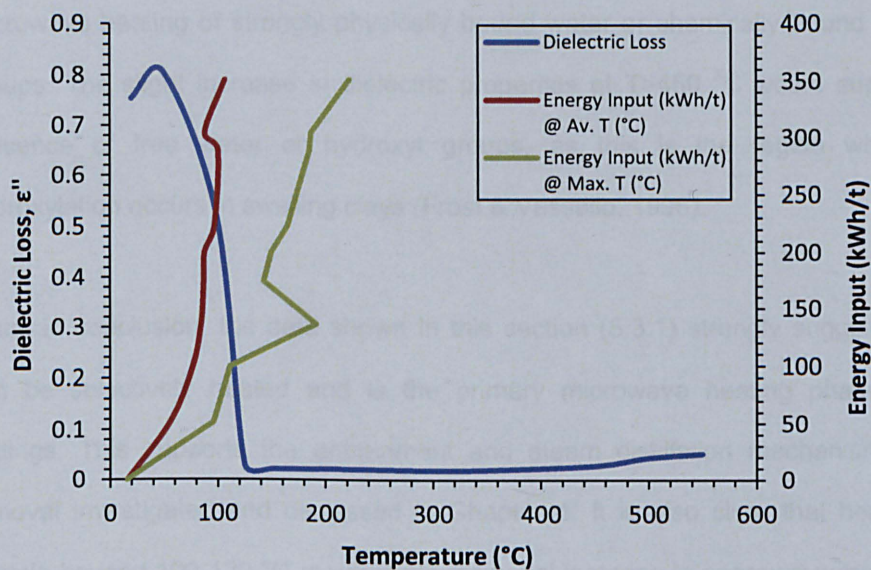


Figure 5.8 - Variation energy input with temperature and equivalent dielectric properties at that temperature.

The increase in energy input with temperature arises as a result of the sensible heating and vaporisation of the water phase as previously discussed, but is also affected by the decrease in the sample's bulk dielectric loss, which according to Equation 4.12 (Section 4.4.9 in Chapter 4) leads to lower heating rates. This in turn results in greater heat loss and a greater energy requirement to heat the material. This is clearly seen at temperatures >140 °C, where the energy input required per 1 °C rises significantly. For example; using the data of the average surface temperature of the sample between 20 and 90 °C, approximately 1.8-2 kWh/t are required per 1 °C rise, whereas between 90 and 110, approximately 12.5 kWh/t are required per 1

°C rise. However, it is also important to consider the maximum temperature measured, as there are some regions in the sample where the temperature is significantly greater than that of the bulk, suggesting microwave absorption and sample heating in those areas is efficient even at temperatures higher than 100 °C and consequently very low moisture content. Thus, the state in which water is present within the cuttings could significantly affect the energy and temperature requirements for vaporisation.

It is possible that local superheating within the cuttings could occur as a result of microwave heating of strongly physically bound water or chemically bound hydroxyl groups. The slight increase in dielectric properties at $T > 450$ °C would support the presence of free water or hydroxyl groups, as this is the region where dehydroxylation occurs in swelling clays (Frost & Vassallo, 1996).

Thus, in conclusion, the data shown in this section (5.3.1) strongly suggests water can be selectively heated and is the primary microwave heating phase in drill cuttings. This supports the entrainment and steam distillation mechanisms of oil removal investigated and discussed in Chapter 4. It is also clear that heating the sample beyond 100-120 °C requires a substantial increase in energy requirement, as lower moisture content, and consequently lower bulk dielectric properties lead to lower heating rates and greater heat loss. Nevertheless, hot spots were observed, and can be resulting from small amounts of highly absorbing microwave phases present in the sample (e.g. pyrite) or due to strongly bound water/hydroxyl groups present in the clays.

5.3.2 *COMPARISON OF CONTINUOUS AND BENCH SCALE TREATMENT*

Following the results shown in Figure 5.4 it is useful to compare results obtained during continuous processing at pilot scale with bench scale experiments, in order to determine potential differences in removal mechanisms and consequently oil removal

efficiency as a function of energy input. Figure 5.9 provides a direct comparison between samples treated using a bench (Chapter 4, Section 4.4.3) and pilot scale experimental setup (Chapter 5, Section 5.2 – Configuration C). In both cases samples containing 3.7 ± 0.4 wt% oil and 12 ± 0.8 wt% water were used. Samples were treated at bench scale at 2500 W for processing times ranging from 15 to 60 seconds.

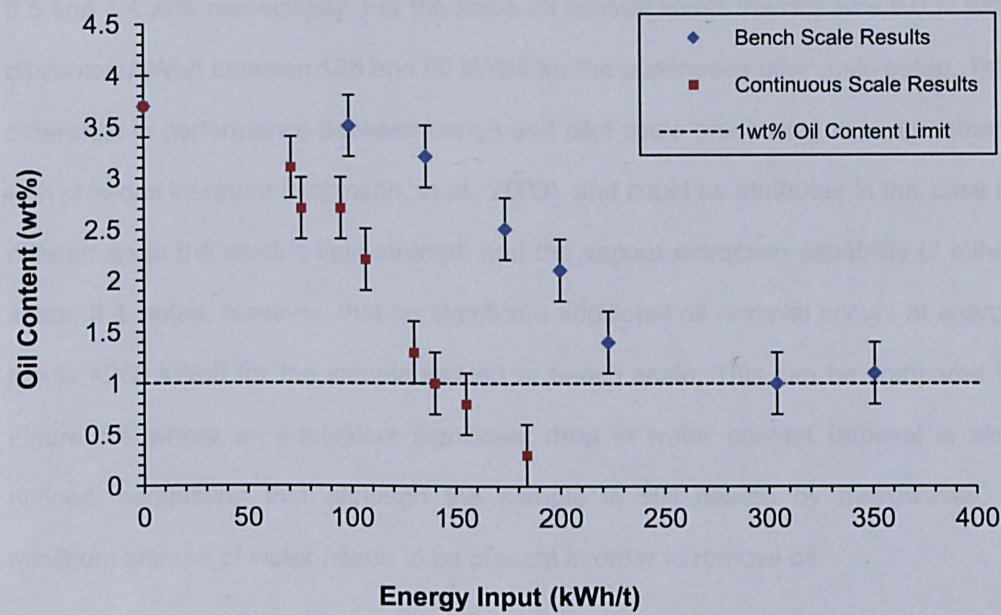


Figure 5.9 - Variation of oil content with energy input for drill cuttings with an oil and water content of 3.7 ± 0.3 and 12 wt% respectively, treated using the pilot scale and bench scale setup (See Chapter 4, Section 4.4.3).

The data shown in Figure 5.9 shows as expected a decreasing trend in oil content with energy input. At bench scale approximately 250-300 kWh/t were required for 1 wt% to be achieved, whereas only 140 kWh/t were required at continuous scale.

There are two key differences between bench scale and pilot scale microwave processing. The first difference is the minimum energy input required for oil removal to be significant (≥ 15 -20% oil removal). At pilot scale, the oil content begins to decrease significantly at >70 kWh/t, whereas at bench scale, the oil content only began to decrease between 100-140 kWh/t. The discrepancy between continuous and pilot scale processing is likely to be a result of greater heat losses and lower

electric field strength in the case of bench scale processing leading to lower power densities in the water phase (Chapter 4, Section 4.4.9 Equation 4.11).

The second difference was the smaller difference in oil content per kWh/t when processing at bench scale. At bench scale, the difference was approximately 0.017 wt% oil/kWh/t between 100 and 225 kWh/t where the oil content was measured as 3.5 and 1.4 wt% respectively. For the same oil content levels the rate was 0.032 wt% oil content/kWh/t between 125 and 60 kWh/t for the continuous pilot scale setup. This difference in performance between bench and pilot scale processing is in agreement with previous literature (Robinson, et al., 2009), and could be attributed in this case to differences in the electric field strength and the vapour extraction capability of either setup. It is noted, however, that no significant additional oil removal occurs at energy inputs >250 kWh/t for the sample treated at bench scale. This can be compared to Figure 5.6 where an equivalent significant drop in water content removal is also noticed, suggesting that although the sample is still heated by microwaves, a minimum amount of water needs to be present in order to remove oil.

In conclusion, according to the data presented in Figure 5.9 there appears to be a significant advantage in operating continuously at pilot scale. This advantage is likely to be a result of the difference in the magnitude of the power forward used in either case, as well as the higher electric field strength in the continuous pilot scale applicator (Robinson, et al., 2009).

5.3.2.1 Effect of power density in the water phase on oil removal

As seen from Figure 5.4 and Figure 5.6 the water content decreases with increasing energy input for both bench and pilot scale treatment. Based on the power absorbed and the residual water content, measured at the end of treatment at a given energy input, it is possible to calculate the final power density in the water phase. This assumes all power is dissipated in the water phase, which will be a good

approximation for water contents >1-2 wt%. Below 1-2 wt% the efficiency of coupling into the water phase decreases and is likely to lead to higher inaccuracies when calculating the power density using this assumption.

Table 5.2 below shows the range of powers used during the continuous treatment of cuttings and includes the corresponding flowrates, energy input and water content. The equivalent data is also shown for bench scale processing; power used, processing time, sample size and the corresponding average water content for each experiment.

Continuous System (Pilot Scale)				Batch System (Bench Scale)				
Power (kW)	Flowrate (kg/hr)	Energy Input (kWh/t)	Water content (wt%)	Power (kW)	time (secs)	Sample mass (kg)	Energy Input (kWh/t)	Water content (wt%)
0	0	0	12	0	0	0	0	12
21	290	71	9.3	2.54	15	0.107	99	11.9
20.5	220	95	8.7	2.57	22.5	0.119	136	7.2
30	250	107	3.07	2.59	30	0.123	174	4.8
32.5	230	130	2.33	2.59	35	0.126	200	3.1
35	230	140	0.74	2.59	37.5	0.121	223	2.3

Table 5.2 - Power, flowrate, processing time, energy input and water content data for bench and continuous processing of cuttings.

Based on the water content data presented in Table 5.2 the power density was calculated using Equation 5.1 below. This assumes all the power is primarily dissipated in the water phase, which is a good approximation at high water contents, but is likely to deviate from the actual power density in the water phase as it approaches <1 wt% water.

$$P_d = \frac{P}{(x_{h2o})(M)(1000)}$$

[Equation 5.1]

Where P_d is the power density in the water phase (W/m³ of water/sec), x_{h2o} is the water content (wt. fraction) and M is the overall mass flowrate of the sample (kg/hr). The density of water is approximated to 1000 kg/m³. Figure 5.10 shows how, for a

given energy input, the power in W dissipated per m³ of water per second is greater in the pilot scale rig in comparison to the bench scale setup.

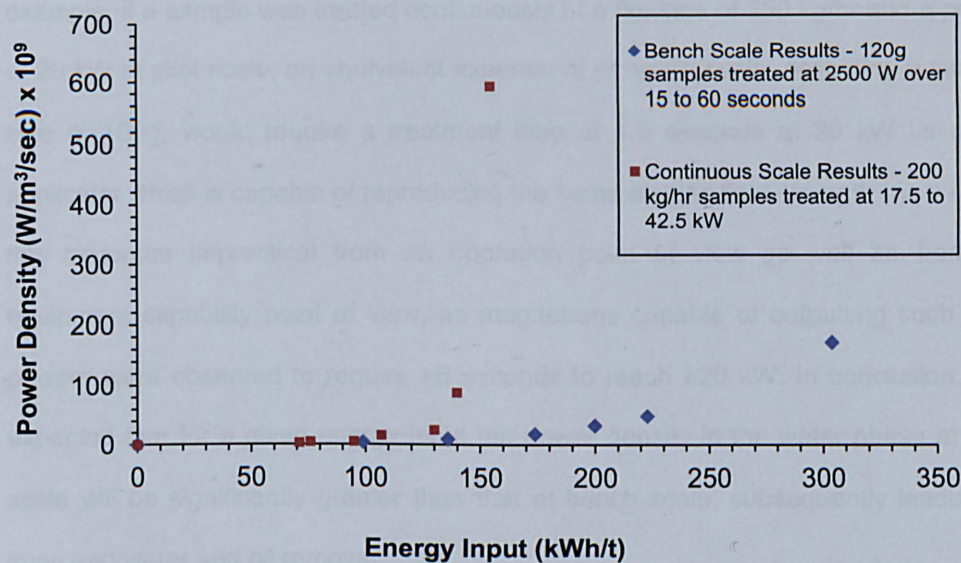


Figure 5.10 - Power density (kW/kg of water/hr) vs. energy input (kWh/t) for drill cutting samples containing 3 and 12 wt% oil and water content respectively, treated using a bench scale and pilot scale setup.

A higher power density for a given energy input means the rate of heating, °C/sec, (Equation 4.12, Chapter 4, Section 4.4.9) in samples treated continuously is higher than that of bench scale experiments. Higher heating rates lead to higher rates of steam generation, which improve heat transfer between the water and oil phase due to higher turbulence and better mixing (Perry & Green, 1997). This improved heat transfer leads to higher rates of oil vaporisation through steam distillation. In addition, higher steam generation rates lead to greater internal pressures and higher vapour velocity, enhancing oil removal through entrainment. Entrainment is desired as latent heat does not need to be overcome, increasing the overall energy efficiency of the process.

As seen from Table 5.2 there is a fundamental difference between the method of processing cuttings in batch at bench scale and continuously at pilot scale. At bench scale, energy input is increased by increasing processing time at a constant power

output, whereas at pilot scale, the energy input is increased by increasing power at a constant flowrate. This difference in mode of operation results in the inability to replicate power densities achieved at pilot scale in bench scale experiments. For example, if a sample was treated continuously at a flowrate of 250 kg/hr and a power of 20 kW at pilot scale, an equivalent experiment at bench scale, assuming a sample size of 100g, would require a treatment time of 1.5 seconds at 20 kW using an applicator which is capable of reproducing the same electric field strength. As a result this becomes impractical from an operation point of view as well as from an equipment capability point of view, as magnetrons capable of outputting such high powers were observed to require >5 seconds to reach ≥ 20 kW. In conclusion, it is expected that for a given energy input the power density in the water phase at pilot scale will be significantly greater than that at bench scale, subsequently leading to improved water and oil removal.

5.3.2.2 Effect of extraction setup on oil removal

During processing in the continuous system the sample moves with the belt through a series of extraction points. The removal of water and oil from the sample is not instantaneous and is time limited (See Appendix 3), due to mass transfer limitations arising from resistance within each individual particle and the bed of cuttings itself. Therefore, passing the sample through a series of extraction points before collection could improve the overall efficiency of the process, by preventing recondensation of the vapour and saturation of the nitrogen immediately above the sample bed. In the case of this particular batch setup the sample was stationary and the water vapour and oil were required to travel a greater length to the extraction point, increasing the potential for vapour re-condensation and re-contamination of the sample.

5.3.3 *EFFECT OF INITIAL OIL CONTENT ON RESIDUAL OIL CONTENT AND ENERGY REQUIREMENTS.*

Using 300kg of Sample 1A containing 5.4 and 6.7 wt% oil and water content respectively as a base material, more oil, analogous to that present in the original mud, was added sequentially to the drill cuttings sample to produce two further samples. An industrial mixer was used to mix the samples for a duration of 7 hours to ensure sample homogeneity as much as possible. However, it is important to note that the actual way the oil is physically distributed within the particles of the newly made samples is likely to differ from actual cuttings produced during drilling. The initial oil and water content of each of the three new samples is provided below in Table 5.3.

Sample	Init. Oil Content (wt%)	Init. Water Content (wt%)
1A	5.4 ± 0.4	6.7 ± 0.3
1B	8.2 ± 0.4	6.7 ± 0.3
1C	10.3 ± 0.4	6.7 ± 0.3

Table 5.3 - Initial oil and water content of Samples 1A, 1B and 1C.

The treatment of 1A-1C samples was carried out using the same procedure as that described in Section 5.2 with an applicator arrangement equal to that of A), as shown in Figure 5.2 The results of these experiments are shown in Figure 5.11.

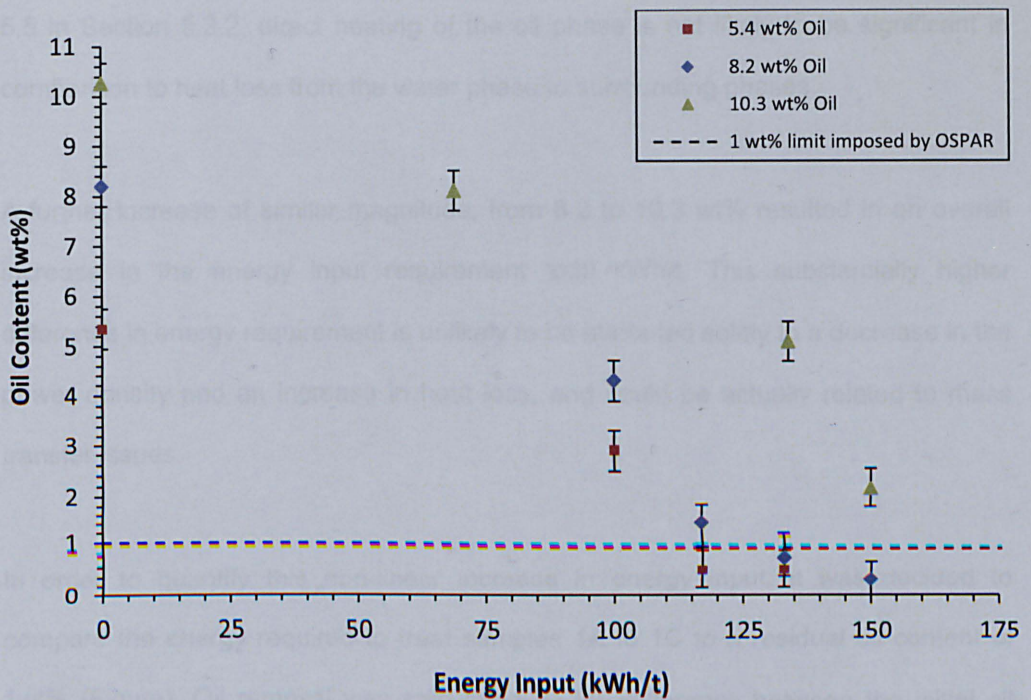


Figure 5.11 - Variation of oil content with energy input for drill cuttings containing different initial oil content.

According to Figure 5.11, energy inputs of 110, 130 and 160 kWh/t were required to treat oil contaminated cuttings containing 5.4, 8.2 and 10.3 wt% initial oil content down to 1 wt% respectively. Increasing the initial oil content resulted, as expected, in an increase in the energy input required to drive the residual oil content down to 1 wt%. However, the large difference in energy input between 10.3 and 8.2 wt% initial oil content was unexpected. The increase of 2.8 wt% oil in the feed from 5.4 to 8.2 wt% initial oil content resulted in an increase in energy input requirement of approximately 20 kWh/t. Using a specific heat capacity of 2 kJ/kg K and a latent heat of vaporization of 800 kJ/kg for the oil phase, the minimum energy input required to vaporize the additional 2.8 wt% oil content is approximately 6 kWh/t. Thus, it is clear that the difference in energy input measured (20 kWh/t) is not directly equivalent to the calculated energy required (6 kWh/t) for the removal of the oil content added to the sample. The 15 kWh/t unaccounted for, could be resulting from a decrease in the overall power density, due to a higher overall liquid volume, and/or heat losses occurring from the water to the various phases present within the drill cuttings, and finally from the sample's surface to the environment. However, as seen from Figure

5.5 in Section 5.3.2, direct heating of the oil phase is not likely to be significant in comparison to heat loss from the water phase to surrounding phases.

A further increase of similar magnitude, from 8.2 to 10.3 wt% resulted in an overall increase in the energy input requirement to 30 kWh/t. This substantially higher difference in energy requirement is unlikely to be attributed solely to a decrease in the power density and an increase in heat loss, and could be actually related to mass transfer issues.

In order to quantify this non-linear increase in energy input, it was decided to compare the energy required to treat samples 1A to 1C to a residual oil content of 1wt% (Figure). Oil removal was calculated as the difference between the initial oil content of each individual sample and a final oil content of 1 wt% divided by the initial oil content of the same sample (Equation 4.18, Chapter 4, Section 4.4.12), which was then plotted against the equivalent energy inputs, previously discussed above.

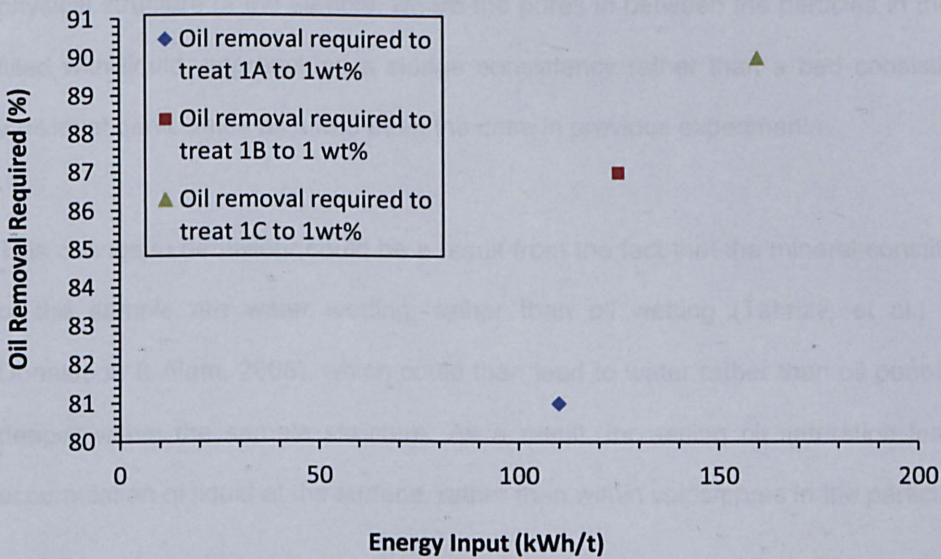


Figure 5.12 - Variation in oil removal requirement with energy input for drill cuttings Samples 1A to 1C.

As expected, an increase in initial oil content leads to an increase in the oil removal required to reach 1 wt% and consequently an increase in the overall energy input

required during treatment. However, a linear increase of energy input with increasing oil removal was expected, which did not occur in practice, especially with Sample 1C. This suggests that the addition of oil to the sample changes the overall sample heat and mass transfer characteristics, resulting in an overall decrease in oil removal efficiency.

5.3.3.1 Effect of initial high oil content on sample structure and mass transfer

The higher oil content in Sample 1C resulted in visible changes to the physical structure of the sample. It was noted that, visually, there was no significant physical structure difference between the samples 1A and 1B containing 5.4 and 8.2 wt% oil content respectively. Samples 1A and 1B consisted of individually separated agglomerated particles without any noticeable surface liquid. When packed in the conveyor belt no significant reshaping of individual particles was observed and there was clear separation between particles. This was not the case with Sample 1C, where surface liquid was clearly visible. This resulted in a significant change in the physical structure of the sample, where the pores in between the particles in the bed filled with liquid, approaching a sludge consistency rather than a bed consisting of individual particulates as it had been the case in previous experiments.

This change in behaviour could be a result from the fact that the mineral constituents of the sample are water wetting, rather than oil wetting (Tabrizy, et al., 2011; Donaldson & Alam, 2008), which could then lead to water rather than oil penetrating deeper within the sample structure. As a result, increasing oil saturation leads to accumulation of liquid at the surface, rather than within voids/pores in the particles.

This change in sample structure could have a number of significant adverse effects in terms of energy input requirements, especially if a final residual oil content of 1 wt% is required. These are summarised as follows:

Increase in boiling point due to increase in internal pressure – A decrease in voids within the sample could impose higher pressures within the pores, which in turn could result in higher boiling points and greater energy input requirements for the removal of oil and water.

Reduced porosity – Further to the point above a decrease in porosity could result in greater resistances to transporting internal water and oil vapour from within the sample outwards. Higher resistance means the time and path taken for the vapour to leave the structure increases, resulting in greater heat loss and re-condensation of vapour. If the pores of the bed are fully saturated, this will also impact mass transfer significantly, as liquid will have to be initially physically expelled from within the pores to the surface of the bed followed by vaporisation at the surface. This presents a further rate limiting step, as the overall surface area for vaporisation becomes equal to that of the outer surface area only, rather than the surface area available within each pore. This could significantly limit the rate at which liquid is removed from the cuttings.

Reduced flow – As a further consequence of lower porosity, the sample requires greater internal pressures in order for vapour to be driven at the same rate from within the voids/pores to the surface of the bed. In order to reach higher pressures, the rate at which energy input is delivered to the sample (i.e. the power) increases, resulting in an overall greater energy requirement.

Thus, from the data presented in Figure 5.11 there is a clear disadvantage, in terms of overall energy input requirement, in treating drill cuttings with a high initial oil content. Potential ways of overcoming this issue are:

1. Pre-drying material with air/nitrogen.
2. Blending of material with dry material to increase overall voidage.
3. Reducing bed depth.

Blending of wet drill cuttings with treated material allows for the successful treatment of cuttings, as previously shown in the literature (Robinson, et al., 2009). However, blending reduces the overall throughput and adds the need for a holding tank and a recycle line, which potentially increases the overall footprint of the unit, which is undesired in this case. Therefore, blending is not investigated further in this work.

Pre-drying wet cuttings with hot nitrogen ($T \gg 300\text{ }^{\circ}\text{C}$) is unlikely to be a feasible solution for cuttings with high oil content as batch scale experiments showed nitrogen/air drying only reduced moisture content and only at drying rates of at most an order of magnitude lower than the measured equivalent microwave drying rates. Thus, high oil content at the surface could still be prevalent even after pre-drying. However, results shown in Section 4.4.11 of Chapter 4 show a significant advantage in having a nitrogen flow present during the microwave treatment, which has also been documented in similar works in the literature where combined microwave and conventional heating has been investigated (Turner, 1991; Marra, et al., 2010). As a result the presence of a nitrogen sweep from a safety and mass transfer enhancement point of view is essential, and was used in all experiments.

Following the results obtained above in Figure 5.12 it was decided to investigate the effect of initial water content in order to answer the following questions:

- Does an increase in water content lead to the same change in structure observed with an increase in oil content?
- Or is the increase in energy requirement proportional to the increase in content?

5.3.4 EFFECT OF INITIAL WATER CONTENT ON RESIDUAL OIL CONTENT AND ENERGY REQUIREMENTS.

Using the same principle as that presented in the beginning of Section 5.3.3, and Sample 1B as the base material, three samples of different water content but equal oil content were generated.

Sample	Initial. Oil Content (wt%)	Initial. Water Content (wt%)
1B	8.2 ± 0.4	6.7 ± 0.3
1D	8.2 ± 0.4	11.3 ± 0.3
1E	8.2 ± 0.4	14.6 ± 0.3

Table 5.4 - Initial oil and water content of Samples 1A, 1B and 1C.

The treatment of samples 1B-1E was carried out using the same procedure as that described in Section 5.2 with an applicator arrangement equal to that of A), as shown in Figure 5.1.2. The results of these experiments are shown in Figure 5.13.

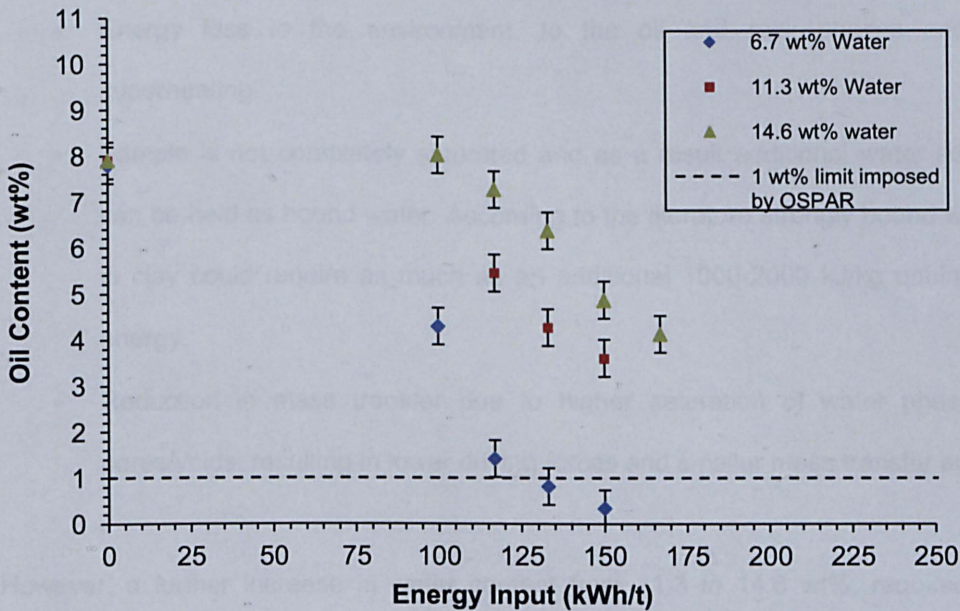


Figure 5.13 - Variation of oil content with energy input for drill cuttings containing different initial water content.

Figure 5.13 shows as expected an increase in energy input requirement with increasing water content. If the data presented is linearly extrapolated, then 125, 200 and 225 kWh/t are required to treat all three samples to 1 wt% oil content. Linear extrapolation was used in this case as previous data has shown (Figure 5.11 and 5.9 for example) that, generally, oil and water content continue to decrease steadily until around 1 wt%, which is expected as drying transitions from constant to falling rate drying only (Meredith, 1998). Interestingly, an increase in water content from 6.7 to 11.3 wt% suggests an additional 75 kWh/t is required, whereas an increase from 11.3 to 14.6 wt% only required an additional 25 kWh/t. This behaviour is opposite to that of oil content

The minimum energy requirement to vaporise 1 wt% water content for a flowrate of 150 kg/hr is 7 kWh/t/wt%. That would suggest that a minimum energy input of 35 kWh/t is required for the additional water content difference between samples containing 6.7 and 11.3 wt% water respectively. The difference between the actual energy input required, 75 kWh/t, and the calculated, 35 kWh/t, could be justified by:

- Energy loss to the environment, to the oil and rock phases and to superheating.
- Sample is not completely saturated and as a result additional water added can be held as bound water. According to the literature strongly bound water in clay could require as much as an additional 1000-2000 kJ/kg unbinding energy.
- Reduction in mass transfer due to higher saturation of water phase in pores/voids, resulting in lower driving forces and smaller mass transfer area.

However, a further increase in water content from 11.3 to 14.6 wt%, required an additional 25 kWh/t to vaporise 3.3 wt% additional water content, which matched

closely the calculated energy requirements. This could be due to the following reasons:

- Water content added could be present as free water and as such would require less energy.
- Increased entrainment – during batch scale experiments higher initial liquid content led to an increase in entrainment (Figure 4.46, Chapter 4, Section 4.4.10.2). As entrainment is a physical process, the boiling temperature of water does not need to be reached in order for removal to occur.
- Higher water content increases the bulk dielectric properties of the material and as a result increases the efficiency at which energy is absorbed and dissipated as heat through the water phase. The higher water content can also increase the contact area between the water and the rock and oil phase increasing heat transfer.

Based on the results obtained in this case (Figure 5.13), it is clear that increasing water content leads to an increase in the overall energy input requirement, without any additional benefit to oil removal. However, previous literature (Shang, et al., 2005) has also shown that a minimum water content is also needed in order for significant oil removal to be observed ($>90\%$). This suggests there is an optimum water content where the minimum amount of water, and consequently energy input, is required to give an oil removal $\geq 90\%$. This is shown diagrammatically in Figure 5.14.

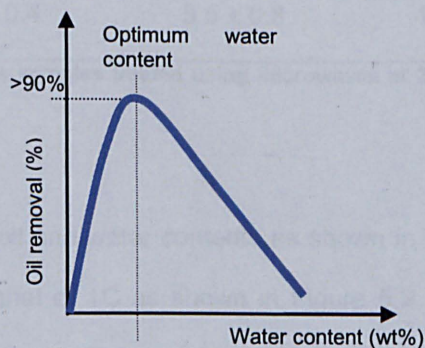


Figure 5.14 - Hypothetical variation of oil removal with water content.

The behaviour illustrated in Figure 5.14 can also be explained from a heat and mass transfer point of view. At low water contents the area of contact between water (Steam) and the oil phases is small, reducing heat transfer from the water phase to the oil phase. At significantly higher water contents heat transfer improves due to higher contact area between both phases, which in theory should allow for higher oil removal. However, energy dissipation into the water phase is likely to be less efficient for 2 reasons: (1) decreasing penetration depth, (2) the additional water content is unlikely to be arranged in the most efficient way for microwave heating (as discussed in Chapter 2, Section 2.9.1. As a result, higher water contents past the optimum will also require a greater overall energy input, decreasing the overall efficiency of the process. The minimum initial water content is likely to depend on the overall sample volume, its initial oil content and physical structure.

5.3.5 EFFECT OF PARTICLE SIZE ON OIL REMOVAL

Drill cuttings samples with the average bulk oil and water content as shown in Table 5.5. were treated using an applicator configuration equal to C) as presented in Figure 5.2.

Sample	Initial Oil Content (wt%)	Initial Water Content (wt%)	Flowrate (kg/hr)	Power Range (kW)
2A	2.9 ± 0.2	12.8 ± 0.3	235 ± 35	0-42.5
2B	2.8 ± 0.4	9.9 ± 0.3	150 ± 7	0-25
2C	7.8 ± 0.4	5.5 ± 0.8	150 ± 17	0-25

Table 5.5 - Drill cuttings samples treated using microwaves at 2.45GHz and analysed at different particle size ranges.

Samples with initial oil and water contents as shown in Table 5.5 were treated using the same setup as that of 1C as shown in Figure 5.2 and were sieved before and after treatment in order to obtain the variation in residual oil content with particle size. Sieve sizes of 6.35 down to 0.3 mm were used in each case, allowing for the particle

size distribution curve to be determined for each sample. The detailed procedure, which was used for sieving samples, is explained in Section 3.6 of Chapter 3. For the purposes of this thesis the particle size is equivalent to sieve aperture size. For example, all particles retained between sieves 6.35mm and 4.75 mm will be referred to as particles with a nominal average size equal to that of the mathematical mean of either sieve sizes (i.e. 5.55 mm). The nominal average particle sizes studied in this case were: 5.55, 4.05, 2.855, 1.777, 1.015, 0.725, 0.513, 0.363 and 0.15 mm. Figure 5.15 shows the cumulative passing particle size distribution of Sample 2A as a function of %weight. The error bars represent the extent of variation in the distribution between feed and treated samples.

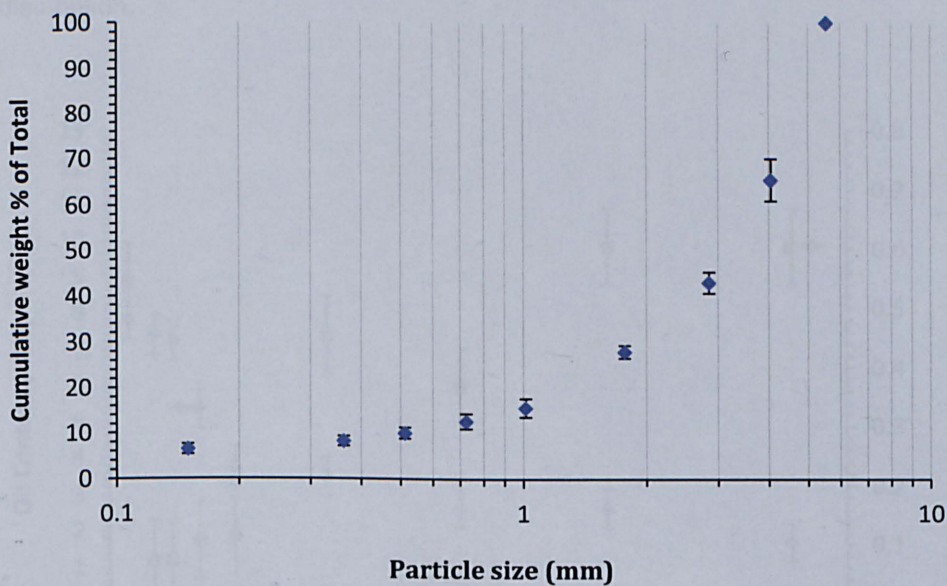


Figure 5.15 - Particle size distribution for Sample 2A.

As seen from Figure 5.15 it is clear that Sample 2A is composed primarily, >85% w/w, of particles of size ≥ 1.015 mm. The oil content was then analysed for each individual particle size class. The oil content was expected to be unevenly distributed, with greater oil content present in the coarser size fractions. Coarser particles will retain oil and water at greater depths within their structure, leading to longer paths lengths for oil and water vapour to travel before removal from the sample. Therefore, oil removal with sieve shaking and subsequent centrifuging would be expected to be

more efficient in finer particle fractions. The measured oil content distribution is shown below in Figure 5.16

As expected the oil content was unequally distributed across the various particle size ranges. However, contrary to what was hypothesised, the oil content was found to be greater in finer particles, and showed an overall decrease in oil content with increasing particle size. This must take into consideration the particle size distribution shown in Figure 5.15, which would suggest that, although the oil content in finer particles is higher, the actual absolute mass of oil within the sample due to larger particles is greater, as the >80% of the sample has a size of >1 mm. This is clearly shown by the data in Figure 5.16 where the oil content is adjusted for the particle size distribution.

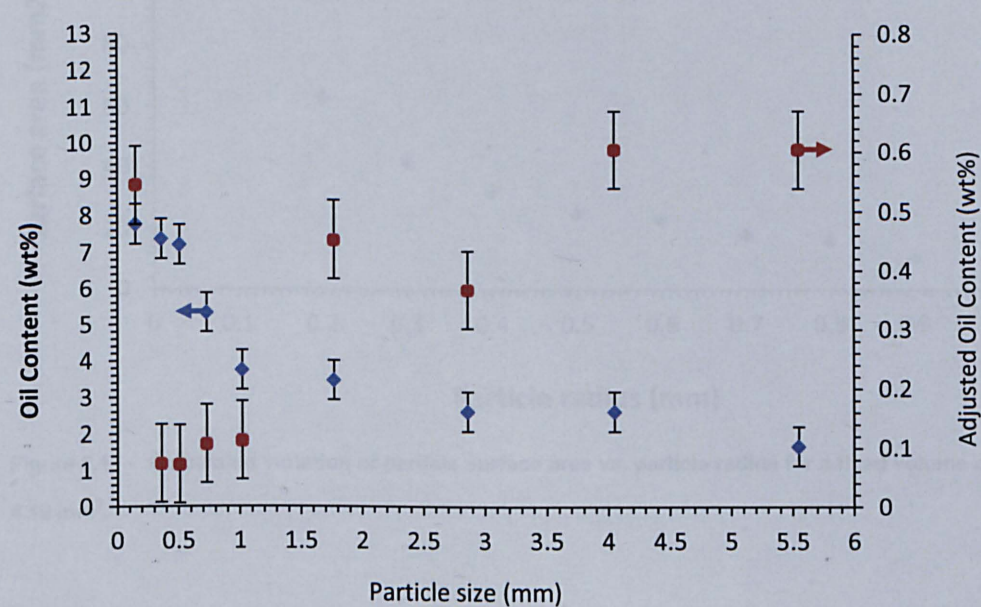


Figure 5.16 - Variation of oil content with particle size for untreated Sample 2A.

Nevertheless, for a given volume of material, the higher oil content in the finer particles can be attributed to a higher overall surface area available in the finer particles in comparison to larger particles. As these drill cuttings particles have high clay content, and are hydrophilic, the oil phase is likely to accumulate at the surfaces. As a result the greater the surface area available the greater the amount of oil

retained per particle, although it is important to note that the finer particles only account for a small fraction of the overall material. Interestingly, there appears to be a clear threshold, around 0.5 mm in the case of Sample 2A, for the minimum particle size required to hold a high amount of oil content. This may be attributed to the fact that the surface area of a sphere is proportional to the square of the radius. As a result, for a fixed volume of sample, finer particles have an exponentially greater surface area in comparison to the coarser particles. This is shown below in Figure 4.17, which shows the calculated variation of overall surface area with increasing particle size for a fixed volume of 4.19 mm^3 , which was calculated based on a sphere with a 1 mm radius.

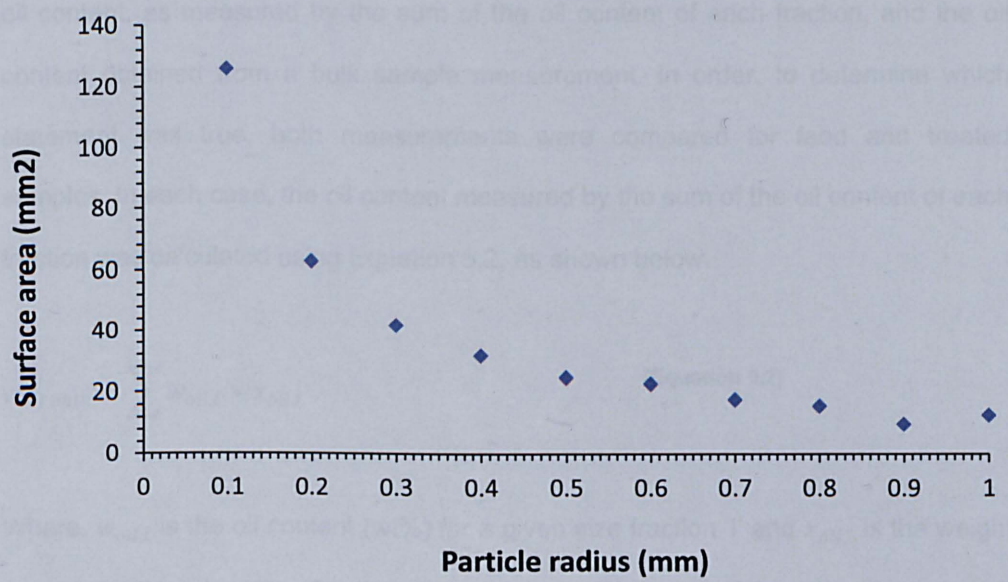


Figure 5.17 - Calculated variation of particle surface area vs. particle radius for a fixed volume of 4.19 mm^3 .

As seen from Figure 5.17, in this hypothetical case, at particles with radii $>0.4 \text{ mm}$ the surface area appears to decrease at a substantially lower rate than at particles $<0.4 \text{ mm}$. This is similar to the trend observed in Figure 5.16 for particles of size $<0.5 \text{ mm}$. However, this would also suggest an exponential increase in oil content with decrease particle size, which was not observed at the finer particle sizes ($<0.5 \text{ mm}$), as discussed. This could be resulting from two reasons:

1. The oil phase does not spread equally across the surface for all particle sizes. In which case you could have a thicker oil film in the coarser particles in comparison to the finer particles. This would still result in higher oil contents in finer particles, but could place a threshold in the overall amount that can be held in finer particles. In this case that amount would be around an oil content of 8 wt% (Figure 5.16).
2. Oil content could have been removed from finer particles, <0.5 mm, mechanically during sieving.

If the latter statement is true, a difference should be observed between the combined oil content, as measured by the sum of the oil content of each fraction, and the oil content obtained from a bulk sample measurement. In order, to determine which statement was true, both measurements were compared for feed and treated samples. In each case, the oil content measured by the sum of the oil content of each fraction was calculated using Equation 5.2, as shown below.

$$w_{oil\ bulk} = \sum w_{oil,i} \times x_{oil,i} \quad \text{[Equation 5.2]}$$

Where, $w_{oil,i}$ is the oil content (wt%) for a given size fraction 'i' and $x_{oil,i}$ is the weight fraction for the same size fraction, 'i', $w_{oil\ bulk}$ (wt%) is sum of the oil content of each size fraction weighted, corrected for the particle size distribution. Figure 5.18 shows the comparison between the variation of oil content as measured from bulk samples with energy input for Sample 2A, as well as the oil content calculated by the sum of oil content contributed by each particle size.

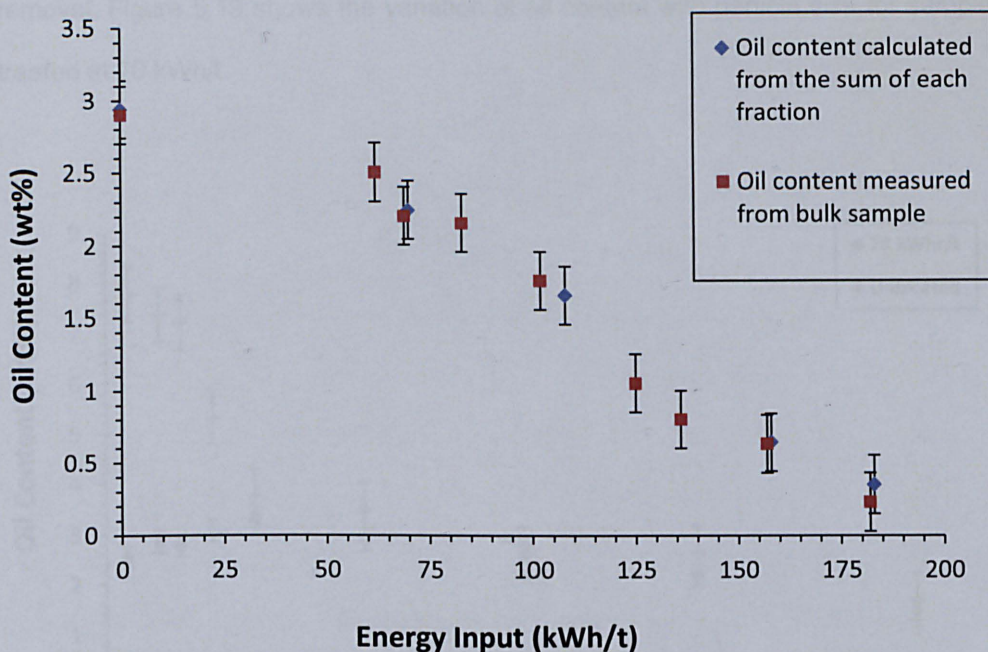


Figure 5.18 - variation of oil content with energy input for Sample 2A as obtained through a bulk sample measurement, and as calculated by the sum of oil content contributed by each particle size.

Both bulk and individual particle size oil content measurements were carried out according to the procedure established in Section 3.3 of Chapter 3. The error bars in Figure 5.18 represent the maximum expected variation for a given sample measurement. The large variation observed results from the natural heterogeneity present in samples. As seen from Figure 5.18, the bulk oil content measured from a bulk sample is within measurement error to the bulk oil content as calculated from the sum of the oil content present in each size fraction. This suggests the results shown in Figure 5.16 are accurate, therefore confirming there is a maximum amount of oil that can be held in the finer size particles, as previously discussed. Figure 5.18 also shows, as expected, a decreasing trend in oil content with energy input, with a residual oil content of 1 wt% being reached at approximately 125 kWh/t.

The variation of oil content with particle size was further investigated for samples treated at 70, 108, 158 and 183 kWh/t. In order to determine whether oil content was removed at equal rates, or whether particular size ranges experienced preferential

removal. Figure 5.19 shows the variation of oil content with particle size for samples treated at 70 kWh/t

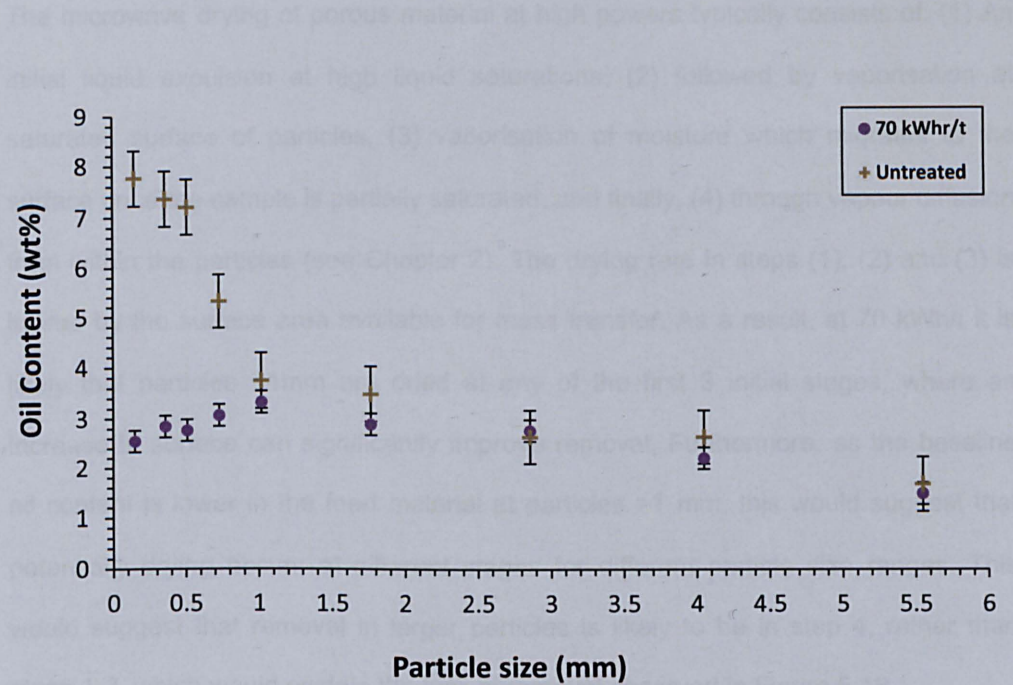


Figure 5.19 - Variation of oil content with particle size for Sample 2A treated at 70 kWh/t.

Figure 5.19 shows a significant drop in oil content within the particle size range of 0.15 and <1 mm. For particles >1 mm, a negligible drop in oil content was observed, suggesting little or no oil removal took place in coarser particles at 70 kWh/t. Between 0.15 and 1 mm the drop in oil content between the feed and the treated material increased with decreasing particle size, with the greatest oil removal being observed at 0.15 mm. Thus, the results presented in Figure 5.19 are clear evidence that oil is preferentially and selectively removed from the <1.0 mm size classes. This could be explained by the difference in the overall mass and heat transfer surface area between particle sizes, the difference in the overall path length vapour generated within the particles needs to travel before exiting the particle, and finally the potential difference in power attenuation between larger and finer particles.

5.3.5.1 Effect of particle surface area

The microwave drying of porous material at high powers typically consists of: (1) An initial liquid expulsion at high liquid saturations, (2) followed by vaporisation at saturated surface of particles, (3) vaporisation of moisture which migrates to the surface once the sample is partially saturated, and finally, (4) through vapour diffusion from within the particles (see Chapter 2). The drying rate in steps (1), (2) and (3) is limited by the surface area available for mass transfer. As a result, at 70 kWh/t it is likely that particles <1mm are dried at any of the first 3 initial stages, where an increase in surface can significantly improve removal. Furthermore, as the baseline oil content is lower in the feed material at particles >1 mm, this would suggest that potentially drying occurs at different stages for different particle size ranges. This would suggest that removal in larger particles is likely to be in step 4, rather than steps 1-3, which would explain the lack of removal observed in Figure 5.19

5.3.5.2 Effect of travel path length

As removal changes from steps 1-2 to 3-4, the drying rate becomes increasingly dependent on the rate of removal of internal oil and water vapour from within the particle. The rate, in turn, is dependent on the tortuosity of internal pores and the length of the path the vapour/liquid needs to travel before reaching the particles surface. It is expected that larger particles would have greater path lengths than finer particles, reducing the rate of mass transfer and increasing the required energy input for oil removal. The increased energy input is likely to occur due to an increase in heat loss as the vapour/liquid travels through the pore, potentially requiring re-vaporisation if condensation occurs. The effect of this increased energy requirement in larger particles would as a result lead to improved removal efficiency in finer particles.

5.3.5.3 Power attenuation

Microwaves attenuate as they propagate through media consisting of phases of high dielectric constant and loss (See Chapter 2). This is the case during the initial stages of drying of drill cuttings, where the water content is significant. The difference in attenuation between coarser and finer particles can be assumed to be entirely dependent on the water content of within the particle. Figure 5.2 shows the variation of water content with particle size for feed material. Note that it was not possible to measure the water content for all sizes due to insufficient sample mass. The variation of oil content with particle size for the same feed material was also provided for comparison purposes.

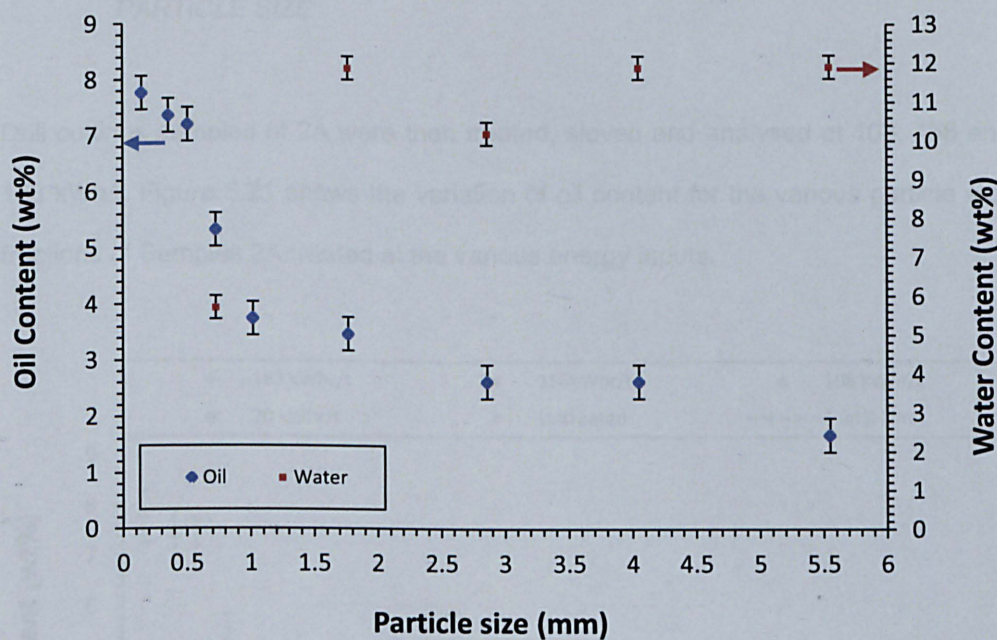


Figure 5.20 - Variation of water and oil content with particle size for Sample 2A feed material.

As seen from Figure 5.2 the water content is relatively constant at particle sizes >1.5 mm, and oscillates around 12 wt%. However, as the particle size decreases and tends to 0, the water content appears to drop sharply, decreasing down to 6 wt% at approximately 0.5 mm. This difference in behaviour between the water and oil content is expected and can be explained in simple terms by the nature of each fluid. Oil is

highly hydrophobic and naturally repels water, as a result regions containing greater volumes of water are unlikely to also contain as high a volume of oil. This can also partially explain the greater oil distribution in finer particles. The high clay content present in many of the formations drilled with oil based muds, which are typically hydrophilic, and as a result are also likely to repel oil, tends to result in oil accumulation at the surface of the formation. Thus, the greater the combined overall particle surface area the greater the expected oil content. The opposite is true for larger particles with high internal volumes and surface areas, which are more likely to contain a greater quantity of water held internally, either within pores or clay interlayers.

5.3.6 VARIATION IN OIL CONTENT DISTRIBUTION AND REMOVAL WITH PARTICLE SIZE

Drill cuttings samples of 2A were then treated, sieved and analysed at 108, 158 and 183 kWh/t. Figure 5.21 shows the variation of oil content for the various particle size fractions of Samples 2A treated at the various energy inputs.

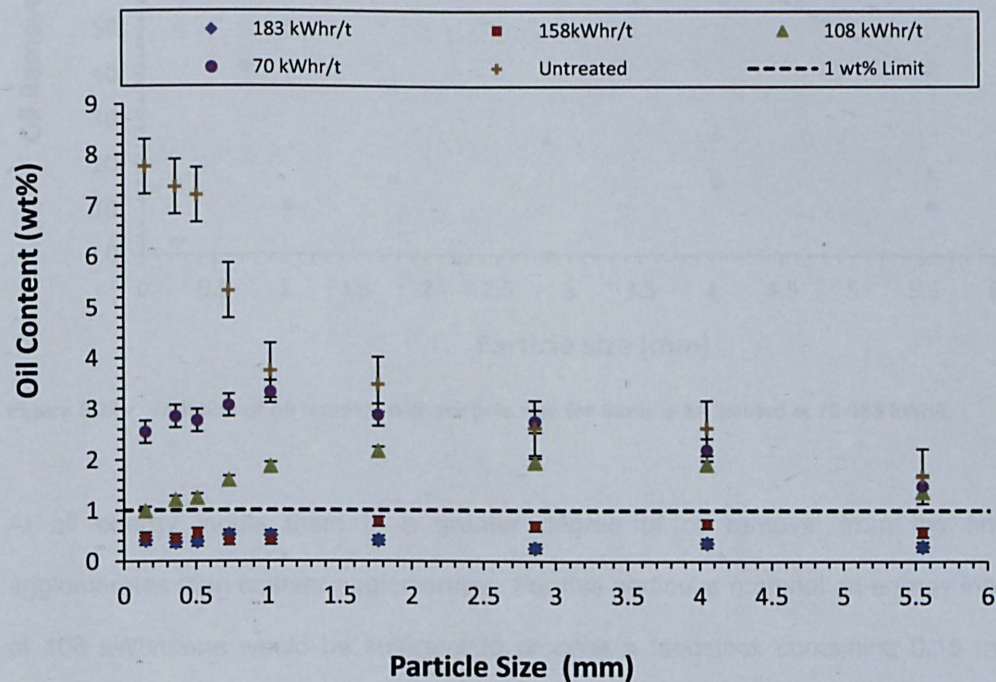


Figure 5.21 - Variation of oil content with particle size for Sample 2A treated at 70-183 kWh/t.

Figure 5.21 shows an overall decrease in the bulk residual oil content present in the material with increasing energy input, which is in agreement with the data presented in Figure 5.18 At 108 kWh/tonne there is a continued improvement in oil removal in <1mm agglomerates compared to 70 kWh/tonne, but a much smaller change in the oil content in the coarser fractions. At 158 and 183 kWh/tonne there is a significant reduction in oil content within all the size classes studied. It is clear from Figure 5.21 that the agglomerate size has a significant effect on oil removal from drill cuttings, and at lower energy inputs oil is preferentially removed from <1mm agglomerates. The efficiency of oil removal across all size classes is shown in Figure 5.22, along with the oil removal efficiency required to attain a residual oil content of 1%. This figure differs according to the size classification as it is a function of the original oil content, and is shown by the dashed line in Figure 5.22.

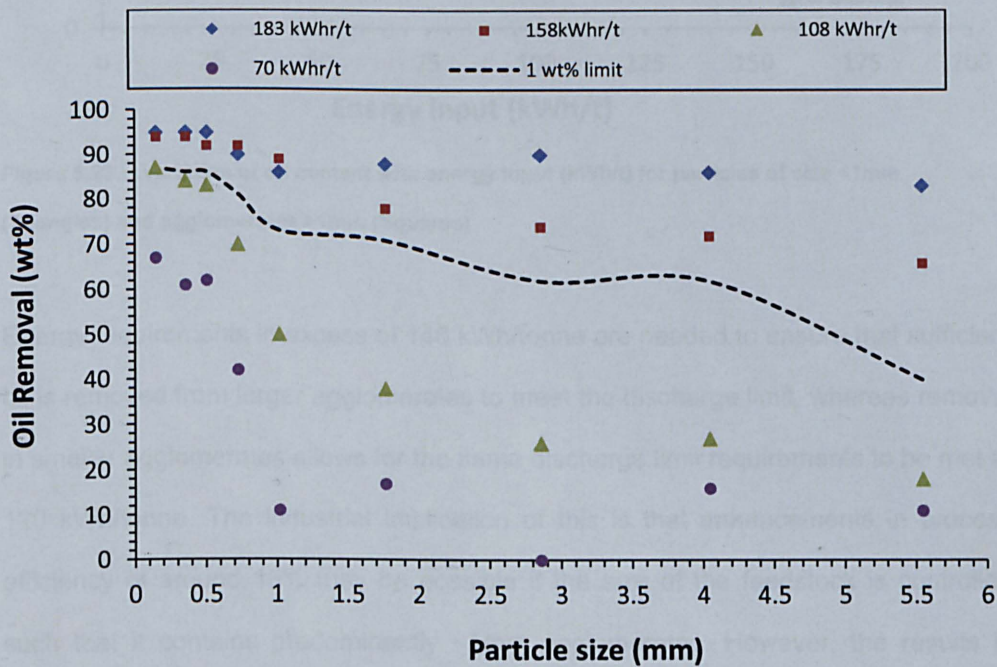


Figure 5.22 - Variation of oil removal with particle size for Sample 2A treated at 70-183 kWh/t.

At all energy inputs there is a greater degree of oil removal from the finer agglomerates than coarser agglomerates. For this particular material an energy input of 108 kWh/tonne would be sufficient to process a feedstock containing 0.15 mm agglomerates, but processing of larger agglomerates will not yield enough oil removal

to meet the 1% environmental discharge threshold. The difference in energy requirement for treatment of fine and coarse sizes is more clearly illustrated in Figure 5.23, which shows the average residual oil content against energy input for agglomerates smaller and larger than 1.0 mm.

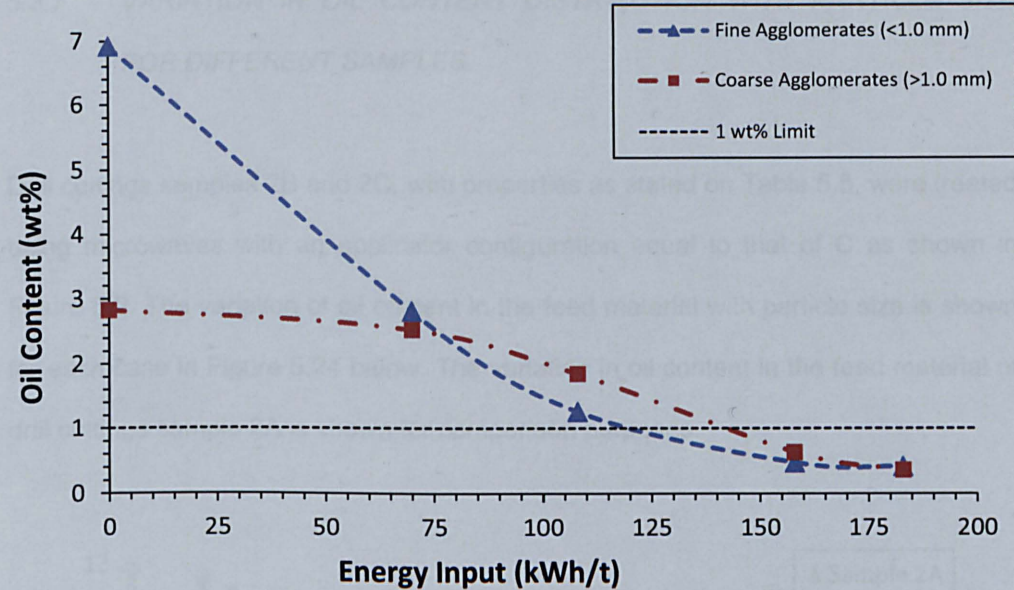


Figure 5.23 - Variation of oil content with energy input (kWh/t) for particles of size <1mm (Triangles) and agglomerates >1mm (Squares).

Energy requirements in excess of 140 kWh/tonne are needed to ensure that sufficient oil is removed from larger agglomerates to meet the discharge limit, whereas removal in smaller agglomerates allows for the same discharge limit requirements to be met at 120 kWh/tonne. The industrial implication of this is that enhancements in process efficiency of around 15% may be possible if the size of the feedstock is controlled such that it contains predominantly <1mm agglomerates. However, the results in Figure 2 indicated that more than 80% of the oil in the bulk sample is located in >1mm agglomerates, so even if the feedstock were separated into two size classes the overall energy requirements will only reduce by up to 3%. It is unlikely, therefore that separating <1mm from coarser agglomerates prior to microwave heating will be viable commercially as the 3% energy saving will not justify the extra footprint, weight and cost of extra bulk materials handling equipment.

However, the results and conclusions shown above are only representative of one type of drill cuttings sample. In order to investigate this further, two other drill cuttings samples with different initial oil and water content were treated using microwaves, sieved and each size fraction tested for oil content.

5.3.7 VARIATION IN OIL CONTENT DISTRIBUTION WITH PARTICLE SIZE FOR DIFFERENT SAMPLES.

Drill cuttings samples 2B and 2C, with properties as stated on Table 5.5, were treated using microwaves with an applicator configuration equal to that of C as shown in Figure 5.2. The variation of oil content in the feed material with particle size is shown for each case in Figure 5.24 below. The variation in oil content in the feed material of drill cuttings sample 2A is shown for comparison purposes.

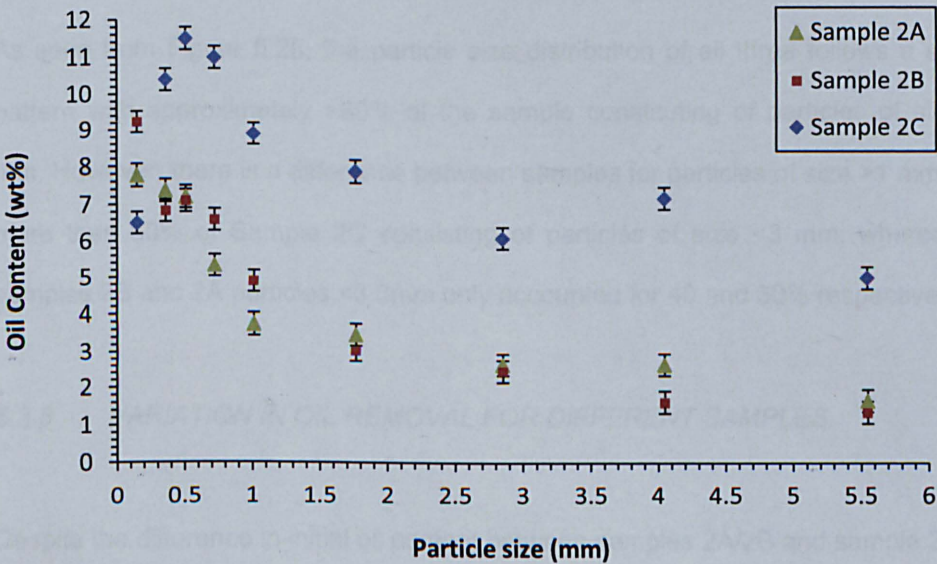


Figure 5.24 - Comparison of the variation in oil content with particle size for samples 2A-2C.

Figure 5.24 shows an overall decrease in oil content with increasing overall particle size for all 3 treated samples. Sample 2A shows an exponential decrease in oil content from just over 9 wt% at 0.15 mm down to approximately 1.6 wt% at 5.5 mm. Similar to the trend previously observed in Sample 2A the variation in oil content for particles of size >1.8 mm was minimal. However, the data shown in Figure 5.24

needs to be analysed in conjunction with the particle size distribution of all three samples (Figure 5.25).

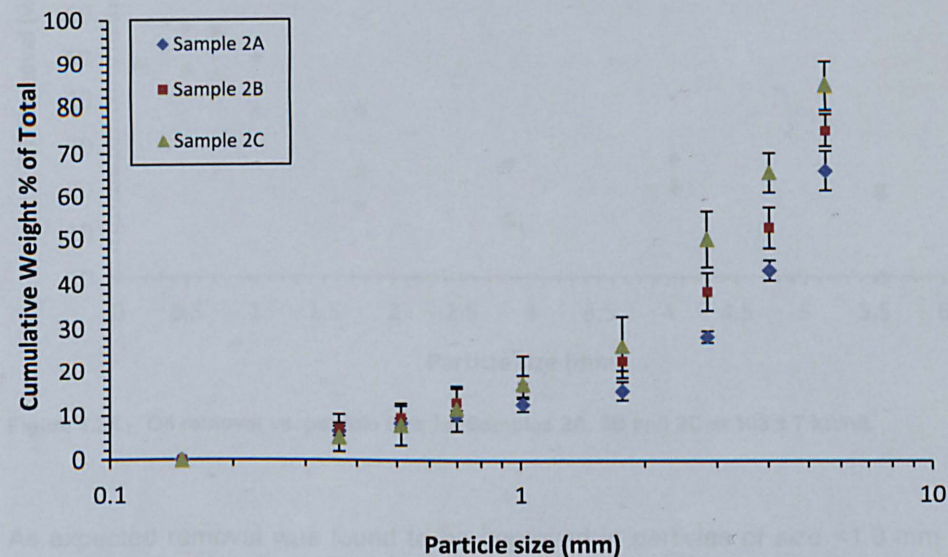


Figure 5.25 - Cumulative particle size distribution for Samples 2A, 2B and 2C.

As seen from Figure 5.25, the particle size distribution of all three follows a similar pattern with approximately >80% of the sample constituting of particles of size >1 mm. However, there is a difference between samples for particles of size >1 mm, with more than 50% of Sample 2C consisting of particles of size <3 mm, whereas for samples 2B and 2A particles <3.0mm only accounted for 40 and 30% respectively.

5.3.8 VARIATION IN OIL REMOVAL FOR DIFFERENT SAMPLES.

Despite the difference in initial oil content between samples 2A/2B and sample 2C, as was the case with sample 2A, removal is expected to be initially more efficient in finer particles than coarser particles. Figure 5.26 below shows the oil removal for all three samples at 103 ± 7 kWh/t.

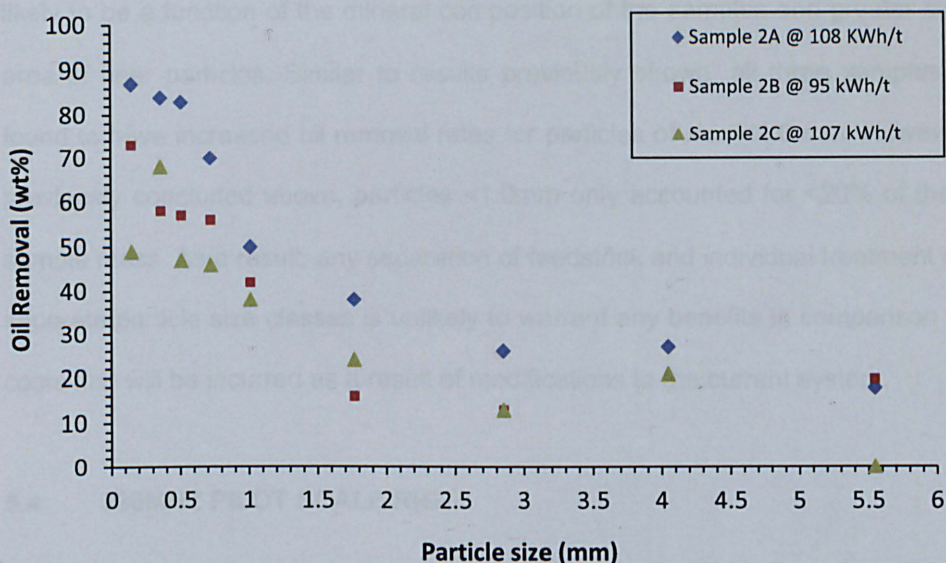


Figure 5.26 - Oil removal vs. particle size for Samples 2A, 2B and 2C at 103 ± 7 kWh/t.

As expected removal was found to be improved in particles of size <1.0 mm for all three different samples treated. Despite having similar initial bulk oil content and oil content distribution across the various particle sizes, oil removal of Sample 2B was not as high as Sample 2A. This could be explained by:

- The difference in the overall energy input between samples - 13 kWh/t discrepancy.
- The difference in power density between samples – 3.5 kWh/kg of sample (Sample 2A) vs. 2.4 kWh/kg of sample (Sample 2B) at around 100 kWh/t. Data presented in the Appendix 4 shows how power density can have a significant impact on removal.

Nevertheless the similarity in the oil removal trend of all three samples suggests the mechanisms of removal in finer and coarser particles are likely to be the same regardless of the sample's initial oil and water content. The initial water content, however, seems to dictate the extent of removal.

In conclusion, the oil distribution with particle size for drill cuttings samples appears to be similar, regardless of differing bulk initial oil and water content in this case. This is

likely to be a function of the mineral composition of the samples and greater surface area of finer particles. Similar to results previously shown, all three samples were found to have increased oil removal rates for particles of size <1.0 mm. However, as previously concluded above, particles <1.0mm only accounted for <20% of the total sample mass. As a result, any separation of feedstock and individual treatment of two separate particle size classes is unlikely to warrant any benefits in comparison to the costs that will be incurred as a result of modifications to the current system.

5.4 896MHZ PILOT SCALE RIG

Oil contaminated drill cuttings were treated using an 896 MHz system located within an existing thermal desorption plant in the UK. Drill cuttings were obtained directly from existing cuttings settling pits and loaded into a rectangular hopper, before being fed through a continuous rectangular conveyor belt system using a series of screw feeders. The material was then passed at a given flowrate through the microwave cavity, where it was treated, leaving the system through an outlet hopper. The entire system was self-contained and maintained inert at all times by supplying nitrogen and monitoring oxygen levels. The power supply was interlocked with an oxygen monitoring device and only started once the oxygen content dropped below 6% v/v. The level in the feed hopper and outlet hopper of the microwave system were monitored continuously and interlocked with the power supply, cutting the power if the level drops below a minimum.

Vapours generated within the cavity were removed at extract points. Steam and condensable vapours were then condensed in a heat exchanger. Extraction points were also present at the feed inlet between the screw feeder and the area of discharge into the belt, as well as at the discharge end of the cavity, where the treated drill cuttings were collected. The flow through the extraction points was controlled was remotely controlled, with nitrogen flowrate into the system

automatically increasing or decreasing in order to maintain the level of inertion required. A representative sample of the treated material leaving the cavity was collected and stored for water and oil content testing. A microwave leakage system was also installed and interlocked with the power supply, however no microwave leakage was detected in any of the experiments. The applicator configuration used in this case was analogous to "B" as shown in Figure 5.2, Section 5.2 with relevant modifications in geometry to reflect the change in frequency.

The microwave cavity consisted of choke sections, which prevented microwave leakage, and the applicator region where treatment took place. The applicator was connected to a magnetron via a number of 90° bends and straight waveguide sections. The magnetron used in this case was capable of outputting a maximum power of 100 kW at 896 MHz. The magnetron was protected by the circulator and was used to absorb any reflected power that was not absorbed by the load. Any heated water leaving the circulator unit is cooled by an air cooled heat exchanger and recycled back in a closed loop. Arc detectors, interlocked with the power supply, were placed in the bend immediately after the applicator and just before the circulator in order to prevent any damage caused through arcing.

Flowrates ranging from 300 to 700 kg/hr and bed heights of 2-3 cm were used. In each case the oil and water content of the feed and product were measured at least 3 times using the standard procedures (ASTM D95 and DCM solvent extraction as per detailed in Chapter 3). Forward powers up to 70 kW were used.

5.5 RESULTS OF 896 MHZ MICROWAVE RIG

Figure 5.27 below shows the variation of oil content with energy input for a drill cuttings sample containing 7.8 ± 0.2 wt% oil and 10.6 ± 0.4 wt% water treated using the 896 MHz system at two flowrates 350 and 800 kg/hr.

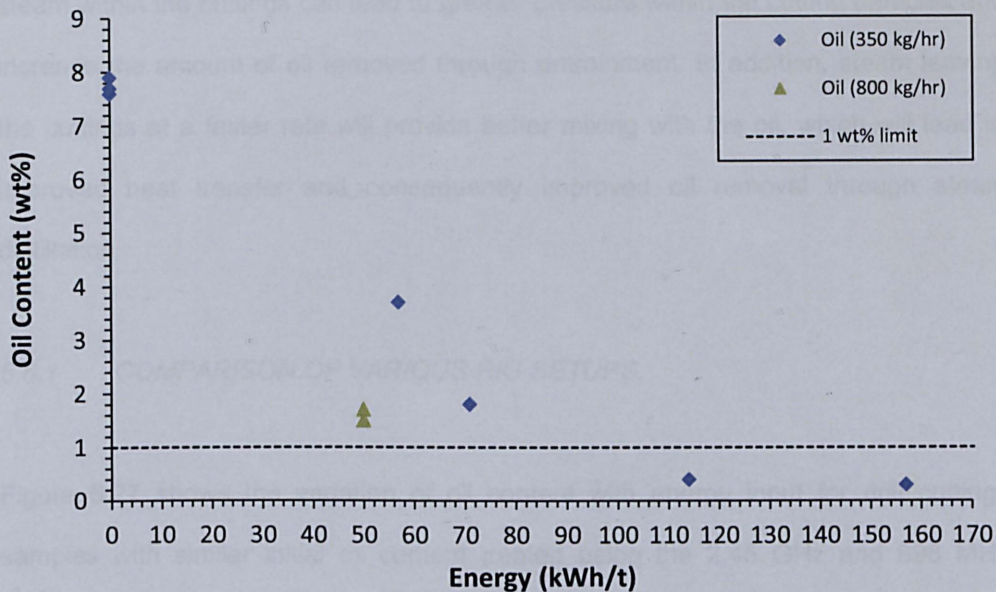


Figure 5.27 - Variation of oil content with energy input for sample treated using the 896 MHz system.

As seen from Figure 5.27, sample treated at 350 kg/hr, decreased below 1 wt% at an energy input in the range of 80-90 kWh/t. Similar to previous tests carried out in the continuous pilot scale rig, once the oil content decreases below 1 wt%, no further significant removal was observed at energy inputs >120 kWh/t. Interestingly, by increasing the flowrate and power by approximately a factor of 2, a significantly greater oil removal was observed. For sample treated at 800 kg/hr and 50 kWh/t the residual oil content was measured at 1.5 wt%, whereas for sample treated at 350 kg/hr and 50 kWh/t the oil content was calculated, based on the data shown, to be approximately in the region of 4-5 wt%.

An increase in flowrate is achieved by increasing the belt speed rather than increasing the sample depth, which decreases sample residence time within the cavity. If the energy input is to be maintained constant, then a reduction in residence time requires an equivalent increase in power. As the power increases, the heating and vaporisation rate of the water and consequently the oil in the drill cuttings also increase, as a result of increasing field strength, which can have a number of positive impacts in terms of oil and water removal from the cuttings. Faster generation of

steam within the cuttings can lead to greater pressure within the cutting particles and increase the amount of oil removed through entrainment. In addition, steam leaving the cuttings at a faster rate will provide better mixing with the oil, which will lead to improved heat transfer and consequently improved oil removal through steam distillation.

5.5.1 *COMPARISON OF VARIOUS RIG SETUPS.*

Figure 5.27 shows the variation of oil content with energy input for drill cuttings samples with similar initial oil content treated using the 2.45 GHz and 896 MHz continuous systems. The respective initial oil and water content conditions, power ranges and system configuration used for the 2.45 GHz pilot system are shown in Table 5.6 for information purposes.

#	Power Range (kW)	Flowrate (kg/hr)	Initial Oil Content (wt%)	Initial Water Content (wt%)	Frequency (MHz)
1B	0-22.5	150 ± 20	8.2 ± 0.4	6.7 ± 0.3	2450
1C	0-22.5	150 ± 20	10.3 ± 0.4	6.7 ± 0.3	2450
1D	0-22.5	150 ± 20	8.2 ± 0.4	11.3 ± 0.3	2450
1E	0-22.5	150 ± 20	8.2 ± 0.4	14.6 ± 0.3	2450
2C	0-25	150 ± 17	7.8 ± 0.9	5.5 ± 0.8	2450
2C (Single Mode, Sample C – Ch. 4, Configuration A)	0-3.3	N/A	7.8 ± 0.9	5.5 ± 0.8	2450
2C (Multi Mode, Sample C – Ch. 4, Configuration B)	0-2.6	N/A	7.8 ± 0.9	5.5 ± 0.8	2450
4A	0-55	350 ± 35	7.8 ± 0.2	10.6 ± 0.4	896

Table 5.6 - Details of experiment conditions for samples shown in Figure 5.28.

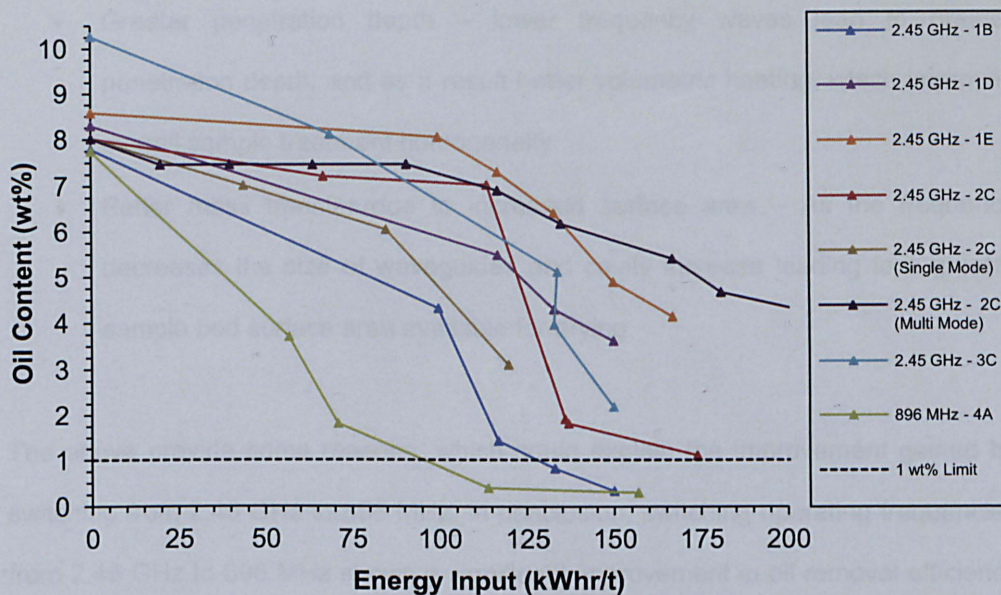


Figure 5.28 - Comparison of residual oil content with energy input for samples treated using the 2.45 GHz and 896 MHz continuous system.

As seen from Figure 5.28 and Table 5.6, for drill cuttings samples containing a similar amount of initial oil content, samples treated at 2.45 GHz required a significantly greater amount of energy to treat samples to a residual oil content below 1 wt%. For example, Sample 1B required an energy input of approximately 125 kWh/t to treat material to ≤ 1 wt%, whereas sample 4A only required an energy input of 90-100 kWh/t. This lower energy requirement occurs despite the lower amount of water content in 4A by comparison to 1B. Sample 1D, which contained similar initial oil and water content to Sample 4A, would suggest based on the data obtained, that more than double the amount of energy (>200 kWh/t) would be required to treat the sample to 1 wt%.

This reduction in energy requirement between processing material using the pilot scale system at 2.45 GHz and the 896 MHz system could be due to the following:

- Improved microwave absorption and heating – a decrease in frequency leads to an increase in microwave heating due to increased microwave absorption through Maxwell-Wagner and ionic polarisation as well as conduction. Better heating of bound water is also expected (**Metaxas, 1993**).

- Greater penetration depth – lower frequency waves lead to greater penetration depth, and as a result better volumetric heating, which improves overall sample treatment homogeneity.
- Better mass transfer due to increased surface area – As the frequency decreases the size of waveguides and cavity increase leading to a greater sample bed surface area available for drying.

The above provide some reasons, which could explain the improvement gained by switching from 2.45 GHz to 896 MHz. In conclusion, switching operating frequencies from 2.45 GHz to 896 MHz shows a significant improvement in oil removal efficiency with energy input, requiring approximately half the energy required to treat a sample of similar initial oil and water content to 1 wt%. However, the difference in physical structure of the sample needs to be taken into account, as the sample treated at 896 MHz was more granular than the sample treated at 2.45 GHz, which consisted of finer grains and particles. Nevertheless, a comparison with Sample 2C (1wt% oil at 175 kWh/t), which was visually similar to Sample 4A (1wt% oil at 90-100 kWh/t), suggests there is a significant benefit in operating at 896 MHz.

In terms of difference in oil removal efficiency between different applicator and operation modes, a significant difference was observed between samples 2C treated using a multimode setup versus samples treated using a single mode/continuous setup. In fact, Figure 5.28 suggests that single mode operation is most efficient between all setups tried, which can probably be attributed to the fact that in single mode operation higher electric field strengths are achievable.

5.6 CONCLUSION

Water was shown to be selectively heated over other drill cuttings phases as expected, leading to average bulk sample temperatures of 100-120 °C. Beyond 100 °C, energy requirement for heating the sample was found to increase significantly,

mainly as a result of lower dielectric properties and thus poor microwave absorption. However, localised heating was found to occur mainly as a result of heating of strongly bound water/hydroxyl groups, as well as small quantities of highly absorbing microwave minerals.

When compared to bench processing, for the a drill cuttings sample with the same initial oil and water content continuous scale microwave processing was found be significantly more efficient. 1 wt% was reached at 150 kWh/t for continuous processing, in comparison to >250 kWh/t for bench scale processing.

The effects of initial water and oil content on oil removal were also investigated for different drill cuttings samples. An increase in oil content in the feed was found to adversely affect oil removal, resulting in an exponential increase in energy input with the oil removal (%) required to treat the sample to 1 wt% residual oil content. This was found to occur due to changes in the mass transfer properties of the sample from a physical change in its structure as a result of added oil content.

An increase in water content in the feed led to an increase in energy input, without any added benefit to oil removal. However, it was found that as the water content was increased, the overall energy input difference between samples approached that which was calculated based on the physical properties of the oil, water and rock contents of the sample. This suggests that heat losses are reduced and heating is more efficient, which could to be due to an overall increase in the dielectric loss and constant properties of the sample as a result of higher water content. In this case at least 6.7 wt% water content was sufficient to allow for a sample containing approximately 8.2 wt% to be treated down to 1 wt% at 125 kWh/t.

The effect of particle size on oil removal during microwave processing of drill cuttings was also investigated and compared for samples containing different initial oil and water content. There was a significant variation in the oil content within the size

fractions of the feed material before processing, with finer agglomerates containing up to three times more oil than coarser particles. When investigating samples with different bulk initial oil and water content a similar oil content distribution was found across all three samples tested.

For all three samples oil was removed from all size fractions during microwave treatment, however removal was preferential in particles of size <1 mm. This was explained by lower electric field strengths in larger agglomerates, which subsequently leads to lower heating rates. In addition, larger increased path lengths in larger agglomerates can increase resistance to mass transfer and reduce removal efficiency.

A 20% reduction in the energy requirement is possible if the feedstock size is restricted to <1 mm, however this size fraction makes up less than 20% of the bulk material. As a result, there is limited scope to exploit this energy reduction commercially due to the increased cost and footprint of bulk handling equipment needed to separate the feedstock into the required size fractions.

Continuous microwave treatment at 896 MHz was also investigated and compared against continuous, bench single and multimode microwave treatment at 2.45 GHz. At 896 MHz, drill cuttings were treated at a flowrate of 300 kg/hr to 1 wt% at approximately 80-90 kWh/t, which was noticeably lower than the >125 kWh/t required for samples with similar initial oil and water content treated continuously at 2.45 GHz. An initial test at 800 kg/hr also appeared to show an improvement in oil removal, leading to a reduction in the residual oil content to 1wt% with approximately 50-60 kWh/t. This was found to be probably a result of increasing forward power input into the sample, and consequently higher field strength and power density in the water phase enhancing steam distillation and entrainment.

Finally, an increase in throughput is still desired when comparing to current commercial conventional thermal desorption systems (800 kg/hr vs. 1-5 tonnes/hr), however, the significant improvement in energy consumption (<100 kWh/tonne vs. approx. 200 kWh/tonne for current commercial solutions) suggests there would be significant benefits in using microwave heated thermal desorption systems.

CHAPTER 6 – Thesis Conclusion & Future Work

Rising offshore oil production has led to increasingly tighter waste management control and policies, which in turn have led to an increase in the cost of offshore waste management. Oil contaminated drill cuttings generated offshore are often hauled to shore generating substantial shipping and further treatment costs. The current maximum residual oil content limit of 1 wt% for direct disposal of contaminated cuttings in the North Sea means there are currently no fit-all, cost effective solutions for the waste management of these oily cuttings offshore.

An opportunity was identified for developing a cost effective microwave heating thermal desorption system, which could be retrofitted to existing platforms, providing a treatment solution offshore. This thesis advanced progress made in previous work through novel investigation of the following 3 key areas:

- 1- Development of key oil and water removal mechanisms during microwave processing.
- 2- Development an understanding of how operating variables (such as power and energy input) as well as inherent drill cuttings variable affect system efficiency.
- 3- Investigations of operational efficiency of the first continuous microwave processing system operating at 896 MHz.

6.1 OIL AND WATER REMOVAL TRANSFER MECHANISMS

This work has shown, through direct quantification, for the first time, that oil and water removal during microwave processing of oil contaminated drill cuttings occurs through two main mechanisms: vaporisation and entrainment. Although removal of oil through evaporation alone using nitrogen was found to be insignificant, nitrogen flowrate during microwave processing was found to have a significant impact in the overall

amount of water and oil removed from the sample. An improvement in combined oil and water removal of 70% was observed when the nitrogen flowrate was increased from $Re_m = 58$ to $Re_m = 203$. This was found to be a result of improved heat distribution across the sample and improved mass transfer from the drill cuttings particle surface to the extraction points as well as a potential for reduced recondensation. The improvement in removal was found to be equal for both water and oil, thus increasing the modified Reynolds Number does not lead to a preferential increase in oil or water removal, but rather increases the overall liquid removal homogenously.

Vaporisation was found to be the main oil removal mechanism, of which most is likely to be removed through steam distillation. Generally, vaporisation accounted for >80-90% of the overall liquid removal. Vaporisation of the oil phase accounted for 70-100% of the overall removal. The relative amount of oil and water removed through vaporisation was found to decrease with increasing energy input and power density. This can be explained by the higher velocity and pressure steam generated at the latter stages of the batch scale processing of the sample.

As water is removed from the sample, the amount of power dissipated per unit volume of water increases leading to an increase in power density in the water phase with processing time, and thus energy input. These in turn lead to higher heating rates, and consequently higher pressure and velocity steam. The latter conditions improve the chance of physical carryover of liquid droplets leading to a higher amount of entrainment.

The sample and applicator type were found to have a significant effect on the extent and ratio of oil and water removal through entrainment and vaporisation. Two samples with different initial oil and water content were investigated. One of the samples contained a greater amount of surface liquid than the other, which led to a higher proportion of oil and water being removed through entrainment.

A method for predicting changes in oil and water removal mechanisms was developed from the variation of oil and water content with energy input. This allowed for relative comparisons between multimode and single mode applicators to be carried out for drill cuttings with equal initial oil and water content treated in both setups. In the multimode setup at low powers, oil removal progressed mainly through low rate steam distillation of the oil until >80-90% of the water was removed. However, when treated at higher powers, a shift to a combined mechanism of high speed steam distillation and entrainment was observed at a much lower water removal percentage 50-60%. By comparison in single mode, treatment appeared to be a combination of high rate steam distillation of the oil from the start followed by a small shift in mechanism, which corresponded to an increase in removal due to entrainment.

6.2 CONTINUOUS MICROWAVE PROCESSING OF DRILL CUTTINGS AT 2.45 GHZ

Drill cuttings with an oil and water content of approximately 3wt% and 12wt% respectively were treated continuously to 1wt% with an energy input of 150 kWh/t, which, was significantly lower than the >250 kWh/t energy required for treatment when using a bench scale setup. This can be explained by the higher electric field strength and higher absolute power forward, which could be achieved using the continuous setup in comparison to the bench scale setup.

Initial oil and water content were also shown to have a significant impact in the overall energy input requirements of the sample. Increasing the initial oil content of the feed material resulted in an exponential increase in energy input required to treat samples down to the required 1 wt%. This was found to occur as a result of changes to the physical structure of the material, which visually changed from a sample which clearly consisted of individual particles, to a sample which resembled more a sludge. This change in structure had a substantial adverse impact in the mass transfer properties

of the sample, as oil and water vapours generated within the sample faced greater restrictions and increased mass flow resistance.

A change in initial water content led to increased energy inputs, without any added benefits in oil removal. Interestingly, as the water content increased, the theoretical energy input required for vaporisation approached that, which was actually used. This suggested the conversion of energy from microwaves to heating improved, which was expected as the bulk dielectric properties of the sample increase with increasing water content.

The effect of particle size was also investigated in detail and found to have a significant impact on the oil distribution over the sample. All three samples tested showed significantly higher oil contents in smaller particles (<1.0 mm) in comparison to coarser particles. This difference in oil distribution was found to be mainly a factor of the increased surface area provided by the finer particles. Initial oil removal was also found to be significantly greater in particles of <1.0mm, however, this effect is diluted by the >80% of the sample consisting of particles >1.0 mm. Although it would be possible to separate finer and coarser particles to treat them separately, therefore reducing overall energy requirement, in practice this increases system complexity and is unlikely to justify increased costs in equipment and system design modifications.

6.3 CONTINUOUS MICROWAVE PROCESSING OF DRILL CUTTINGS AT 896 MHZ

Microwave processing of oil contaminated drill cuttings at 896 MHz was carried out for the first time and showed a significant improvement over continuous processing at 2.45 GHz and batch scale processing. For samples with an initial oil content of approximately 7 wt% treated at 300 kg/hr, 80-90 kWh/t was required to reduce the oil content down to 1 wt%. By comparison, at 2.45 GHz, >125 kWh/t was required to continuously treat a sample with similar initial oil and water content. Preliminary

testing at 800 kg/hr showed a further improvement in energy input requirements, suggesting approximately 50-60 kWh/t would be required to reduce the oil content of the same sample to 1 wt%. This can be explained by the results obtained previously during batch and continuous scale experiments, where an increase in the flowrate requires a proportional increase in power input to maintain a given energy input, however increasing the power appears to lead to an exponential increase in oil removal rather than linear. This is mainly a result of faster heating rates at higher powers due to higher field strengths and consequently power densities in the water phase. As previously explained, increasing power density, allows for the rapid generation of superheated and high speed, pressurised steam, which have been shown to improve the overall extent of oil vaporisation and entrainment, and thus oil removal.

6.4 IMPLICATIONS OF WORK ON INDUSTRIAL SYSTEM DESIGN

The work carried out in this thesis helps to define the optimum sample characteristics and operating parameters for any microwave system designed to treat oil contaminated drill cuttings to the 1 wt% residual oil content limit. The key characteristics, in this case, can be broken down into: agglomerate particle size, nitrogen modified Reynolds's numbers, initial oil and water content and energy input requirements.

Based on the results generated in this work, it was clear that finer agglomerates provided better oil removal, suggesting samples with particles of average size <1.0 mm would be ideal. A modified nitrogen Reynold's number $Re_m \geq 203$ is also suggested based on results obtained, with a nitrogen temperature ≥ 80 °C being advisable in order to prevent premature condensation of oil and water vapours within the cavity. However, significantly higher nitrogen temperatures should be balanced against excessive pre-drying of the sample, as this may lead to poor oil removal.

Although the oil and water removal mechanisms were confirmed and quantified in this work, further work could be carried out to physically demonstrate, through imaging techniques or otherwise, how the water and oil physically move from within each of the individual cuttings particles. This work would also allow for the confirmation of the location of the water and oil within individual cuttings particles and potentially allow for the development of a micro-scale model, which predicts the movement of the oil and water phase within the porous medium during microwave processing. This could ultimately be useful in accurately predicting heat and mass transfer coefficients for porous materials containing multi-component liquid phases (free and physically bound). This would then further allow for minimum processing times to be established.

A variable, which appears to have a significant impact in the efficiency of oil and water removal, but cannot be easily quantified, is the physical structure of the sample (e.g. how the particles pack and how the liquid is distributed, at the macro-scale, within it). Progress in this area, by providing a clear structure, which can be used to quantify the effect of sample structure on oil removal, could be very useful in developing a predictive model for microwave processing of drill cuttings. The data obtained in this work could be combined with data regarding the effect of sample structure, such that for a given initial oil and water content, applicator configuration/type and sample structure it would be possible to estimate the approximate energy input required to treat samples to a given final residual oil content.

REFERENCES

(EPA), U. s. E. P. A., 1999. *Economic analysis of proposed effluent limitations guidelines and standards for synthetic-based drilling fluids and other non-aqueous drilling fluids in the oil and gas extraction point source category.*, Washington: U.S. Environmental Protection Agency.

Ahmed, T., 2001. Fundamentals of Rock Properties.. In: *Reservoir Engineering Handbook*.. Houston: Gulf Professional Publishing, pp. 189-287.

Al-Ansary, M. S. & Al-Tabbaa, A., 2007. Stabilisation/solidification of synthetic petroleum drill cuttings.. *Journal of Hazardous Materials* , Volume 141, pp. 410-421.

Aleklett, K. et al., 2010. The peak of the oil age - analysing the world oil production reference scenario in world energy outlook 2008.. *Energy Policy*, 38(3), pp. 1398-1414.

Al-Harabsheh, M. & Kingman, S. W., 2004. Microwave-assisted leaching - a review.. *Hydrometallurgy*, June, 73(3-4), pp. 189-203.

Appleton, T. J., Colder, R. I., Kingman, S. W. & Lowndes, I. S., 2005. Microwave technology for energy-efficient processing of waste.. *Applied Energy*, May, 81(1), pp. 85-113.

Asami, K., 2002. Characterisation of heterogeneous systems by dielectric spectroscopy.. *Progress in Polymer Science*, October, 27(8), pp. 1617-1659.

Ayappa, K. G. et al., 1991. Microwave heating: an evaluation of power formulations.. *Chemical Engineering Science*, 46(4), pp. 1005-1016.

Bäder, H. & Schlunder, E.-U., 1996. High frequency drying of porous material. *Drying Technology*, 14(7-8), pp. 1499-1523.

Bagad, V. S., 2009. Travelling Wave Tubes (TWT). In: *Microwave Engineering - I*. Pune: Technical Publications Pune, pp. 4.1-4.18.

Baricz, A., 1994. *Generalised bessel functions of the first kind*.. New York: Springer.

Barker, G. W., Armstrong, K. W. & Adamson, T. J., 1992. *Land treatment of petroleum hydrocarbon-based drill cuttings: Pilot scale field study*.. Washington, s.n., pp. 149-162.

Benenson, W., Stocker, H., Harris, J. W. & Lutz, H., 2001. Charges and currents.. In: *Handbook of physics*. New York: Springer-Verlag, pp. 421-436.

Benes, J. et al., 2012. *The future of oil: geology versus technology*., s.l.: International Monetary Fund.

- Bengtsson, N. E. & Risman, P. O., 1971. Dielectric properties of foods at 3GHz as determined by a cavity perturbation technique. II. Measurements on food materials.. *Journal of Microwave Power*, 6(2), pp. 107-123.
- Berger, D. & Pei, D. C. T., 1973. Drying of hygroscopic capillary porous solids - a theoretical approach.. *International Journal of Heat and Mass Transfer*, February, 16(2), pp. 293-302.
- Bernier, R. et al., 2003. *Environmental aspects of the use and disposal of non aqueous drilling fluids associated with offshore oil & gas operations.*, London: s.n.
- Breuer, E. et al., 2004. Drill cutting accumulations in the Northern and Central North Sea: a review of environmental interactions and chemical fate.. *Marine Pollution Bulletin*, January, 48(1-2), pp. 12-25.
- Budd, C. J. & Hill, A. D. C., 2011. A comparison of models and methods for simulating the microwave heating of moist foodstuffs.. *International Journal of Heat and Mass Transfer*, November, Volume 54, pp. 807-817.
- Bykov, Y. V., Rybakov, K. I. & Semenov, V. E., 2001. High-temperature microwave processing of materials.. *Journal of Physics D: Applied Physics*, Volume 34, pp. R55-R75.
- Caenn, R. & Chillingar, G. V., 1996. Drilling fluids: State of the art.. *Journal of Petroleum Science and Engineering*, Volume 14, pp. 221-230.
- Cameron, C. & Baroid, H., 2005. *Deepwater drilling fluids - What's New?*. Houston, s.n., pp. 1-6.
- Canadian Association of Petroleum Producers, 2001. *Offshore drilling waste management review.*, Alberta: s.n.
- Carlton, R. A., 2011. *Pharmaceutical Microscopy*. New York: Springer.
- Ceaglske, N. H. & Hougen, O. A., 1937. Drying granular solids.. *Industrial & Engineering Chemistry*, July , 29(7), pp. 805-813.
- Chilingarian, G. V. & Vorabutr, P., 1981. *Drilling and drilling fluids.*. Amsterdam: Elsevier Scientific Publishing Company.
- Chodorow, M. & Susskind, S., 1964. *Fundamentals of Microwave Electronics*. New York: McGraw-Hill .
- Coker, A. K., 2010. Distillation. In: *Ludwig's applied process design for chemical and petrochemical plants. (Volume 2)*. Oxford: Gulf Professional Publishing, pp. 1-263.
- Constant, T., Moyne, C. & Perré, P., 1996. Drying with internal heat generation: Theoretical aspects and application to microwave heating.. *AIChE Journal*, February, 42(2), pp. 359-368.

- Cosenza, P. & Tabbagh, A., 2004. Electromagnetic determination of clay water content: role of the microporosity.. *Applied Clay Science*, February, Volume 26, pp. 21-36.
- Dargay, J. M. & Gately, D., 2010. World oil demand's shift toward faster growing and less price-responsive products and regions.. *Energy Policy*, 38(10), pp. 6261-6277.
- Das, A. & Das, S. K., 2007. Propagation of electromagnetic waves. In: *Microwave Engineering*. New Delhi: Tata McGraw-Hill, pp. 26-50.
- Dean, E. W. & Stark, D. D., 1920. A convenient method for the determination of water in petroleum and other organic emulsions.. *The Journal of Industrial and Engineering Chemistry*, 12(5), pp. 486-490.
- Devereux, S., 1998. *Practical well planning and drilling manual*.. Tulsa: PennWell Corporation.
- Deysel, K., 2007. *Leucoxene study: a mineral liberation analysis (MLA) investigation*.. Natal, The Southern African Institute of Mining and Metallurgy.
- Dhir, R. K., Csetenyi, L. J., Dyer, T. D. & Smith, G. W., 2010. Cleaned oil-drill cuttings for use as filler in bituminous mixtures.. *Construction and Building Materials*, October, Volume 24, pp. 322-325.
- Dionex, 1999. *ASE® 200 Accelerated Solvent Extractor Operator's Manual*. California: Dionex Corporation.
- Donaldson, E. C. & Alam, W., 2008. *Wettability*. Houston: Gulf Publishing Company.
- Dye, W. M. et al., 2006. New Water-Based Mud Balances High-Performance Drilling and Environmental Compliance.. *SPE Drilling & Completion*, December, 21(4), pp. 255-267.
- Ellison, W. J., Lamkaouchi, K. & Moreau, J.-M., 1996. Water: a dielectric reference.. *Journal of Molecular Liquids*, Volume 68, pp. 171-279.
- Elridge, R. B., 1996. Oil contaminant removal from drill cuttings by supercritical extraction.. *Industrial & Engineering Chemistry Research*, June, 35(6), pp. 1901-1905.
- Energy Information Administration, 2011. *U.S. Average Depth of Crude Oil, Natural Gas, and Dry Exploratory and Developmental Wells Drilled (Feet per Well)*, s.l.: s.n.
- Erickson, P., Fowler, B. & Thomas, D., 1988. *Oil-based drilling muds: offstructure monitoring - Beaufort Sea*., Ottawa: s.n.
- Erle, U., Regier, M., Persch, C. & Schubert, H., 2000. Dielectric properties of emulsions and suspensions.. *The Journal of Microwave Power and Electromagnetic Energy*., 35(3), pp. 185-190.

- Evans, N. G., 1997. *Dielectric property measurement at Staffordshire University*. s.l.:s.n.
- Fandrich, R., Gu, Y., Burrows, D. & Moeller, K., 2007. Modern SEM-based mineral liberation analysis.. *International Journal of Mineral Processing*, 84(1-4), pp. 310-320.
- Fink, J. K., 2003. *Oil field chemicals*. Burlington: Gulf Professional Publishing.
- Frost, R. L. & Vassallo, A. M., 1996. The dehydroxylation of the kaolinite clay minerals using infrared emission spectroscopy.. *Clays and Clay Minerals*, 44(5), pp. 635-651.
- Gabriel, C. et al., 1998. Dielectric parameters relevant to microwave dielectric heating.. *Chemical Society Reviews*, February, 27(3), pp. 213-223.
- Gray, G. R. & Darley, H. C. H., 1980. The development of drilling fluids technology.. In: *Composition and Properties of Oil Well Drilling Fluids*. . Houston: Gulf Publishing Company, pp. 37-89.
- Growcock, F. & Harvey, T., 2005. Drilling Fluids. In: *Drilling Fluids Processing Handbook*. Burlington: Gulf Professional Publishing, pp. 15-68.
- Gupta, M. & Wong Wai Leong, E., 2007. Microwaves - theory.. In: *Microwaves and Metals*. s.l.:John Wiley & Sons (Asia), pp. 25-43.
- Gurr, C. G., Marshall, T. J. & Hutton, T. J., 1952. Movement of water in soil due to a temperature gradient.. *Soil Science*, November, 74(5), pp. 335-348.
- Gu, Y., 2003. Automated scanning electron microscope based mineral liberation analysis.. *Journal of Minerals & Materials Characterization & Engineering*, 2(1), pp. 33-41.
- Hall, C., Hoff, W. D. & Nixon, M. R., 1984. Water movement in porous building materials - VI. Evaporation and drying in brick and block materials.. *Building and Environment*, 19(1), pp. 13-20.
- Halliburton , 2007. *Baroid Surface Solutions*, s.l.: s.n.
- Harris, C., 1972. Determination of water.. *Talanta Review*, 19(12), pp. 1523-1547.
- Ho, C. K. & Udell, K. S., 1995. Mass transfer limited drying of porous media containing an immobile binary liquid mixture.. *International Journal of Heat and Mass Transfer*, January, 38(2), pp. 339-350.
- Hudgins, C., 1994. Chemical use in north sea oil and gas E&P. *Journal of Petroleum Technology*, January, 46(1), pp. 67-74.
- Instrumentation Systems & Services Ltd, 2003. *ThermoView Ti30 User's Manual*. s.l.:s.n.

- Ji, G. D. et al., 2004. Phytodegradation of extra heavy oil-based drill cuttings using mature reed wetland: an in situ pilot study.. *Environmental International*, June, 30(4), pp. 509-517.
- Jones, D. A., Kingman, S. W., Whittles, D. N. & Lowndes, I. S., 2007. The influence of microwave energy delivery method on strength reduction in ore samples.. *Chemical Engineering and Processing*, 46(4), pp. 291-299.
- Jones, P. L. & Rowley, A. T., 1996. Dielectric drying. *Drying Technology* , 14(5), pp. 1063-1098.
- Jorissen, F. J. et al., 2009. Impact of oil-based drill mud disposal on benthic foraminiferal assemblages on the continental margin off Angola.. *Deep-Sea Research II*, November, 56(23), pp. 2270-2291.
- Joshi, D. R., 2010. *Engineering Physics*. New Delhi: Tata McGraw Hill.
- Kao, K. C., 2004. *Dielectric Phenomena in Solids*. London: Elsevier, Inc..
- Kappe, C. O., 2002. High-speed combinational synthesis utilizing microwave irradiation.. *Current Opinion in Chemical Biology*, June, 6(3), pp. 314-320.
- Kappe, C. O. & Stadler, A., 2005. *Microwave in organic and medicinal chemistry*.. Weinheim: Wiley-VCH.
- Kennedy, M. J., 1995. *Microwaves: Theory and application in materials processing III*. Westerville, s.n., pp. 43-54.
- Khan, M. I. & Islam, M. R., 2007. Sustainable Waste Management. In: *Petroleum Engineering Handbook - Sustainable Operations*. Houston: Gulf Publishing Company, pp. 135-188.
- Kitagawa, K. & Kanuma, Y., 1986. The reliability of magnetrons for microwave ovens.. *Journal of Microwave Power*, 21(13), pp. 149-158.
- Kjärstad, J. & Johnsson, F., 2009. Resources and future supply of oil.. *Energy Policy*, 37(2), pp. 441-464.
- Krokida, M. & Maroulis, Z., 2000. Quality changes during drying of food materials.. In: *Drying technology in agriculture and food sciences*.. s.l.:Science Publishers Inc., pp. 61-98.
- Lee, B., 1998. *The use of synthetics in well drilling fluids for the offshore oil field*.. Dallas, s.n., pp. 233-237.
- Leonard, S. A. & Stegemann, J. A., 2010. Stabilisation/solidification of petroleum drill cuttings.. *Journal of Hazardous Materials*, February, 174(1-3), pp. 463-472.
- Lidström, P., Tierney, J., Wathey, B. & Westman, J., 2001. Microwave assisted organic synthesis - a review.. *Tetrahedron*, November, 57(45), pp. 9225-9283.

Love, W., 1995. Magnetrons. In: *Handbook of Microwave Technology - Components and Devices (Volume 2)*. San Diego: Academic Press, Inc., pp. 33-55.

Ludwig, E. E., 1997. *Applied process design for chemical and petrochemical plants*. 3 ed. Houston: Gulf Professional Publishing.

Luque de Castro, M. D. & Priego-Capote, F., 2010. Soxhlet extraction: past and present panacea. *Journal of Chromatography A*, 1217(16), pp. 2383-2389.

Marcos, C. & Rodriguez, I., 2011. Expansibility of vermiculites irradiated with microwaves.. *Applied Clay Science*, 51(1-2), pp. 33-37.

Marra, F., De Bonis, M. V. & Ruocco, G., 2010. Combinedmicrowaves and convection heating: A conjugate approach.. *Journal of Food Engineering*, 97(1), pp. 31-39.

McAdams, W. H., 1926. Basic principles of evaporation, distillation and drying.. *Journal of Chemical Education*, February, 3(2), pp. 157-165.

McNair, H. M. & Miller, J. M., 2009. *Basic gas chromatography*. Hoboken: John Wiley & Sons, Inc.

Mehdizadeh, M., 2010. Single-mode microwave cavities for material processing and sensing.. In: *Microwave/RF applicators and probes for material heating, sensing and plasma generation - a design guide*.. Oxford: Elsevier inc., pp. 109-150.

Mehdizadeh, M., 2010. The impact of fields on materials at RF/Microwave frequencies.. In: *Microwave/RF applicators and probes for material heating, sensing and plasma generation - a design guide*.. Oxford: Elsevier Inc., pp. 1-34.

Meng, B., Booske, J. & Cooper, R., 1995. Extended cavity perturbation technique to determine the complex permittivity of dielectric materials.. *IEEE Transactions on Microwave Theory and Techniques*., 43(11), pp. 2633-2636.

Meredith, R., 1998. *Engineers Handbook of Industrial Microwave Heating*. London: Institute of Electrical Engineers.

Metaxas, A. C., 1993. *Applicators for industrial microwave processing*.. Westerville, s.n., pp. 549-562.

Metaxas, A. C. & Meredith, R. J., 1983. *Industrial microwave heating*. London: Peter Peregrinus Ltd..

MI SWACO, 2006. *Thermal desorption: three ways to treat oil-contaminated drill cuttings, reducing waste and recovering valuable resources*., Houston: s.n.

Miao, J., Ishikawa, T., Shen, Q. & Earnest, T., 2008. Extending X-Ray crystallography to allow the imaging of noncrystalline material, cells, and single protein complexes.. *Annual Review of Physical Chemistry*, Volume 59, pp. 387-410.

Miller, R. G., 2011. Future oil supply: the changing stance of the International Energy Agency.. *Energy Policy*, 39(3), pp. 1569-1574.

Minton, R. C. & Secoy, B., 1992. *Annular re-injection of drilling wastes*.. Cannes, s.n., pp. 247-253.

Minton, R. & McGlaughlin, J., 2003. Rising drilling-waste costs promote novel technologies, approaches. *Oil & Gas Journal*, 101(31), pp. 51-55.

Moore, D. M. & Reynolds Jr., R. C., 1997. *X-Ray diffraction and the identification and analysis of clay minerals*. New York: Oxford University Press, Inc..

Moyers, C. G. & Baldwin, G. W., 1997. Psychrometry, evaporative cooling, and solids drying.. In: *Perry's Chemical Engineers' Handbook*. New York: McGraw-Hill, pp. 12-1 to 12-90.

Mujumdar, A. S. & Devahastin, S., 2004. Fundamental principles of drying.. In: *Guide to industrial drying: principles, equipment and new developments*.. Mumbai: Colour Publications, pp. 1-22.

Munro, P. D. et al., 1998. Solid-phase test for comparison of degradation rates of synthetic mud base fluids used in the off-shore drilling industry.. *Environmental Toxicology and Chemistry*, October, 17(10), pp. 1951-1959.

National materials advisory board, 1994. *Microwave processing of materials*, Washington: National Academy Press.

Neff, J. M., 2005. *Composition, environmental fates, and biological effects of water based drilling muds and cuttings discharged to the marine environment: a synthesis and annotated bibliography*., Duxbury: s.n.

Nelson, S., Lindroth, D. & Blake, R., 1989. Dielectric properties of selected minerals 1 to 22 GHz. *Journal of Microwave Power and Electromagnetic Energy*, 24(4), pp. 213-220.

Newman, A. B., 1931. The drying of porous solids: diffusion and surface emission equations.. *Transactions of the American Institute of Chemical Engineers*, Volume 27, pp. 203-216.

Nielsen, J. K. & Maiboe, J., 2000. Epofix and Vacuum: An easy method to make casts of hard substrates.. *Palaeontologia Electronica*, 3(1), pp. 1-10.

Norton, M. G. & Suryanarayana, C., 1998. *X-Ray Diffraction: A practical approach*.. New York: Plenum Press.

Oghbaei, M. & Mirzaee, O., 2010. Microwave versus conventional sintering: a review of fundamentals, advantages and applications.. *Journal of Alloys and Compounds*, April, 494(1-2), pp. 175-189.

- Orsat, V., Yang, W., Changrue, V. & Raghavan, G. S., 2007. Microwave-assisted drying of biomaterials.. *Food and Bioproducts Processing*, September, 85(3), pp. 255-263.
- Orzechowski, K., Slonka, T. & Glowinski, J., 2006. Dielectric properties of intercalated kaolinite.. *Journal of Physics and Chemistry of Solids*, May-June, 67(5-6), pp. 915-919.
- OSPAR, 2000. *OSPAR convention for the protection of the marine environment in the north-east atlantic.*, Copenhagen: s.n.
- Perkin, R. M., 1983. The drying of porous materials with electromagnetic energy generated at radio and microwave frequencies.. *Progress in Filtration and Separation*, Volume 3, pp. 205-266.
- Perry, R. H. & Green, D. W., 1997. *Perry's Chemical Engineers' Handbook*. 7th ed. New York: McGraw-Hill.
- Pickles, C. A., 2009. Microwaves in extractive metallurgy: part 1 - review of fundamentals.. *Minerals Engineering*, October, 22(13), pp. 1102-1111.
- Piper, W., Harvey, T. & Mehta, H., 2005. Waste management.. In: *Drilling fluids processing handbook*.. Burlington: Gulf Professional Publishing, pp. 367-412.
- Puder, M. G. & Veil, J. A., 2006. *Offsite commercial disposal of oil and gas exploration and production waste: availability, options, and costs.*, Argonne: s.n.
- Reader, H. C., 2006. Understanding microwave heating systems: a perspective on state-of-the-art.. In: *Advances in microwave and radio frequency processing*.. New York: Springer-Verlag, pp. 3-14.
- Reimer, L., 1998. *Scanning Electron Microscopy: Physics of image formation and microanalysis*.. 2nd ed. New York: Springer-Verlag.
- Remya, N. & Lin, J., 2011. Current status of microwave application in wastewater treatment - a review.. *Chemical Engineering Journal*, February, 166(3), pp. 797-813.
- Richardson, J. F., Harker, J. H. & Backhurst, J. R., 2002. *Chemical engineering (Volume 2) - particle technology and separation processes*.. 5th ed. Oxford: Butterworth-Heinemann.
- Roach, B., 1995. Klystrons. In: *Handbook of Microwave Technology - Component and Devices (Volume 2)*. San Diego: Academic Press, Inc., pp. 1-30.
- Robinson, J. et al., 2009. Microwave treatment of oil-contaminated drill cuttings at pilot scale.. *SPE Drilling & Completion* , September, 24(3), pp. 430-435.
- Robinson, J. P. et al., 2009. Remediation of oil contaminated drill cuttings using continuous microwave heating. *Chemical Engineering Journal*, may, Volume 152, pp. 458 - 463.

Robinson, J. P. et al., 2009. Remediation of oil-contaminated drill cuttings using continuous microwave heating.. *Chemical Engineering Journal*, October, Volume 152, pp. 458-463.

Roebuck, B. D. & Goldblith, S. A., 1972. Dielectric properties of carbohydrate-water mixtures at microwave frequencies.. *Journal of Food Science*, Volume 37, pp. 199-204.

Saarenketo, T., 1998. Electrical properties of water in clay and silty soils.. *Journal of Applied Geophysics*, October, 40(1-3), pp. 73-88.

Sakai, N. & Wang, C., 2004. An analysis of temperature distribution in microwave heating of foods with non-uniform dielectric properties.. *Journal of Chemical Engineering of Japan*, 37(7), pp. 858-862.

Sandrea, I. & Sandrea, R., 2007. Exploration Trends show continued promise in world's offshore basins. Growth expected in global offshore crude oil supplies.. *Oil & Gas Journal*, 105(9).

Schiffmann, R. F., 2006. State of the art of microwave applications in the food industry in the USA.. In: *Advances in microwave and radio frequency processing*.. New York: Springer-Verlag, pp. 417-426.

Scomi Oiltools, 2010. *Drill Cuttings Thermal Desorption*.. [Online] Available at: http://www.scomi.com.my/core/DWM/pdf/treatmentDisposal/Thermal_Desorption_1208.pdf

Scott, G., Bradshaw, S. M. & Eksteen, J. J., 2008. The effect of microwave pretreatment on the liberation of a copper carbonatite ore after milling.. *International Journal of Mineral Processing*, January, 85(4), pp. 121-128.

Seaton, S., Morris, R., Blonquist, J. & Hogan, B., 2006. *Analysis of drilling fluid base oil recovered from drilling waste by thermal desorption*.. San Antonio, s.n., pp. 1-9.

Shang, H. et al., 2007. Theoretical Study of Microwave Enhanced Thermal Decontamination of Oil Contaminated Waste.. *Chemical Engineering Technology*, 30(1), pp. 121-130.

Shang, H., Snape, C. E., Kingman, S. W. & Robinson, J. P., 2005. Treatment of oil-contaminated drill cuttings by microwave heating in a high-power single-mode cavity.. *Industrial & Engineering Chemistry Research*, 44(17), pp. 6837-6844.

Shang, H., Snape, C. E., Kingman, S. W. & Robinson, J. P., 2006. Microwave treatment of oil-contaminated North Sea drill cuttings in a high power multimode cavity. *Separation and Purification Technology*, August, Volume 49, pp. 84-90.

Shepherd, C. B., Hadlock, C. & Brewer, R. C., 1938. Drying materials in trays - evaporation of surface moisture.. *Industrial & Engineering Chemistry*, April, 30(4), pp. 388-397.

Sherwood, T. K., 1929. The drying of solids - I.. *Industrial & Engineering Chemistry*, January, 21(1), pp. 12-16.

Sherwood, T. K., 1929. The drying of solids - II.. *Industrial & Engineering Chemistry*, October, 21(10), pp. 976-980.

Sherwood, T. K., 1930. The drying of solids - III.. *Industrial & Engineering Chemistry*, February, 22(2), pp. 132-136.

Sisodia, M. L. & Gupta, V. L., 2005. Microwave tubes: Magnetrons. In: *Microwave Engineering*. New Delhi: New Age International (P) Limited, Publishers, pp. 6C.1-6C.20.

Sparkman, O. D., Penton, Z. & Kitson, F. G., 2011. *Gas Chromatography and Mass Spectrometry: A Practical Guide*.. Oxford: Elsevier, Inc.

Stangle, G. C. & Aksay, I. A., 1990. Simultaneous momentum, heat and mass transfer with chemical reaction in a disordered porous medium: application to binder removal from a ceramic green body.. *Chemical Engineering Science*, 45(7), pp. 1719-1731.

Staprans, A., McCune, E. W. & Ruetz, J. A., 1973. High-power linear-beam tubes. *Proceedings of the IEEE*, March, 61(3), pp. 299-330.

Stratton, J. A., 2007. *Electromagnetic Theory*. New Jersey: John Wiley & Sons, Inc..

Stuart, B., 2003. *Practical Laboratory Skills Training Guides: Gas Chromatography*. Cambridge: Royal Society of Chemistry.

Tabrizy, V. A., Denoyel, R. & Hamouda, A. A., 2011. Characterization of wettability alteration of calcite, quartz and kaolinite: Surface energy analysis.. *Colloids and Surfaces A: Physicochemical and Engineering Aspects*, 384(1-3), pp. 98-108.

Tang, J., Hao, F. & Lau, M., 2002. Microwave heating in food processing.. In: *Advances in bio-processing engineering*.. London: Word Scientific Publishing Co. Pte. Ltd., pp. 1-44.

Terselius, B. & Ranby, R., 1978. Cavity Perturbation Measurements of the Dielectric Properties of Vulcanizing Rubber and Polyethylene Compounds. *Journal of Microwave Power and Electromagnetic Energy*, 13(4), pp. 327-336.

Thostenson, E. T. & Chou, T. W., 1999. Microwave processing: fundamentals and applications.. *Composites: Part A*, February, Volume 30, pp. 1055-1071.

Tsimring, S. E., 2007. Traveling-wave tubes and backward-wave oscillators (O-type tubes). In: *Electron beams and microwave vacuum electronics*. Hoboken: Wiley-Interscience, pp. 297-360.

Turner, I. W., 1991. *The modelling of combined microwave and convective drying of a wet porous material*., s.l.: s.n.

- TWMA, 2010. *TWMA integrated drilling waste management - TCC RotoMill*, Aberdeen: s.n.
- Tyrrell, H. J. V., 1964. The origin and present status of Fick's diffusion law.. *Journal of Chemical Education*, July, 41(7), pp. 397-400.
- van der Veen, M. E. et al., 2004. On the potential of uneven heating in heterogeneous food media with dielectric heating.. *Journal of Food Engineering*, August, Volume 63, pp. 403-412.
- Veil, J. A., 1997. *Costs for off-site disposal of nonhazardous oil field wastes: salt caverns versus other disposal methods.*, Argonne: s.n.
- Veil, J. A., Dusseault, M. B. & Laboratoy, A. N., 2003. *Evaluation of slurry injection technology for management of drilling wastes.*, Pittsburgh: U.S. Department of Energy.
- Veil, J. et al., 1996. *Preliminary technical and legal evaluation of disposing of nonhazardous oil field waste into salt caverns.*, Washington: s.n.
- Venkatesh, M. S. & Raghavan, G. S. V., 2005. An overview of dielectric properties measuring techniques.. *Canadian Biosystems Engineering*, Volume 47, pp. 7.15-7.30.
- Vongpradubchai, S. & Rattanadecho, P., 2009. The microwave processing of wood using a continuous microwave belt drier.. *Chemical Engineering and Processing: Process Intensification*, May, 48(5), pp. 997-1003.
- Wait, S. T. & Sharma, S., 2009. *The discharge of synthetic based mud cuttings offshore - a legislative comparison between india and other parts of the world.* New Delhi, s.n., pp. 856-860.
- Westphal, W. B., 1997. *Dielectric constant and loss data.*, s.l.: s.n.
- Whitaker, S. & Chou, W. T.-H., 1983. Drying granular porous media - theory and experiment.. *Drying Technology*, 1(1), pp. 3-33.
- Wilmanski, K., 2010. *Permeability, tortuosity, and attenuation of waves in porous materials.*, Berlin: s.n.
- Yacobi, B. G., Holt, D. B. & Kazmerski, L. L., 1994. *Microanalysis of solids*. New York: Plenum Press.
- Yeskis, D., Koster van Groos, A. F. & Guggenheim, S., 1985. The dehydroxylation of kaolinite.. *American Mineralogist*, Volume 70, pp. 159-164.
- Yoshikawa, N. et al., 2007. Brief review on microwave (MW) heating, its application to iron & steel industry and to the relevant environmental techniques.. *The Iron and Steel Institute of Japan International*, November, 47(4), pp. 523-527.

Zhang, H., Zhang, J. & He, L., 2010. *Effects of the sample's porous structure on the process of vacuum freeze drying..* Chengdu, s.n., pp. 1-4.

Zittel, W. & Schindler, J., 2002. *Future world oil supply*, Ottobrunn: L-B-Systemtechnik GmbH.

APPENDIX 1 – Additional Characterisation Data

This appendix contains additional data on sample characterisation. Figure A.1 below shows the glycolated XRD Spectra for three different samples.

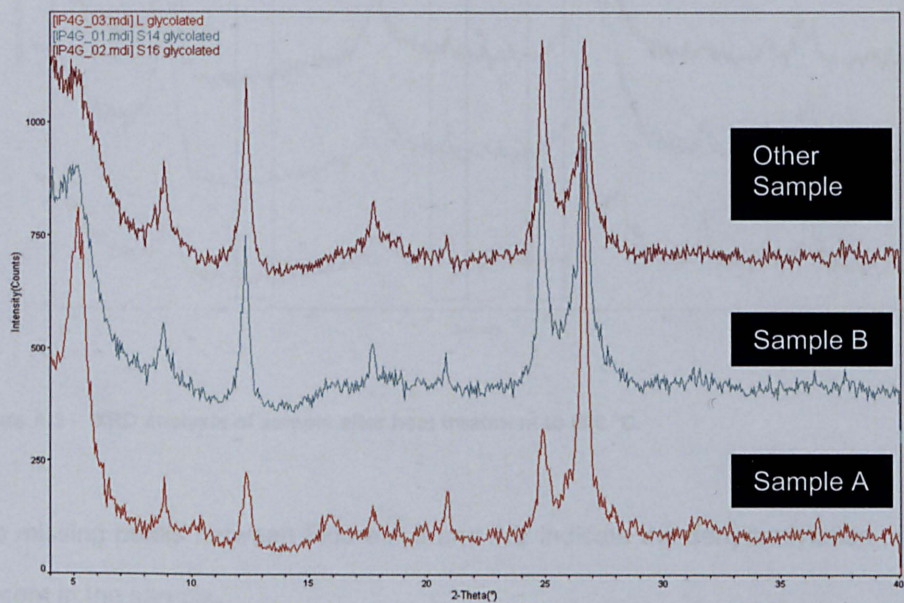


Figure A.1 - XRD analysis of Samples A and B after glycolation.

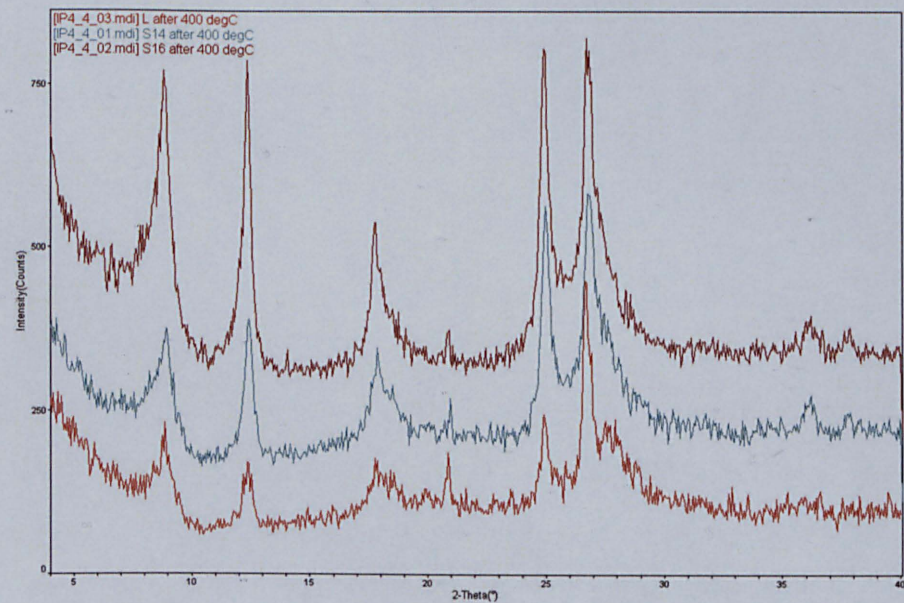


Figure A.2 - XRD analysis of sample after heat treatment to 400 °C.

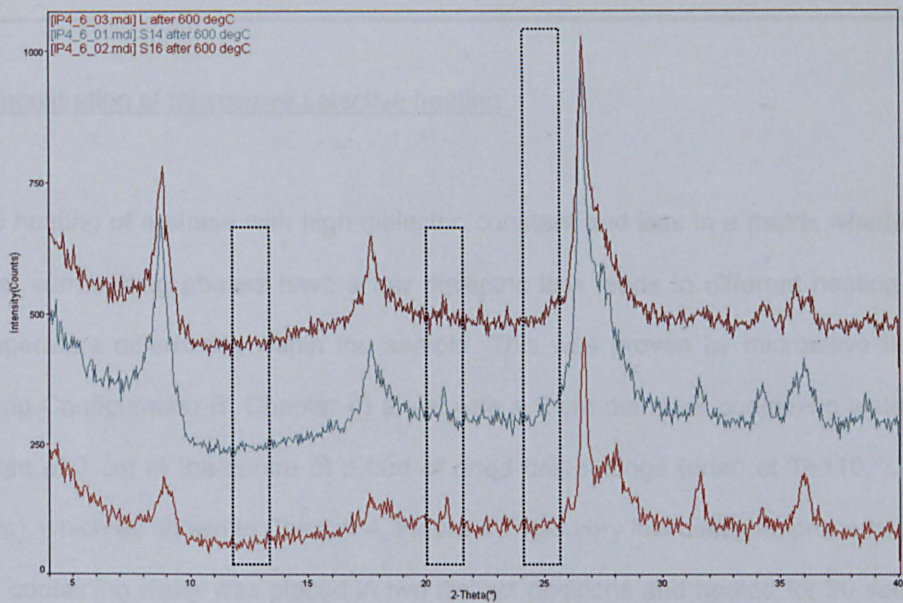


Figure A.3 - XRD analysis of sample after heat treatment to 600 °C.

The missing peaks between Figure A.3 and A.2 indicate the dehydroxylation of clays present in the sample.

APPENDIX 2 – Microwave Surface Temperature Data

Demonstration of microwave selective heating

The heating of a phase with high dielectric constant and loss in a matrix whether the other surrounding phases have a low dielectric loss leads to different heating rates temperature differences within the sample. This was proven by microwave heating (using Configuration B, Chapter 4) a vial with a 2 cm diameter containing water to a height of 3 cm at the centre of a bed of dried drill cuttings (dried at $T \approx 110^\circ\text{C}$ for 2 days), which as shown in Chapter 4, Figure 4.7 has very low dielectric properties. The vial containing water was placed in two distinct positions and heated for 30 seconds. A vial containing oil was also placed in the same location and heated for 30 seconds. The surface temperature was recorded for each experiment and is shown below.

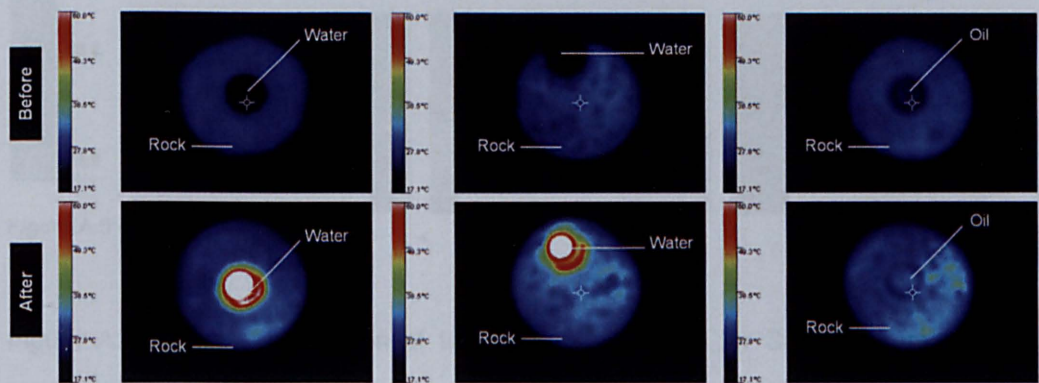


Figure A.4 - Variation of surface T (°C) for water, oil and dried cuttings during MW treatment for 30 secs.

The temperature before and after heating was taken, and the scale was maintained constant throughout (17.1 – 60 °C). Water (Left) at 17 °C and drill cuttings at 25 °C were heated to >60 °C and 30 °C respectively after 30 seconds of microwave treatment, with the same result being observed when the water vial was placed in a different location (Centre). A vial containing oil placed in the same position as the one containing water, was also heated but only showed a small temperature increase; 20-25 °C to 30-35 °C at most (Right).

Surface temperature measurements with time for two samples with significant difference in structure.

Sample B consists of larger, individually separated particulates, with little observed surface liquid. Sample C consists of much finer grains, with clear surface liquid joining particles.

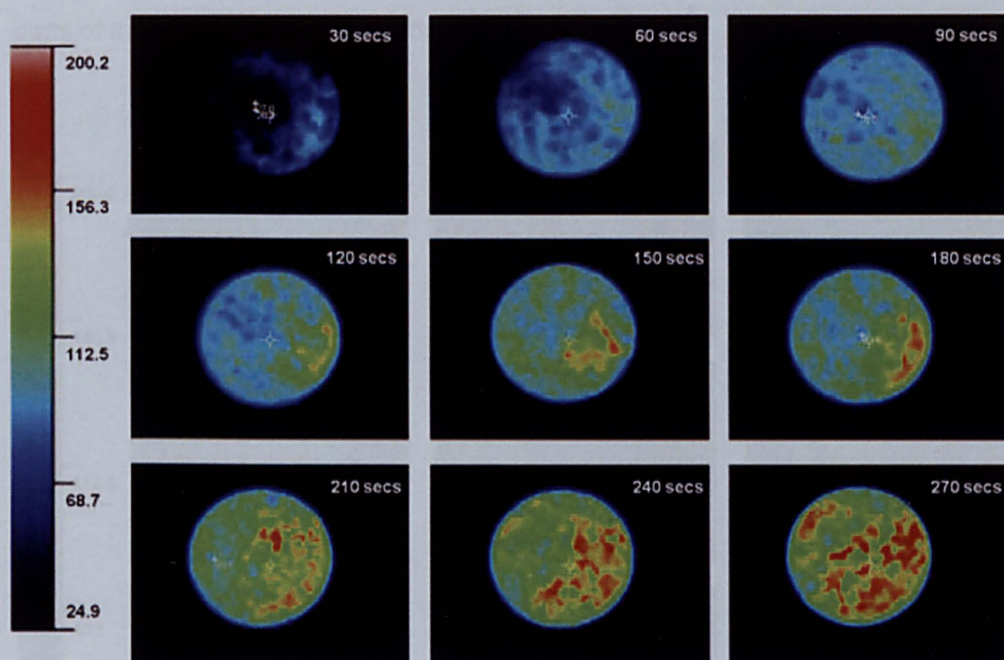


Figure A.5 - Sample B

Figure A.4 shows the variation of temperature with time for Sample B treated at 508W. The temperature of the sample surface increased with time, initially faster near the walls of the container and then at the centre. The temperature difference between individual particles was clear, with certain individual particles being heated to higher temperatures than others. Over the entire experiment the temperature of the sample heated to higher temperatures in the bottom right corner. Overall, the temperature rose from an initial minimum of 25 °C to a maximum of approximately 190 °C at 270 seconds. A significant proportion of the surface of the sample reached a temperature of 100 °C between 60 and 90 seconds, with treatment times >180 seconds leading to sample temperatures >150 °C.

The same measurements were taken for Sample C and are shown in Figure A.5. The temperature increased from a minimum of 25 °C to a maximum of 160 °C at 270 seconds. A similar trend was observed to the results presented for Sample B, with surface temperatures being higher at the edges for the first 120 seconds rather than the centre. Unlike Sample B the temperature gradient of Sample C across the surface was smoother throughout. Beyond 210 seconds, the surface of the sample dried out and the temperature distribution approached that observed for Sample B, with certain parts of the sample heating more than others.

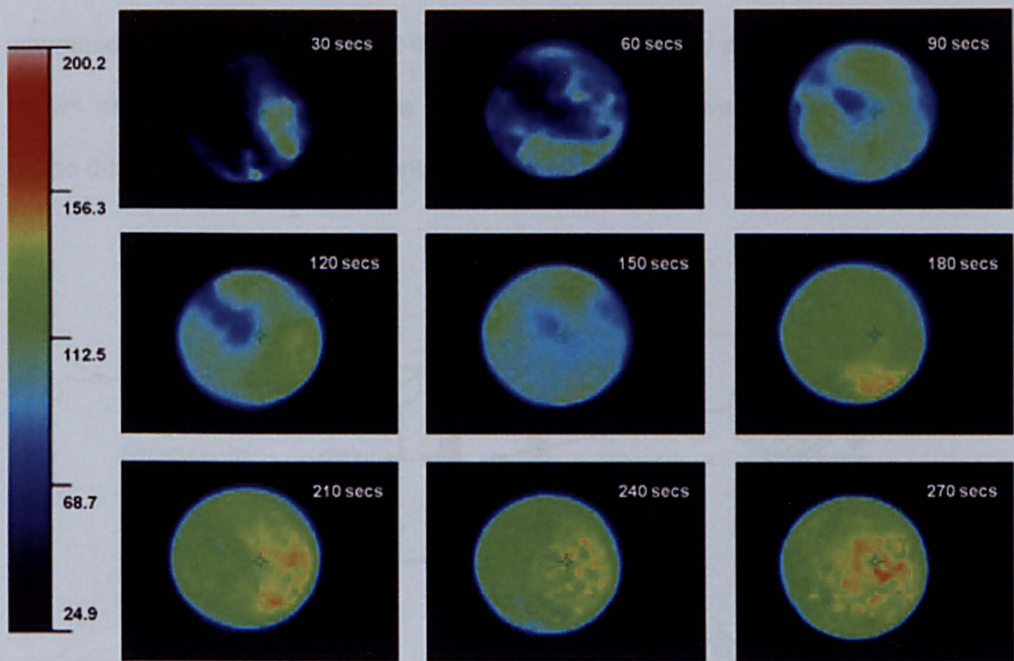


Figure A.6 - Sample C.

APPENDIX 3 – Weight Loss and Drying Rate Data

This section provides data of variation in weight, water and oil content with time collected using Sample A and the experimental setup shown in Figure A.6 below.

Method

Sample A was used for these experiments. Samples weighing approximately $181\text{g} \pm 5$ were placed into cylindrical Pyrex® containers with an inner diameter of 0.075m , and filled to a 3 cm height. The samples were placed 3 cm directly above the waveguide inlet, into the cavity at the centre of a PTFE tray attached to a balance as shown on Figure A.6 below. The balance recorded the weight loss of the sample online during microwave processing every 2 seconds.

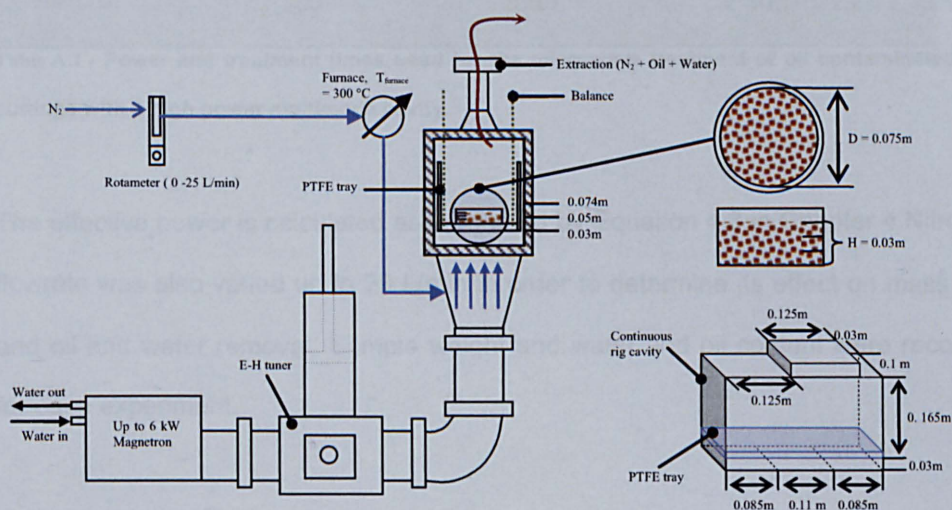


Figure A.7 - Continuous processing cavity used for batch treatment of drill cuttings.

The cavity was connected perpendicularly to WR-430 e-plane bend, which was attached to a straight waveguide section, an automatic E-H Tuner for load impedance matching, followed by another straight waveguide section, a circulator, to avoid any damage to the magnetron, and the magnetron itself. A magnetron capable of outputting a maximum power of 6 kW was used for this set of experiments.

Nitrogen heated to 80 ± 5 °C was fed into the cavity from below at a flowrate of 10 L/min in order to maintain an inert atmosphere and prevent early condensation of oil and water in the cavity. Extracted oil and water vapour as well as nitrogen were removed from the cavity through an extraction section, which was connected directly to the main extraction line in the laboratory. The sample was treated with microwaves at a range of different powers and times as shown on Table A.1

Power in (W)	Power Ref. (W)	Power Ab. (W)	Time (sec)
515	25	490	60, 90, 120, 150, 180
1075	75	1000	15, 30, 45, 60, 90
1625	110	1515	15, 30, 45, 60
2110	120	1990	15, 30, 45
3200	275	2925	10, 20, 30, 40
4010	360	3650	5, 10, 15, 22

Table A.1 - Power and treatment times used for the microwave treatment of oil contaminated drill cuttings with a high power multimode cavity.

The effective power is calculated as presented by Equation 4.3 in Chapter 4. Nitrogen flowrate was also varied up to 20 L/min in order to determine its effect on mass loss and oil and water removal. Sample weight and water and oil content were recorded for each experiment.

Results

Figure A.7 shows the variation of weight with time for sample A treated at an average effective power of 490 W and a number of processing times. Weight varied with time in two stages:

- (1) The first stage was present between 0 and 1.5 minutes and showed little variation in sample weight.
- (2) The second stage took place between 1.5 and 3 minutes, where the weight of the sample decreased constantly and linearly with time.

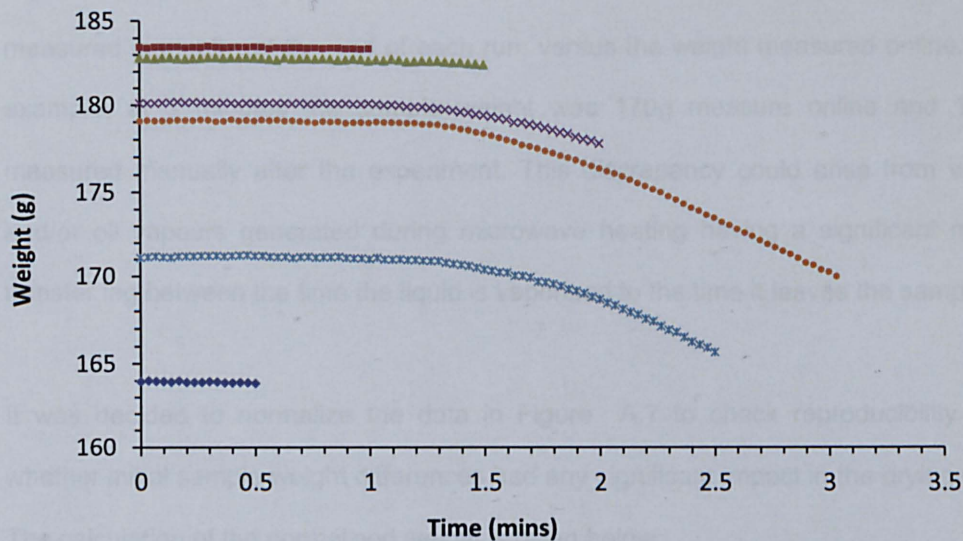


Figure A.8 - Variation of weight vs. time for Sample A treated at 490W in a multimode cavity setup as shown in Figure A.6

Figure A.8 compares the difference in the variation of weight vs. time with data recorded online and with sample mass measured after the sample was removed from the applicator and had its final weighing.

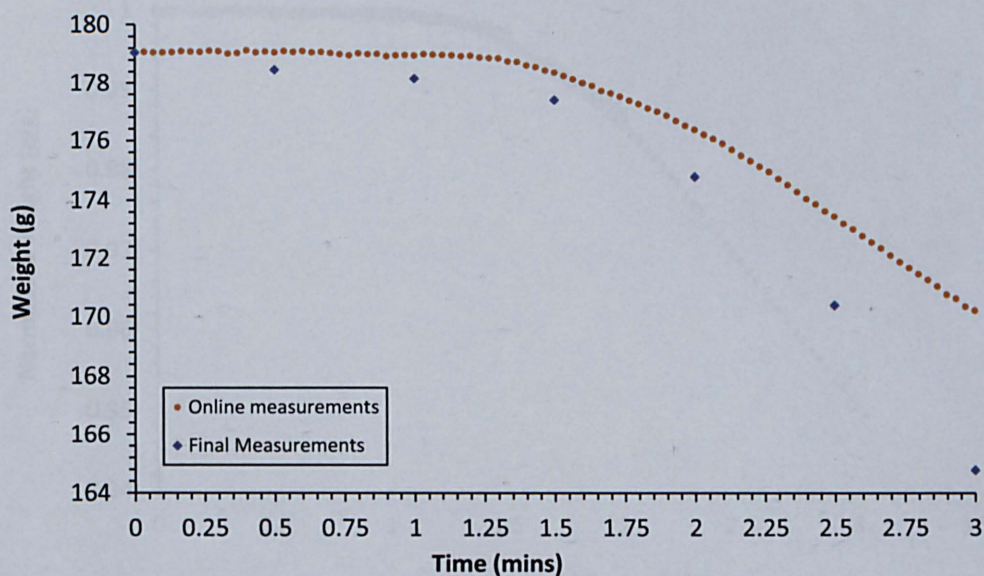


Figure A.9 - Online measurements vs. manual weighing measurements for samples treated at 180 seconds and an average power of 490 W.

Figure A.8 shows an increasing difference with time between the sample weight measured manually, at the end of each run, versus the weight measured online. For example, at 3 minutes the sample weight was 170g measure online and 165g measured manually after the experiment. This discrepancy could arise from water and/or oil vapours generated during microwave heating having a significant mass transfer lag between the time the liquid is vaporised to the time it leaves the sample.

It was decided to normalize the data in Figure A.7 to check reproducibility and whether initial sample weight differences had any significant impact in the drying rate. The calculation of the normalised weight is given below:

$$W_{normalised} = \frac{W_t}{W_{initial}}$$

[Equation A.1]

Figure A.9 shows a normalised plot of the variation of weight vs. time for the various samples treated at the various times.

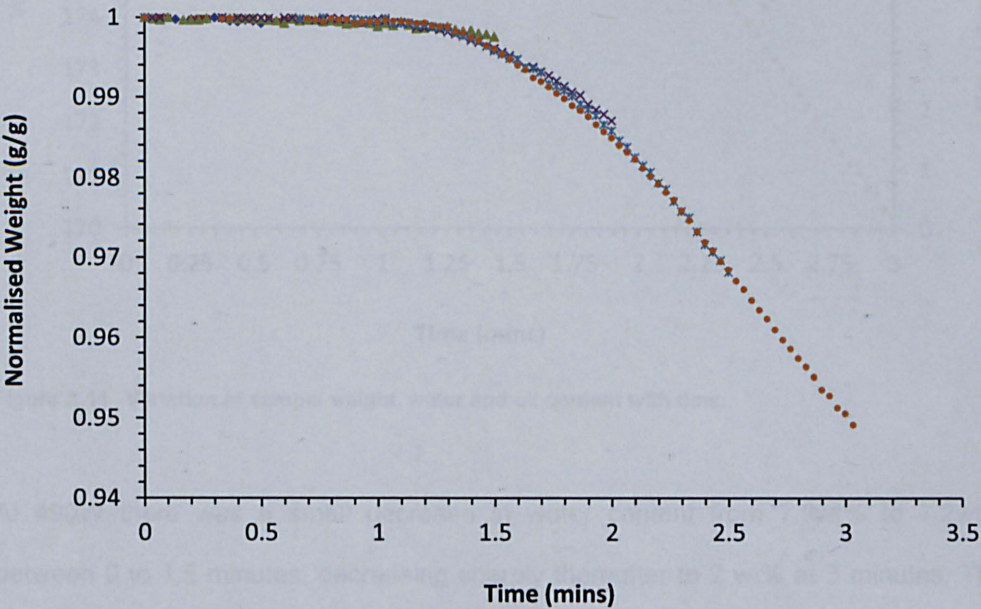


Figure A.10 -Normalised weight vs. time for Sample 4 treated in a high power density multimode cavity at 490 W.

Where the $w_{normalised}$ is the normalise weight of the sample (g/g), w_t is the weight of the sample (g) for a given run at a time (mins) "t" and $w_{initial}$ is the initial weight (g) of a sample for a given run. As seen from Figure A.9 all samples tested at different times superimpose with little variation (<0.01g), suggesting good reproducibility. From this it is also possible to conclude that initial weight did not affect drying rates. Note this observation is only valid for the range of sample weights and experimental conditions tested.

Figure A.10 shows the variation of oil and water content for the same time period as measured from the final sample collected after the experiment was completed.

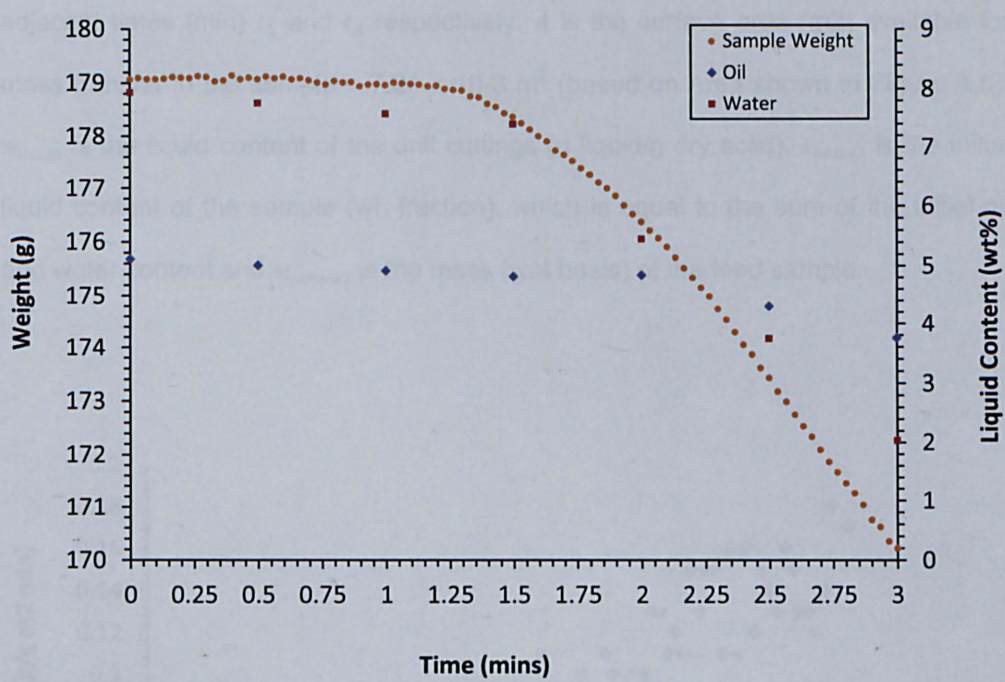


Figure A.11 -Variation of sample weight, water and oil content with time.

At 490W there was a small decrease in water content from 7.9wt% to 7.2wt% between 0 to 1.5 minutes, decreasing sharply thereafter to 2 wt% at 3 minutes. The oil content remained constant around 5 wt% until 2 minutes, decreasing to 4 wt% at 3 minutes. The variation of water content against time matched well the variation of weight with time. The drop in oil content, however, lagged behind the transition time of 1.5 minutes, being present only after 2 minutes.

Figure A.11 below shows the drying rate for the sample treated at 490 W. The drying rate was calculated using the online measurements as it provided the best representation of the process during operating conditions. The drying rate was calculated using the following equations:

$$\frac{dW}{dt} = \frac{w_2 - w_1}{A \times (t_2 - t_1)} \tag{Equation A.2}$$

$$W_{liquid} = \frac{x_{liquid,i} \times m_{sample,i} - dW}{m_{sample,i} - x_{liquid,i} \times m_{sample,i}} \tag{Equation A.3}$$

Where $\frac{dW}{dt}$ is the drying rate (g/m² min), w_1 and w_2 are the weight of the sample (g) at adjacent times (min) t_1 and t_2 respectively. A is the surface area (m²) available for mass transfer in the sample = 7.24 x 10⁻³ m² (based on Area shown in Figure A.6). W_{liquid} is the liquid content of the drill cuttings (g liquid/g dry solid), $x_{liquid,i}$ is the initial liquid content of the sample (wt. fraction), which is equal to the sum of the initial oil and water content and $m_{sample,i}$ is the mass (wet basis) of the feed sample.

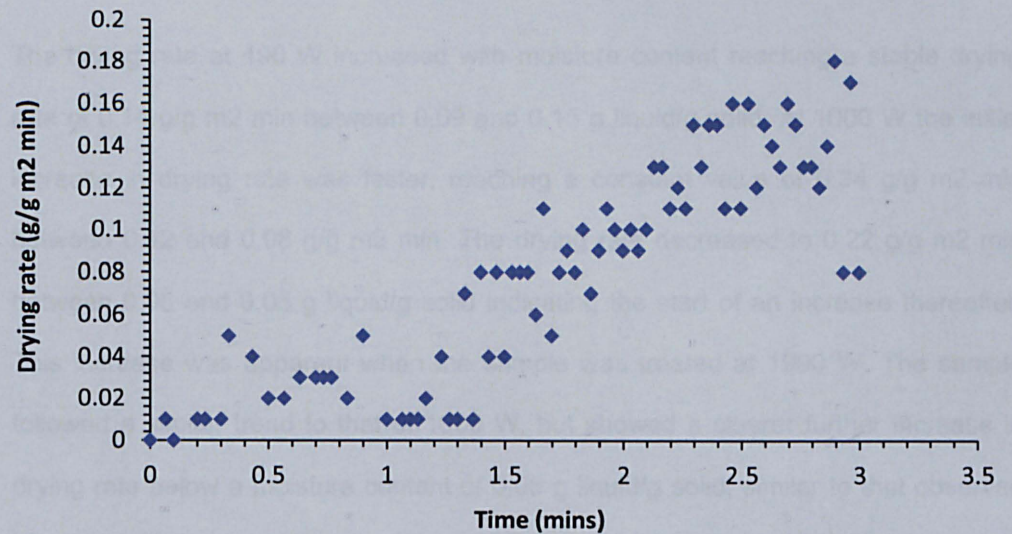


Figure A.12 -Drying rate for drill cutting samples treated at 490 W. Drying rate calculated based on Data presented on Figure A.10 and Figure A.6.

As seen from Figure A.11 the drying rate remains low until 1.5 mins, where it then increases linearly until around 2.5 mins, where it then appears to become constant, falling slightly as it approaches 3 mins. Based on these initial results a number of other powers were tested. Figure A.12 shows the drying rate for samples treated at 490, 1000 and 1990W against water content.

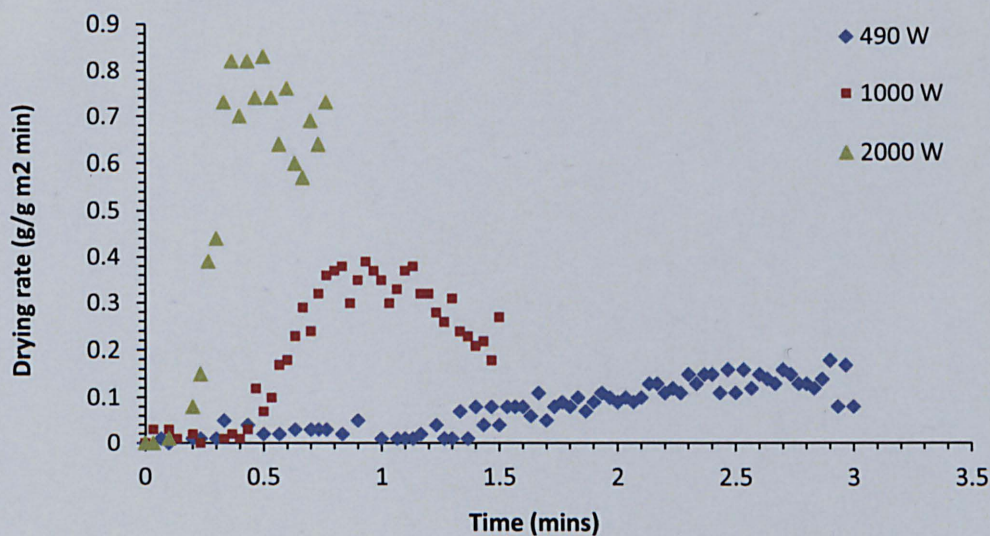


Figure A.13 -Drying rate for drill cutting samples treated at 490, 1000 and 1990 W. Drying rate calculated based on Data presented on Figure A.10 and Figure A.6.

The drying rate at 490 W increased with moisture content reaching a stable drying rate of 0.14 g/g m2 min between 0.09 and 0.15 g liquid/g solid. At 1000 W the initial increase in drying rate was faster, reaching a constant value of 0.34 g/g m2 min between 0.12 and 0.08 g/g m2 min. The drying rate decreased to 0.22 g/g m2 min between 0.08 and 0.05 g liquid/g solid indicating the start of an increase thereafter. This increase was apparent when the sample was treated at 1990 W. The sample followed a similar trend to that of 1000 W, but showed a clearer further increase in drying rate below a moisture content of 0.05 g liquid/g solid, similar to that observed in the initial multimode experiments previously carried out.